Aromatization over Platinum/Zeolite L Catalysts: The effect of Oxygenates

Robin John Nash

B.Sc. Hons. (Chem.,1991)
M.Sc. (Appl. Sci.,1994)

Submitted in fulfillment for the degree of
DOCTOR OF PHILOSOPHY

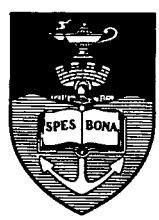

University of Cape Town

February 1997

The copyright of this thesis vests in the author. No quotation from it or information derived from it is to be published without full acknowledgement of the source. The thesis is to be used for private study or non-commercial research purposes only.

Published by the University of Cape Town (UCT) in terms of the non-exclusive license granted to UCT by the author.

University of Cape Town

Acknowledgements

Whole hearted thanks to my supervisor, Professor Mark Dry. Without your help and guidance this project may well have never been finished. Thanks for your time and your expert opinion.

I would like to thank Leslie Petrik for her help with the instrumental analyses. Thanks also to Susana Vasic for perservering with the (at times frustrating) chemisorbtion analyses.

Also to all the my fellow postgrads who contributed to such a great spirit in our department - keep it up guys and girls. There are too many names to mention, but special thanks to Peter, Chappie, Ashli, Shehnaaz, Dave, Ansgar, Rein, Gary, Stefan and Mary. Also a big thanks for my laboratory partner, Jannie, who handled the stress well. Good luck with your new job and success with your thesis.

To the workshop staff, Mr. Peter Dobias and Mr. Joachim Petersen, for always being able to fix whatever the postgrads managed to break. At times we must have worn your patience thin. A special thanks to Mr. Tony Barker for all the advice as well as the excellent job you preformed on my motorbike.

I would also like to thank my family for their support and guidance. Don't worry I am finally going to get a real job.

I would like to acknowledge the farsighted policy of SASOL Ltd. in financially supporting students like myself during their postgraduate studies. Without this very valuable support this project could not have been undertaken.

And lastly to a very special person, Dorothee. Your positive spirit and energy was an inspiration to me. I hope to spend the rest of my life with you.

Synopsis

In 1980, Bernard reported that platinum dispersed on zeolite LTL (Pt/KL) had exceptionally high selectivity for the aromatization of n-hexane to benzene. The selectivity was *ca.* 95% at 99% conversion of n-hexane. This Pt/KL catalyst has been extensively studied to determine the reasons for the exceptional stability and benzene yields relative to platinum supported on silica (Pt/SiO_2) and alumina (Pt/Al_2O_3). The Pt/KL catalyst was found to be monofunctional with all the activity occurring on platinum metal clusters inside the pores of zeolite L. The catalyst exhibits excellent stability and the Aromax Process developed by Chevron Ltd., using a barium doped Pt/KL catalyst, PtBa/KL, has been reported to operate continually for the equivalent of one year during accelerated deactivation testing at 450°C and a hydrogen partial pressure of 6 bar. However, sulphur-containing compounds such as thiophene, result in rapid and irreversible deactivation of the catalyst due to sintering of platinum clusters. Thus the level of sulphur-containing compounds, especially thiophene, must be kept below 50 ppb of the feed to avoid deactivation by sintering. SASOL Ltd. may be in a unique position to use Pt/KL as a catalyst for the aromatization of hexanes and heptanes to benzene and toluene respectively, as their products which are produced by the Fischer-Tropsch process are sulphur free. However, a substantial amount of oxygenates are formed in the Fischer-Tropsch process and as yet no study has been undertaken to determine the effect of these compounds on the activity and selectivity of the catalyst.

n-Hexane was used as the principal hydrocarbon feed during this project. Platinum/KL was synthesized by incipient wetness impregnation of $Pt(NH_3)_4Cl_2.H_2O$ with potassium exchanged zeolite L (KL). The loading of platinum was 1% by mass. The effect of co-feeding ethanol, n-butyraldehyde, i-butyraldehyde, methylethylketone, water and carbon monoxide with n-hexane was studied. The variables were reaction temperature, hydrogen partial pressure and the molar ratio of the oxygenated co-feed to n-hexane.

For n-hexane aromatization the Pt/KL catalyst underwent deactivation at low hydrogen partial pressures (< 6 bar hydrogen partial pressure) and a reaction temperature of 450°C. The deactivation was almost completely reversible by calcination of the deactivated Pt/KL catalyst in air. The deactivation of the catalyst was modelled by the empirical equation (exponential decay with time on stream) of Voorhies and is assumed to be mainly due to coking. As the catalyst was not completely regenerated, it is postulated that a small degree of sintering occured. This is attributed to the formation of local "hot spots" during the regeneration procedure. At hydrogen partial pressures of 6 bar no deactivation was observed. Increasing the hydrogen partial pressure from 1 bar to 2 bar resulted in an increase in the conversion of n-hexane and the selectivity to benzene as a result of the suppression of hexene products, which presumably cause fouling of the platinum clusters. At higher partial pressures of hydrogen (3 bar to 6 bar) the selectivity to benzene and MCP is markedly suppressed, as consistent with thermodynamics considerations. This leads to a decrease in the conversion of n-hexane. Hydrogenolysis reactions to form non-aromatizable C_1-C_5 products are favoured by increase in hydrogen partial pressure. However, terminal hydrogenolysis, from which methane is a major product, is suppressed at high partial pressures of hydrogen (6 bar) relative to low hydrogen partial pressures (1 bar).

The co-feeding of oxygenated compounds with n-hexane at 450°C and 1 bar hydrogen partial pressure resulted in a decrease in n-hexane conversion and benzene selectivity. The deactivation effect is reversible as the activity and selectivity of the catalyst is restored after co-feeding of the oxygenated compound was terminated. In all cases carbon monoxide was detected as a product. The oxygenated compounds were found to undergo two competing reactions over Pt/KL, *viz.* hydrogenation and hydrogenolysis. Complete hydrogenation will result in the formation of an alkane and water while hydrogenolysis will result in the formation of a smaller alkane (or two alkanes) and carbon monoxide. The deactivation observed during the co-feeding was initially postulated to be enhanced either by water or carbon monoxide formed by the reactions of the oxygenated co-feeds over Pt/KL. The co-feeding of water, however, resulted in no observable

effect. On the other hand the co-feeding of carbon monoxide caused rapid deactivation, similar to that observed for the other oxygenated co-feeds.

At 500°C the deactivation caused during co-feeding is postulated to be the result of reversible chemisorption of carbon monoxide and other oxgenated species on platinum clusters. The platinum clusters in zeolite KL are reported to be slightly basic, and hence electron rich. Thus the absorbing molecule will form a interaction with the platinum cluster via a carbon atom adjacent to an electronegative oxygen atom. Water, will interact via hydrogen atoms. However, this hydrogen bond to platinum will be weak relative to the carbon atom, which explains the negligible effect of water on the activity of Pt/KL. The carbon atom bond to platinum is stabilized by π-back donation of electrons from platinum into the empty 2π orbitals of carbon. This interaction is absent in the case of water. The interaction of the oxygenated compounds with platinum is much weaker than in the case of sulphur-containing compounds where a strong S-Pt bond forms. This Pt-S bond results in the weakening of the interactions anchoring the platinum cluster and accelerated sintering occurs. Sintering of platinum does not occur as the result of feeding oxygenated compounds over platinum. The exact nature of the bonding of carbonyl compounds with platinum is unknown as platinum carbonyl species are unstable and are not expected to occur at reaction temperatures of 450°C. However, the platinum-oxygenate species formed alters the reactivity of the platinum cluster, resulting in lower selectivity to benzene (at the same conversion of n-hexane) relative to deactivation as a result of coke formation only.

The different oxygenated co-feeds, with the exception of water, were observed to result in a similar degree of deactivation of Pt/KL, for similar molar ratio of co-feed to n-hexane. The molar ratio of co-feed to to n-hexane was found to be an important factor deteriming the extent of deactivation during co-feeding. Increasing the molar ratio of co-feed to n-hexane, at constant hydrogen partial pressure resulted in a larger extent of deactivation. Thus competitive adsorbtion of n-hexane and the oxygenated co-feed take place on platinum clusters. The oxygenated

compounds form stronger interactions with platinum than the alkanes due to the electronegative oxygen atom resulting in slightly electron deficient carbon atoms, which interact more strongly with platinum clusters than the carbon atoms of n-hexane.

Increase in the hydrogen partial pressure also had an inhibitory effect on the deactivation caused by co-feeding. This presumably was the result of increased hydrogenation of carbon monoxide to methane and water, both of which do not interact with platinum in the same manner as the carbonyl compounds.

In summary the Pt/KL catalyst is suitable for use in industrial aromatization reactions as long as the feedstocks are sulphur-free. The presence of oxygenated compounds will at worst lower conversion and aromatics selectivity. However, operating at higher hydrogen partial pressures (6 bar) should reduce this effect. It is recommended that the molar ratio of oxygenates to the alkane feed be kept as low as possible, however, as the magnitude of deactivation is directly related to this ratio. The deactivation is, however, reversible and the catalyst can be regenerated by calcination in an oxidising atmosphere. The reactivity of the platinum clusters is altered during the co-feeding of oxygenated compounds resulting in less benzene formation. This result tends to support the hypothesis that the superior performance of the Pt/KL catalyst with regard to benzene selectivity and stability is due to unique electron interactions existing only within the channels of Pt/KL.

Table of Contents

List of Figures

List of Tables

Nomenclature

BPSD	Barrels per standard day
BTX	Benzene, toluene, xylene
BuHO	Butyraldehyde
C_1-C_5	Alkanes from methane to pentane
C_6=	Hexene
DME	Dimethylether
EtOH	Ethanol
EXAFS	Extended X-ray adsorption fine structure
FTIR	Fourier transform infrared spectroscopy
H-ZSM-5	Acidic form of ZSM-5 zeolite (MFI structure)
KL	Potassium-exchanged zeolite L
LN	Light naphtha
LPG	Liquified petroleum gas
LTL	Linde type L zeolite (IUPAC nomenclature)
MCP	Methylcyclopentane
MFC	Mass flow controller
MEK	Methylethylketone
MFI	IUPAC nomenclature for zeolites with 5-membered ring structure
ppb	Parts per billion
Pt/KL	Platinum supported on potassium exchanged zeolite L
RON	Research octane number
TCI	Terminal cracking index (n-C_5/n-C_4 for n-hexane cracking)
t.o.s.	Time on stream
XRD	X-ray diffraction

Chapter 1

Literature Review

1. Literature Review

1.1 Introduction

Benzene, toluene and xylenes (BTX) are important upstream building blocks for the fibre, agricultural, fine chemicals and pharmaceutical industries. Benzene finds broad applications as a precursor for many important organic intermediates and cycloaliphatic compounds[1]. Of these applications the two most important are alkylation to ethylbenzene and cumene and hydrogenation to cyclohexane. Ethylbenzene and cumene are precursors to styrene and phenol respectively. Demand for styrene and phenol is growing in Western Europe and Japan respectively. BTX is also used in the manufacture of a wide variety of fine and speciality chemicals[2].

Until recently, BTX was used in gasoline blending because of its high octane rating. However, legislation has reduced the allowed level of aromatics in the blend. Commencing in 1996, Phase II of the Clean Air Act Amendments limits the maximum aromatics allowed in the gasoline blend in the United States of America to only 20% by volume, with the limit for benzene being less than 1% by volume[3].

1.1.1 Traditional methods of obtaining BTX aromatics

At present BTX hydrocarbons are recovered from the following:

- Coking products from hard coal.
- Reformate gasoline from crude gasoline (heavy naphtha) processing.
- Pyrolysis gasoline formed during ethylene or propene production from the steam cracking of naphtha.

The major process is the catalytic reforming of naphthas, in which benzene is formed in small amounts compared to toluene and C_8 aromatics such as xylenes and ethylbenzene. Benzene can also be produced by steam cracking of naphtha, in which C_8 aromatics are underproduced compared to benzene and toluene[4]. Both these processes yield a thermodynamic equilibrium mixture of xylenes (o:m:p $\approx$ 25:50:25). Reforming yields a C_8 cut that contains 15% - 20% ethylbenzene and steam cracking yields a C_8 cut that contains 35% - 55% ethylbenzene[5]. The amount of benzene produced in both processes is small relative to the sum of toluene and C_8 aromatics. Recently several new technologies have been developed for the production of BTX aromatics from light naphtha (LN, C_6-C_8) and from liquified petroleum gas (LPG, C_3-C_4). These are discussed further in Section 1.2.1 and Section 1.2.2 respectively.

BTX recovered from reformer or pyrolysis gasolines does not meet the needs of the chemical industry because both processes result in a shortage of benzene, which is the most important aromatic raw material. Benzene is used in the production of ethylbenzene, cumene, long chain alkylbenzenes, cyclohexane, halogen and nitrogen derivatives. Of the xylenes produced, the most abundant is m-xylene, which has only limited application, whereas the demand for o-xylene and p-xylene in particular is high. p-Xylene is used in the production or phthalic anhydride and terephthalic acid.

1.1.2 Economics of LPG and LN aromatization

Any new technologies for the production of BTX, particularly by aromatization of light alkanes must be strongly competitive with current processes. The viability of the processes will depend greatly on feedstock availability and price. In 1989 world production of BTX was 42 000 000 tons of which 30%, 23% and 7% were produced in the United States, Western Europe and Japan respectively[1,4]. Catalytic reformate accounted for about 60% of world BTX production. Hence, BTX availability depends greatly on the availability of heavy naphtha.

In the early 1980's, the aromatization of LPG and light naphtha to yield BTX received increasing attention as a reforming process. The reasons were that high octane BTX could then be blended directly into the gasoline pool and that demand for BTX as source of basic chemical intermediates was growing. A further advantage is that these technologies produce substantial amounts of hydrogen. Most of the catalysts developed for the dehydrocyclization of light hydrocarbons are derived from medium-pore zeolites with a MFI structure, *viz.* ZSM-5. The catalysts are generally promoted by a dehydrogenating function such as zinc, gallium or platinum (Section 1.2.2).

The economics of LPG and LN aromatization processes depend very much on local and site specific factors. However, the relative economics of LPG and LN aromatization processes can be evaluated as shown below.

- Thermochemistry of aromatization

  Standard enthalpies (298K) per mole of aromatic compound produced in aromatization are as follows:

$2C_3H_8$	→	C_6H_6	+	$5H_2$	290.4 kJ/mol
$3C_4H_{10}$	→	$2C_6H_6$	+	$9H_2$	269.7 kJ/mol
$2C_4H_{10}$	→	C_8H_{10}	+	$5H_2$	267.1 kJ/mol
C_6H_{14}	→	C_6H_6	+	$4H_2$	249.9 kJ/mol

  Due to the high endothermicity of the aromatization of light alkanes, an estimated 15% of the feedstock combustion energy must be used to reach and maintain reaction temperature.

- Feedstock and fuel prices[2]

  The highest prices predicted for the feedstocks and products are shown. These predictions were made in 1989. However, it is notoriously difficult to make accurate predictions in this regard and thus these values should at best be used as an approximate guide.

Propane	$140/ton	$6.2/kmol
Butane	$155/ton	$9.0/kmol
Light naphtha	$165/ton	$14.2/kmol, n-hexane basis
Benzene	$420/ton	$32.7/kmol
Toluene	$340/ton	$31.3/kmol
Xylenes	$350/ton	$37.1/kmol
Hydrogen	$400-1000/ton	$0.8-2.0/kmol

The large variation in the value of hydrogen is dependant on whether hydrogen is valued as a fuel or as a chemical. The added values, per kmol of carbon, for the various reactions, with and without the recovery of hydrogen are shown in Table 1-1, based on the data of Szmant (1989)[2]. Hydrogen is valued at $1.4/kmol. Only the aforementioned aromatization reactions are assumed to take place and only the added value, as a result of these aromatization reactions, is shown.

Table 1-1 Relative economics of LPG and LN aromatization processes

	Added value per kmol of carbon (US$)	
	No hydrogen recovery	100% hydrogen recovery
Propane to benzene	3.4	4.5
Butane to benzene	3.2	4.2
butane to xylenes	2.4	3.3
hexane to benzene	3.1	4.0

Hence the following conclusions can be drawn with regard to process economics for both LPG and LN aromatization:

- Hydrogen is a valuable product and must be recovered, as full hydrogen recovery improves process economics, on average, by 32%. A key requirement for the efficient recovery of hydrogen is the minimization of methane yield in the fuel gas product as this reduces separation costs. Actual hydrogen recovery is typically only 2-5 wt%.

- Aromatics selectivity must be optimized. However, a large amount of feedstock must be sacrificed to satisfy the reaction temperature requirements dictated by thermodynamics.

However, light naphtha aromatization economics are less favourable than LPG economics for the following reasons:

- LN aromatization is in direct competition with classical reforming processes.

- Added value per mol of carbon is less than for LPG. See Table 1-1.

- Carbon loss via coking or cracking to give fuel gas is higher than for LPG.

- Hydrogen recovery, both relative and absolute, is less than for LPG.

- No decrease in feedstock cost is predicted, since there is no likelihood of a significant surplus of LN.

1.2 Processes available for obtaining BTX aromatics

1.2.1 Processes for the reforming of naphtha

1.2.1.1 Platforming

Platforming is the earliest process for the catalytic reforming of naphtha[6] , being introduced by United Oil Products Ltd. (UOP) in 1949. Major advances in plant design and catalyst performance have increased attainable product octanes, however the liquid yield still declines severely at the highest octanes. The reason may be a selectivity limit intrinsic to conventional bifunctional reforming catalysts that contain acidic, halided-alumina supports[10]. Most petroleum derived aromatics are obtained by catalytic reforming of naphthas. In the catalytic reforming process low octane naphthas, boiling between 65°C and 200°C, are converted to high octane gasolines containing a high concentration of aromatics[10,12]. The important reactions leading to aromatics are:

- dehydrogenation of six-membered ring naphthalenes;
  e.g. methylcyclohexane (RON 75) to toluene (RON 124)

- dehydroisomerization of five-membered ring naphthalenes;
  e.g. 1-*trans*-3-dimethylcyclopentane (RON 81) to toluene (RON 124)

- dehydrocyclization of paraffins.
  e.g. n-heptane (RON 0) to toluene (RON 124)

Present day catalytic reforming processes are incapable of converting light hydrocarbons with carbon numbers of five or less to aromatics[12]. Much higher yields of liquid reformate and hydrogen can be attained by decreasing the reactor pressure. However, operation at lower pressure causes rapid deposition of coke on the catalyst which consequently causes run lengths to be prohibitively short. In addition, deactivation of monometallic Pt/alumina catalysts is accompanied by a

large decrease in the yield of C_5+ reformate[10]. To this end UOP[7] introduced Continuous Platforming in 1971 and IFP[8] introduced Regenerative Reforming in 1973. Both UOP and IFP now refer to the technology as Continuous Catalyst Regeneration (CCR). CCR is also the technology used to maintain catalyst activity in the Cyclar process.

It was observed that the addition of small amounts of Re to the basic monometallic Pt/Al_2O_3 increases the life time of the catalyst substantially. Kluksdahl of Chevron Research achieved this goal by inventing the first bimetallic reforming catalyst which was commercialized in 1967[10]. These $Pt\text{-}Re/Al_2O_3$ catalysts have both superior activity and selectivity stability.

Catalytic reforming of naphtha has remained the dominant process for increasing aromatics content and octane rating of hydrocarbon streams in the gasoline range. In todays' Platforming technology, new catalyst development has reduced pressures to approximately 4 bar, increased space velocity, reduced the hydrogen to hydrocarbon molar ratio by a factor of two and increased research octane number (RON). Benzene concentration has decreased by 20% by volume[9].
The Platforming process has very limited ability to reform C_6-C_7 alkanes. However, recent developments using monofunctional catalysts, consisting of highly dispersed platinum or palladium particles in a non-acidic large pore zeolite, have increased the aromatics selectivity of C_6-C_7 alkanes (Section 1.2.1.2).

1.2.1.2 Aromax

The Aromax process was developed by Chevron Research Ltd. for the aromatization of C_6 to C_7 hydrocarbons. The catalyst is platinum dispersed on zeolite LTL. Barium and potassium are commonly used as the exchanging ions, *viz.* the nomenclature: Pt/KL or Pt/BaKL. Metallic platinum is nearly 100% dispersed as the active phase. The barium exchanged form of the catalyst is calcined at 600°C, as at this temperature the barium(II) cations move from open positions in the pore system to locked exchange sites in the cages. The platinum metal particles should

have a maximum diameter of 8Å - 10Å. The use of a monofunctional metal-catalyzed process avoids acid-catalyzed isomerization of n-alkanes to branched alkanes. Cracking and polymerization reactions which lower the aromatic product yield and deactivate the catalyst are also minimised[40].

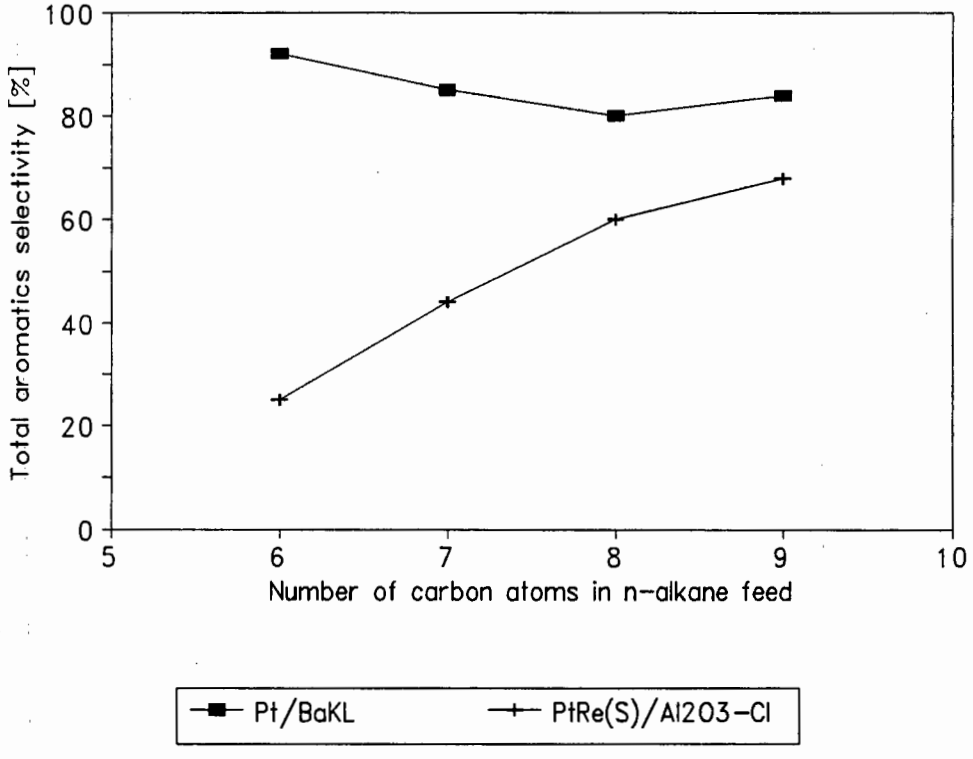

Figure 1-1 Effect of n-alkane chain length on the selectivity to aromatics at 766K (493°C), 6.5 bar and LHSV of 18/hr (Hughes T.R. *et al.*, 1987)

The capability of greatly increasing the selectivity for aromatization of light alkanes by monofunctional catalysts over that of conventional reforming catalysts have recently been demonstrated by Hughes *et al.* (1987)[6] using Pt/BaKL (Figure 1-1). The advantage in aromatization activity and selectivity is particularly large for hexane and heptane. The ability of the Pt/BaKL catalyst to achieve a commercially practical cycle length during reforming of desulphurized naphtha has been demonstrated[6].

1.2.1.3 STAR

Another type of process, steam active reforming (STAR), using a monofunctional catalyst, is also capable of dehydrocyclizing alkanes to aromatics with a high selectivity. The process was developed by Phillips Petroleum[6]. Steam is used as a diluent to favour dehydrocyclization equilibrium and to supply heat to maintain the reaction temperature. The catalyst is reported to contain multiple metal promoters on a neutral support, so that acid catalyzed isomerization is minimized. Although the composition of the STAR catalyst has not been divulged, the one used in a Phillips patent that describes the process, was platinum and tin supported on zinc aluminate spinel[6].

1.2.1.4 Selectoforming[10]

Selectoforming uses a small pore zeolite, erionite, to catalyze the shape selective cracking of n-paraffins. The main by-product is LPG, principally propane. In this process the aromatics in the feed are concentrated, no aromatization reactions take place.

1.2.2 Processes for the Aromatization of Light Hydrocarbons

1.2.2.1 M2-forming[11,12]

The M2-Forming process, developed by Mobil Research and Development Corporation, converts light alkenes and alkanes to BTX aromatics using a H-ZSM-5 type catalyst. M2-Forming is a refinement of M-Forming. M-Forming selectively cracks straight chain alkanes in the reformate on a ZSM-5 catalyst to give light alkenes. These alkenes are mostly reacted with aromatics present in the reformate to yield alkylaromatics. However, the alkenes can also oligomerize and cyclize to form aromatics. This led to the development of a zeolite based process, M2-Forming, specifically tailored to produce aromatics from light hydrocarbons by

maximizing alkene oligomerization and aromatization. The minimum temperature varies considerably, ranging from less than 370°C for alkenes to 538°C for propane. The maximum yield of aromatics is determined by the stoichiometric constraint imposed by the hydrogen content of the feed and the products. The reactions involved in the M2-forming are complex, consecutive, acid-catalyzed reactions[11,175], as discussed below.

Light hydrocarbons, other than methane and ethane can be converted to aromatics and light gases over H-ZSM-5. In the reactions promoted by H-ZSM-5, the aromatics are suggested to be formed in an acid catalyzed, consecutive reaction scheme:

- alkanes → small alkenes → C_2-C_{10} alkenes → aromatics.

Excess hydrogen from reactants is rejected in the form of hydrogen rich products, such as methane and ethane. Introduction of a dehydrogenation compound, platinum, into H-ZSM-5 increased the conversion of propane. However, the aromatization selectivities of the Pt/H-ZSM-5 catalysts were low[6]. The exchange of either Ga(III) or Zn(II) ions into H-ZSM-5 increased aromatization selectivities by increasing the formation of dihydrogen (reverse hydrogen spillover). However, loss of zinc from the catalyst caused deactivation at elevated temperatures. Gallium was found to be stable[6].

1.2.2.2 Cyclar

The Cyclar process was developed jointly by BP and UOP in 1984 and converts LPG into aromatics in a single step. The aromatization reactions are termed dehydrocyclodimerization by BP and UOP. The Cyclar process converts the majority of the excess hydrogen from aromatization in the form of H_2, rather than as light alkanes. BP have disclosed that the Cyclar process is based on a gallium doped zeolite catalyst developed in their laboratories. Although the detailed composition of the Cyclar catalyst has not been disclosed it seems more than likely to be

gallium doped acidic H-ZSM-5[6].

In January 1990, a 1000 bpsd unit was commissioned at Grangemouth, Scotland to evaluate the following[13]:

- Various LPG feeds, *viz.* propane, butane and mixed LPG.

- Different catalysts: a first-generation catalyst with proven physical strength and a second-generation catalyst with *ca.* 30% higher activity. In both cases the catalyst is a gallium-modified MFI zeolite with a binder that has low activity and high attrition resistance.

- A wide range of reactor conditions, including high pressure (<6.5 bar) corresponding to minimum investment and low aromatics yield and low pressure operation, corresponding to higher investment, but producing maximum aromatics yield.

This demonstration unit was decommissioned at the end of 1991, but could still be operated as a small commercial unit, with BTX products being blended into the refinery process streams.

1.2.2.3 Pyroform

The Pyroform process produces aromatic products from ethane, propane or mixtures of these compounds[6]. There are two versions, one thermal and the other thermal/catalytic. In the case of propane, Pyroform is inferior to the Cyclar process in terms of aromatic products. However, with ethane as feed the Pyroform process may be superior to the Cyclar process as ethane is relatively unreactive over gallium doped H-ZSM-5 catalysts[6].

1.2.2.4 Z-Forming[14]

Z-forming was developed by Mitsubishi Oil Corporation and Chiyoda Corporation to manufacture BTX and hydrogen from LPG and LN. A 200 bpsd demonstration plant operated at Kawasaki, Japan from November 1990 until December 1991[14]. The process uses a fixed-bed switching reactor system in which two stacks of four reactors are arranged in series. A multistage reactor is used because of the endothermicity of the reaction. The catalyst is regenerated by progressively increasing first the concentration of oxygen in circulating nitrogen and then the regeneration temperature. Water produced by burning coke is removed from the regeneration loop to avoid catalyst deterioration. For LN and butane aromatization a train of reactors can be operated continuously for 4 days with only a small decline in activity and aromatics selectivity. Decline in aromatization activity and selectivity can be off-set by increasing the reaction temperature.

The reported performance of the Z-Forming process is slightly inferior to that of the Cyclar process[14]. With the present data it is not possible to determine whether the differences are the result of catalyst formulation or differences in process operation. Cyclar and Z-Forming, however, compare quite well when operated at high pressure on a mixed propane/butane feed as well as for propane and butane separately. At low pressure (high aromatization mode with recycle to reactor), Z-forming produces 30% more fuel gas and 10% less total aromatics than the Cyclar process. However, the selectivity to benzene is higher for Z-Forming than for Cyclar. The reaction temperature range for the Z-Forming process is not known, but be may be assumed to be higher than the Cyclar process as more benzene and fuel gas are produced.

1.2.2.5 Aroforming[15,16]

The Cyclar process is not intended to convert light naphtha feedstocks, especially C_5 and C_6 hydrocarbons into aromatics, while the Aroforming process, developed by IFP and SALUTEC, has been designed to aromatize a large range of aliphatic

hydrocarbons[17] (LPG and LN). Its performance for LPG conversion is reported to be close to that of the Cyclar process. No pilot plant or demonstration plant data are available for the Aroforming process. As with Cyclar and Z-Forming, the catalyst is most likely a Ga-MFI zeolite, possibly including a group VIII metal. Aroforming is based on multiple fixed bed reactors that switch between operation and regeneration modes.

1.2.2.6 Topas

Only a few details have been released on the Topas (Topsoe Aromatics Synthesis) process of Haldor Topsoe A/S. According to Topsoe[18] the Topas process uses a zeolite catalyst that does not contain exotic or expensive metal components. Specifically it does not contain gallium. However, the product distribution is identical to that of a gallium containing catalyst. The stability of the Topsoe catalyst appears to be much better than that of gallium containing catalyst. The longer lifetime makes the use of a single fixed-bed reactor possible. The Topas process operates at 475°C - 525°C and pressures up to 10bar. A modified version of the process, which produces only benzene and hydrogen is also available.

1.2.3 Summary of the processes for the production of BTX

A summary of the processes discussed in Section 1.2.1 and 1.2.2 are shown in Table 1-2.

Table 1-2 Summary of the processes available for BTX production

Process	Catalyst	Feed	Operating temperature	Operating pressure
Reforming	$Pt\text{-}Re/Al_2O_3$	$C_7\text{-}C_{11}$	490°C	10-20 bar
Aromax	Pt/BaKL	$C_6\text{-}C_7$	450°C	2-7 bar
STAR	$Pt\text{-}Sn/ZnAl_2O_4$	$C_6\text{-}C_8$		
Selectoforming	Erionite	$n\text{-}C_6+$		
M2-Forming	H-ZSM-5	$C_3\text{-}C_4$	538°C	1-20 bar
Cyclar	Ga/H-ZSM-5	$C_3\text{-}C_4$	500°C	1 bar
Pyroforming		$C_2\text{-}C_3$		
Z-Forming	ZSM-5	$C_3\text{-}C_8$	>500°C	
Aroforming	Ga/H-ZSM-5	$C_5\text{-}C_6$		
Topas	Zeolite	$C_3\text{-}C_4$	500°C	10 bar

1.2.4 Research challenges in LPG and LN aromatization

In principle LPG aromatization is a bifunctional catalytic process that reqires both dehydrogenation and acidic sites, while LN aromatization is ideally a monofunctional catalytic process that involves only dehydrocyclization. In LPG aromatization C-H bonds must be activated and C-C bonds constructed. In LN aromatization C-H bonds must also be activated, but, other than in cyclization, C-C bonds must be neither created or broken. Coke formation is also a problem when zeolite catalysts are used, although medium pore size zeolites, *e.g.* MFI (ZSM-5), reduce coke formation by steric restriction of the coke transition states[19].

Hence basic research in the area of LPG and LN aromatization faces a variety of challenges:

- The addition and preservation of the hydrogen-transfer-dehydrogenation functions in modified zeolite catalysts.
- The optimization of catalyst formulations to reduce coke deposits.
- The regeneration of coked or deactivated catalysts without irreversible changes in their structural or chemical properties.

1.3. Aromatization of Hexane

1.3.1 Thermodynamic considerations for hexane aromatization

The aromatization of hexane is endothermic (the standard enthalpy of reaction for the conversion of n-hexane to benzene at 298K is 249.9 kJ/mol). Thus high reaction temperatures are required to achieve practical levels of conversion. In principle several cyclization products can be obtained, including methylcyclopentane (MCP), cyclohexane and benzene as well as various isomerization products (methylpentanes). Under conditions of temperature of 783K (510°C), hydrogen pressure of 20 bar and hydrogen/hydrocarbon ratio of 4 the following thermodynamic equilibrium results are obtained[20]:

- Dehydrogenation of n-hexane (to hexenes) is negligible (<0.3%)
- Hexane isomerization is extensive, leading to a predicted equilibrium composition of 25% n-hexane, 28% 2-methylpentane, 18% 3-methylpentane, 18% 2,2-dimethylbutane and 10% 2,3-dimethylbutane.
- n-Hexane is relatively stable with respect to the formation of naphthenes (*ca.* 5% MCP and *ca.* 1% cyclohexane).
- High pressure strongly limits the formation of benzene (100% benzene at 1 bar and 45% benzene at 50 bar).

Equilibrium ratios of several reversible reactions that occur in the aromatization of n-hexane have been calculated (Tamm *et al.*, 1988)[21] at 738K (465°C), 6.5 bar hydrogen partial pressure and a hydrogen/hydrocarbon ratio of 6:

1-hexane	⇄	benzene	$k^1/k^{-1} = 5$
MCP	⇄	n-hexane	$k^2/k^{-2} = 7$
MCP	⇄	3-methylpentane	$k^3/k^{-3} = 5$
MCP	⇄	2-methylpentane	$k^4/k^{-4} = 10$

Implicit in these calculations was the assumption that the cracking rate constants are small. This was shown to be a valid assumption for the reaction of n-alkanes over Pt/KL[21].

Thermodynamic equilibrium calculations were also made using Hysim[22] (Section A.1.6.2) and these show that the ratio of 2-methylpentane to 3-methylpentane is not affected by change in the hydrogen partial pressure. Also, as expected, increasing the hydrogen partial pressure results in less MCP relative to methylpentanes. At lower hydrogen partial pressures (1 bar), benzene is the major product. Formation of benzene is of course inhibited by increase in hydrogen partial pressure. Increase in reaction temperature is also favourable to the formation of benzene. The spontaneous formation of benzene from n-hexane and 1-hexene becomes feasible (Gibbs free energy of reaction, ΔG_r, becomes negative) at temperatures above 350°C and 175°C respectively.

The maximum achievable aromatics yield will be adversely affected by competing isomerization reactions and thus efficient aromatization catalysts must minimize n-hexane isomerization.

1.3.2. Catalysts for hexane aromatization

1.3.2.1 Zeolite catalysts

Bernard[23] (1980) and Besoukhanova[24] *et al.* (1981) reported that platinum containing (0.6wt%) potassium-exchanged neutral zeolite L, Pt/KL, had a remarkable selectivity for the dehydrocyclization of n-hexane to benzene when

compared to zeolites X, Y, Omega and mordenite (The selectivity was *ca.* 80% at 59% conversion of n-hexane). The system behaves as a monofunctional catalyst with the metal solely responsible for the activity. These results were rationalized in various ways[24]:

- Unidentified pore size effects
- Possible interactions between alkaline cations and platinum leading to changes in the electronic structure or morphology of the platinum particles.

Modification of the electronic state of the metal particles has been proposed but is not conclusive[25,26]. However, infrared data for adsorbed carbon monoxide suggests an effect attributable to nearby cations when carbon monoxide adsorption occurs on the metal[27]. Platinum containing zeolites of the mordenite and LTL types, modified by alkaline soaking and halocarbon treatment have been shown to increase the aromatics yield from 81% to *ca.* 90% at nearly complete conversion of n-hexane[28]. The preferred halocarbon is CF_3Cl. The halocarbon treatment does not noticeably change the framework aluminum content but rather replaces terminal hydroxyl groups with halogen atoms, including hydroxyl groups from silanol nests. The platinum particles become more electron rich following halocarbon treatment.

Catalysts based on zeolite ZSM-5 (MFI) containing gallium or tellurium modifiers have also been investigated[29,30,31]. However these catalysts do not give the high selectivity to aromatics when compared to platinum/zeolite L catalysts.

1.3.2.2 Nonzeolite catalysts

High aromatization activities and selectivities have been observed for platinum supported on the following nonzeolitic catalysts:

- Carbon, with additional promotion by alkaline earths[32].
- Silica[33]
- Aluminum-modified magnesia[34,35,36]
- Layered silicalite[37]

In addition, high aromatic selectivities were observed for palladium supported on aluminum modified magnesia[34]. A comparison of the effect of different supports for platinum and palladium[34] are shown in Figure 1-2. Two different kinds of platinum particles exist on the surface of aluminum-modified magnesia. One type exhibits normal behaviour to the adsorption of carbon monoxide and probably corresponds to platinum with low dispersion. The second type probably corresponds to small platinum clusters and has unusual properties similar to those of platinum in platinum-loaded alkaline and alkaline-earth forms of zeolites. Infrared spectroscopy of adsorbed carbon monoxide indicates there could be excess negative charge on the platinum in the latter case[38,39].

Catalysts consisting of platinum on alumina-stabilized magnesia have activities and selectivities for the aromatization of n-hexane similar to those of zeolite catalysts[34]. Plots of selectivity to aromatics as a function of n-hexane conversion are similar for platinum on alumina stabilized magnesia, Pt/Mg(Al)O, and for Pt/Zeolite L. These catalysts differ in the nature of the support as well as the size of the platinum particles which have a slightly larger size distribution for Pt/Mg(Al)O of *ca.* 2 nm than for Pt/Zeolite L which has a platinum size average of *ca.* 1 nm[34]. The data analysis appears to be independent of metal loading, metal dispersion and the nature of the support. The nature of the support has negligible effect provided it is not acidic.

Very high aromatics selectivity for catalysts consisting of palladium on stabilized magnesia has been observed by Derouane *et al.* (1993)[34] (Figure 1-2) and is of

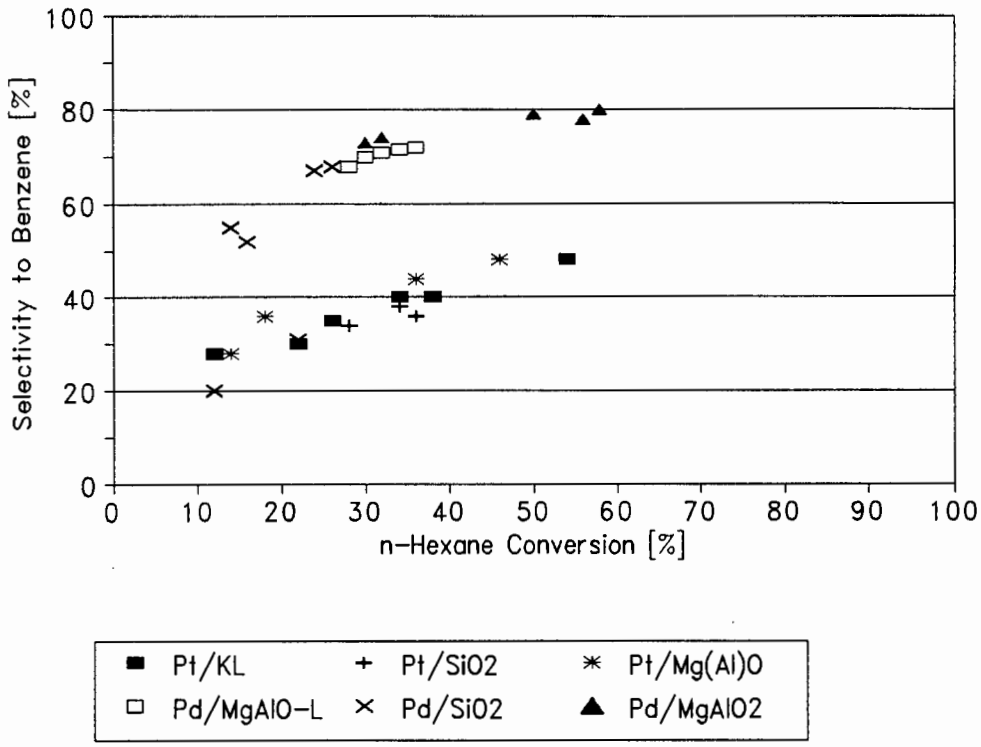

Figure 1-2 Selectivity to aromatics at 477°C, 1 bar and a hydrogen/hydrocarbon molar ratio of 6 for platinum and palladium catalysts (Derouane E.G. *et al.*, 1993)

interest from practical and fundamental viewpoints. The high aromatics selectivity seems to be a result of the suppression of isomerization reactions. Thus supported palladium catalysts, dispersed on non-acidic supports, have much higher aromatization selectivities, than supported platinum catalysts, at similar n-hexane conversions, due to decreased isomerization of n-hexane. The reason for the large difference between platinum and palladium catalysts remains unclear, however, ^{13}C MAS NMR results indicate unambiguously that:

- Pt/KL and Pt/MgO show an identical aromatics selectivity versus conversion relationship. However, the reaction pathways are not identical at the molecular level. Conversion pathways involving cyclic species (MCP) are more prevalent on the zeolite supported catalysts for both platinum and palladium[40].

- Methylcyclopentane (MCP) plays a central role in n-hexane conversion on palladium supported catalysts. MCP can be formed from n-hexane, but it is more readily converted into the methylpentane isomers on palladium than on platinum. In contrast to Pt/KL, MCP can undergo 1,6 ring enlargement to yield benzene on supported palladium catalysts. Hydrogenolysis of the methyl group of MCP (demethylation) explains why more methane is produced with palladium based catalysts[41].

A schematic diagram of the reaction pathways involved in aromatization of n-hexane for platinum and palladium catalysts is shown in Figure 1-3.

1.3.2.3 Mechanisms for n-hexane aromatization on supported Pt and Pd catalysts

The acid-catalyzed cyclization of n-hexane (to cyclohexane) is not favoured because it requires a primary carbenium ion. Acid catalyzed isomerization produces iso-hexanes, with MCP (formed by a more favoured secondary carbenium ion) as an intermediate[42]. These iso-alkanes are more difficult to cyclize than n-alkanes. In addition acid-catalyzed polymerization and cracking deactivate the catalyst and result in lower aromatics yield. It is thus apparent that acidity should be avoided in hexane aromatization catalysts.

A comprehensive scheme for the conversion of n-hexane on monofunctional nonacidic metal catalysts is shown in Figure 1-3 and Figure 1-15. n-Hexane can isomerize to the methylpentanes by either a cyclic mechanism, with MCP as an intermediate, or by a carbon-bond shift mechanism. Cracked products (C_1-C_5) are obtained by hydrogenolysis of n-hexane and its isomers. Demethylation of MCP occurs only on supported palladium catalysts. Aromatization can occur by dehydrogenation of n-hexane to monoalkenes, dialkenes or acetylenic compounds that then cyclize to form benzene. Aromatization may also occur by direct ring closure of n-hexane to form cyclohexane which can then undergo dehydrogenation

to benzene. On supported palladium catalysts MCP can undergo dehydrogenation to methylcyclopentene followed by ring enlargement to yield benzene.

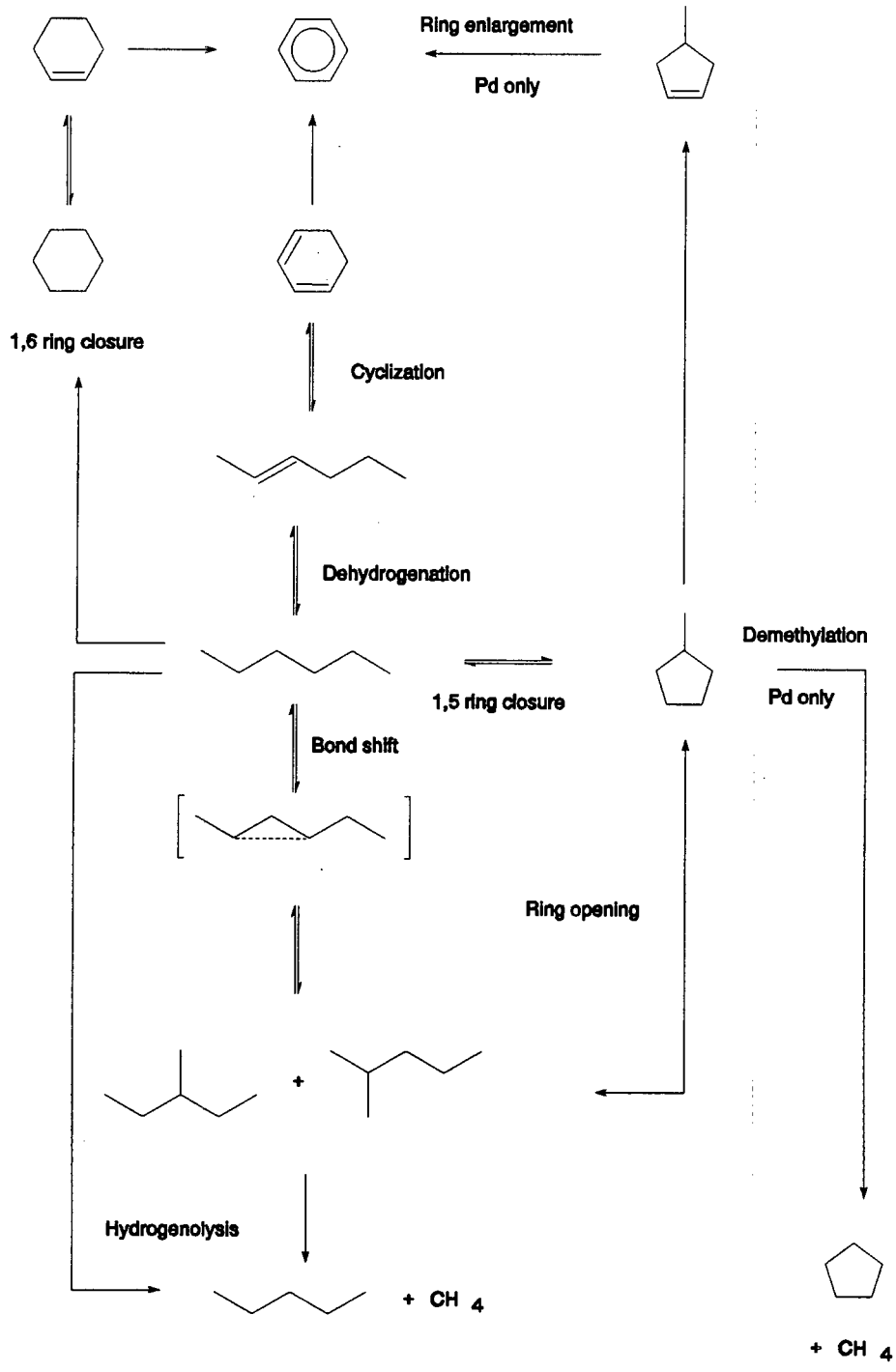

Figure 1-3 Schematic diagram of the reaction pathways for n-hexane aromatization over supported platinum and palladium catalysts (Germain 1969)

1.3.3 Platinum/KL as an aromatization catalyst

In view of the discussion in Section 1.3.2, it can be seen that Pt/KL is a well researched catalyst for the aromatization of n-hexane and n-heptane. A summary of the properties of Pt/KL as an aromatization catalyst is discussed below.

The relative aromatization rate decreases with increase in hydrocarbon chain length possibly due to diffusional constraints in the zeolite pores or some steric hinderance in the zeolite L cages[55]. Experimental observations for n-hexane aromatization support a metal catalyzed mechanism that involves direct 1,6-ring closure and dehydrogenation to benzene. The confinement model developed to rationalize this involves the formation of a metallocycle or ring intermediate followed by classical metal-catalyzed dehydrogenation chemistry[43]. A role for the zeolite cage or channel structure cannot be excluded in the Pt/KL catalyst, but appears unlikely due to the similar activities and selectivities observed on both zeolitic and non-zeolitic supports[34]. Other possibilities are listed below:

- The zeolite channels collimate the flux of n-hexane molecules for end-on adsorption at the platinum surface (Tauster and Steger, 1988)[44].

- Single file diffusion resulting from partial plugging of the zeolite L channels could affect the product distribution (Karpinski *et al.*, 1993)[45].

- The zeolite channels inhibit reactions that lead to the formation of coke and catalyst deactivation (Iglesia and Baumgartner, 1993)[46].

Thus, several probably co-existing mechanisms have been proposed for n-hexane conversion on monofunctional metal catalysts and are discussed in more detail in Section 1.8.

1.4 Properties of Zeolite L

1.4.1. Basic description

The basic structure of zeolite L was determined in 1969 from powder X-ray diffraction of the sodium and potassium form of the zeolite[47]. The IUPAC nomenclature is LTL (Linde type L). The LTL structure is based on polyhedra cages formed by five six-member and six four-member rings, similar to that found in erionite, cancrinite and offretite. This arrangement results in the formation of a unidimensional channel system. In the hydrated form of zeolite L, the structure has four cation positions. Only the cations positioned within the 12 member ring channel will readily exchange[48]. The other three cations are located outside the main channels and occupy sites in close proximity to the framework oxygen atoms. The preferred Si/Al ratio is 3.0 with ordering of Si and Al. Upon dehydration the cations sited at the walls of 12-member ring channels migrate into the six member rings[49].

Table 1-3 Structural parameters of zeolite L (LTL)

Chemical composition	$K_9[((AlO_2)_9(SiO_2)_{27}].22H_2O$ $K_6Na_3[Al_9Si_{27}O_{72}].21H_2O$
Symmetry	hexagonal
Space group	P6/mmm
Unit cell constants (Å)	a = 18.4 Å c = 7.5 Å
Framework density	1.61 g/cm^3 16.4 T/1000Å^3
Void fraction (determined from water content)	0.32
Pore structure	unidimensional 12-member rings (7.4Å)
Secondary building units	single 6-rings

The pores of zeolite L are unidimensional and consist of ellipsoidal polyhedra cages of internal free dimensions of 4.8Å x 12.3Å x 10.7Å connected via 12-membered

oxygen ring windows of 7.4Å free opening[50,40]. This is illustrated schematically in Figure 1-4.

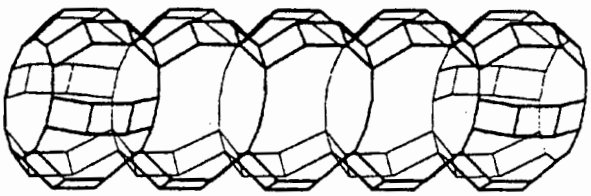

Figure 1-4 Schematic diagram of the unidimensional pore system of zeolite LTL

When fully hydrated, zeolite L has four cation positions, labelled A to D in Figure 1-5 in the projected view. During dehydration, the cations from site D withdraw from the channel walls to a fifth site E, located between the A sites. This also occurs during calcination at high temperatures of *ca*. 600°C, leaving the zeolite pores free of cations that could hinder molecular diffusion[40]. In site D, the cations are co-ordinated with two water molecules in the channels. Cations at site D are most readily exchanged. It has been observed that for barium exchanged zeolite L, the barium can be transferred from the C and D sites to the A and B sites by calcination at temperatures between 590°C and 650°C[51].

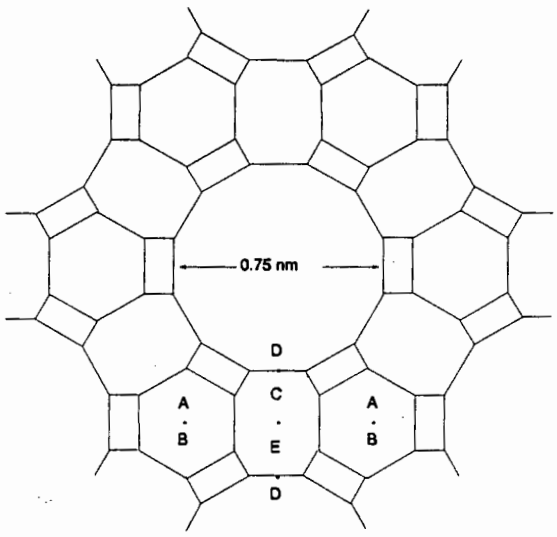

Figure 1-5 Schematic diagram of the channel system of zeolite L.

1.4.2 Synthesis of zeolite L

Zeolite L was first prepared from a batch composition containing a mixture of potassium and sodium oxides. The ratio of $K_2O/(K_2O + Na_2O)$ ranges from 0.33 to 1.0 and the $(K_2O + Na_2O)/SiO_2$ is between 0.35 and 0.5. The SiO_2/Al_2O_3 ratio falls between 10 and 28 and water to alkali oxide ratio ranges from 15 to 41. Crystallization takes place at 100°C after 64 hours[48].

1.4.3 Infrared spectrum

The mid infrared spectrum[48] for Linde type L is shown below in Figure 1-6. The zeolite exhibits strong infrared absorption at 1105, 608 and 438 cm^{-1}.

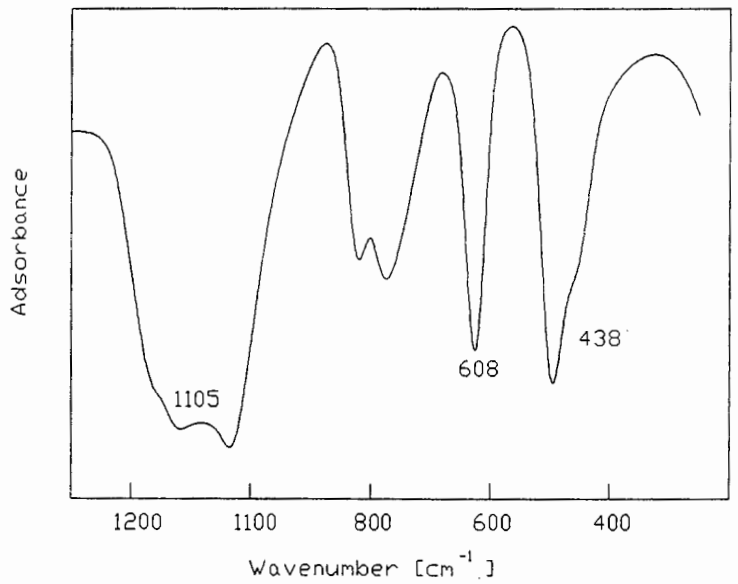

Figure 1-6 Mid-infrared spectrum of zeolite L (Szostak R., 1992).

1.4.4 X-ray diffraction spectrum

The simulated (von Ballmoos and Higgins, 1990)[52] and experimental (Szostak, 1992)[48] X-ray diffraction data of zeolite L is shown in Table 1-4. There is good correspondence between the relative intensities.

Table 1-4 X-ray powder diffraction data

d [Å]	2Θ	I/I_o	I/I_o
		(Szostak, 1992)	(von Ballmoos and Higgins, 1990)
15.80	5.4	100	100
5.98	14.6	25	22
4.57	19.3	32	25
3.91	22.7	30	28
3.48	25.6	23	15
3.17	28.0	34	29
3.07	29.1	22	22
2.91	30.7	23	36
2.65	33.8	19	16
2.42	36.9	11	8
2.19	41.0	11	2

1.5 Synthesis of Platinum/L Zeolite catalysts

1.5.1 Comparison between impregnation and ion exchange[53]

The properties of Pt/KL catalysts prepared by ion-exchange (IE), incipient wetness impregnation (IWI) and co-impregnation with KCl (IWI+KCl) were compared (Ostgard *et al.*, 1992). TPR shows significant differences between IE and IWI catalysts. After calcination (in oxygen) at temperatures up to 400°C the IWI samples contain Pt^{+4} ions that are reduced at 250°C, but the IE catalysts contain PtO particles that are reduced at 11°C as well as two Pt^{+2} species. After reduction, the IWI catalysts contain smaller platinum particles located inside the zeolite channels, while IE catalysts have larger platinum particles some of which are located on the external surface. At high temperatures KCl reacts with the zeolite to form HCl which escapes. The IWI catalysts are less acidic, less active for n-hexane conversion, more selective for dehydrocyclization, but less selective for hydrogenolysis and they deactivate less.

Table 1-5 Comparison of Pt/KL catalysts synthesized by ion-exchange and impregnation (Ostgard *et al.*, 1992)

Product selectivity	Pt/KL (IE)	Pt/KL (IWI)	Pt/KL (IWI+KCl)
C_1-C_5	46.7	20.2	10.7
2m-C_5	13.3	13.2	13.7
3m-C_5	7.8	9.3	10.7
MCP	17.1	23.8	31.1
Benzene	15.0	33.4	33.7
n-C_6 conversion	20	15	12

350°C, 0.5 wt% platinum

Hydrogenolysis requires large platinum ensembles and hence the small platinum particles in the IWI catalysts produce less C_1-C_5 compounds and less coke[53]. These catalysts are also less acidic than catalysts prepared by ion-exchange, which may

also account for the lower selectivity to cracked products. In the IE catalysts $Pt(NH_3)_4^{2+}$ ions are exchanged for K^+ ions.

$$Pt(NH_3)_4^{2+}{}_{(aq)} + 2Cl^-_{(aq)} + 2K^+_{(zeol)} \rightarrow [Pt(NH_3)_4]^{2+}{}_{(zeol)} + 2Cl^-_{(aq)} + 2K^+_{(aq)}$$

The K^+ and Cl^- ions are removed by washing while in the IWI technique these ions remain in the zeolite. After destruction of the NH_3 ligands in the calcination step, Pt^{+2} ions coordinated to zeolite walls should be produced in the IE procedure while some unknown distribution of Pt^{2+} and $PtCl_2$ particles located in the zeolite channels will result after drying in the IWI preparation. In addition some reduction of Pt^{+2} or $PtCl_2$ can occur by the action of decomposing NH_3. As a result of this autoreduction, platinum particles will be formed which are oxidized to PtO or PtO_2 during further calcination in air. The calcination step is followed by hydrogen reduction and protons of considerable Bronsted acidity will be formed from Pt^{+2} ions[11, 53].

$$Pt^{+2} + H_2 \rightarrow Pt^0 + 2H^+$$

However, HCl and water are a co-products of the reduction of $PtCl_2$ and platinum oxides respectively. The addition of KCl to the impregnation solution should further ensure that no Bronsted protons are formed as surface protons will react at elevated temperature with KCl. The HCl formed will be driven off at the temperature of reduction (350°C)[11, 53].

$$H^+_{zeol} + KCl \rightarrow K^+_{zeol} + HCl$$

1.5.2 Platinum dispersion

Effects of the temperature and time of reduction in hydrogen on the apparent dispersion of platinum[55] in 0.8Pt/BaKL are shown in Figure 1-7. The sizes of approximately spherical platinum particles is also shown, based on the assumption

that the average platinum particle diameter is related to the ratio of surface to total platinum atoms by the equation suggested by Anderson (1975)[54]. The maximum concentration of surface platinum atoms accessible to CO molecules is reached after reduction at *ca.* 590K (317°C). The accessible platinum surface decreases appreciably after reduction at higher temperatures.

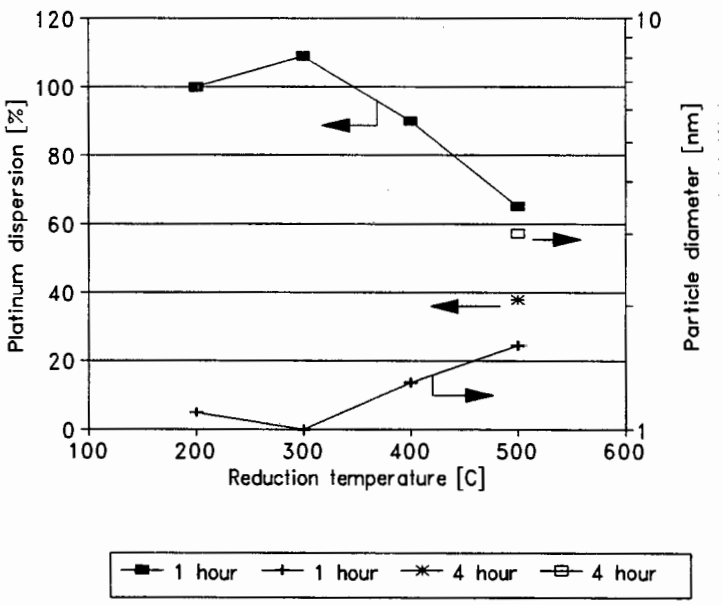

Figure 1-7 Effects of reduction temperature and time on platinum dispersion in 0.8Pt/BaKL (Hughes *et al.*, 1987)

Transmission electron micrographs (TEM) of Pt/BaKL reduced at 755K (482°C) show that the largest platinum particles are *ca.* 0.8-1 nm in diameter[55]. The particles are presumed to be non-spherical in shape and are thus small enough to fit within the large intracrystalline zeolite channels (0.75nm) and appear to be inside the zeolite crystals[55]. The platinum particle sizes determined by TEM are considerably smaller than the average size estimated by CO chemisorption. The principal cause of this discrepancy may be restricted access of CO molecules to surface platinum atoms. As the metal clusters grow the spaces between the surfaces of the platinum particles and the zeolite channel walls become smaller than the CO molecule and hence some surface platinum atoms cannot chemisorb

CO. Thus the decrease in CO chemisorption with increasing reduction temperature and time exaggerates the extent of platinum particle growth[55].

1.5.3 Effect of alkali cations and basicity

Platinum was deposited on a series of BaL zeolites containing different alkali cations (Li to Cs) by Hicks *et al.* (1993)[56]. The specific activity of Pt/BaL for heptane reforming was sensitive to the type of the alkali cation and the turnover frequency for formation of C_1 to C_6 hydrocarbons, benzene and toluene increased with increasing molecular mass of the alkali cation[56]. An increase in selectivity to benzene for n-hexane aromatization was shown by Besoukhanova *et al.* (1981)[57] and the results are tabulated in Table 1-6. They suggested that the properties of platinum particles are strongly dependent on the surrounding zeolite structure and field, which is altered as result of different cations.

Table 1-6 Effect of the exchanging cation on platinum impregnated zeolite L catalysts (Hicks *et al.*, 1993)

Selectivity	Li	Na	K	Rb	Cs
C_1-C_5	13.2	4.6	2.6	2.2	2.2
i-C_6	10.2	6.3	5.2	4.8	4.9
MCP	33.7	19.9	12.8	7.4	7.6
Benzene	42.4	69.4	79.0	88.2	85.2
n-C_6 conversion	20.5	34.7	50.0	73.1	70.8

460°C, 0.6 wt% platinum

However, Mielczarski *et al.* (1992)[186] has pointed out that the selectivity to benzene was compared at different levels of conversion, thereby complicating the interpretation of the results. However, they also noted that the trends observed in Table 1-6 closely resembled their results, except for the sample containing lithium. The low selectivity to benzene associated with a Pt/LiL catalysts may be due to the

presence of acid sites generated by lithium incorporation[58]. They further point out that the results of Besoukhanova *et al.* (1981)[57] are consistent with the observation that changing the alkali cation of non-acidic Pt/KL has little or no effect on the selectivity to benzene during n-hexane aromatization (at the same conversion of n-hexane).

Metal-support interactions have been observed in the Pt/L system by comparing the ratio of toluene and benzene adsorption equilibrium constants, $K_{T/B}$, for samples containing different alkaline earth cations[187]. A decrease of $K_{T/B}$ with incorporation of heavy alkaline earth cations into the zeolite indicates platinum clusters become more electron rich, which is consistent with the idea of negative charge transfer from the zeolite to the cluster. An influence of zeolite basicity on the electronic structure of supported platinum clusters has been reported to explain the interaction of adsorbed CO with Pt/L, as detected by infrared spectroscopy[187]. This may indicate that platinum clusters inside the channels of zeolite L are more electron rich than for other supports.

Recently it was shown by Fukanaga and Ponec (1995)[93] that potassium cations increase the aromatization activity of Pt/SiO_2. It was assumed that K^+ promoted catalysts were electron rich relative to unpromoted catalysts and are thus less sulphur tolerant for the aromatization reaction (n-hexane to benzene). But, they also observed that K^+ containing catalysts were less senstive to sulphur for dehydrogenation reactions (cyclohexane to benzene). This would not be expected if the electron structure changes in platinum (platinum becoming more electron rich) due to K^+ were the only reason for the changes in catalytic behaviour. Thus it was concluded[93] that the extraordinary properties of the Pt/KL catalyst should not be based on the assumed changes in the electron structure of platinum by potassium cations. The decrease, by sulphur, of the amount of surface adsorbing CO is smaller in the presence of K^+ than in the absence of K^+. This indicates that a part of the sulphur was bound somewhere other than the platinum particles, namely to potassium.

1.6 Reaction Kinetics on Platinum/KL

1.6.1 Dependence on hydrogen partial pressure

1.6.1.1 Low pressure

The rate of reaction for n-heptane aromatization was shown by Kooh *et al.* (1993)[59] to decline sharply over the first 10 hours (50% reduction) at a hydrogen partial pressure of 0.95 atm and 6.7 atm helium. This decline was as a result of coke formation. A best fit to the power law dependence of rate on time is shown in Figure 1-8. The equation for the line was:

$$r = 0.017 \times t^{-0.22} \quad (\text{mol } C_7/h.g)$$

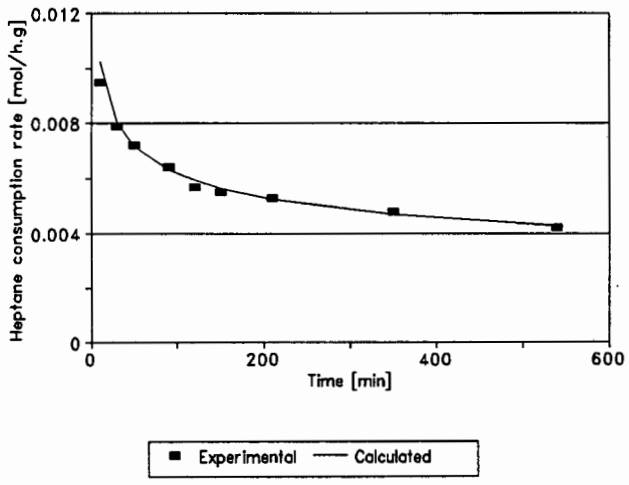

Figure 1-8 Dependence of heptane consumption rate on time over Pt/KBaL (Kooh *et al.*, 1993)

The preference for terminal cracking was evaluated by comparing the hexane selectivity relative to C_5 and C_4 hydrocarbons. The terminal cracking index (TCI) for n-hexane and n-heptane feedstocks is defined as follows:

$$TCI\ (n\text{-}C_6) = C_5/C_4$$

$$TCI\ (n\text{-}C_7) = C_6/(C_5 + C_4)$$

The TCI decreased slightly from 1.4 to 1.2 after 10 hours time on stream (t.o.s). Activation energies and reaction orders for heptane conversion for the main products at low hydrogen partial pressure (< 2.0 atm) are shown in Table 1-7. The kinetic parameters were obtained by varying the conditions from 425°C to 475°C, 0.05 atm to 0.4 atm heptane, 0.2 atm to 2.0 atm hydrogen partial pressure and 3 atm to 10 atm total pressure. The rates of hydrogenolysis, isomerization and dehydrocyclization exhibit positive, fractional order dependencies on heptane and hydrogen pressures[59].

Table 1-7 Kinetic constants for heptane reforming over Pt/KBaL at low hydrogen pressure (Kooh *et al.*, 1993)

Product	Activation energy	Reaction orders in terms of:		
	[kJ/mol]	Heptane	Hydrogen	Total pressure[a]
C_1 and C_2	230	0.5	0.2	0.7
ECP[b]	0	0.7	0.8	1.3
Benzene (B)	155	0.0	0.3	0.4
Toluene (T)	113	0.3	0.6	0.6

(a) For $H_2/C_7 = 6.0$
(b) ethylcyclopentane

Plotting selectivities as a function of conversion was suggested as a way of distinguishing between primary and secondary products[60]. If the selectivity of the given product approaches zero when conversion approaches zero, it is most likely not a primary product. A primary product should show a finite selectivity at conversions near zero. This method was applied for testing skeletal reactions of n-hexane over platinum/alumina at 500°C. On a non-acidic catalyst, Pt-Sn/Al_2O_3, treated with lithium, aromatization occured by series reactions, with increasing alkene selectivity at low conversions[61] and low hydrogen partial pressure (8 kPa).

All other products have negligible selectivities, the value of which was taken as zero by extrapolation to zero conversion. Thus the alkenes are primary products. At a higher partial pressure of hydrogen (32 kPa) all C_6 reaction pathways result in a finite ordinate intercept for the products at zero conversion. The ratio of 2-methylpentane:3-methylpentane is *ca.* 2 in all cases, as expected statisically from the ring opening of MCP by cyclic mechanisms. A predominance of 2-methylpentane is regarded as evidence of a prevailing bond shift reaction[62] (See Section 1.8.1.2).

1.6.1.2 High hydrogen pressure

When the hydrogen pressure was increased to 12 atm, the Pt/BaKL catalyst no longer deactivated during n-heptane aromatization[59]. In contrast to operation at lower hydrogen pressure, the reaction rate increased by about 50% over the first 30 minutes of the run and remained constant thereafter. No benzene or alkenes were formed under these conditions. The selectivity to toluene was 15% at 12 atm and 43% at 0.95 atm of hydrogen. The rates of hydrogenolysis and isomerization increased relative to the rate of dehydrocyclization (to toluene). In agreement the TCI was 0.61, which was lower than the TCI value of 1.3 observed at low hydrogen pressure. The apparent activation energies and reaction orders measured for n-heptane conversion at high pressure are shown in Table 1-8.

Table 1-8 Kinetic constants for heptane hydrogenolysis, isomerization and dehydrocyclization over Pt/BaKL at high hydrogen pressure (Kooh *et al.*, 1993)

Reaction	Activation energy	Reaction orders in	
	[kJ/mol]	heptane	hydrogen
hydrogenolysis	163	0.7	-1.9
isomerization	251	0.6	-2.8
dehydrocyclization	243	0.4	-2.7

Error in activation energy ± 20%

At high pressure the rates of hydrogenolysis, isomerization and dehydrocyclization exhibit positive, fractional order dependencies on the heptane pressure and large, negative order dependencies on the hydrogen pressure. At high hydrogen pressure the activation energy for hydrogenolysis is lower than that for isomerization and dehydrocyclization. These results may be contrasted to those obtained at low hydrogen pressure. Below 6 atm of hydrogen the reaction rates are less sensitive to the hydrogen pressure, whereas above this pressure the rates decrease rapidly with pressure. The change in product selectivities at low and high partial pressures of hydrogen are shown Table 1-9.

Table 1-9 Comparison of product selectivities and n-heptane conversion at low and high hydrogen pressure at 450°C (Kooh *et al.*, 1993)

Product selectivity	0.95 atm hydrogen	12 atm hydrogen
C_1-C_5	14.8	31.4
C_6	4.8	10.0
i-C_7	2.1	16.4
ECP[a]	11.6	27.1
alkenes	11.7	0
benzene	11.8	0
toluene	42.8	15.0
ΣSelectivities	99.6	99.9

(a) ethylcyclopentane

The effect of hydrogen on the rate of heptane reforming over Pt/KBaL is similar to that observed for hydrocarbon reforming over platinum on alumina[63] where the rate of heptane dehydrocyclization over Pt/Al_2O_3 increases with hydrogen partial pressure from 0 atm to 6 atm and then falls as the hydrogen partial pressure increases further. This was attributed to the influence of coke formation on the catalyst activity. Below 6 atm hydrogen the platinum surface is covered with carbon residues which block the reforming reaction. This carbon can be hydrogenated off the surface, freeing up sites for catalysis. Above 6 atm hydrogen the platinum surface is kept clear of carbon, but now hydrogenation of adsorbed

hydrocarbon intermediates limits the rate of reaction, *i.e.* the dehydrogenation rate is suppressed. This change is evident in Figure 1-9.

The deactivation of Pt/KBaL catalyst at low hydrogen pressure provides additional evidence that carbon accumulates on the platinum under these conditions. The activity of the catalyst falls at a rate proportional to the -0.22 power of time[59]. This power law dependence is the same observed by Pacheco and Petersen (1984)[64] for carbon fouling of Pt/Al_2O_3 during dehydrogenation of methylcyclopentane (MCP) where the activity decayed with -0.2 power of time.

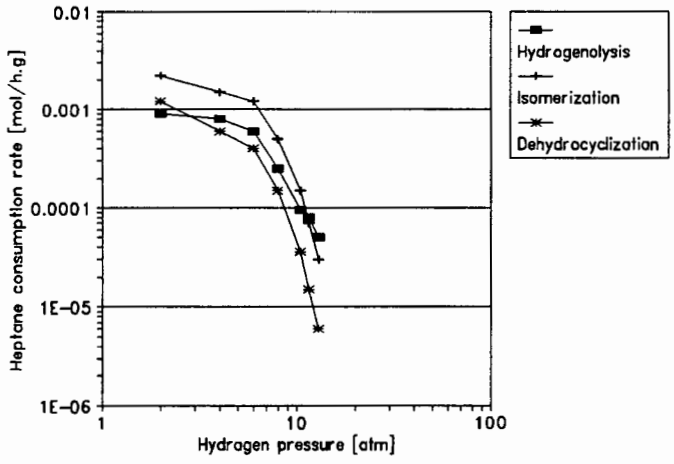

Figure 1-9 The effect of hydrogen partial pressure on rates of reaction (Kooh *et al.*, 1993)

The negative dependency of dehydrocyclization rates for n-hexane reforming on Pt/BaKL catalysts was also reported by Sharma *et al.* (1994)[65] The hydrogen orders for benzene and MCP production were -2.3 and -0.88 respectively. This behaviour is characteristic of dehydrogenation reactions where hydrogen pressure has an inhibiting effect on reaction rate. It was also noted that the hydrogen orders for alkane hydrogenolysis exhibit maxima as the hydrogen partial pressure is increased.

1.6.2 Isomerization Kinetics

The characteristic of alkane isomerization over platinum on acidic supports is that the dependence of the rate on hydrogen pressure is inverse to the dependence of rate on alkane pressure[66].

$$r = k([HC]/[H_2])^n \qquad \text{where HC = alkane}$$

The rate limiting step on these catalysts is proposed to be alkene isomerization on acid sites[67]. However, when alkane isomerization is catalyzed by platinum alone, such as on Pt/BaKL, the rate limiting step involves the reaction of a dehydrogenated hydrocarbon intermediate on the platinum surface. The formation of the intermediate is inhibited by hydrogen and yields a large, negative-order dependence on the hydrogen pressure. The similarity of the heptane and hydrogen dependencies for hydrogenolysis, isomerization and dehydrocyclization over Pt/BaKL (Table 1-8 and Figure 1-9) suggests these reactions have similar mechanisms. In each case the rate limiting step most likely involves the transformation of a dehydrogenated, adsorbed hydrocarbon species.

The isomerization of n-hexane over platinum can proceed by either a ring-opening or a bond shift-mechanism. The ring-opening pathway is dominant on clean platinum surfaces[65]. The ratio of the rates of formation of methylpentanes to MCP is equal to 0.88 for Pt/BaKL. For deactivated Pt/SiO_2, this ratio is 3.0 which may imply that contributions to the isomer product distribution by the bond shift mechanism may have become important. These results suggest that the ring opening mechanism may have a stricter site requirement and be more sensitive to surface carbonaceous material than is the bond-shift mechanism.

MCP conversion was studied on various faces of platinum crystals by Zaera *et al.* (1986)[68]. The main products were methylpentanes, with smaller amounts of n-hexane, methane and cyclopentane. A negative order on hydrogen partial pressure was observed for methylpentane formation. The activation energies for

MCP conversion over Pt(111) and Pt(100) crystal faces of platinum is shown in Table 1-10. Even with the 20% error inherent in these activation energies it appears that the P(111) face is more reactive for methylpentane formation, but less reactive for methane formation.

Table 1-10 Activation energies (kJ/mol) for MCP conversion over Pt single crystal surfaces (Zaera *et al.*, 1986)

	methylpentanes	cyclopentane	methane	$< C_6$	benzene
Pt(111)	38	79	75	104	>125
Pt(100)	46	-	58	108	

Error in activation energies ± 20%

The selectivity ratios of 2-methylpentane:3-methylpentane was reported to increase with platinum dispersion and the ratio is approximately 2.2 at a platinum dispersion of 100% by Moretti and Sachtler (1989)[69]. The ratio decreases with decreasing platinum metal dispersion to a value of 1.8, corresponding to a platinum dispersion of 65%. According to Moretti and Sachtler (1989) a ratio of 1.8 is significantly lower than the statistical value of two. This result can be rationalized in geometric terms as the MCP molecule has a length to width ratio of about 1.7. Ring opening can only occur when the impinging molecule is orientated toward the metal with its flat bottom end[69]. The preferred products thus becomes 3-methylpentane. Hence, the decreasing ratio of 2-methylpentane:3-methylpentane with decreasing dispersion is in agreement with this model. MCP ring opening is strongly suppressed in the presence of cyclohexene or cyclohexane in the gas feed. These molecules are rapidly dehydrogenated to benzene and hence probably preferentially displace MCP from platinum particles.

In the study of hydrogen partial pressure on MCP ring opening on Pt/KL by Vaarkamp *et al.* (1995)[70] it was found that the ratio of 2-methylpentane:3-methylpentane decreased only slightly from 1.2 to 1.1 over a 10 fold hydrogen:MCP partial pressure. This is lower than the expected statisical value of

2. The thermodymanic value for the ratio is 1.6 and would be independent of hydrogen partial pressure. The selectivity to "total n-hexane" (n-hexane + benzene) was also constant over the same H_2:MCP partial pressure ratio range. The turnover frequency of MCP, however, exhibited a maximum at a H_2:MCP ratio of *ca.* 20 - 30. The rate of MCP ring opening is a function of the surface reaction rate and the surface concentration of hydrogen and MCP. Thus the optimal H_2:MCP ratio at which maximum activity is achieved is affected by the adsorption energies of hydrogen and MCP. The heat of adsorption of hydrogen on Pt/KL is *ca.* 10 kJ/mol higher than for Pt/SiO_2 or for acidic Pt/KL[71]. This is consistent with the lower H_2:MCP ratio at which maximum activity is obtained for the Pt/KL catalysts relative to Pt/SiO_2 and Pt/Al_2O_3. At low H_2:MCP partial pressure ratio the surface reaction is limited by the rate of hydrogen dissociation. At higher H_2/MCP ratio the surface is saturated with hydrogen and hence this decreases aromatics production. The decreased stability of the catalysts at low H_2:MCP ratio is due to the larger rate of coke deposition on hydrogen deficient platinum particles[70]. An alternate explanation is that the peak in the turnover frequency of MCP is the result of coke at low partial pressures of hydrogen and thermodynamics at high partial pressures of hydrogen. Pt/KL will exhibit a maximum in turnover frequency at a lower H_2:MCP ratio than for Pt/SiO_2 and Pt/Al_2O_3 due to decreased coke formation on Pt/KL. Pt/KL is less acidic than Pt/SiO_2 and Pt/Al_2O_3 and is hence expected to produce less coke.

1.6.3 Hydrogenolysis Kinetics

In a study of the comparative activities of Pt/BaKL and Pt/SiO_2 by Sharma *et al.* (1994)[65], it was shown that Pt/BaKL displayed a higher selectivity for terminal cracking than the Pt/SiO_2 catalyst for n-hexane aromatization. The TCI for n-hexane ($n\text{-}C_5/n\text{-}C_4$) was 1.2 for Pt/BaKL and 0.76 for Pt/SiO_2. At high conversions, increased contributions from secondary hydrogenolysis will tend to decrease the ratio. However, the TCI correlates well with aromatics selectivity, *i.e.* a high TCI is indicative of a high aromatics selectivity. This was also the case for Pt/BaKL and

Pt/SiO_2 where the Pt/BaKL was an order of magnitude more reactive for the formation of benzene than Pt/SiO_2.

On neutral supported platinum catalysts, the primary hydrogenolysis reactions of n-hexane produce $C_4 + C_2$ and C_5 and C_1 hydrocarbons. Lighter hydrocarbons C_1 - C_3 are produced mainly from secondary hydrogenolysis reactions[65]. Propane can, of course still be produced from the acid catalyzed conversion of n-hexane. The increased terminal cracking observed on Pt/L zeolite catalysts has been attributed to geometric effects imposed by the zeolite structure[72]. However, high terminal cracking is also observed on clean platinum surfaces on supports other than zeolite L. However, these catalysts are more sensitive to coke formation, which causes rapid deactivation.

The dehydrocyclization selectivity exhibited by Pt/BaKL is sensitive to the reaction conditions. The ratio of the rate of dehydrocyclization (r_d) to the rate of hydrogenolysis (r_h) is:

$$r_d/r_h = 1.2 \times 10^6 \, p(C_7)^{-0.3} \, p(H_2)^{-0.8} \exp(-19000/RT)$$

$p(C_7)$: heptane partial pressure
$p(H_2)$: hydrogen partial pressure
T : temperature [K]
R : gas constant = 8.314 [J/(K.mol)]

The ratio was found to be 0.36 at 430°C, 0.16 atm heptane and 12 atm hydrogen[59] with a toluene selectivity of 27%. At 500°C, 1 atm heptane and 6 atm hydrogen the ratio of the rates was 1.21 with a toluene selectivity of 55%.

Lane *et al.* (1991)[190] has shown that the hypothesis of terminal adsorption does not adequately explain the enhanced aromatic selectivity of the Pt/KL catalyst and does not provide a satisfactory basis for the rationalization of the increased reaction rate for Pt/KL. They proposed that the non-binding interactions of

n-hexane with the zeolite lead to adsorption of n-hexane as a pseudo-cycle. Based on molecular modelling calculations, the L zeolite pore size is optimum for preorganization of n-hexane as a six ring pseudo-cycle, which resembles the transition state in the formation of benzene[40]. This model is also proposed to be consistent with the increased activity of 1,5 ring closure in Pt/KL relative to Pt/KY as the rate of MCP formation is expected to increase when the adsorption of hexane leads to preorganization of a five ring pseudo-cycle. The smaller pore size of L zeolite more closely matches the steric requirements for a 1,5 ring closure transition state. The turnover frequency of MCP on Pt/KL is 3.3 times higher than for Pt/KY despite the lower 1,5 ring closure selectivity for Pt/KL.

1.6.4 Dehydrocyclization Kinetics

When n-hexane was fed over Pt/BaKL by Iglesia and Baumgartner (1993)[76], the ratio of the formation rates of benzene to MCP was 2.3, thus indicating that 1,6 ring closure is more active than 1,5 ring closure. However, on Pt/SiO_2 this ratio was 0.43 at steady state, indicating the opposite reactivity. The accumulation of carbonaceous species on the silica supported platinum catalysts appears to inhibit the 1,6 ring cyclization pathway more severely than the 1,5 cyclization pathway. The initial 1,6 ring closure activity on clean Pt/SiO_2 was as high as on Pt/BaKL and was greater than the initial 1,5 ring closure activity[76]. However, a selective decrease in 1,6 ring closure activity with time on stream was noted on Pt/SiO_2.

The apparent activation energies for 1,6 and 1,5 ring closure were determined by Lane *et al.* (1991)[190] for n-hexane aromatization over Pt/KL based on turnover frequency (moles product/s Pt surface sites). The space velocity was chosen such that the n-hexane conversions would be less than 15% at all temperatures. By using the assumption of differential conversion over this conversion range the rates of the back reactions could be neglected. The observed turnover frequencies (TOF) were fitted to an Arrhenius-type temperature dependence and the kinetic parameters obtained are shown in Table 1-11.

Table 1-11 Kinetic parameters for n-hexane on Pt/KL (Lane *et al.*, 1991)

Product	Activation energy [kJ/mol]	$\ln(k_o)^a$
Benzene	226	37
MCP	163	25

(a) k_o is the Arrhenius pre-exponential factor which includes any entropy effect in units of s^{-1}

The rate of 1,6 ring closure dominates at high temperature, whereas at low temperature the rate of 1,5 ring closure exceeds the rate of 1,6 ring closure. It was also shown that both the reaction pathway and activation energies of Pt/KL and Pt/KY are identical[190], but that the Pt/KL zeolite exhibits a much higher selectivity to benzene, especially at high n-hexane conversions, than Pt/KY. This effect was ascribed to either geometric effects or more likely to coke formation. Coke formation occurs more rapidly on Pt/KY and results in deactivation of the catalyst. This loss of active platinum sites by coke deposition results in lower activity and lower selectivity to benzene.

1.7 Deactivation of Platinum/KL Catalysts

Platinum/KL catalysts exhibit excellent stability, with regards to deactivation by coking, during aromatization reactions relative to other supported platinum catalysts. However, Pt/KL catalysts are extremely sensitive to the sulphur content in the feed. An uninterrupted one-year run was attained (with constant selectivity to aromatics and conversion of light naphtha) when the feed sulphur concentration was below 0.05 ppm (wt%)[55]. This sulphur level is much lower than that common in reforming with monometallic platinum catalysts or the bifunctional platinum-rhenium catalysts that have replaced monometallic catalysts in commercial reformers[55].

The uniqueness of the zeolite L support has been understood to derive from the ability of the L zeolite support to stabilize extremely small platinum particles in an non-acidic environment (Larsen and Haller, 1992)[25]. It was further proposed that further stabilization against deactivation, by geometric constraints of bimolecular coke precursor reactions, is what distinguishes these catalysts relative to SiO_2 supported small platinum particles[25]. Two opposing hypotheses have been developed to explain the resistance to deactivation by Pt/KL catalysts relative to other supported platinum catalysts. The initial proposal was that interaction of the platinum particles with the basic zeolite L walls caused the particles to be electron rich[165]. The alternative proposal was that was that the zeolite channels might orientate the reactant in such a way as to make 1,6-adsorption more probable[34]. Extensive experimental evidence was provided for the correlation of aromatization and terminal cracking on a large number of Pt/L zeolites of varying dispersion and cation exchange[72] and is is discussed in more detail in Section 1.5.1.2. This correlation has been confirmed by Mielczarski *et al.* (1992)[186]. However they also found that other platinum supported catalysts exhibited the same correlation. Thus the high aromatization selectivities are independent of the support, as long as it is non-acidic. Dehydrocyclization turnover rate and terminal hydrogenolysis selectivity are similar on Pt/KL and fresh Pt/SiO_2, but the rate and selectivity decrease rapidly on Pt/SiO_2 as it deactivates. Platinum particle size determination, by H_2

chemisorption and TEM, demonstrate that deactivation occurs as a result of coking of the platinum particles[76].

1.7.1 Deactivation by coke formation

Iglesia and Baumgartner (1993)[73] propose that inhibited deactivation is a protective effect of L zeolite channels and apparently reflects shape selective restriction on bimolecular transition states required in polymerization steps needed to form coke. The probability of bimolecular encounters is particularly low in one dimensional L zeolite channels[74]. Such bimolecular reactions to form deactivating coke would presumably involve alkene precursors. However, other possibilities that need to be considered are:

- Catalyst deactivation by polymerization reactions that lead to coke formation may occur primarily between gas phase precursors (between alkenes and/or aromatics) and condensed carbonaceous residues (Hughes R., 1984)[75].

- Unimolecular formation of carbon fragments may take place when the generation of hydrogenated species is experimentally kept to a minimum.

Neopentane is a valuable catalytic probe for purely metal catalyzed reactions, as it has a molecular inability to yield alkenyl products. Hydrogenolysis of neopentane (to methane and isobutane) is a strong function of L zeolite support acidity. The effect of zeolite acid/base properties on other different hydrocarbons was tested by 2-methyl-2-pentene isomerization in the absence of hydrogen. The deactivation results are correlated to the kinetically derived ratio of toluene to benzene (K_T/K_B) adsorption coefficients, which is known to be a very sensitive parameter of the electronic nature (support acidity) of small metal clusters[165].

According to Larsen and Haller (1993)[165], low temperatures, or high hydrogen pressure, inhibit rapid initial deactivation of platinum under aromatization conditions. Their results show that the unidimensional L zeolite framework does not inhibit coke formation in the general sense of shape selectivity. Rather the same interactions that stabilize the small size of platinum particles in L zeolite also stabilize these particles against unimolecular deactivation mechanisms that operate with non-acidic supports such as silica. The results observed may reflect only the metal deactivation and/or the initial deactivation step. The smaller platinum particles in acid-free L zeolite are less active but more stable with regard to coke formation than larger platinum particles[165].

Iglesia and Baumgartner (1992)[76] propose that inhibited deactivation of platinum clusters within zeolite channels accounts for the selective dehydrocyclization and terminal hydrogenolysis on Pt/KL. The zeolite channels inhibit bimolecular reactions leading to coke. Selective terminal adsorption and dehydrocyclization are intrinsic properties of clean platinum sites, with by may be inside or outside of the zeolite channels. Clean platinum sites survive only within the L-zeolite channels at reaction temperatures that favour dehydrocyclization thermodynamics. Inhibited deactivation reflects a protective effect of L-channels as well as stabilization against deactivation by platinum cluster interactions with alkaline cations. Platinum surface planes with hexagonal close-packed microfacets catalyze selective dehydrocyclization and terminal hydrogenolysis[76]. The data suggests that terminal adsorption does require collimation and that such a binding mode favours dehydrocyclization and that surface 1,6-ring closure steps are structure sensitive on platinum. This structural sensitivity leads to the observed selective inhibition of these pathways on platinum clusters poisoned by carbon deposits in mesoporous supports or by chemisorbed sulphur atoms within L-zeolite channels[76]. Electron micrographs of a Pt/L zeolite crystal clearly show multilayer carbon deposits form readily on platinum clusters outside the L-zeolite channels. The surface of extracrystalline platinum clusters (100Å in diameter) are totally covered with graphitic carbon, yet the sample retained 50% of its initial dehydrocyclization rate, suggesting that many intracrystalline platinum sites remain available for catalytic

dehydrocyclization reactions[76].

An increase in the platinum particle size distribution from sub 7Å clusters to 13Å clusters was observed with exposure to sulphur-free feed in an accelerated deactivation test. The platinum clusters grow along the channels forming elongated particles, which may facilitate the migration of platinum to the outside surface of the channels[91]. Thus platinum agglomeration, rather than coke formation (less than 2% of the mass of catalyst) is suggested as the cause of catalyst deactivation.

The dissociation of hydrocarbons on the surface of metal aggregates should result in the formation of Pt-C bonds. For the adsorbtion of n-butane on 1 nm platinum particles this has been suggested by RED (radial electron distribution) studies[77] and is consistent with change in platinum particle morphology. In the presence of higher partial pressures of hydrogen (H_2:n-C_4 > 1) this structure change does not form. The temperatures for these experiments was 300°C[78]. Modification of platinum particle structure was also observed after cracking of benzene at 325°C which leaves a carbon deposit[77] on the platinum aggregate. Increase in hydrogen partial pressure eliminates the Pt-C bond and hydrogen atoms cover the surface.

1.7.2 Discussion of fouling and poisoning

Any process which decreases the activity of a catalyst can be classified as deactivation. In many cases deactivation may be accompanied by large changes in selectivity as well. Several processes which cause deactivation by the mechanism of poisoning are listed[79]:

- Irreversible adsorption or reaction of poison precursors on or with the surface

- Competitive reversible adsorption of poison precursor

- Poison induced restructuring of catalyst surfaces

- Physical and/or chemical blockage of support pore structure

Poisoning may be identified as selective or nonselective and/or reversible or irreversible. A material that acts as an irreversible poison at one temperature level may become reversible at higher temperatures. Observations that a catalyst may become completely deactivated by an amount of poison well below the amount corresponding to the adsorption capacity of the catalytic surface have led to the concept of selective poisoning. In this case an initial increment of poison on the surface causes a large relative deactivation with subsequent amounts giving decreasing rates of activity change. This has often been modeled by exponential or hyperbolic functions of poison uptake. Conversely for nonselective poisoning all active sites appear identical and the resultant activity-poison uptake relationship is linear.

For monofunctional catalysts in which there are no interactions between adsorbate poison molecules or alterations of site energetics upon adsorption, then nonselective poisoning would be expected. However, even if all sites are equivalent in geometry and energetics, the relationship between activity and extent of poison uptake can still be complicated (Herrington and Rideal, 1944)[80]. Multisite adsorption phenomena can yield selective poisoning behaviour on uniform surfaces. Diffusional effects can also be important in apparent selective poisoning. Distribution of active site strengths has been used as an explanation of selective poisoning[81]. Multifunctionality is often associated with metal-solid acid catalysts such as Pt/Al_2O_3, which is widely encountered in reforming reactions. In these catalysts the overall selectivity as well as the activity is altered by poisoning.

1.7.2.1 Poisoning and structure sensitivity

Recent work on the poisoning of supported metal catalysts has developed the concept of structure-sensitive deactivation derived from the corresponding concepts of structure-sensitive reactions on supported metals. Several observations of structure-insensitive reactions becoming apparently structure-sensitive under poisoning conditions have been reported[82,83,84].

Recent work has been directed towards poisoning of Pt/SiO_2 and Pt/Al_2O_3 by carbon monoxide for the hydrogenolysis of methylcyclopropane. A $CO:Pt_S$ ratio of one has been reported for Pt/SiO_2[85], where Pt_S are the exposed platinum atoms. The unpoisoned reaction was mildly structure-sensitive at metal percentages exposed > 40%, with activity increasing with increasing percentage of metal exposed. However, a notable structure-senstive effect was seen upon carbon monoxide poisoning which became more pronounced as surface coverage of the poison increases. The CO/Pt_s ratio decreased from 1.0 to 0.8 with increasing percentage metal exposed for Pt/Al_2O_3 and a mild structure sensitivity of the unpoisoned catalyst was observed with activity decreasing with increasing percentage of metal exposed[86]. The general pattern of structure sensitivity did not change with progressive poisoning. The different results between Pt/Al_2O_3 and Pt/SiO_2 may be due to differing support interactions and this is currently under investigation[79].

1.7.2.2 Influence of metal accessibility

Metals encaged in zeolites can be inaccessible to reactant molecules because the pore system is blocked by partial or total structure breakdown. The deactivation is then irreversible. Pores clogged by carbon deposits or polymeric materials can be unblocked by calcination in air, thus reactivating the catalyst.

1.7.2.3 Effects of electronic structure

Modifications of the electronic structure of bulk metals are expected theoretically when the aggregates are smaller than 1.5 nm[79]. Simultaneously the electronic structure could be modified by the environment, including the electron donor/acceptor sites of the support, other cations, metal atoms and adsorbates. It was reported that the rate of n-hexane isomerization on PtCaY zeolite containing highly dispersed platinum was only slightly affected by the presence of sulphur, whereas large particles are rapidily deactivated[87]. The weaker Pt-S bonding was attributed to the electron deficient character of small platinum aggregates decreasing the interaction with electronegative sulphur. This was substantiated by investigations of the electronic structure of encaged platinum as well as by poisoning and regeneration experiments[88]. Inhibited accessibility of the platinum aggregate surface to hydrogen and thus the removal of poison could account for any sulphur resistance of platinum on Pt/KL where there is excess charge density on platinum[89]. The electron deficiency of platinum should have an adverse effect on the resistance to poisoning by base compounds since stronger bonds can be formed via electron donation from the adsorbate to the metal.

1.7.3 Sensitivity to sulphur

The sulphur sensitivity of monofunctional Pt/KL hexane aromatization catalysts is qualitatively known to be substantially higher than that of conventional Pt/Cl-Al_2O_3 and Pt-Re/Cl-Al_2O_3 bifunctional reforming catalysts[90]. Presently, acceptable Pt/KL aromatization cycle lengths can only be achieved by reducing feed sulphur concentrations to ultralow levels ($<$ 50 ppb). Extremely low thiophene feed sulphur concentrations in the range 50 ppb to 200 ppb accelerate platinum agglomeration. Catalyst deactivation, resulting primarily from metal agglomeration, occurs by multiple blockages of KL channels by platinum or platinum-sulphur clusters (10Å - 20Å)[90]. Platinum agglomeration is the primary deactivation mechanism for initially well dispersed Pt/KL catalysts with little or no platinum outside of the zeolite

channels. The role of agglomeration is to create multiple blockages within the one dimensional KL channels, thereby entombing active platinum sites. Sulphur accelerates agglomeration, but does not appear to modify the intrinsic catalytic properties of accessible platinum sites within the channels of KL zeolites[90].

However, Kao *et al.* (1993)[91] reported that sulphur in the form of thiophene functions as a stoichiometric poison and lowers, thereby, the number of active platinum sites. The sulphur sensitivity is highly dependent on the sulphur source. The order of sensitivity at constant sulphur level is:

thiophene > > 1,2-benzodiphenylene sulphide > propanethiol > sulphonane[91].

The effect of steric hinderance was investigated by comparing the poisoning effect bulky 1,2-benzodiphenylene sulphide relative to the much smaller propanethiol. These results were rationalized in terms of the reactivity of the sulphur compounds. In general the poisoning effect of a molecule on a catalyst is related to its ability to form a chemisorbed species. Organo-sulphur compounds which possess one or two lone pairs of electrons on sulphur often exhibit enhanced toxicities towards noble metals[92]. The highly conjugated π electron system present in thiophene and 1,2-benzodiphenylene sulphide would be expected to be more strongly chemisorbed than aliphatic propanethiol. Differences in toxicity between thiophene and 1,2-benzodiphenylene sulphide might reflect a steric effect, as the bulky molecule will have more difficulty in diffusing into the channels of KL. In the case of sulfolane, a two step reduction of hexa-valent sulphur to the divalent sulphur is needed to poison platinum metal particles[91].

TEM measurements suggest that large platinum agglomerates block access to the active platinum sites within the KL channels[91]. Platinum agglomerates tend to form at the KL channel entrance which supports the contention that sulphur deactivation, at least in the initial stages, of Pt/KL occurs by pore mouth blocking of the KL channels (Figure 1-10) by platinum or platinum-sulphur particles[91]. It is

also reported that platinum outside the channels are less sensitive to poisoning by platinum as the catalyst retains some residual, yet stable, activity after poisoning by sulphur[91]. This further supports the contention that it is pore mouth blocking, which results in the feed being denied access to platinum particles in the channels. The platinum in the channels have high aromatization activity and inhibited acess to these platinum particles is the cause of deactivation of Pt/KL.

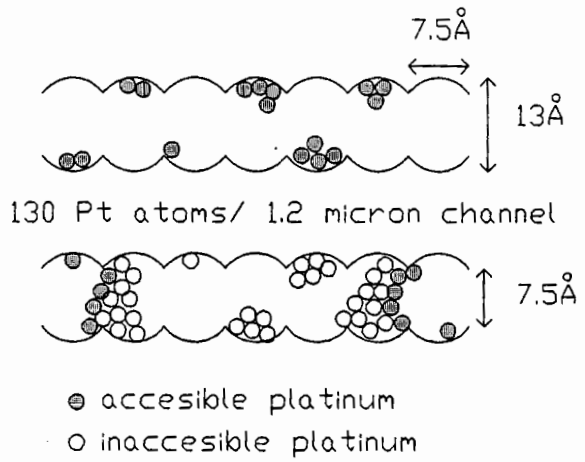

Figure 1-10 Proposed model for pore mouth blockage of Pt/KL catalysts (Kao *et al.*, 1993).

A plot of benzene selectivity against n-hexane conversion results in a curve that is shared for sulphur-free as well as sulphur containing feeds[91]. This strongly suggests that sulphur deactivation occurs by the loss of active platinum sites and not by the modification of the catalytic platinum sites. Even at sulphur to platinum ratios of 0.1 there is rapid deactivation. Thus only 10% of active platinum atoms need to be poisoned for deactivation to occur. This is further support for the pore blockage model for deactivation.

1.7.3.1 The effect of potassium

In a recent paper, Fukunaga and Ponec (1995)[93] showed that the high aromatization yields and the high sensitivity to sulphur poisoning in n-hexane conversion on Pt/LTL, could be related to the presence of K^+ cations. They also

showed that the decrease in dehydrogenation activity only (cyclohexane to benzene), caused by sulphur, was more pronounced on a K^+ free catalyst. It was suggested that K^+, which stabilizes an intermediate of aromatization, loses this property by interaction with sulphur, which explains the selective and significant loss of aromatization activity in the presence of sulphur.

The sulphur sensitivity of the catalyst was studied by changing the nominal S/Pt ratio. A significant decrease in benzene yield occurs, primarily as a result of the decrease in n-hexane conversion[90,93]. When the selectivities to benzene and C_1-C_5 are plotted (Figure 1-11) as a function of n-hexane conversion for platinum catalysts of different S/Pt ratios it is clear that catalysts with high S/Pt showed lower benzene, and higher C_1-C_5, selectivity when compared to catalysts with lower S/Pt ratios. It was also shown that Pt/KL and Pt-K/SiO_2 are more sensitive to sulphur poisoning for the aromatization of n-hexane, than the corresponding catalysts without potassium as a promoter. Sulphur also caused a change in the product distribution, with an increase in both the i-hexane and MCP selectivities. The change in C_1-C_5 selectivity depends on the presence of K^+. The C_1-C_5 selectivity increased with K^+ containing catalysts and decreased with K^+ free catalyst, after sulphur addition.

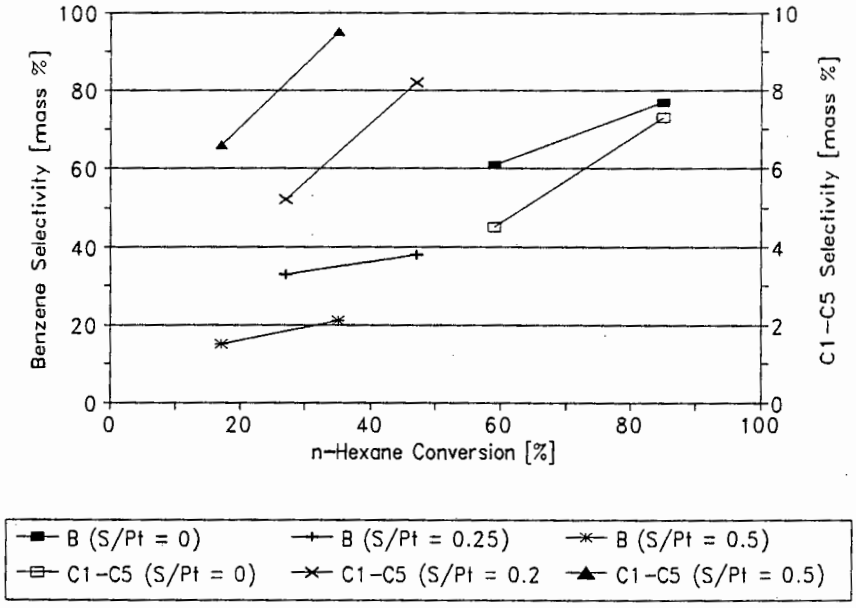

Figure 1-11 Changes in benzene selectivity of the Pt/KL catalysts caused by sulphur, at two different residence times (Fukunaga and Ponec, 1995) B = benzene

If sulphur, when added in increasing amounts, were selectively poisoning an increasing amount of equivalent sites, then a common curve would be expected for a plot of benzene selectivity as a function of n-hexane conversion[90]. However, the points in Figure 1-11 do not lie on a common curve[93] which is an indication that that sulphur is subsequently poisoning sites of different quality (this contradicts data from Kao et al., 1993[91]). An increase in hydrogenolysis activity is observed[93,172] and is a strong indication that the activity loss observed after sulphurization of Pt/KL is not due to a simple ensemble size decrease by sulphur adsorption. Hydrogenolysis, which requires a large platinum ensemble size, should have been suppressed preferentially if the ensemble size decrease were the only reason for the change in selectivity. Dehydrogenation of cyclohexane to benzene has been described as a structure-insenstive reaction[94] and only a small ensemble is considered to be involved in the rate determining step of the dehydrogenation reaction[95]. Thus the benzene yield should reflect the changes in the accessible platinum surface area of the catalyst, for the dehydrogenation of cyclohexane to

benzene. It was found that the presence of potassium on Pt/SiO_2 causes a decrease in the dehydrogenation activity of the catalyst (cyclohexane to benzene), but an increase in the aromatization activity (n-hexane to benzene). In addition the K^+ free catalyst, Pt/SiO_2, is more sensitive to sulphur poisoning in the dehydrogenation reaction and less sensitive in the n-hexane aromatization than $Pt\text{-}K/SiO_2$[93]. The reasons for these results are discussed below.

TEM observations made by Fukanaga and Ponec[93] were not consistent with platinum particle size changes. An increase in C_1-C_5 selectivity would be expected if platinum particle growth by sulphur had occurred. However, the smaller decrease in cyclohexane dehydrogenation activity by sulphur poisoning than in n-hexane aromatization is not compatible with the agglomeration mechanism. Both reactions produce the same products and hence blockage of KL zeolite channels and subsequent diffusion hindrance should have influenced both reactions to the same extent. Only benzene formation was suppressed and the formation of MCP, i-hexanes and C_1-C_5 were influenced little by sulphur, suggesting that the simple loss of platinum active sites by particle agglomeration is not the main cause of the aromatization activity loss.

Hence in summary[93], on Pt/KL and $Pt\text{-}K/SiO_2$, K^+ stabilizes an intermediate of aromatization for the reaction cyclohexane to benzene. This leads to high and selective benzene formation from n-hexane relative to K^+-free catalysts. However, in the presence of sulphur, an interaction occurs between K^+ and sulphur which reduces the stabilization ability of K^+. Hence sulphur induces a significant loss of aromatization activity and also leads to a relatively high hydrogenolysis selectivity. Dehydrogenation of cyclohexane to form benzene, a structure insensitive reaction, is less suppressed by sulphur on K^+-containing catalysts, because some of the sulphur added is adsorbed on K^+. Lastly, it is noted that the formation of strong interactions between sulphur and K^+ has been observed[96,97], resulting in the formation of K_2S and KHS from sulphur compounds with K_2O and KOH-promoted iron catalysts.

Pt/KL catalysts were individually poisoned with K_2SO_4, H_2S, thiophene and sulphur diphenyl by Besoukhanova *et al.* (1980)[98] and the effect on hexane aromatization and benzene hydrogenation was followed. These results and the conclusions derived therefrom tend to be in conflict with the aforementioned work. Some of these conclusions follow. Only a part of surface platinum atoms seem to be catalytically active. Small sulphur amounts are selectivity fixed on sites responsible for hydrogenolysis. The platinum in Pt/KL zeolites have an excess of electrons due to interaction with basic sites but are more sulphur resistant than Pt/NaY catalysts containing only Pt^0 atoms. Various factors such as zeolite field and platinum particle location are suggested to give the higher sulphur resistance to platinum particles in KL than in Pt/NaY[98]. The sulphur resistance is less than that of acidic platinum catalysts. Thiophene and H_2S are less effective poisons for L zeolites than the Y type. The average platinum dispersion is not changed by sulphur poisoning. As already stated these results are in conflict with those mentioned at the beginning of this section.

1.7.4 Discussion of the effect of sintering

Oxygen alone does not result in the redispersion of platinum supported on alumina[99]. The presence of chlorine is needed for redispersion to occur. Chlorine may be present in the support, which accounts for previous reported platinum redispersion during oxygen treatments[100],[101]. Foger and Jager (1985)[102] reported that platinum supported on alumina can be redispersed by treatment in Cl_2-N_2 mixtures. Redispersion of platinum generally occurs between temperatures of 200°C to 450°C while for Pt/SiO_2 redispersion was only observed at temperatures between 150°C and 200°C[103].

Redispersion of platinum in oxidising atmospheres (Cl_2 or Cl_2/O_2) requires the formation of oxidised metal compounds or complexes, which have to migrate over the support surface and form stable oxidized metal-support complexes. Subsequent reduction of these well dispersed metal-support complexes results in high metal

dispersions. Sintering in oxidising atmospheres can result if conditions (temperature and concentration) are such that the oxidised metal or metal-support complex is unstable. Significant redispersion of supported noble metal catalysts has not been observed as a result of treatment in reducing or inert atmospheres[104]. Furthermore the rates of sintering are much lower in inert or reducing atmospheres than in oxygen atmospheres.

Several models have been proposed to account for sintering and redispersion. These are discussed briefly.

1.7.4.1 Empirical model

The introduction of Platforming in the 1950's resulted in the first quantitative study of sintering data[105,106]. The catalysts studied were platinum supported on alumina. A power-law rate model was used to describe the sintering data.

$$dD/dt = -k\,D^n$$

Integrating for $n \neq 1$ gives

$$D^{(1-n)} = D_o^{(1-n)} + (n-1)kt$$

D = metal dispersion
t = sintering time
D_o = initial metal dispersion (t = 0)
k = temperature dependent rate constant
n = sintering order

The fitting of sintering data has been reviewed by Wanke *et al.* (1975)[107]. Power- law orders ranging from 2 to 16 have been observed and often no single value of n will describe the sintering data over larger sintering times, *i.e.* the sintering order is a function of dispersion. The sintering order does not appear to be correlated with the type of metal, sintering atmosphere or nature of the support.

Hence, the power law model cannot be used for predictive purposes and is at best an approximate method for correlating sintering data.

1.7.4.2 Phenomenological models

These models postulate a set of general processes by which sintering can occur without specifying details of these processes. There are two phenomenological models for sintering that have received considerable attention:

- Sintering is postulated to occur by migration of atomic or molecular metal species.

- Sintering is postulated to occur by the migration of entire metal particles.

Both these types of phenomena were proposed by Mills *et al.* (1961)[108] as possible processes responsible for the sintering of supported platinum catalysts. Ruckenstein and Pulvermacher (1973)[109] and Flynn and Wanke (1974)[110] performed quantitative calculations of these models for supported catalysts. A brief summary is presented here, for a fuller description see Wanke (1982)[111]. The particle diffusion model assumes that sintering occurs by diffusion of entire metal particles upon the support followed by collision and merging of the migrating metal particles. This model predicts that the rate of sintering can be described by the power-law rate function (Section 3.3.3.1) with a sintering order of 1 to 10. The magnitude of the sintering order depends on whether the rate of diffusion or the rate of merging of metal particles is rate limiting[112]. This model does not predict increases in dispersion since merging of colliding metal particles always results in an increase in the average metal particle size. The splitting of metal particles was proposed to account for the observed decrease in average particle size observed during regeneration treatments[113].

The alternative model proposes that sintering occurs by the migration of atomic or molecular species. The metal atoms or metal containing molecules move from the metal particles to the support surface and then migrate over the support surface until they either encounter a trapping site on the support surface or are captured by a metal particle. Redispersion occurs if the migrating species become immobilized at trapping sites and sintering occurs if the capture of migrating metal species by metal particles predominates. This model also predicts that sintering can be described by a power-law rate function. The sintering order may change as sintering progresses, in accordance with observations.

1.7.4.3 Mechanistic model

The mechanistic models involve the identification of the chemical species formed during sintering and redispersion. The proposed mechanisms for sintering and redispersion of platinum supported on alumina are summarized in Figure 1-12 by Wanke *et al.* (1987)[104]. It is assumed that sintering in hydrogen and inert atmospheres occurs by migration of platinum atoms or small platinum clusters. However, little direct evidence is available to support this assumption. The intermediates shown in Figure 1-12 for the sintering and redispersion in oxidising atmospheres are well established.

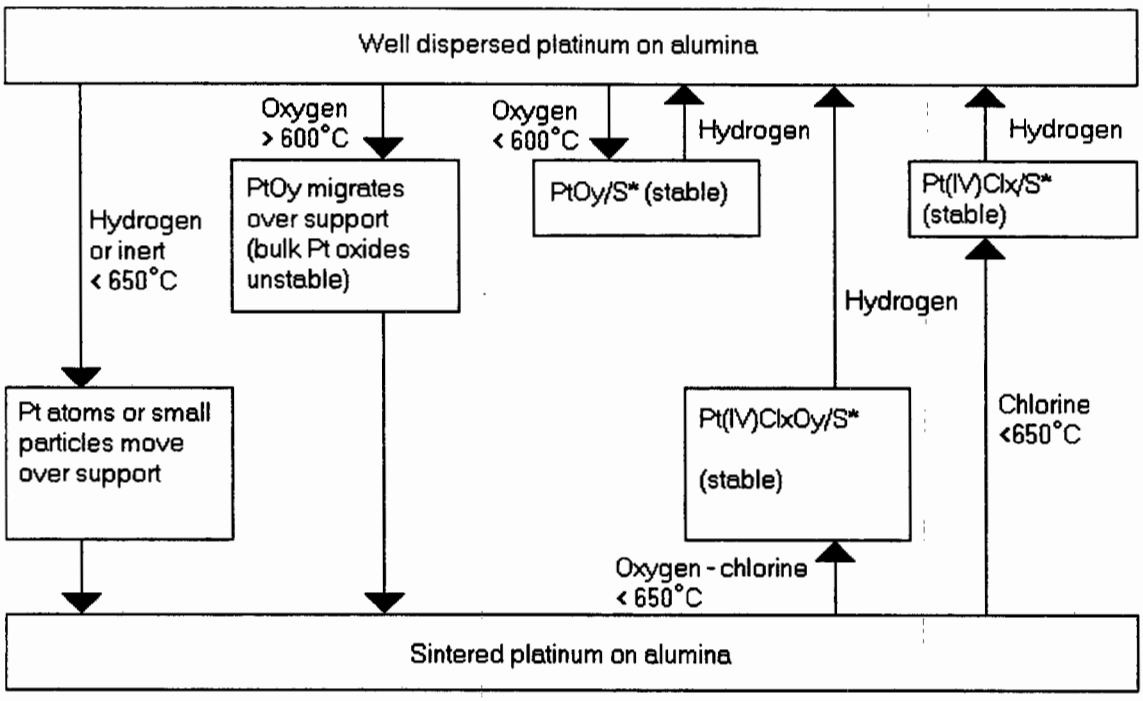

Figure 1-12 Schematic representation of sintering and redispersion for platinum supported on alumina in different atmospheres (Wanke *et al.*, 1987)

The changes in platinum dispersion during treatment in oxidising atmospheres are governed by the formation of Pt^{+4} species[114]. The stability and mobility of Pt^{+4}-support complexes determine whether sintering or redispersion occurs. Platinum oxides are formed during low temperature oxygen treatment of Pt/Al_2O_3 catalysts. Subsequent reduction restores the platinum to a well dispersed state. Bulk platinum oxides are unstable at high temperatures and sintering occurs during treatment in oxygen at high temperatures. Reduction of Pt/Al_2O_3, which has been treated in oxygen at high temperature, results in a catalyst with a bimodal platinum particle size distribution. The temperature at which sintering starts depends on the chlorine content of the alumina. High temperatures are required to sinter platinum supported on chlorine-containing alumina. Sintering in oxygen usually starts at

600°C to 650°C.

Chlorine not only stabilizes Pt/Al_2O_3 catalysts, but it is also required for redispersion of sintered catalysts. Surface species such as $Pt(IV)O_yCl_x/Al_2O_3$ and $Pt(IV)Cl_x/Al_2O_3$ have been identified as the agents responsible for redispersion[115,102]. These species are well dispersed over the surface of the alumina and are formed during treatment in O_2-Cl_2 or Cl_2 at temperatures below 650°C. At higher temperatures these species are unstable and sintering occurs.

1.7.5 Redispersion of Platinum

Platinum/KL zeolite catalysts, applied to industrial processes, need restoration treatment at suitable intervals, as they are deactivated by the accumulation of coke and sulphur as well as the sintering of platinum particles. Treatment of KL zeolite with CF_3Cl increased the catalytic activity for the aromatization of C_6 feedstock. Deactivation of this Pt/FKL catalyst was caused by sintering of the platinum particles, loss of halogen atoms and coke formation during aromatization of C_6 feedstocks[116]. The catalyst performance was restored by decoking in flowing CCl_4(0.005%)/O_2(2%)/N_2(97.995%) from room temperature to 500°C followed by treatment in flowing freon(0.8%)/O_2(10%)/N_2(89.2%) at 500°C. The results of IR spectra of chemisorbed CO and terminal OH groups suggest that the most important goal of regenerating the used Pt/FKL is to redisperse the platinum particles and restore their electronic state. A small amount of aluminium is removed from the L zeolite framework during the CF_3Cl treatment and terminal hydroxyl groups, including silanol nests formed by dealumination, are replaced by halogen atoms during CF_3Cl treatment. Halogen atoms also suppress sintering and/or promote redispersion during reduction, as well as maintaining platinum dispersion during n-hexane aromatization and the low accumulation rate of carbon deposits as a result of the hydrogenolysis activity. The regenerated catalyst, which restored the catalytic performance, exhibited the same amount of terminal OH groups as the fresh Pt/FKL and had electron rich platinum particles compared with those of the

fresh Pt/FKL[116].

As terminal hydroxyl groups are replaced by halogen atoms, no increase in acidity was expected or observed[28]. However, based on the results of infrared spectroscopy of adsorbed CO, it was found that platinum particles supported on CF_3Cl treated KL become electron rich by decreasing the interaction with oxygen atoms on the zeolite framework and that in the case of Pt/FKL, the electronic state of the platinum particles in an important factor for its catalytic activity. The Pt/FKL catalysts exhibits a high stability and a low carbon accumulation rate even at a low hydrogen/hexane ratio of 0.5 compared with untreated Pt/KL[117]. Due to the high aromatization rate, the Pt/FKL was able to attain the same aromatics yield at a lower reaction temperature than Pt/KL as the carbon formation rate increases with reaction temperature. This is one the reasons why Pt/FKL showed a lower carbon accumulation rate and high stability, even at a low hydrogen/hexane ratio. The low accumulation rate of carbon deposits is also a result of the low hydrogenolysis activity of these catalysts (Table 1-12). At low hydrogen partial pressure the difference between the catalysts is small, due to the suppression of hydrocracking at low hydrogen partial pressures. The ratios of n-pentane to iso-pentane ($n\text{-}C_5/i\text{-}C_5$) differ significantly between Pt/KL and Pt/FKL being 5 and 2 respectively. Cyclopentadiene, an intermediate for coke precursors[118], seems to be more easily produced on Pt/KL than Pt/FKL by the dehydrocyclization and dehydrogenation of n-pentane, especially at low hydrogen to hydrocarbon ratios. Although it is not clear that n-pentane and iso-pentane are produced directly through hydrocracking of n-hexane and/or iso-hexanes or through isomerization of pentane isomers, the differences among the aromatization, isomerization and hydrocracking rates over Pt/FKL and Pt/KL seem to affect the $n\text{-}C_5/i\text{-}C_5$ ratios considerably.

Additionally it was shown by TPD of n-hexane and benzene from Pt/KL and Pt/FKL that n-hexane diffuses more slowly in Pt/FKL than Pt/KL, while benzene diffuses more rapidly through Pt/FKL than Pt/KL. The easier diffusion of benzene through the Pt/FKL leads to the expectation that the formation of carbon and polycyclic

Table 1-12 Product distribution of Pt/KL and Pt/FKL catalysts

	Pt/KL	Pt/FKL
n-C_6 Conversion	2.2	14.2
C_1-C_5 selectivity	10.4	4.6
Aromatics selectivity	89.6	95.4

480°C, H_2/n-C_6 = 5, WHSV = 80 /hr, p(H_2) = 5 kg/cm^2

aromatics via benzene will be lower on Pt/FKL. In agreement Pt/FKL is more stable than Pt/KL[117].

Platinum supported on zeolites K-L,H-L, H-ZSM-5 and silica was treated with Cl_2 in nitrogen or HCl in air at 347°C. Platinum redispersion was found to be linked to the formation of strongly bonded Pt(IV) chloride species of which the concentration depends on the aluminium content of the zeolite. A redispersion scheme was proposed which involves splitting of some Si-O-Al linkages and bonding of platinum halide species to the aluminium. No crystalline platinum chlorides were formed in 2wt% Pt/L zeolites. After reduction metal particles (<10Å) were present on the zeolite surface and within the channels. Medium and poorly dispersed Pt/KL catalysts were successfully redispersed by treatment at 347°C with 10% chlorine in nitrogen. Platinum was not lost from H-L and K-L zeolite until a level of 3.5wt% platinum was exceeded. Thus agglomerated platinum in zeolite channels can be redispersed successfully by treatment with chlorine or a combination of HCl and oxygen. Zeolite crystallinity is retained. The amount of platinum chloride compound strongly adsorbed on the zeolite is linked to the aluminium content. Only strongly bound Pt(IV) species lead to catalysts of high dispersion upon reduction[119].

1.8 Reaction of Hydrocarbons on Platinum Surfaces

The reactions of hydrocarbons on platinum surfaces include:

- hydrogenation
- dehydrogenation
- isomerization
- hydrogenolysis
- cyclization (including dehydrocyclization)

The cyclization reactions include the cyclization of n-alkanes to 5-membered ring and to aromatic compounds, as well as ring opening reactions of methylcyclopentanes to cyclohexanes and aromatics[120].

The rates of these reaction have been measured with single-crystal platinum catalysts[121] and the results are summarized in Figure 1-13.

Alkene hydrogenation, especially ethene hydrogenation, has been investigated intensively and is regarded as one of the best test reactions to provided detailed information about the catalytic nature of metal surfaces. The hydrogenation reaction occurs readily on many metal surfaces. At high temperatures the working surface of platinum is nearly clean, but at low temperatures is covered in carbonaceous (alkenyl) deposits[122]. Experiments with a pulse reactor containing platinum operated at -31 °C showed that carbonaceous deposits were formed rapidly, but were not involved in the ethene hydrogenation[122].

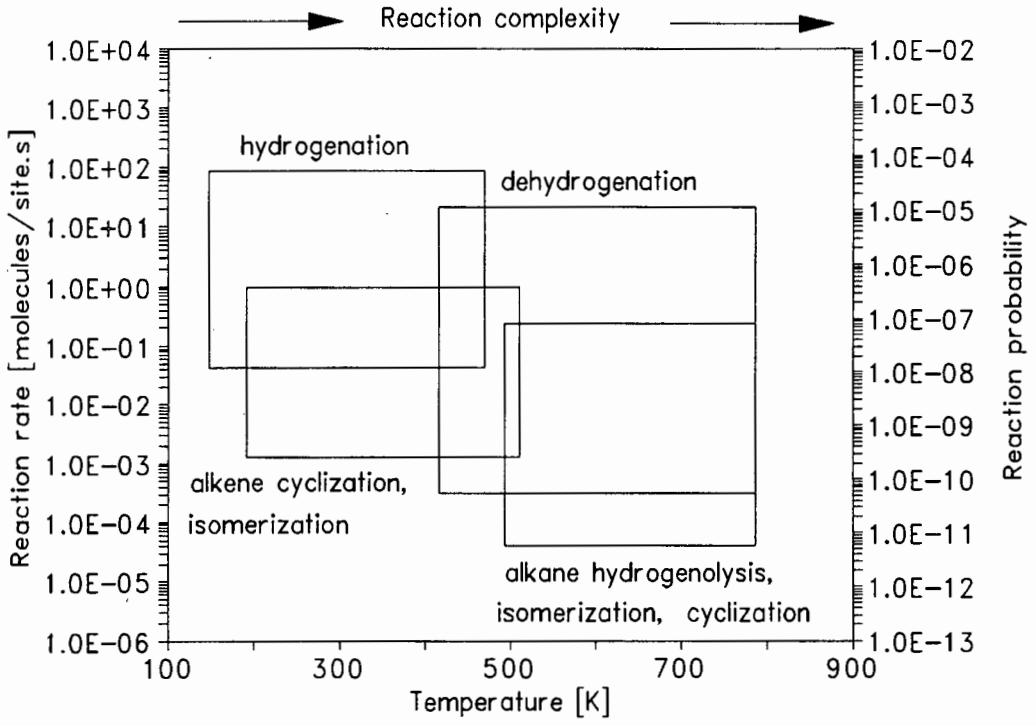

Figure 1-13 Approximate rates of hydrocarbon conversion reactions on platinum catalysts (Somorjai G.A., 1987).

A number of hydrocarbon rearrangement reactions have been investigated with single crystals cleaved to expose various densities of terraces, steps and kinks[123]. Experiments were carried out to measure the rates of catalytic reactions such as:

- the dehydrocyclization of n-hexane to benzene;
- the simultaneous dehydrocyclization to methylcyclopentane (MCP);
- isomerization to methylpentanes;

- hydrogenolysis.

The results of these experiments showed that the activity of platinum for hydrocarbon conversion varies from one crystal face to another. The conversion of n-hexane to benzene occurs most readily on platinum surfaces with the flat hexagonal (111) structure (these surfaces are several times more active than the (100) surface). Many other experiments give evidence for the dependence of catalytic activity for hydrocarbon conversion on the structure of the platinum surface[122]. The exact catalytic sites for each of the aforementioned reactions is not known, but extensive research with isotopic tracers to elucidate details of the reaction pathways and to allow inference of the nature of surface reaction intermediates has been carried out. This research has shown that cyclic structures (analogues of metallocycles), some bonded to the metal surface at more than one position are present. The platinum catalyst is also largely covered with hydrocarbon overlayers[122,120].

1.8.1 Skeletal reaction mechanisms

1.8.1.1 The bond shift mechanism

The initial act of chemisorption of an alkane molecule at a metal surface is dissociative and considerable insight into this process has been obtained by the use of deuterium exchange reactions[124]. Butane, reacted over platinum films underwent isomerization at 507K (234°C), accompanied by hydrocracking and it was further shown the platinum was the sole seat of the catalytic activity[125]. A π-bonded complex was suggested as a reaction intermediate. The essential feature of such a complex was that it should not have less than three adjacent non-quaternary carbon atoms. Thus n-butane would be able to form a π-complex, but neopentane would not. However, the fact that the isomerization of neopentane was observed to occur at a similar rate to n-butane indicates that a π-bonded complex is not necessary for isomerization. In the absence of a π-bonded

intermediate complex, the adsorbed intermediates must be bonded to the surface by σ-bonds. As a consequence of that work a mechanism of isomerization was proposed for aliphatic hydrocarbons at a platinum surface, *viz.* initially the 1 and 3 carbon atoms were probably singly bonded to the surface by dissociative adsorption through conventional σ-bonds (Figure 1-14, A). One of the adsorbed carbon atoms changes its hybridization to sp^2 by the loss of further hydrogen atoms (B). The model proposes that the surface precursor is 1,3 diadsorbed with a double bond to the surface at one carbon atom (A) and that isomerization occurs by the transformation of this to a bridged structure (B) as shown in Figure 1-14.

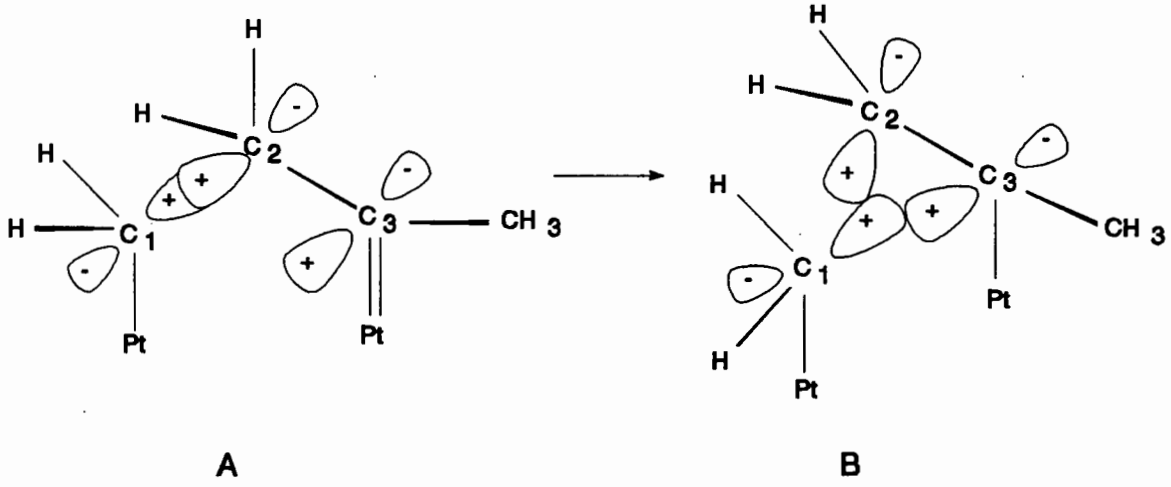

A B

Figure 1-14 Andersons' mechanism for isomerization of n-butane on platinum surfaces.

1.8.1.2 Bond shift and cyclic mechanisms

A comparative study of the hydrogenolysis of methylcyclopentane (MCP) to methylpentanes and the isomerization of n-hexane isomers on platinum catalysts was perfomed by Barron *et al.* (1963)[126]. The almost complete absence of 2,3-dimethylbutane and the formation of MCP was observed during isomerization of n-hexane. These results strongly suggest that a common intermediate with a five-membered ring structure (Figure 1-15) is responsible for these reactions[126]. Further investigations at high temperatures on platinum films and on supported

catalysts with a low metal content have shown that a similar distribution is obtained with any cyclic hydrocarbon, corresponding to an equal chance of breaking the different cyclic bonds (Figure 1-17). For this type of non-selective hydrogenolysis, π-allylic triadsorbed species were proposed to be present[120]. At low reaction temperatures only the secondary CH_2-CH_2 cyclic bonds of cyclopentanes and cyclobutanes were broken. This selective hydrogenolysis was associated with $\alpha,\alpha,\beta,\beta$, tetraadsorbed species. The analysis of product distributions obtained from MCP suggests a third mechanism takes place on platinum, namely a partly selective hydrogenolysis which involves the breaking of secondary bonds as well as secondary-tertiary bonds to a lesser extent[127].

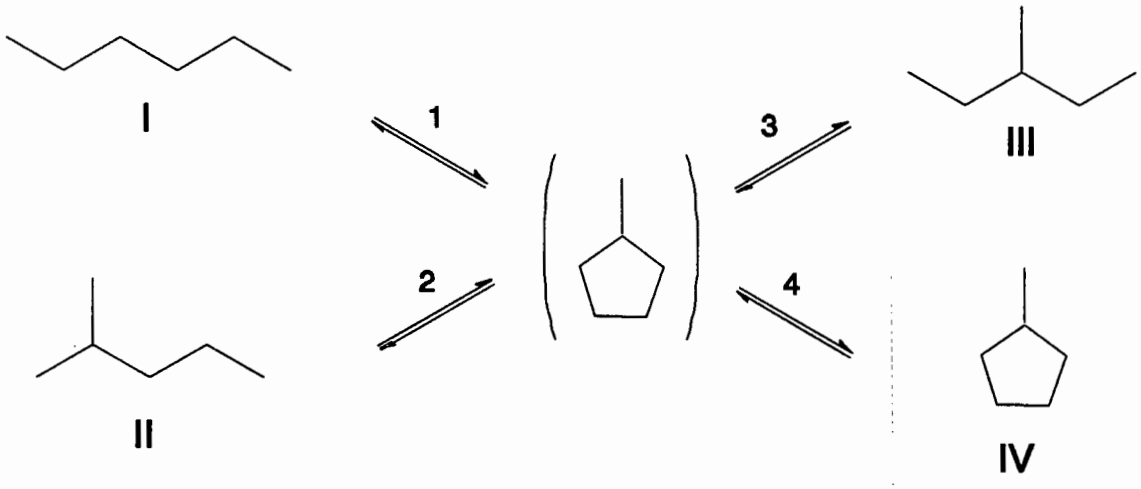

Figure 1-15 Proposed reaction pathways for C_6 alkanes on platinum.

Among these mechanisms, one corresponds to an equal chance of rupturing the five cyclic bonds of MCP. Tertiary CH-CH bonds were opened and cis-trans equilibrium of substituted cyclopentanes was reached during hydrogenolysis. It was thus assumed that the species responsible for isomerization and dehydrocyclization of hexanes were α,β,τ, triadsorbed species[128]. The first elementary step of isomerization is in Figure 1-16.

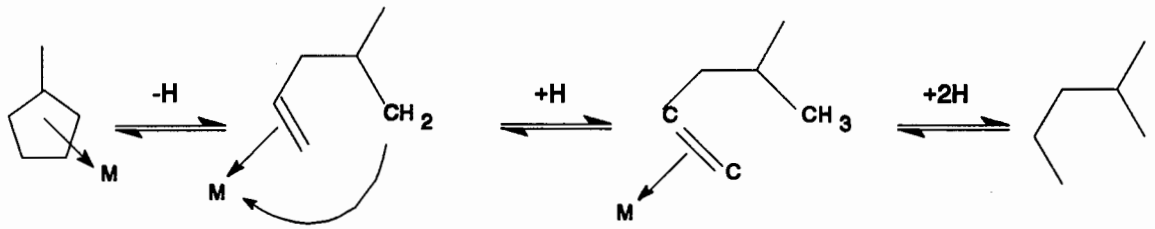

Figure 1-16 First elementary step of MCP isomerization.

In summary, there are at least two different mechanisms of isomerization on platinum catalysts. One of these involves a cyclic intermediate and the other an alkyl shift. Aromatization also occurs under the same conditions provided the reactant molecule is sufficiently large. In highly dispersed platinum catalysts the cyclic mechanism dominates (for molecules with five or more carbon atoms). The percentage of cyclic products increases with:

- decreasing hydrogen pressure
- increasing hydrocarbon pressure
- increasing reaction temperature

The ratio of cyclic to acyclic products varies widely with conversion, decreasing sharply with contact time. The correct manner to compare the contribution of the cyclic mechanism for various catalysts is to determine the percentage of cyclic products at various contact times and extrapolate to zero conversion.

1.8.1.3 Cyclic mechanisms

In the study[129] of the ring opening (hydrogenolysis) of methylcyclopentane (MCP) on a series of Pt/Al_2O_3 catalysts with different metal loadings from (0.15 to 20% platinum) it was found that the distribution of reaction products changed substantially with changing the percentage of platinum on the carrier. In addition, a more selective rupture of CH_2-CH_2 bonds was found on the catalysts with more

than 2% platinum while on the catalysts with less than 1% of platinum the probabilities of rupturing the five C-C bonds of the five member ring were approximately equal (Figure 1-17)[122].

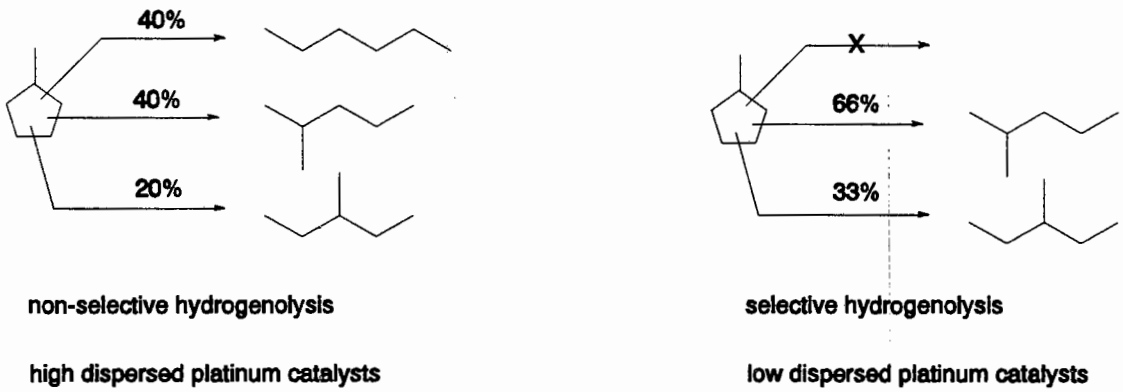

Figure 1-17 Reaction product probabilities on high and low dispersed platinum catalysts.

A more careful study of MCP hydrogenolysis made with two catalysts of extreme dispersion showed that on 0.2% Pt/Al_2O_3 the product distribution did not vary with temperature between 493K - 593K (220 - 320°C), while it varied significantly on the catalyst with low dispersion[128].

Three reaction mechanisms (Figure 1-18) for hydrogenolysis of cyclopentanes were proposed[127]. The non-selective (A) mechanism corresponds to equal chance of breaking any cyclic bond. Of the two other mechanisms, the completely selective (B) mechanism results in only the fission of secondary CH_2-CH_2 bonds, while the partly selective (C) mechanism involves the breaking of secondary and secondary-tertiary bonds. These two mechanisms (B and C) compete on catalysts of low dispersion.

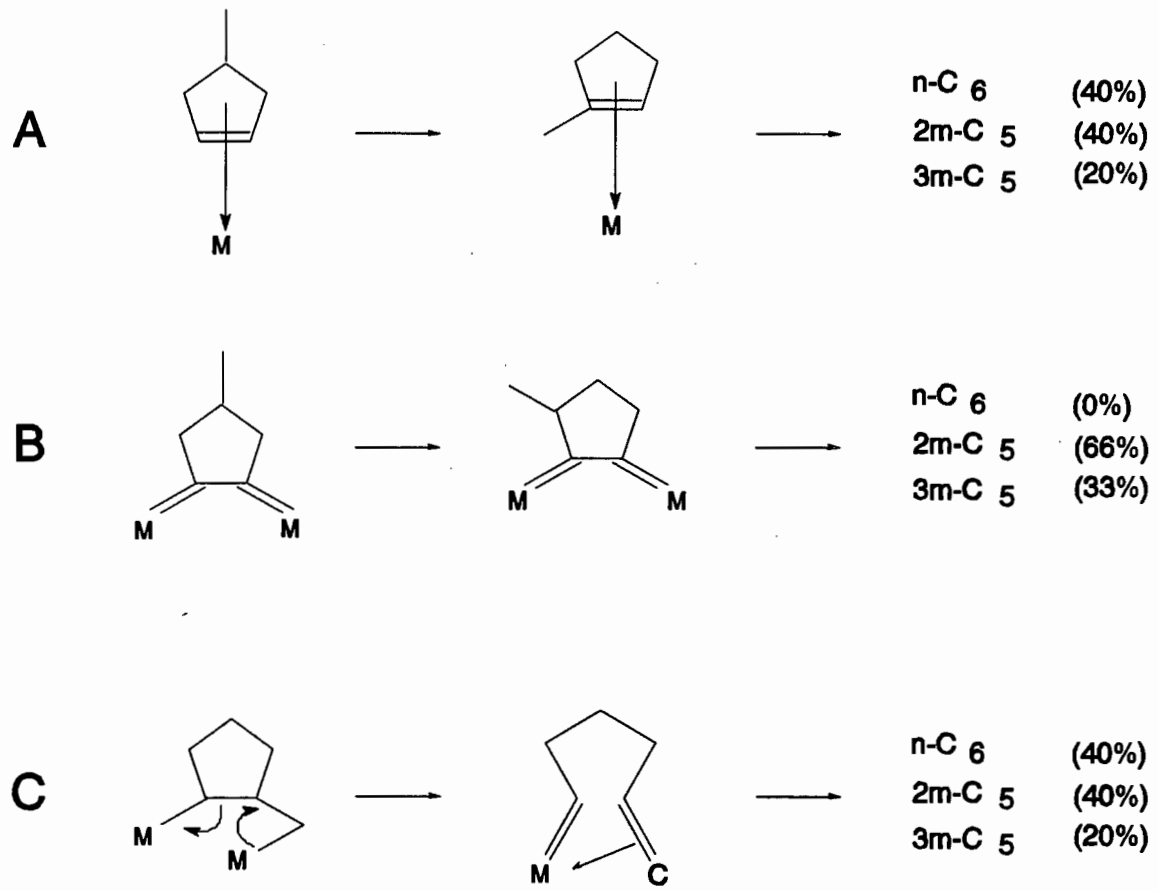

Figure 1-18 Mechanisms for cyclopentane hydrogenolysis.

On platinum the precursor for the dehydrocyclization process of pentane is necessarily attached to the metal by two carbon atoms, *i.e.* 1 and 5 and not by three carbon atoms 1,2 and 5. The precursor species does not require alkene formation. As shown in Figure 1-19, a 1,1,3-triadsorbed precursor (such as B) was suggested to be responsible for the bond shift rearrangement on platinum[130,131]. A 1,1,5-triadsorbed species (C) was suggested, along with a more energetically favoured transient intermediate (E), in which the two *p* orbitals of carbon atoms 1 and 5 are coupled together with a *d* metal orbital[132]. This is illustrated in Figure 1-19.

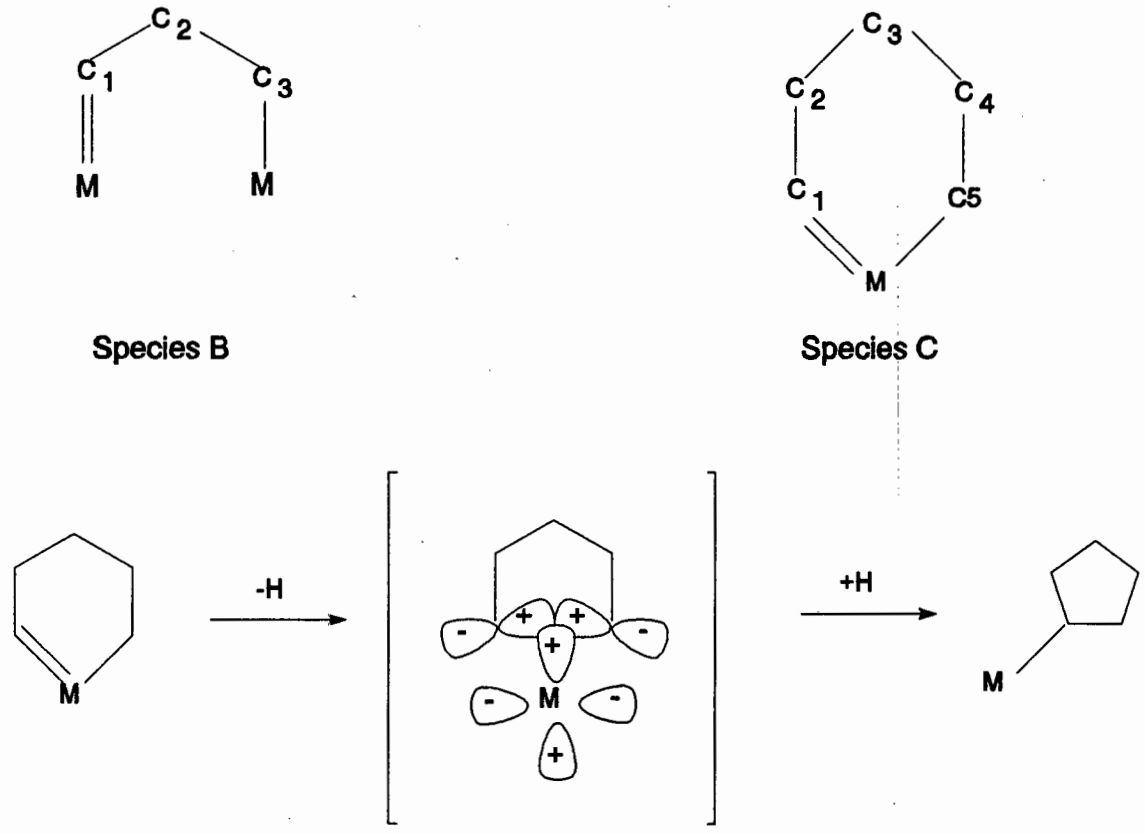

Figure 1-19 Reaction intermediates for pentane dehydrocyclization.

1.8.1.4 Hydrogenolysis

On platinum catalysts the activation energy for hydrogenolysis is very much larger for ethane than for larger molecules[133]. As ethane reacts at a considerably higher temperature range it was concluded that a mechanism involving a 1-2 adsorbed intermediate will not be of much importance in hydrogenolysis reactions over platinum for hydrocarbons other than ethane[133]. A mechanism involving a 1,3 adsorbed intermediate can operate for other hydrocarbons. Alkane isomerization is accompanied by hydrocracking and the activation energies for the two processes are identical. Thus both reactions proceed via a common intermediate and a bridged intermediate is suggested[134] as shown in Figure 1-20. Thus

hydrocracking may be represented by the failure to form a bond between C_1 and C_3, probably as a result of attack by a surface hydrogen atom at C_1. The slow step is the formation of the bridged intermediate B from the 1-3 adsorbed species A. This process requires two nearest neighbour surface platinum atoms.

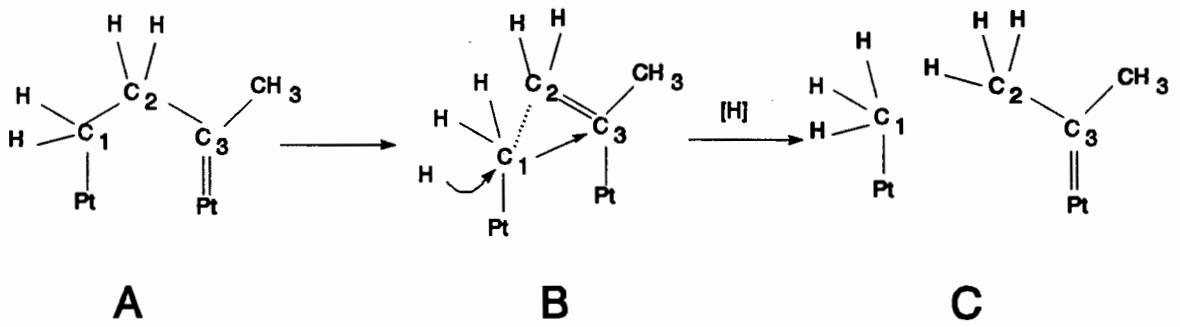

A B C

Figure 1-20 Bridged reaction pathway for hydrocracking

Another mechanism was proposed by Anderson and Shimoyama (1973)[135] to account for the formation of isopentane from 3-methylpentane as well as for the increase of the specific hydrogenolysis rate when the metal particle size decreases. These mechanisms, which involve a catalytically active site consisting of a single platinum atom, are referred to as π-alkene hydrogenolysis mechanisms (Figure 1-21). The species (E) and (G) could subsequently be hydrogenated off the surface. This mechanism explains why the overall hydrogenolysis rates decrease with increasing crystallite size.

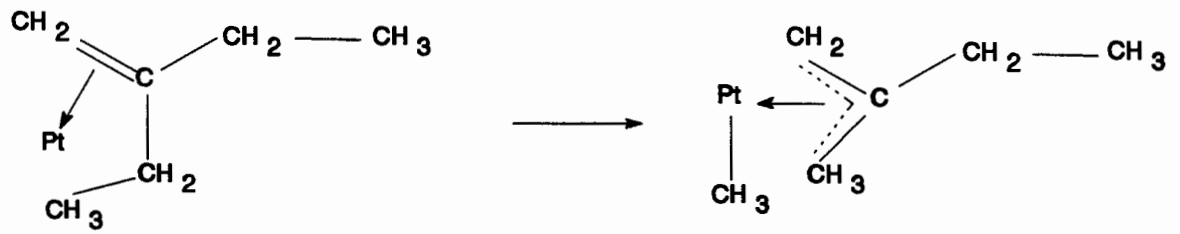

E G

Figure 1-21 π-Alkene hydrogenolysis mechanisms.

1.8.1.5 Dehydrocyclization

The stepwise mechanism of hexane dehydrocyclization was shown by kinetic[136] and radiotracer studies[137] to predominate over unsupported platinum-black. The same mechanism was also found over supported platinum catalysts[138]. TPD studies confirmed the stepwise n-hexane → n-hexadiene → benzene reaction sequence over platinum alumina[139]. The nature of the ring closure remained undecided. Three schemes were proposed[140]:

- (A) hexadiene → cyclohexene → cyclohexadiene → benzene
- (B) hexadiene → cyclohexadiene → benzene
- (C) hexadiene → hexatriene → cyclohexadiene → benzene

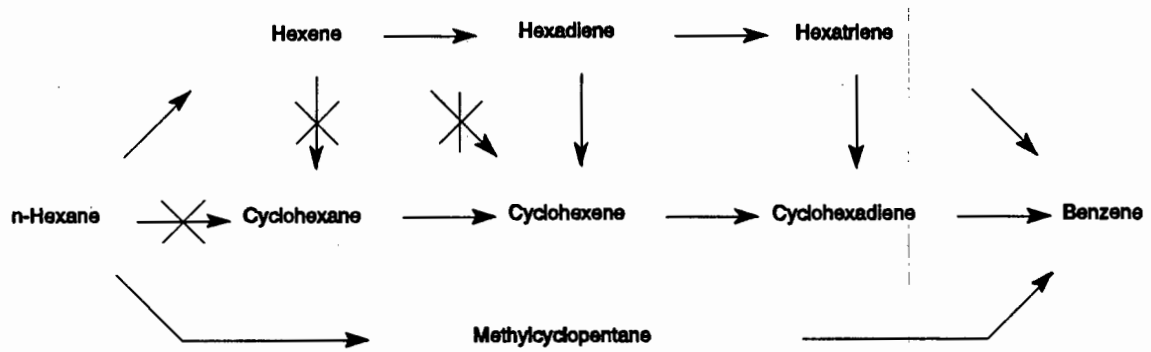

Figure 1-22 Reaction pathways for n-hexane on Pt/Al_2O_3 catalysts (Zimmer *et al.*, 1982)

All three schemes are theoretically equally possible. Radiotracer studies[141] disproved the reaction of hexadiene to cyclohexene (A) and gave evidence in favour of the formation of hexatriene (C)[142]. In addition 2,4-hexadiene gave benzene, practically without any hexatriene intermediate. Thus pathway (A) can be excluded, but both pathways (B) and (C) can be regarded as possible on the basis of catalytic studies.

The very large differences between the rates of cyclization of cis and trans

hexatriene isomers point to the importance of the trans to cis isomerization as one of the possible rate determining steps, especially in the absence of hydrogen[140]. Cyclization of cis-hexatriene proceeds easily, without any catalyst[136] at high temperatures (500°C).

The evidence from TPD and TPR data presented by Zimmer *et al.* (1982)[140] suggests that scheme (C) is the pathway for aromatization of n-hexane. However, two factors influencing the reaction pathway are:

- The amount of hydrogen available.
- The position of the double bond.

Aromatization activity and selectivity had maxima as a function of hydrogen partial pressure on platinum-black as well as for platinum on other supports[143]. Structural factors are more marked on unsupported platinum-black. Most conspicuous is the difference between 1-hexene and 2-hexene. The terminal double bond is more favourable for futher dissociation, *viz.* benzene formed from 1-hexene is generally more deeply dissociated than that from 2-hexene. Thus the dissociative adsorption of the terminal double bond of 1-hexene represents a pathway of higher barrier for benzene formation than for stepwise cyclization. The ample amount of hexadiene formed from 2-hexene and its easier aromatization point to the possibility of the cyclization of 2,4-hexadiene having two double bonds[140].

1.8.2 Metal particle size and reaction mechanism

The specific rates of a number of reactions have been shown to remain remarkably independent of the platinum dispersion. Examples include:

- dehydrogenation of cyclohexane[144]
- hydrogenolysis of cyclopentane[145]
- hydrogenolysis of cyclohexene[146]

- hydrogenation of cyclopropane[147]
- dehydrogenation of 1,1,3-trimethylcyclohexane[148]

The first reported case of a reaction with a large dependance of specific rate on catalyst crystal structure was for neopentane on platinum[149]. This led to the classification of reactions as:

- facile or structure-insensitive, for which the specific rate does not depend on the size of metal particles.

- demanding or structure sensitive, for which the specific rate is highly dependent on the metal dispersion.

Specific sites with special geometric requirements are involved in structure sensitive reactions, while all metal atoms of the surface are available for structure insensitive reactions. The dehydrocyclization of n-heptane on platinum catalysts is a structure sensitive reaction[150]. All reactions thus far discovered to be structure sensitive for the rate of reaction are also structure sensitive for selectivity, since the product distributions vary widely with the metal particle size. The isomerization of hexanes are typically structure sensitive for the selectivity in the sense that the cyclic mechanism is largely predominant on highly dispersed catalysts, while bond shift mechanism is the major reaction pathway on supported platinum catalysts with low dispersion[150].

1.8.2.1 Existence of different types of sites

Maire and Garin (1984)[120] suggest that there is good evidence that isomerization by bond shift and cyclic mechanisms involves different types of sites on a platinum surface. The percentage of cyclic mechanism in the isomerization of 2-methylpentane to 3-methylpentane remains constant as long as the mean platinum particle diameter, d, is larger than 1-2 nm and increases steeply for more highly dispersed catalysts. This observed increase in the percentage of cyclic

mechanism with decrease in platinum particle is taken as evidence that there are two types of platinum sites active for cyclic and bond shift mechanisms. For the most highly dispersed catalysts the proportion of bond shift becomes negligibly small. However, the constancy of the proportion of cyclic mechanism for d between 2 and 15 nm suggests that the sites responsible for bond shift and cyclic mechanisms are topographically similar, both involving either face or edge atoms[120].

1.8.2.2 Weak and strong adsorption sites

It can be assumed that all superficial atoms are available for weak adsorption and may be used for reactions in which only C-H bond fission and formation take place, and that sites required for isomerization and cyclopentane hydrogenolysis involve strong adsorption and hence C-C bond fission and formation. The latter case may involve sites on very specific parts of the metal crystallites, *e.g.* the edge. If the weakly adsorbed species are precursors of the strongly adsorbed species then the following sequence of reactions has been proposed[120]:

(1) Indiscriminate adsorption of a gaseous molecule on a crystal face site of the metal to form a weakly adsorbed molecule.

(2) Superficial migration from the adsorption site S_A to a reactive site S_R located on some specific region of the metal particle.

(3) Formation on the reactive site of a highly dehydrogenated species.

(4) Skeletal rearrangement of this strongly adsorbed species.

(5) Rehydrogenation of the strongly adsorbed species, superficial migration and desorption of the weakly adsorbed molecule, to yield the reaction products.

Weak indiscriminate adsorption (step 1) and superficial migration (step 2) could be much faster than strong adsorption (step 3) and the surface reaction (step 4). Thus the rate determining step in isomerization was proposed[120] to be reactions (3) and (4) which occur on active sites, S_R. Kinetic data for the isomerization of hexanes[151] strongly suggests that the rate determining step is surface reaction (step 4), while successive dehydrogenation species are equilibrated.

1.8.2.3 Relationships between selectivity and specific rates

The model proposed above accounts for the various situations which arise concerning the dependence of specific rates and selectivity on the size of the metal species (This is shown schematically on the following page).

On most crystallites the total number N_R of reactive sites S_R is much larger than the number N^*_A of weakly adsorbed hydrocarbon molecules since only a small fraction of the catalyst surface is covered by chemisorbed alkanes. Only some of the available reactive sites are occupied, N^*_R, which is proportional to the number of weakly adsorbed molecules, N^*_A. Since N^*_A is proportional to the number of superficial metal atoms, N_S, the number of reacted molecules is hence proportional to N_S. Therefore the turnover number is expected to be independent of the size of the metal crystallites. However, distribution of the various reaction sites, N_{R1}, N_{R2}, ... ($\Sigma N_{Ri} = N_R$), associated with various parallel reaction pathways, generally depends on the size of the metal particles. This explains the situation where the selectivity varies widely with metal dispersion, while the specific rate remains constant.

A second possibility is that the number N_R of reactive sites of any type is much smaller than the number N^*_A of weakly adsorbed hydrocarbons. All the reactive sites are then occupied ($N^*_R = N_R$) and consequently the number of reacted molecules is no longer proportional to either the number of weakly adsorbed hydrocarbon, N^*_A or the number of superficial metal atoms. In this case not only the selectivity, but also the specific rate depends upon the metal particle size. This

situation, which is that of the structure sensitive reaction rate, arises especially when the change in particle size has been obtained by sintering a supported metal catalyst. The effect of sintering is to smooth the metal surface, thus reducing the number of the irregularities (steps, kinks, etc.) with which the reactive sites may be associated.

This discussion is best shown schematically, where:

N_S : number of superficial metal atoms
N_R : number of reaction sites
N^*_A : number of weakly adsorbed hydrocarbons
N^*_R : number of occupied reactive sites

Case 1 $N_R \gg N^*_A$ ∵ only a small fraction of catalyst covered
$\Rightarrow N^*_R \propto N^*_A$
also $N^*_A \propto N_S$
$\therefore$ number reacted molecules $\propto N_S$

Case 2 $N_R \ll N^*_A$
$\Rightarrow N^*_R = N_R$
$\Rightarrow$ number reacted molecules not $\propto N^*_A$ nor N_S

A third scenario is that the rate of superficial migration becomes much smaller than the rate of weak adsorption or desorption. In this case the molecules adsorbed in the vicinity of the active site may be strongly adsorbed and react. The reaction rate is proportional to the number of reactive sites and not to the total number of surface atoms, so that the reaction is again structure sensitive for the rate.

1.8.2.4 Bonding energy of small platinum clusters

It is well known that the free energy of small metal clusters is significantly higher

than that of bulk metal and that the former are highly reactive[166]. The reason for this is the smaller number of bonds per metal atom in the clusters compared to the bulk metal. The atomization energy for Pt_2 was shown experimentally by Gingerich (1980)[152] to be only 340-360 kJ/mol compared to 570 kJ/mol for the bulk metal[153]. Moreover, for small metal clusters, the strength of the Pt-Pt bond may be lower than that in the bulk metal. In the case of transition metal clusters containing less than 15-20 atoms the average bond energy may be 2-3 times lower than that for the bulk metal[154], which is slightly higher than that reported by Gingerich et al. (1985)[155]. The energy passes through a minimum for clusters containing 6-10 atoms and reaches the values specific for bulk metal for clusters of 20-30 atoms. The platinum clusters in Pt/KL are extremely small, possibly containing only 5-6 atoms[172,156].

1.8.3 Reactions of carbon monoxide on platinum

As carbon monoxide was detected as a reaction product for the reactions of oxygenated compounds over Pt/KL it is of interest to examine the reactivity of platinum towards CO. Stakheev and Kappers (1995)[166] report that it can be expected that a substantial fraction of the platinum particles inside the KL zeolite are highly reactive towards CO. Lower Pt-Pt bond energy for these clusters facilitates the disruption of Pt-Pt bonds, followed by the formation of CO bonds in the course of platinum-carbonyl formation.

Carbon monoxide is one the principal products in any process that involves partial oxidation (or gasification) of methane, coal, shale oil, etc. The subsequent hydrogenation of CO to form a range of products is of importance economically, the major problem being to control the selective production of the desired products. During the overall process the reaction between CO and water is important, via the water gas shift reaction, which is used to control H_2/CO ratio in the gas stream:

- $CO + H_2O \rightarrow CO_2 + H_2$ water gas shift

- $CH_4 + H_2O \longleftrightarrow CO + 3H_2$ steam reforming (the forward reaction dominates at reaction temperatures > 700°C)

1.8.3.1 The CO molecule and chemisorption[157]

The CO molecule is isoelectronic with the N_2 molecule, however, localization occurs with the orbitals of lower energy existing on the more electronegative oxygen atom. A comparison of the molecular orbital energy levels of N_2 and CO are shown in Figure 1-23.

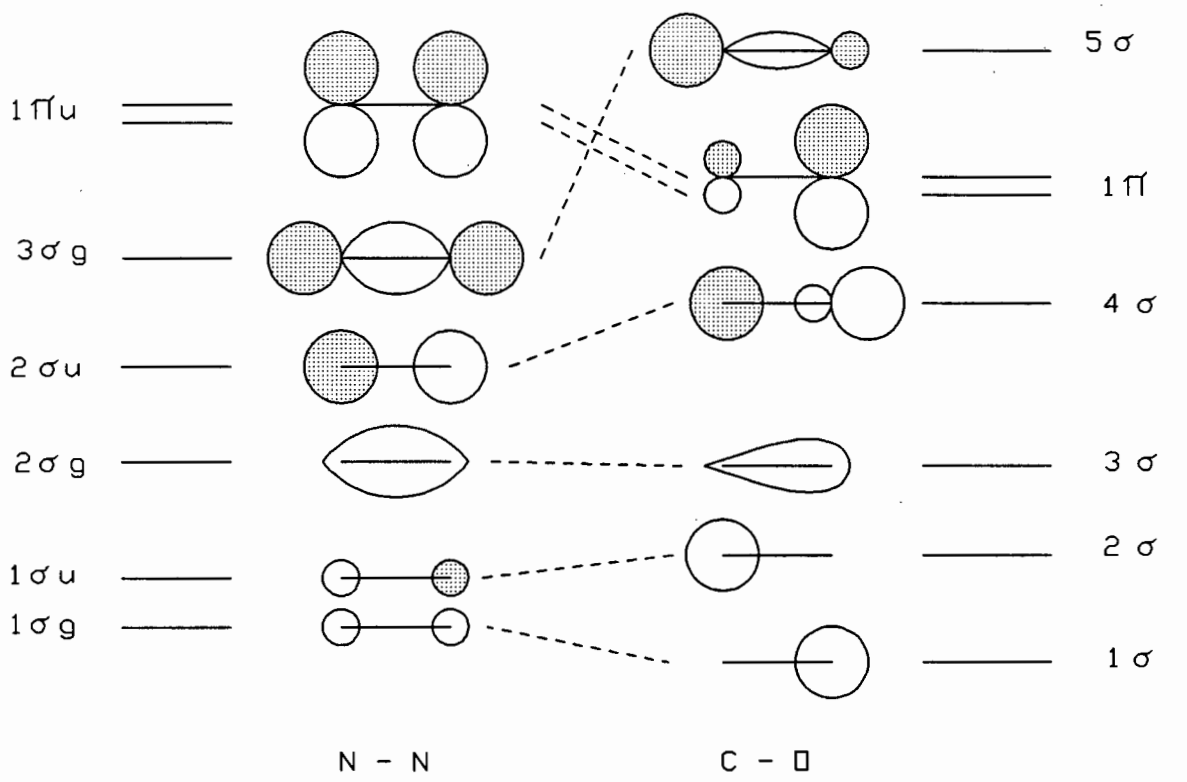

Figure 1-23 Comparison of N_2 and CO molecular orbital energy levels

The CO molecule has a poorly localized oxygen lone pair character, which results in the small dipole moment of CO. This is responsible for allowing a strong interaction between CO and metal surfaces since it has the high energy and requisite direction character to donate electrons into empty metal orbitals. The antibonding 2π orbitals, which represent the next higher level and tend to be localized on the carbon atom facilitates back donation from the metal to the CO molecule[158].

Any catalytic event on a solid surface must be preceded by an adsorption step which significantly perturbs the electronic structure of the surface. The formation of a bond between CO and a transition metal is widely thought to occur according to the Blyholder model[159] which invokes a donor-acceptor mechanism qualitatively similar to the bonding of metal-carbonyl clusters[160]. In this model the bond occurs through a concerted electron transfer from the highest filled (5σ) molecular orbitals of CO to unoccupied metal d orbitals with back donation occurring from occupied metal orbitals to the lowest unfilled (2π) orbital of CO. This process is illustrated schematically in Figure 1-24 (Broden *et al.*, 1976)[161].

Thus, as a first approximation, the transfer electrons from the 5σ orbitals will not significantly effect the C-O bond strength in the chemisorbed state[162]. However the 2π orbitals are anti-bonding and back donation into these orbitals will tend to weaken the C-O bond.

1.8.3.2 CO adsorbed on platinum metal surfaces

A summary by Frotzhein *et al.* (1977)[163] and Hopster and Ibach (1978)[164] of different studies of the adsorption of CO on platinum surfaces suggests a model for the coordination of CO molecules on close packed surfaces which assumes single coordination bonding on top of platinum at low coverage followed by bridged bonding at higher coverage. This model reconciles infrared (IR) and electron energy loss spectroscopy (EELS) patterns and predicts 1-fold coordination instead of 3-fold coordination at low coverages of platinum. This is due to the different bonding

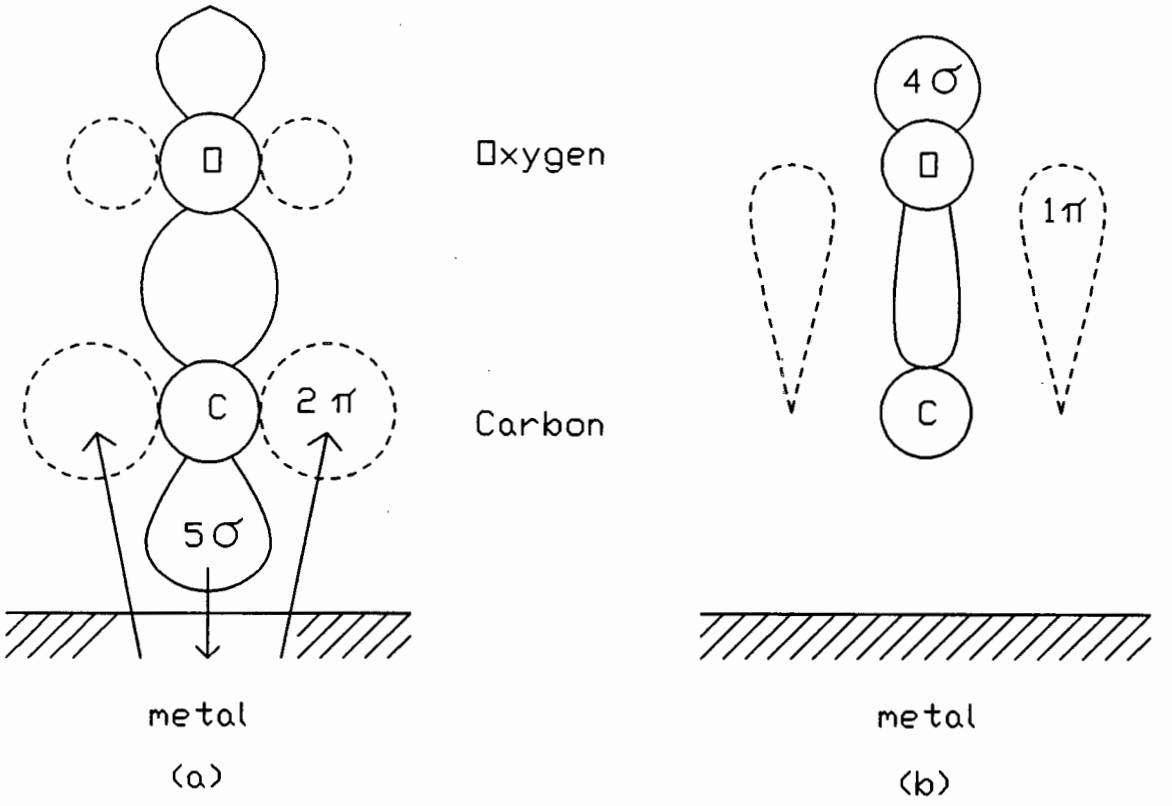

Figure 1-24 The chemisorption of CO on a metal surface involves the 5σ and 2π orbitals (a), with insignificant participation of the 4σ and 1π orbitals (b) (Broden *et al.*, 1976)

energies of linear and bridged CO, *viz.* bridged CO has a lower bonding energy on platinum (111) surfaces than linearly bonded CO.

1.8.3.3 Infrared spectroscopy of CO adsorbed on Pt/KL catalysts

Several studies have revealed that platinum dispersed on KL zeolite exhibits unusual adsorption sites for carbon monoxide. These sites are distinguished by a series of peaks appearing between 2050 and 1950 cm^{-1} in the infrared spectrum. It has been suggested that these bands are due to CO adsorbed on platinum clusters which are disturbed by their close proximity to the zeolite lattice. Through interactions with the framework oxygen, and possibly also involving protons, the electronic states of the platinum particles are changed, causing the infrared bands to shift to lower frequency[189].

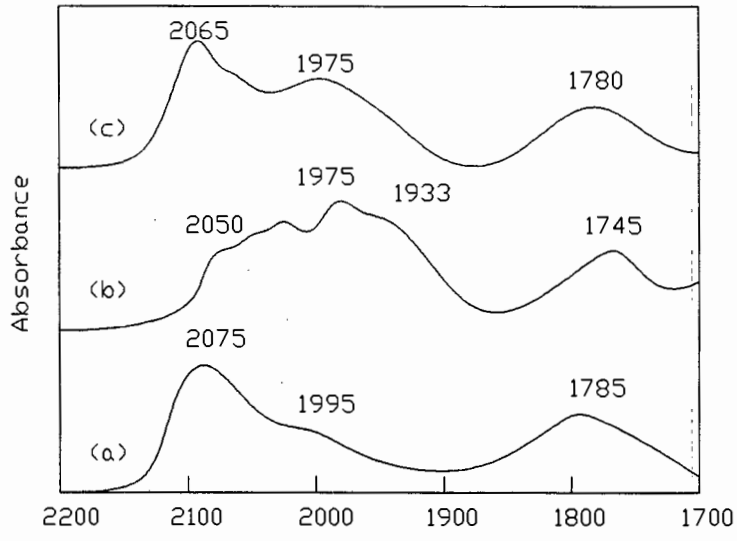

Figure 1-25 IR spectra of CO adsorbed on 0.76% Pt/NaBaL

When CO was adsorbed on Pt/BaL (Figure 1-25) a series of infrared peaks between 2050 and 1950 cm^{-1} were not observed after exposure to CO at 25°C (a), but instead appeared when the catalyst was heated to 225°C (b), and remained after it was cooled to room temperature (c). However, when the sample was exposed to several Torr of oxygen at 65°C, the peaks disappeared in a few minutes. It was proposed that the bands between 2050 and 1950 cm^{-1} are due to CO adsorbed on platinum in which the oxygen atoms of the CO molecules weakly bond to zeolite cations. Heating may be required to allow platinum atoms and CO molecules to move into positions that may facilitate bonding to the zeolite. Oxygen adsorption apparently rapidly destroys this arrangement[189].

Figure 1-25 shows the IR spectra for a saturation coverage of CO on 0.76% Pt/NaBaL at 25°C and 225°C. Two broad adsorptions appear in all three spectra. The first band (2100-1900cm^{-1}) is due to CO adsorbed on platinum. The second band (1900-1700cm^{-1}) is due to either some form of bridge-bonded CO on platinum or to a carbonate species adsorbed on the support. This latter feature was not observed when the zeolite support was exposed to CO. At room temperature the

IR band for CO adsorbed on platinum consists of a main peak at 2075cm^{-1} and shoulders at 2115 and 1955 cm^{-1}. The peak at 2075cm^{-1} is characteristic of CO adsorbed on supported platinum catalysts such as Pt/SiO_2 and Pt/Al_2O_3. This feature is due to adsorption on platinum clusters inside the pores. The platinum clusters do not interact strongly with the zeolite lattice since the position of the this peak is no different from that observed for conventional catalysts[189]. The shoulder at 2115 cm^{-1} may be assigned to one of two adsorption sites. The first possibility is on large platinum particles outside the pores, since the peak frequency is the same as that observed at saturation coverage of CO on Pt(111). The second possibility is platinum atoms on the small clusters adjacent to oxygen atoms of the zeolite lattice. Additional results indicate that this assignment is most likely correct. The other shoulder in the spectrum at 1995cm^{-1} is assigned to CO adsorbed on platinum clusters which interact strongly with the zeolite walls[189].

The appearance of overlapping bands indicates that heating the sample generates new adsorption sites for CO on the platinum clusters (b and c). It was concluded that the new adsorption sites are formed by restructuring the CO covered platinum clusters in such a way that they interact strongly with the zeolite walls[189].

IR spectra of CO adsorbed on a series of 0.6wt% Pt/BaL catalysts at 25°C are shown in Figure 1-26. Each catalyst exhibits a broad band near 2050cm^{-1} due to CO adsorbed on platinum clusters. The position of the band shifts from 2065 to 2020cm^{-1} as the alkali element is changed from Li to Cs. This shift may be ascribed to the electronic interaction between the platinum clusters and supports. The heavier alkali elements negatively polarize the platinum clusters. The increased charge on the platinum leads to more back donation of electron into the CO π^* orbital and a downward shift in frequency. An analogous effect is observed for CO adsorbed on platinum in acidic Y zeolites, where the IR bands shift up in frequency with increasing acidity of the support[189].

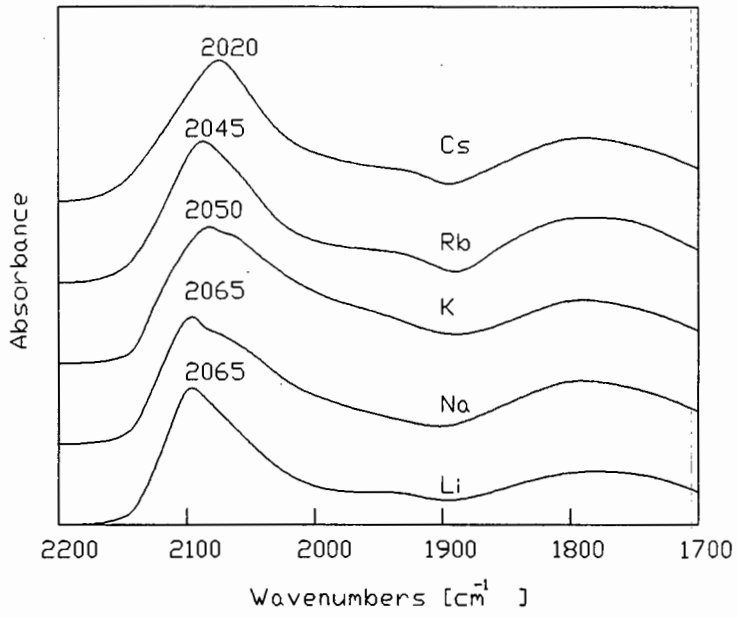

Figure 1-26 IR spectra of CO adsorbed on 0.6wt% Pt/BaL at 25°C

FTIR spectra of Pt/KL samples were measured in the region of the stretching vibration of hydroxyl groups[165]. An intense band at 3740 cm^{-1} is ascribed to terminal silanols located at the external surface of the zeolite. Bands at 3690 cm^{-1} are assigned to nonacidic hydroxyl groups and bands in the region 3650-3630 cm^{-1} are assigned to acidic bridging hydroxyls. Both acidic and nonacidic hydroxyls are produced during reduction of platinum ions. These bands are weak for all the Pt/KL samples studied[165]. For CO adsorbed on Pt/KL the predominant band is in the range 2070-1950 cm^{-1} with maxima at 2067, 2051, 2031, 2008, 1998, and 1979 cm^{-1}. These are due to linearly bonded CO on platinum and show remarkable dependence on sample preparation. Bands which may be attributed to bonding CO are very weak and the band typical for CO adsorbed on large platinum particles is absent. The total intensity of the bands attributed to platinum carbonyls 2067-1760 cm^{-1} is significantly higher for catalysts prepared by incipient wetness than by impregnation, indicating the former have a much higher dispersion[165]. The results can be rationalized in terms of different electronic states of Pt. A low frequency for platinum carbonyls is indicative of the low extent of electron deficiency of the platinum particles, which is a result of the formation of Pt-proton

adducts. In the absence of protons (catalysts prepared by incipient wetness and by back exchanging with KCl) the positive charge on the platinum particles is expected to be low, which is in agreement with the low frequency bands[165].

The formation of platinum carbonyls, at room temperature, has been inferred from infrared data of CO adsorbed on Pt/KL was reported by Stakheev *et al.* (1995)[166]. The temperature of CO adsorbtion was 25°C. The formation of Pt-carbonyl species leads to drastic transformation of Pt/CO stoichiometry. This conclusion is supported in the work of Kappers *et al.* (1991)[167] and Kustov *et al.* (1991)[168]. The formation of neutral platinum carbonyls in zeolites has not been previously reported, however, the formation of anionic carbonyl complexes[169] may also be excluded as the infrared spectra for bridged and linearly bonded CO are different to those observed. At present it is only possible to speculate on the possible structure of platinum-carbonyl complexes. Platinum complexes containing only CO ligands are unknown or very unstable[170] and $Pt(CO)_4$ has been prepared only under low temperature conditions[171]. However, the complex is stabilized by σ-donation, normally by PPh_3 ligand substitution. Since the oxygen atoms in the KL zeolite exhibit strong basic properties, it can be assumed that they act as σ-donor ligands and stabilize a platinum-carbonyl species of the following structure:

$$(Zeol\text{-}O:)_m Pt_x(CO)_y$$

Evidence for this interaction was inferred from EXAFS data, which indicate that small particles of platinum are coordinated with framework oxygen. The existence of a Pt-O bond was found for both Pt/H-ZSM-5 and Pt/KL[172] with a distance of 2.06 Å - 2.14 Å. Recently a Pt-O bond length of 2.04 Å has been confirmed from EXAFS measurements[166]. These are comparable to a P-Pt distance of 2.25 Å reported from platinum complexes containing phosphine ligands[173] if the smaller radius of the oxygen atoms is accounted for. Metal-carbonyl species exhibit high mobility inside zeolite micropores which can lead to redistribution and agglomeration of the metal[174]. This agglomeration occurs both on the outer surface and inside the channels and occurs at elevated temperature of *ca.* 500°C.

Platinum particle growth occurs at the expense of the finest particles which are reactive towards platinum-carbonyl formation and causes a decrease in the number of platinum carbonyls.

1.8.4 Reactions of oxygenated compounds

1.8.4.1 Alcohols

On acidic catalysts, alcohols are dehydrated to form alkenes and water. However, on non-acidic metal catalysts, dehydrogenation to form aldehydes (from primary alcohols) or ketones (from secondary alcohols) can occur. Tertiary alcohols cannot be easily dehydrogenated. In the presence of hydrogen, hydrogenation to form an alkane and water should occur. Aldehydes and ketones can be reduced by catalytic hydrogenation to form alcohols or by complete reduction to form alkanes and water. It is reported that platinum dispersed on basic KL zeolite exhibited dehydrogenation activity in isopropanol decomposition (to acetone)[175], while platinum supported on acidic NH_4L zeolite enhanced the conversion of isopropanol to form water and propene. Isopropanol can be dehydrated over acid sites or dehydrogenated over basic sites[176]. At 225°C almost 100% conversion of isopropanol to propene only occurred on NH_4L. At the same reaction temperature the conversion of isopropanol on KL was 12% with a selectivity of 41% to acetone and 59% to propene. Platinum, loaded on NH_4L, was found to suppress dehydration and to accelerate the dehydrogenation reaction to acetone (94.2% selectivity). Interestingly, the Pt/KL exhibited less sensitivity to thiophene poisoning for the isopropanol reaction relative to the n-hexane aromatization reaction[175]. The NH_4L zeolite deactivated rapidly during isopropanol conversion, even in hydrogen atmosphere. This was presumably due to coke formation on acid sites. The Pt/NH_4L kept it's high activity (100% conversion of isopropanol at 170°C) under the same reaction conditions with hydrogen as the carrier gas. With helium as the carrier gas rapid deactivation was observed. The authors[175] ascribe the positive effect of platinum in maintaining the catalyst activity as being due to "platinum

keeping the acid sites clean". Coke precursors on the acid sites are removed by platinum catalyzed reaction with hydrogen[177].

1.8.4.2 Carbonyl compounds

Acetone is a common molecule used for studying the reaction of carbonyl compounds on metals. Isopropanol and propane are the two primary products of hydrogenation of acetone over transition metals (Chen and Chen, 1996)[178]. Isopropanol is observed at near 100% selectivity on most transition metals at low reaction temperatures (25°C). Propane is formed in detectable amounts on platinum foils, platinum films and unsupported platinum powders as well as platinum supported on SiO_2. A fully reduced platinum catalyst that exhibits stronger catalytic activity only catalyzes mild hydrogenation of acetone to isopropanol. A partially oxidised catalyst exhibits greater activity for hydrogenation of acetone to propane. These reactions took place at 25°C with a molar ratio of hydrogen to acetone of 2. The enhancement of propane formation from the acetone hydrogenation reaction by oxygen perturbed platinum catalysts is a general phenomenon that can be extended to increase the selectivity toward methylene group formation from ketone hydrogenation reactions. This behaviour is more pronounced when aromatic substituent ligands exist in ketone compounds, *i.e.* benzaldehyde. A non-zero extrapolated value of the methylene group formation rate to zero conversion of ketones on platinum catalysts, suggests that alcohols are not necessary as an intermediate for the production of alkanes from ketones. The formation of alkanes and alcohols may hence proceed by parallel reaction pathways[178].

1.9 Review of Chemisorption on Pt/KL Catalysts

Gas molecules which collide with a surface may stick to it for a short interval. This excess of gas on the surface is regarded as the adsorbed amount. There are no special adsorption forces. The intermolecular forces or van der Waals forces are well known to cause cohesion of molecules in liquids and solids. These forces cause physical adsorption of a gas on a solid. Similarly the valency forces which lead to combinations of chemical elements to form compounds can also cause surface combinations between elements on the surface of a solid, as well as adsorption or chemisorption. Physical adsorption is nonselective. For example nitrogen can adsorb on any surface at sufficiently low temperatures ($<100K$). Although adsorption of nitrogen and other gases at low temperatures may lead to multilayer adsorption on a solid substance, a value for only the unimolecular coverage of the entire surface may be derived from the adsorption data. This is the basis of the Brunauer-Emmet-Teller (BET) method for the determination of the total surface area of finely divided solids. Emmet and Brunauer later developed specific chemisorption methods to measure areas of distinctly different chemical species exposed on the surface[179].

Chemisorption of hydrogen on platinum is instantaneous at ambient temperature and it readily reaches a complete monolayer coverage on the exposed platinum surface. However, the following conditions must be fulfilled to measure the extent of platinum surface coverage:

- The H/Pt stoichiometry is mostly assumed to be unity and a site density for H atoms on a platinum surface or the effective area per H atom on the surface is experimentally determined.

- Physical adsorption on the metal surface and on the support surface is negligible. This is reasonable for hydrogen, but for nitrogen and CO a correction for physical adsorption must be subtracted from the totally measured adsorption.

- The chemisorption of H_2 should occur without further complications, like dissolution of hydrogen into the metal, spillover of hydrogen from the metal to the support, strong metal-support interactions, etc. Such complications can cause deviation from the H/Pt ratio of unity.

In 1965 Benson and Boudart[180] introduced a surface gas tritration method as a measure of the dispersion of supported platinum. This method is based on the chemisorption of O_2 on the surface, and the subsequent reaction of H_2 with the oxygen (or vice versa). All these surface reactions are carried out at room temperature. The stoichiometries are as follows:

$Pt + \frac{1}{2}H_2$	→	Pt-H	(H chemisorption, HC)
$Pt + \frac{1}{2}O_2$	→	Pt-O	(O chemisorption, OC)
$Pt\text{-}O + 1\frac{1}{2}H_2$	→	$Pt\text{-}H + H_2O$	(H tritration, HT)
$2Pt\text{-}H + 1\frac{1}{2}O_2$	→	$2Pt\text{-}O + H_2O$	(O tritration, OT)

In the case of Pt/Al_2O_3 catalysts, the water is retained on the alumina and does not interfere with the tritration. There has been considerable controversy as to the exact stoichiometry (HC:OC:HT) of the tritration reactions[181]. Much of this controvery was attributed to research groups using the very first H_2 chemisorption on the freshly reduced catalyst as the basis for all calculations. However, this first value is often not reproducible since the surface was still in a metastable condition after reduction. More reproducible results could be obtained after the sample had been annealed by a few H_2-O_2 cycles[181]. The stoichiometry of HC:OC:HT was always found to be 1:1:3 if the H_2 titer values were used as the basis for calculations. This was independent of the platinum crystallite size and independent of pretreatment of the catalysts. Recent studies[182],[183] have suggested that residual hydrogen retained on supported platinum catalysts after a reduction is responsible for the metastable condition of freshly reduced platinum catalysts.

Hydrogen to metal (H/M) ratios commonly exceed unity for platinum and often exceed 2 for highly dispersed platinum, rhodium and iridium supported on Al_2O_3

and SiO_2. Since the coordination of hydrogen to metal atoms is unknown for highly dispersed catalysts, the metal surface area of these catalysts cannot be calculated from hydrogen chemisorption values[184]. EXAFS measurements were performed to determine metal particle size and thereby calibrate hydrogen chemisorption results. The H/M ratio determined by chemisorption is a linear function of the average metal coordination number determined by EXAFS[184]. This linear relationship is independent of support and varies with the H/M ratio, increasing in the order Pt<RH<Ir. Spillover and subsurface hydrogen are excluded as explanations and only multiple adsorption of hydrogen on metal surface atoms is capable of explaining the experimental observations[184].

Selective chemisorption of gaseous molecules, especially hydrogen, has been extensively used to estimate the degree of dispersion of group VIII metal catalysts. Chemisorption methods are of special importance since it is often difficult to determine the degree of dispersion by other techniques such as XRD or electron microscopy measurements. Hydrogen chemisorption data can be directly used to compare dispersions of a metal in different catalysts in a relative way. However, to calculate metal surface areas in an absolute manner the hydrogen to metal stoichiometry must be known. For platinum metal the H/M stoichiometry of one has been used and this assumption has been justified by calibration with XRD and TEM[184]. Surface science studies furthermore proved that a maximum of one hydrogen atom per metal atom could be chemisorbed on the (111) faces of fcc metal single crystals. Under the assumption that the surface of metal particles larger than 2 nm consist mainly of (111) faces it is understandable that the empirical assumption of H/M = 1 was successful in many early studies. However, in the 1960's data began to appear in the literature with stoichiometries exceeding one. The value of H/Pt = 1.5 -1.65 has been measured for Pt/Al_2O_3 catalysts and H/Pt = 1.3 - 1.6 have been quoted for Pt/SiO_2 catalysts, while a value of H/Pt = 2 has been observed for platinum deposited on a zeolite[184].

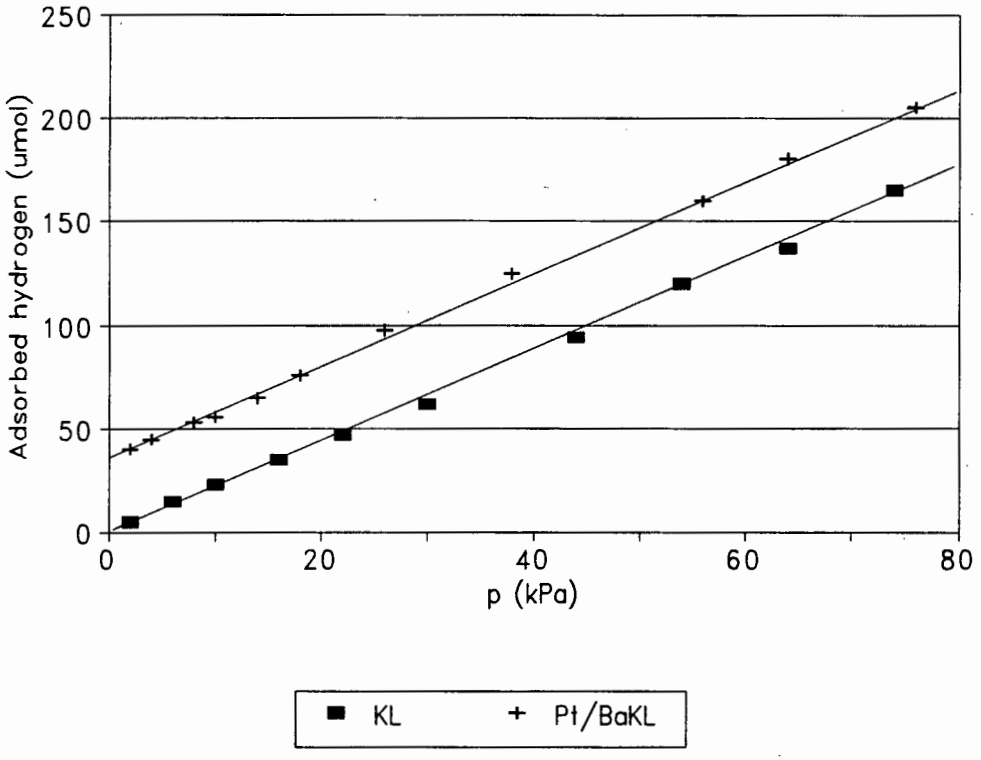

Figure 1-27 Desorption isotherms for hydrogen adsorbed on 0.867g Pt/BaKL (1.2 wt% platinum) and KL zeolite catalysts at room temperature (Vaarkamp *et al.*, 1990)

The ratio of H/Pt can be used as a rough guide to average platinum cluster size. For clusters greater than about 1 nm in average diameter, the stoichiometry of hydrogen to platinum surface atoms is about one. However, H/Pt ratios exceeding unity have been found for many catalysts. Vaarkamp *et al.* (1990)[185] reported H/Pt ratios of 1.3 for platinum clusters in BaKL (Figure 1-27). The mass of the catalyst was 0.867g with a platinum loading of 1.2% by mass (0.0104g platinum). Extrapolation by linear least squares fitting of the data of Pt/BaKL (*ca.* 35 μmol H_2) gives a H/Pt ratio of 1.3. The chemisorption of hydrogen on the support was negligible. An average Pt-Pt coordination number of 3.7 determined by EXAFS for the same sample was consistent with platinum clusters composed of only 5 or 6 atoms. The H/Pt ratio was correlated with average Pt-Pt coordination number and

showed that H/Pt ratios greater than unity contain information on relative cluster sizes[186].

The occurrence of electronic effects in supported metal catalysts and their influence on catalytic properties has been a matter of controversy for many years. An example is the case of very small metal particles encaged in the internal pores of zeolites. In addition to the intrinsic electronic effects due to the small size exhibited by the metal particles, a modification of the electronic structure of the metal by the different environment provided by the support should be considered. In the case of zeolites this kind of metal support interaction may be more pronounced than on non-zeolite supports because the particle may interact with the zeolite cage over a substantial fraction of its surface. Larsen and Haller (1989)[187] report that there is empirical evidence from chemisorption and reaction chemistry that the different direction of electron transfer between the platinum particle and the zeolite support may be a reality and have catalytic consequences. The H_2 and CO chemisorption results[187] for a series of Pt/L catalysts are shown in Table 1-13.

Table 1-13 Hydrogen and carbon monoxide chemisorption data (Larsen and Haller, 1989)

Catalyst	H/Pt	CO/Pt
Pt/KL	1.10	0.47
Pt/MgL	1.12	0.45
Pt/CaL	1.17	0.34
Pt/BaL	1.15	0.29

Hydrogen chemisorption suggests that platinum particle dispersion is not much affected by exchange of cations and that all the platinum particles are still accessible. However, CO adsorption is more interesting since the capacity is changed. CO/Pt decreases systematically as the ratio of radius to charge is increased for the alkaline earth metals. There appears to be significant decrease in the CO chemisorption capacity and the hydrogen chemisorption suggests that this

is unlikely to be a result of accessibility of platinum particles because no change is noted for H_2. If replacement of Mg by Ca or Ba exchange resulted in increasing electron transfer to Pt, it might be expected to inhibit CO chemisorption in the order Ba > Ca > Mg, as observed, since the primary bond to platinum is by electron donation from the 5σ orbital to Pt. However, this should also affect the hydrogen chemisorption[188].

Larsen and Haller (1992)[25] report that CO/H ratios of 0.7 are observed for Pt/L, independent of particle size, for H_2 and CO chemisorption on a series of Pt/L catalysts prepared with different platinum dispersions (Figure 1-28). Previous results from their work indicate that 30% of hydrogen adsorbed on Pt/L catalysts can be removed by room temperature evacuation. They ascribe the difference between H/Pt and CO/Pt adsorption stoichiometries to the presence of some degree of reversiblity in the H_2 uptakes at 298K (25°C). However, if one corrects for this 30% then the CO/H ratio would be $\approx$ 1. When H/Pt ratios are plotted against the corresponding EXAFS-derived coordination numbers, a nearly linear relationship is found. These results are in agreement with those reported for Pt/Al_2O_3 catalysts[25].

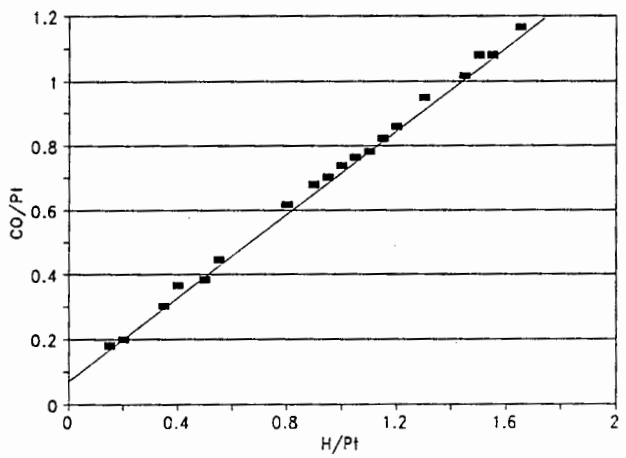

Figure 1-28 Linear relationship between CO and H_2 chemisorption on Pt/L (Larsen and Haller, 1989)

Platinum dispersions of 0.6wt% Pt/BaL were determined by hydrogen tritration of adsorbed oxygen by Han *et al.* (1993)[189]. To check the consistency of these results against other chemisorption methods, hydrogen and CO adsorption isotherms were recorded. In addition H_2 tritration, H_2 adsorption and CO adsorption isotherms were recorded for NaBaL support. The isotherms of the support yielded straight lines which intersected the origin at zero uptake for CO adsorption. The platinum dispersions measured by hydrogen tritration, hydrogen adsorption and CO adsorption were 50%, 54% and 51% respectively, assuming reaction stoichiometries for H/PtO_s, H/Pt and CO/Pt_s are 3,1,1 respectively. The latter value for CO is obtained in the case where the support adsorption isotherm is subtracted from the catalyst adsorption isotherm. The results show good consistency among the different chemisorption techniques. Thus hydrogen tritration of adsorbed oxygen is a suitable method for estimating the platinum dispersion[189].

Lane *et al.* (1991)[190] has reported that TEM data has shown that platinum clusters in L zeolite are much smaller than in Y zeolite. However, CO chemisorption results showed the same CO/Pt ratio on Pt/KL and Pt/KY samples. Their calculations for turnover frequency (TOF) assume that only sites capable of chemisorbing CO are accessible for n-hexane[190,186]. They report that calculations based on CO chemisorption overestimate platinum particle size (*i.e.* underestimate platinum dispersion). Hydrogen chemisorption values are about a factor of three higher than CO chemisorption for L zeolite catalysts[190]. When Larsen and Haller[187] studied platinum clusters on a series of alkaline zeolites, they found the CO/Pt ratio varied strongly with cation while the H/Pt ratio remained constant. Their results show that CO chemisorption data should not be used to determine platinum cluster sizes in Pt/L catalysts and cast doubt on basing turn over frequencies (TOF) on CO chemisorption[187,186].

In the literature, several explanations have been given for H/M values exceeding unity. Often a distinction has been made between reversibly and irreversibly adsorbed hydrogen. In many cases only the irreversibly adsorbed hydrogen has been assumed to be important for the determination of metal surface area. Several

authors have ascribed the high H/M values to hydrogen spillover to the support or to an increased hydrogen-to-metal stoichiometry for metal atoms situated at the corners and edges of the small metal particles. Another explanation has been the positioning of part of the hydrogen under the surface of the metal particle. However, Kip *et al.* (1987)[184] reports that only multiple adsorption of hydrogen on metal surface atoms can explain all experimental observations.

Several effects which could explain high H/M ratios were excluded as discussed below[184]:

- Unreduced M^{n+} was not present, as can be concluded from TPR experiments. All metal was reduced to M^0.

- Contamination of the catalysts with carbon did not occur. Elemental analysis showed that no carbon deposits existed initially on the catalyst. TPD values resulted in high H/M values.

- Partial reoxidation during outgassing at high temperature can be excluded because oxygen consumption during oxidation at 773K (500°C) after reduction and evacuation at 773K was measured to be O/Ir = 1.96 for 1.5wt% Ir/Al_2O_3. IrO_2 is the most stable oxide of iridium and hence Ir was in the zero valent state after reduction.

In a recent paper Ehwald and Leibnitz (1996)[191] showed that the activation energy for desorption of hydrogen chemisorbed on platinum dispersed on alumina, depends strongly on hydrogen surface coverage. The hydrogen chemisorption was investigated by temperature programmed desorption (TPD). Exposure of the reduced Pt/Al_2O_3 catalyst to trace amounts of water results in hydrogen desorption, even if no hydrogen was previously adsorbed. These results were explained in the following manner:

- Under high temperature conditions the alumina surface is reduced by spillover hydrogen, thus forming hydroxyl groups (-OH).

- In the absence of hydrogen and at high temperatures, the surface hydroxyl groups can oxidise the reduced centres and release hydrogen. The hydroxyl groups formed by surface reduction transform to oxygen bridges.

The investigation by Miller *et al.* (1993)[192] and Modica *et al.* (1994)[193] of platinum supported on K-containing LTL zeolites showed that the amount of high temperature desorbed hydrogen depends on the K/Al ratio and the hydrogen desorption temperature was similar to the dealumination temperature of such kind of zeolites. For a given zeolite module the K/Al ratio defines the amount of the acid -OH groups and dealumination would produce water.

1.9.1 Summary of chemisorption

In view of the discussion in this section, the following summary can be made:

- The accurate determination of platinum dispersion by chemisorption for highly dispersed supported platinum catalysts is complex. Thus the use of chemisorption to determine platinum dispersion should be used in conjunction with other analytical methods, such as TEM and EXAFS, to allow quantitative results to be obtained .

- Carbon monoxide and hydrogen, which are the most commonly used gases for the determination of platinum dispersion, do not form a 1:1 stoichiometry with platinum. In addition, especially in the case of hydrogen, the reaction stoichiometry may change with platinum dispersion (Vaarkamp *et al.*, 1990)[185].

- The stoichiometry of carbon monoxide with platinum is affected by the exchanging cation in the case of platinum supported on zeolite L (Larsen and Haller, 1989)[187].

- Although CO chemisorption tends to underestimate platinum dispersion (Lane *et al.*, 1991)[190], it is less susceptible to spurious effects, such as water content of the support and spillover reactions, than hydrogen. Thus carbon monoxide is the gas of choice in determing platinum dispersions by chemisorption[194]. However, the platinum dispersions obtained by this method will at best be relative.

1.10 Research Objectives

Platinum supported on zeolite L has been extensively researched as a catalyst for the aromatization of hexane and heptanes. Very high selectivity to aromatics are obtained over these Pt/KL catalysts. However, the Pt/KL catalysts exhibit extreme sensitivity towards sulphur containing compounds which causes rapid and irreversible deactivation by sintering of the platinum clusters. The Pt/KL catalyst may find application in the aromatization of the sulphur-free feedstocks from the Fischer-Tropsch process. However, the Fischer-Tropsch process produces appreciable amounts of alkenes as well as oxygenated compounds, mainly alcohols, ketones and aldehydes. As yet no study has been made to quantify the effect of these compounds on the activity and selectivity of n-hexane aromatization over Pt/KL catalysts.

Thus the research objectives of this study are:

- Synthesize Pt/KL by incipient wetness impregnation.
- Characterize the platinum loading by atomic absorbtion spectroscopy and platinum dispersion by CO chemisorption.
- Test the Pt/KL catalyst for n-hexane aromatization and compare the results obtained to those reported in literature.
- Quantify the deactivation of the catalyst during n-hexane aromatization at low and high hydrogen partial pressure. Determine whether deactivation is the result of coke formation or sintering.
- Determine whether deactivated catalysts can be regenerated by calcination in air.

- Co-feed various oxygenates with n-hexane at different hydrogen partial pressures. The effect of the molar ratio of oxygenate to n-hexane is also to be investigated.

- Feed the oxygenates individually over Pt/KL to determine the reaction products.

- Feed 1-hexene over Pt/KL to test the suitability of the catalyst to aromatize alkene feedstocks.

Chapter 2

Experimental Procedures

2 Experimental Procedures

2.1 Catalyst synthesis

2.1.1 Platinum/potassium L (Pt/KL)

Tetraammineplatinum(II) chloride monohydrate, $Pt(NH_3)_4Cl_2.H_2O$ (Mm 352.13 g/mol), obtained from Strem Ltd. (code 78-2000, 99% purity) was used as the platinum salt for the synthesis of Pt/KL. The addition of the platinum salt to zeolite KL was by standard incipient wetness impregnation. The following method was used to synthesize Pt/KL:

- Zeolite KL (50 g) was dried in an oven at 150°C for 16 hours.
- The wetting volume was determined and found to be 0.740 ml water/g catalyst.
- $Pt(NH_3)_4Cl_2.H_2O$ (0.3609 g) was dissolved in de-ionized water (14.8 ml) and added dropwise to dry zeolite L (20 g). The addition was accompanied by vigorous shaking.
- The impregnated zeolite was dried in a dessicator, at room temperature, for 24 hours and then dried in an oven at 100°C for a further 24 hours.
- The catalyst was calcined in air (300ml/min) in a glass reactor (20 mm i.d.). The reactor temperature was increased from ambient to 350°C over 2 hours in 25°C increments. The temperature was held at 350°C for 2 hours.

- The catalyst was flushed with nitrogen (300ml/min) at 350°C for 15 minutes and then reduced in hydrogen (300ml/min) at 350°C for 2 hours followed by an increase in temperature to 450°C which was held for two hours. This catalyst is henceforth referred to as Pt/KL.

2.1.2 Potassium back-exchanged catalyst (Pt/KKL)

To remove any acidity induced during the synthesis procedure a 2.0 g batch of the Pt/KL catalyst, as synthesized in Section 2.1.1, was heated under reflux in 2.0 M solution of potassium chloride (Saarchem Ltd., purity 99.0%) for 2 hours. The catalyst was dried, calcined and reduced as explained above. This catalyst is denoted by the acronym Pt/KKL.

2.2 Reaction system

A schematic diagram of the rig is shown in Figure 2-1 . A stainless steel down-flow plug reactor, 4.5 mm internal diameter (cross sectional area of 15.9 mm^2), was used. The reactor was wrapped in copper wire and covered with aluminum foil to ensure good heat transfer between the furnace and the reactor walls. The temperature profile of the reactor is shown in Section 3.1. An internal standard, dimethylether (DME), was fed downstream of the reactor by a mass flow controller (MFC). Mixing of the internal standard with the products as well as mixing of the feedstocks was facilitated by the use of two mixers as shown in Figure 2-1 (denoted as 'b'). The mixers consisted of ¼ inch stainless steel tubes, 10 cm in length, filled with 1 mm diameter glass beads. With the exception of the mixers and the reactor the diameter of the tubing was all 1/8 inch (stainless steel). The tubing between the saturators and the reactor was heated to 80°C while the tubing downstream of the reactor was heated to 220°C to prevent condensation in the lines.

The hydrocarbon feed was delivered via a saturator with hydrogen or nitrogen as a carrier gas (Section 2.3). All gases were fed via mass flow controllers. Air and nitrogen could be fed for calcination and flushing. Analysis of the reaction products was by on-line sampling to a gas chromatograph (HP5890).

2.2.1 Product analysis

2.2.1.1 Gas chromatography analysis

The reaction products were analysed by online gas chromatography (Hewlett Packard 5890. The chromatograph was operated isothermaly, typically at 25°C. The product compounds were resolved by use of a 50m PONA capillary column (0.5mm i.d., 0.53μm cross-linked methyl silicone film thickness). Detection was by flame ionization detector (FID) and the data was integrated by a Hewlett

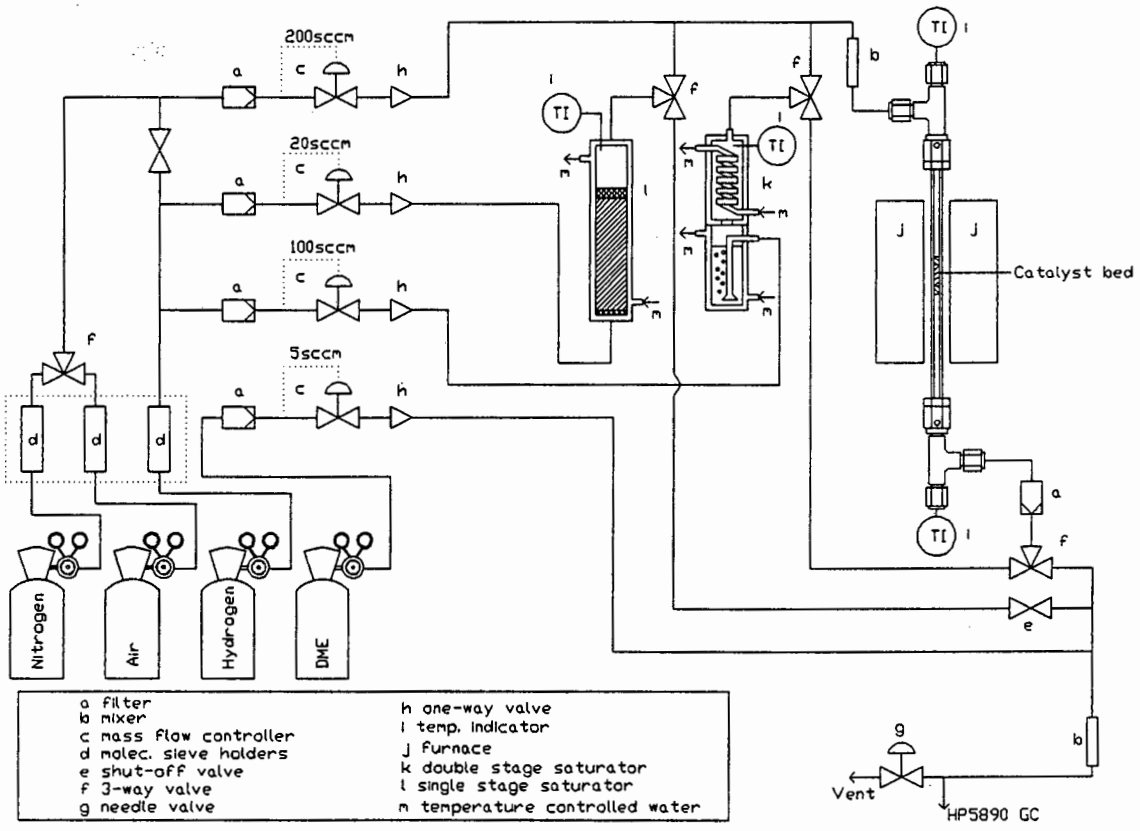

Figure 2-1 Schematic diagram of the reaction system.

3396 Series II integrator. Ethane/ethene and propane/propene could only be resolved by using cryogenics to lower the oven temperature to -10°C. The response factors for the hydrocarbons was assumed to be unity. A relative response factor of 0.70 by carbon mass was determined for n-alkanes/DME by the use of calibration gas containing known amounts of DME, methane,propane and butane. A list of the product compounds is tabulated in Appendix A.3. A typical GC trace for n-hexane aromatization at 450°C and 1 bar hydrogen partial pressure is shown in Figure 2-2.

2.2.1.2 Resolution of products

The products were resolved by means of a 50m PONA capillary column at an isothermal GC temperature of 25°C. This allowed complete resolution of all products, except ethane\ethene and propane\propene. These latter compounds could only be resolved by using cryogenics to lower the GC oven temperature to

10°C. However, ethene and propene were found to be negligible products even at 1 bar hydrogen partial pressure and zero at higher partial pressures of hydrogen. The resolution of the hexene isomers was also possible at 25°C. However, a decline in resolution was noticed towards the end of the project, presumably as a result of the deterioration of the stationary methyl silicon phase of the capillary column. This deterioration is accelerated by the analysis of oxygenated compounds[195] and affected the resolution of hexene isomers the most. However, operation at higher partial pressures of hydrogen (>2 bar) towards the end of the project resulted in no hexene (or other alkene) isomers being produced during this time.

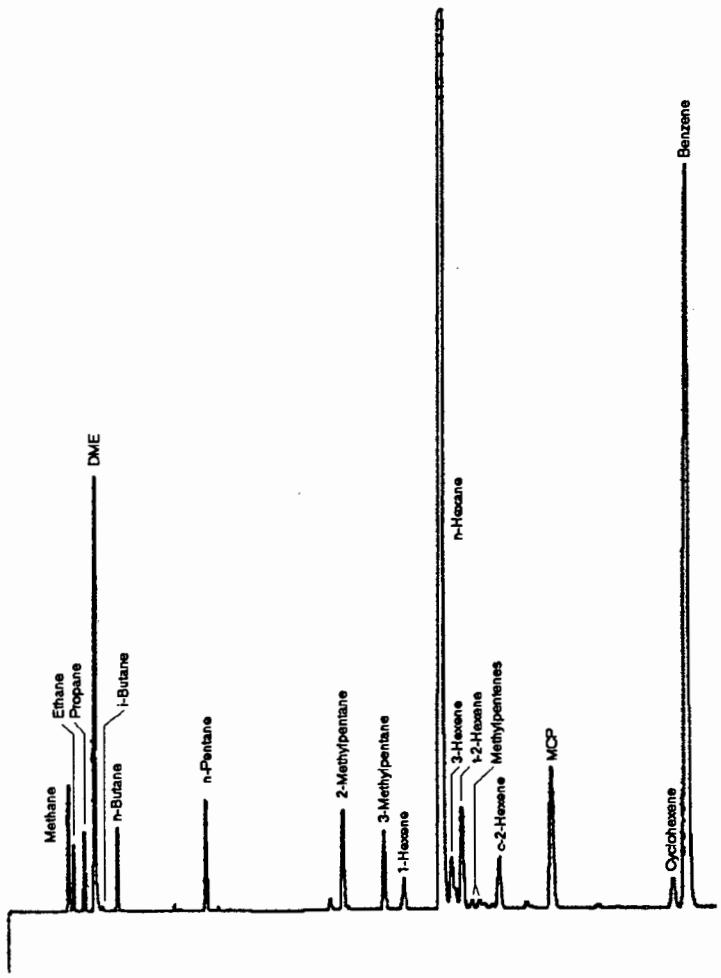

Figure 2-2 A typical GC trace for n-hexane aromatization at 450°C and 1 bar hydrogen partial pressure

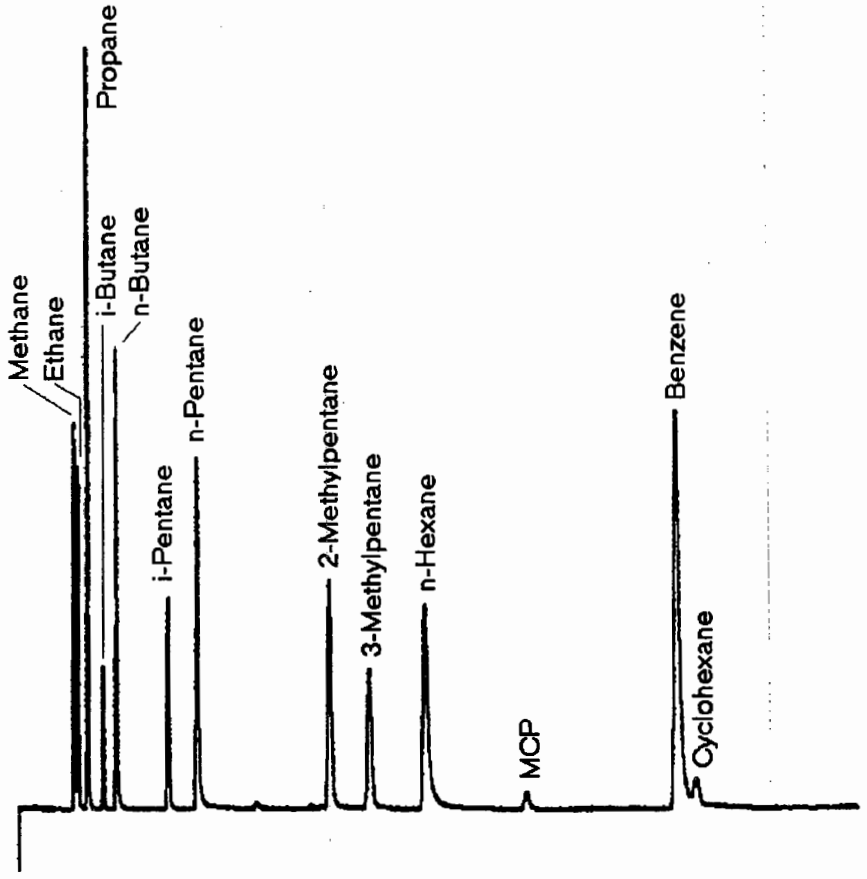

Figure 2-3 GC trace for n-hexane aromatization over Pt/KL at 450°C and 6 bar hydrogen partial pressure

2.2.1.3 Mass balances

Mass balances were determined on a carbon mass basis, relative to the carbon mass flow of feed on bypass and resulted in good balances of 100 ± 2.5%. This was typical for most runs throughout the project. Mass balances are shown for most experiments in the proceeding sections.

2.2.1.4 Repeatability

One batch of catalyst was used throughout the project and the sythesis thereof is explained in detail in Section 2.1. A summary of results, obtained under identical experimental conditions, but using newly loaded Pt/KL catalyst, is show in

Table 2-1. These results indicate that repeatability was satisfactory, as determined by the standard deviation. There is, however, some difference between run C and the others (A,B,D).

Table 2-1 Repeatibility between different experiments for n-hexane aromatization at 450°C

		Selectivity					
Run	Conversion	Benzene	MCP	2,3m-C_5	Hexenes	C_1-C_5	Σ
			$p(H_2)$ = 1 bar				
A	35	58	9.3	8.1	11.4	11.3	98.1
B	35	59	9.9	8.7	11.3	9.7	98.6
C	34	58	13	10.5	10.8	7.6	99.9
D	31	57	8.5	8.4	12.5	11.8	98.2
Std. dev.[a]	1.64	0.71	1.70	0.93	0.62	1.64	
			$p(H_2)$ = 6 bar				
E	84	28	1.6	27	-	42	97.6
F	85	28	2.3	25	-	44	99.3
G	87	31	1.3	23	-	44	99.3
H	86	30	1.0	24	-	43	98.0
Std. dev.[a]	1.12	1.30	0.48	1.41	-	0.83	

A-D t.o.s = 50 hr, E-F t.o.s. = 24 hr
(a) Standard deviation

2.2.1.5 Analysis of carbon monoxide and carbon dioxide

The flue gas was analyzed on-line for carbon monoxide and carbon dioxide by the use of a Hartmann and Braun Uras 10E infrared spectrometer.

2.2.2 Experimental procedures

2.2.2.1 Loading of catalyst

In all cases, with the sole exception being during the testing for film diffusion (section 2.4.3), 0.100 g (± 0.0005 g) of catalyst was loaded (Figure 2-6). The catalyst was in the form of a fine powder (0.1μm mean particle size) and was not diluted. There was a pressure drop of 15kpa ± 5 kPa over the bed at a gas flowrate of 30 sccm.

2.2.2.2 Start of experimental run

After loading the catalyst, hydrogen at a flowrate of 30 sccm, was allowed to flow over the bed while the reactor temperature was increased to 450°C over about 45 minutes. The feed flow was started when the reactor temperature reached 350°C.

2.2.2.3 Variation of reaction temperature

When the reaction temperature was varied the following method was used:

- The catalyst was allowed to reach steady-state operation with respect to conversion at 450°C.

- The temperature was then decreased from 450°C, to the lowest reaction temperature to be tested, in 25°C or 50°C decrements. The catalyst was allowed 30 minutes stabilization time after each temperature decrement, during which time on-line sampling of the product gases took place.

- The reaction temperature was then returned to 450°C in 25°C or 50°C increments with on-line sampling taking place at each

temperature increment after 30 minutes had elapsed.

- If higher reaction temperatures were to be tested then they would now be performed, after which the reaction temperature was allowed to return to 450°C.

2.2.2.4 Variation of WHSV

The WHSV was varied by varying the flow through the feed saturator which changed the residence time of the feed through the catalyst bed. After a series of different WHSV's were tested the WHSV was returned to the starting value. A time interval of about 30 minutes was allowed between changes in WHSV during which time sampling of the product gases took place.

2.2.2.5 Regenerations

Regenerations by calcination in air (60 sccm) were performed at 350°C and 450°C *in situ*, *i.e.* in the reactor, by use of the following method:

- The deactivated catalyst was first flushed with nitrogen (60 sccm), at the calcination temperature (*viz.* 350°C or 450°C), for 15 minutes.
- Calcination, in air (60 sccm), was then performed for a period of between 2 hours and 12 hours.
- The catalyst was then flushed with nitrogen (60 sccm) for 15 minutes at the calcination temperature.
- Reduction in hydrogen (60 sccm) at 450°C for 2 hours was then performed, after which further reaction work was carried out on the catalyst.

2.2.2.6 Co-feeding of oxygenates

Oxygenates were fed using a single-stage stainless steel saturator, described in greater detail in Section 2.3.2. Initially a run was started using n-hexane only as feed, with auxillary hydrogen being co-fed. The oxygenates were initially fed with an identical carrier gas flowrate to that of the auxillary hydrogen, bypassing the reactor, until stable flows were obtained (2-4 hours). Then the flow of the auxillary hydrogen was terminated and the oxygenated co-feed was allowed to flow over the catalyst bed. In this manner, both the residence time over the catalyst bed, as well as the hydrogen partial pressure, was kept constant.

2.3 The feed delivery system

The hydrocarbon feed, *viz.* n-hexane or 1-hexene, was fed by the use of a saturator. Both a single stage stainless steel saturator (for pressures > 200 kPa) and a double stage glass saturator (for reaction pressures < 200 kPa) were used. The temperature of the saturators was controlled by water baths, which allowed a temperature range of -5°C to 40°C to be obtained. Vapour pressure data, obtained from Reid *et al.* (1987)[196] was used to calculate the feed flowrates (Appendix A.4). The saturators were also calibrated relative to the DME internal standard and these results are summarized in section 2.1.3.1 The oxygenated co-feed was fed by use of a single stage stainless steel saturator. The co-feeding of CO was performed by using a calibrated mass flow controller.

2.3.1 Mass flow controller calibration

The mass flow controllers were calibrated relative to a bubble meter and the flows, in ml/min, normalized to STP (sccm, standard cubic centimeters per minute). The DME flow controller could not be calibrated using a bubble meter due to the high solubility of DME in water (0.071 g DME/ g H_2O)[197]. Thus the DME flow controller was calibrated reative to propane on the gas chromatograph, using a response factor of 0.70 for DME relative to propane. The results of the mass flow controller calibrations are shown in Appendix A.2.

2.3.2 Calibration of the saturators

The delivery of a binary organic feed was made possible by the use of two saturators. This method of feed delivery is recommended, for system pressures less than 150 bar by Weitkamp[198]. A single stage saturator was used for the oxygenated co-feeds and a double stage saturator for the n-hexane feeds. The

single-stage saturator was packed with Chromosorb B and a constant temperature was obtained by the use of a water jacket. Experiments at various pressures (1-6 bar) were carried out with the experimental conditions such that the residence time of carrier gas in the reactor would remain constant, *i.e.* by increasing the carrier gas molar flowrate for increase in pressure. A summary of the experimental conditions is shown in Table 2-2.

Table 2-2 Experimental conditions for the calibration of saturators

DME flowrate	2.2 ml/min
R_f (n-C_6/DME)	0.7
R_f (EtOH/DME)	0.5
Saturator temperature (EtOH)	14-16°C
Saturator temperature (n-C_6)	9°C and 5°C
Vapour pressure (EtOH)	0.017 bar (@ 15°C)
Vapour pressure (n-C6)	0.10 bar (@ 9°C) and 0.075 bar (@ 5°C)

Flame ionization detectors (FID) exhibit a linear response to hydrocarbons over a wide range of concentrations (*ca.* 10^6)[199]. The response to all hydrocarbons is assumed to be equal. However, the detection of oxygenated compounds is more complicated as the FID does not show equal sensitivity to non-hydrocarbons. In addition the oxygenated compounds tend to exhibit a greater degree of tailing on the PONA column which affects the integration of the areas on the GC trace adversely. The response factor for DME relative to n-alkanes was determined by use of calibration gas, in which the molar ratios of DME and propane were known, and were calculated as 0.7. The response factor for DME relative to ethanol was calculated relative to the flowrates calculated by the vapour pressure (Appendices A.1.3 and A.1.4) and found to be 0.5. The flowrates of the other oxygenated compounds were calculated by means of their vapour pressure and the flow of the carrier gas (A.1.3).

2.3.2.1 Calibration of n-hexane

The calibration of the n-hexane flowrate from a double stage saturator relative to the internal standard, DME (relative response factor 0.7), was carried out over a range of carrier gas flowrates at a pressure of 1 atmosphere. The lower stage of the saturator was operated 20°C higher than the top, as recommended by Weitkamp[198]. The vapour pressure was determined by the temperature of the upper stage of the saturator. At low carrier gas flowrates (< 25 sccm) higher experimental n-hexane feed rates, compared to the theory, were observed (and vice versa for carrier gas flowrates > 25 sccm). This is illustrated in Figure 2-4 for the upper stage saturator temperature of 5°C and a n-hexane vapour pressure of 0.075 bar. The percentage difference between the theoretical and the experimentally derived flowrates is also shown. At a higher temperature for the upper stage of the saturator (9°C) there is an increase in the feed flowrate of 33% (for a 4°C increase in the saturator temperature). However, a linear response to carrier gas is exhibited by the feed system for n-hexane. The feed rate of n-hexane, F_r (mol/s), for both the theoretical and experimental results, can be expressed, for a n-hexane vapour pressure of 0.075bar, as a function of carrier gas flowrate, by the following equations:

$$F_r = 5.87 \times 10^{-8} \times \text{carrier gas flow} \qquad \text{(Theory)}$$

$$F_r = 4.68 \times 10^{-8} \times \text{carrier gas flow} + 2.91 \times 10^{-7} \qquad \text{(Experimental)}$$

The experimental feed flow rate does not intersect with the origin, even though the MFC flowrates intersect the origin (section A.2.1). The deviations between the experimental and theoretical results must thus be the result of undersaturation of the gas at high flowrates (and oversaturation at low flowrates).

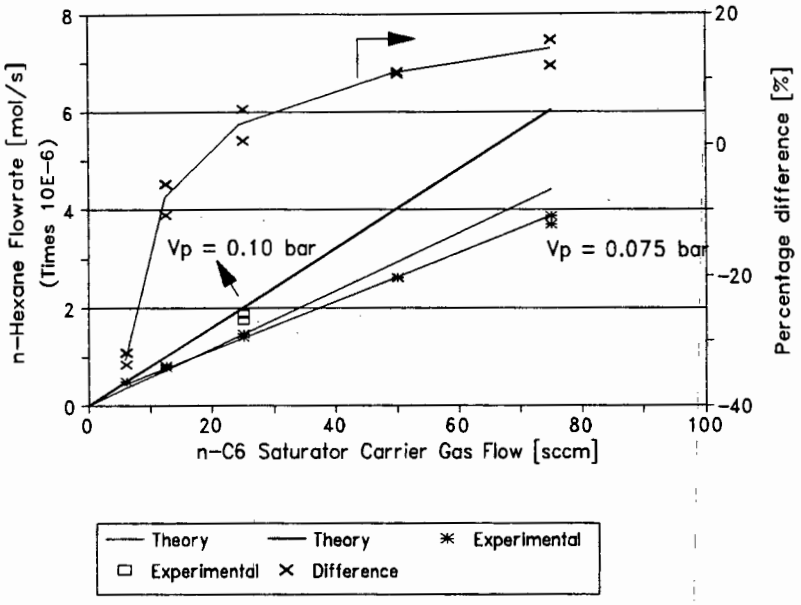

Figure 2-4 Calibration of the n-hexane saturator at two vapour pressures (0.1 bar and 0.075 bar)

2.3.2.2 Calibration of ethanol flowrates

The calibration of the ethanol flowrate from a single stage saturator was performed relative to a constant flowrate of both DME and n-hexane for different carrier gas flowrates through the ethanol saturator. This was to determine if the single stage ethanol saturator would exhibit a linear response to carrier gas flowrate, as well as to determine if changes in the flowrate of the ethanol saturator would effect the flowrate of reactant from the other (n-hexane) saturator. The carrier gas flowrate through the n-hexane saturator was 25 sccm. The results are shown in Figure 2-5. A linear response of ethanol to the flow of carrier gas through the saturator is observed. The flowrate of n-hexane remains constant and is not affected by the increase in carrier gas flow through the ethanol saturator. The flowrates of ethanol, in mol/s, were calculated by the use of the formula in the Appendices (A.1.3). Due to the lower carrier gas flowrates (< 20 sccm) through the ethanol saturator, no undersaturation occurs. A FID response factor of 0.5 of ethanol, relative to DME was determined from the data using the equation in A.1.4.

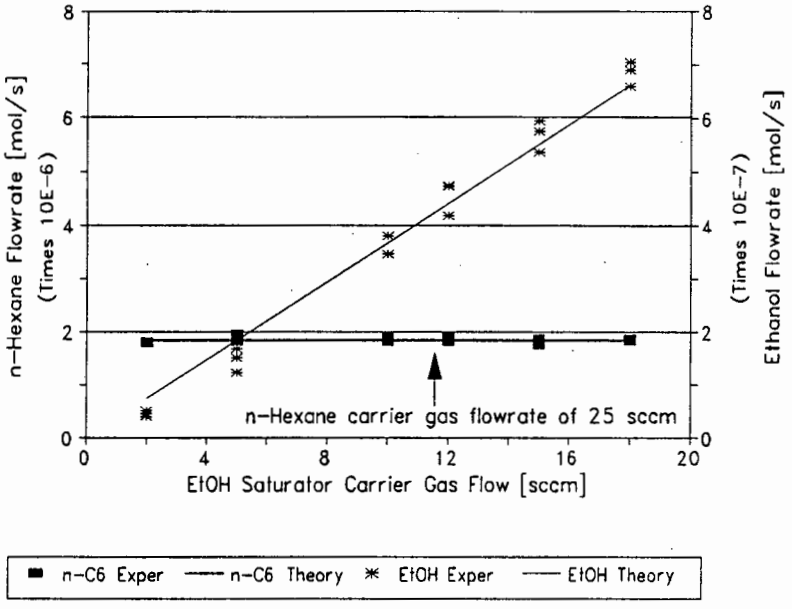

Figure 2-5 Calibration of ethanol and n-hexane saturators

2.3.2.3 Conclusions on saturator calibration

The calibration of the saturators show that good agreement between the theory and experimental results is obtained for both ethanol and n-hexane. The flowrates of the other oxygenated feeds are calculated by use of their vapour pressure and the carrier gas flowrate. The flowrates are very sensitive to changes in temperature of the saturators as vapour pressure increases exponentially with temperature. The total pressure of the system is also a factor influencing flowrates, *i.e* a two-fold increase in total pressure will necessitate a two-fold increase in the carrier gas flowrate to obtain the same feed flowrate and residence time. The flowrates of n-hexane reported in this work are those determined by calibration with DME, as described in Section 2.3.2.1.

2.4 The catalyst bed

The catalyst bed in shown schematically in Figure 2-6. The catalyst was supported on a bed of silica wool. A thermocouple protruded into the bed from both the top and the bottom. The length of the bed was *ca.* 5mm.

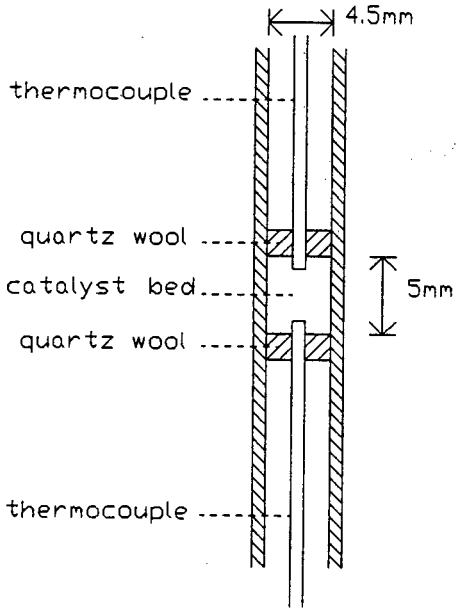

Figure 2-6 Schematic diagram of the catalyst bed.

2.4.1 Reactor temperature profile

The longitudinal temperature profile of the reactor was tested by moving a thermocouple inside the empty reactor at two different furnace temperatures, *viz.* 450°C and 550°C. Nitrogen was used as carrier gas at 100 ml/min. No organic feed were fed through the reactor during this test. The results are shown in Figure 2-7 and illustrate that an isothermal bed length of *ca.* 60 mm was available.

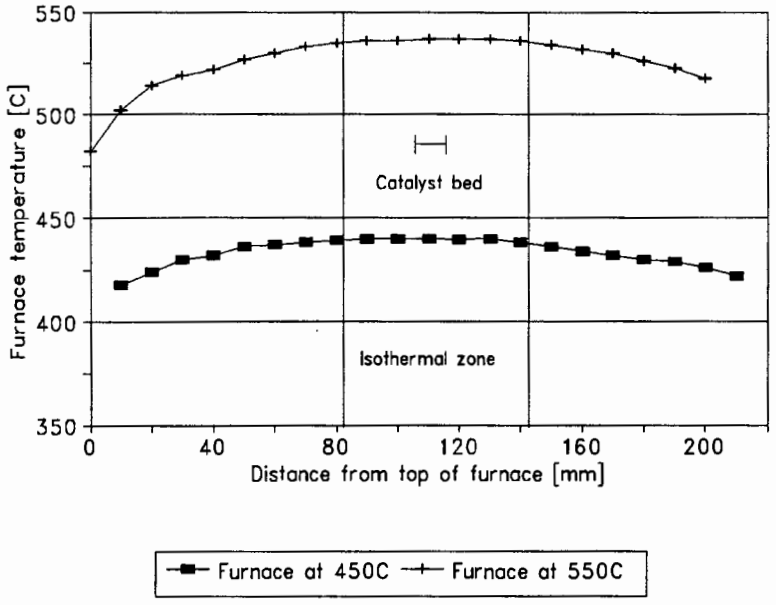

Figure 2-7 Longitudinal reactor temperature profile

The radial temperature of the reactor was not measured due to the small clearance between the reactor walls and the thermocouple (1.5mm). The average catalyst bed length used for experiments was *ca.* 5 mm. The reactor temperature declined more sharply towards the bottom of the reactor. This is a result of the four heating elements in the furnace being positioned nearer the bottom than the top of the furnace. The reactor temperature is *ca.* 15°C and 10°C lower than the furnace temperature settings of 550°C and 450°C respectively. All reaction temperatures quoted are for the temperature inside the reactor as measured by the internal thermocouples.

2.4.2 Activity of the reactor and of KL zeolite

The activity of both the reactor and zeolite KL were tested for residual activity. The stainless steel reactors are reported to be catalytically active due to the presence

of chromium and nickel in the metal. Nickel is well know to catalyze the complete hydrogenolysis of alkanes to methane[200].

2.4.2.1 Reactivity of reactor walls

n-Hexane was fed through the empty reactor at 550°C to test for latent activity. A small amount of thermal cracking was observed (methane), however, the conversion of n-hexane was less than 3%. Hence, it can be reasonably assumed that if there was negligible activity at 550°C, then there will be even less at lower temperatures. The bulk of the studies were, in any case, carried out at reaction temperatures of 450°C and lower.

2.4.2.2 Reactivity of zeolite KL

The reactivity of n-hexane on zeolite KL was tested over a wide reaction temperature range (250°C - 550°C). The n-hexane feed was 98% pure with pentane, methylpentanes and MCP as contaminants. These have been calculated out from the products, but at low n-hexane conversions this is difficult as the errors in analysis tend to be magnified. The conversion of n-hexane was zero below 350°C, increasing to 2.5% and 7.5% at 450°C and 550°C respectively (Figure 2-8). A selectivity of 0% and 22% to benzene was observed at 450°C and 550°C respectively. Dehydrogenation of hexane to linear hexenes was prevalent at reaction temperatures greater than 400°C (Figure 2-9). The selectivity to the linear hexenes decreases sharply at reaction temperatures above 500°C, presumably by conversion to benzene or by hydrogenation to n-hexane. Hexane isomerization activity is low and declines with reaction temperature. The ratio of MCP to methylpentanes (0.4) and the ratio of 2-methylpentane to 3-methylpentane (0.75) remains constant above 500°C (Figure 2-11). Methane is the major cracked product with a small amount of ethane and propane observed above 500°C (Figure 2-10). The absence of butanes or pentanes, and the prevalence of methane, is indicative of nickel catalyzed hydrogenolysis, which is well known to

complete hydrogenolysis of alkanes to methane (nickel is present in the stainless steel reactor walls). Propane, which appears at reaction temperatures above 525°C is mostly likely formed by acid catalyzed cracking. The appearance of ethane above 475°C may be due to a shift in the desorption equilibria at high temperatures, thus allowing ethane to desorb before it is cracked to methane. A similar mechanism may also hold for propane, in addition to the acid-catalyzed cracking pathway.

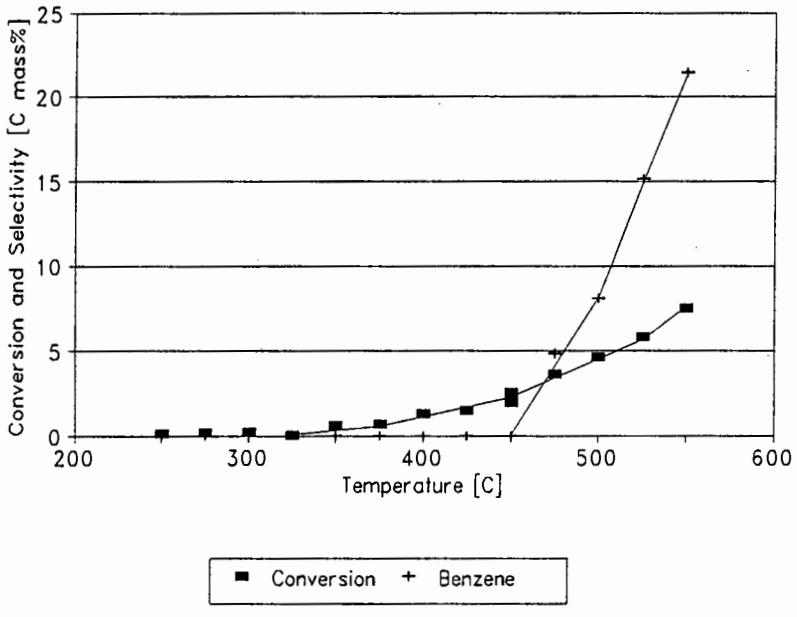

Figure 2-8 Conversion of n-hexane and selectivity to benzene over KL

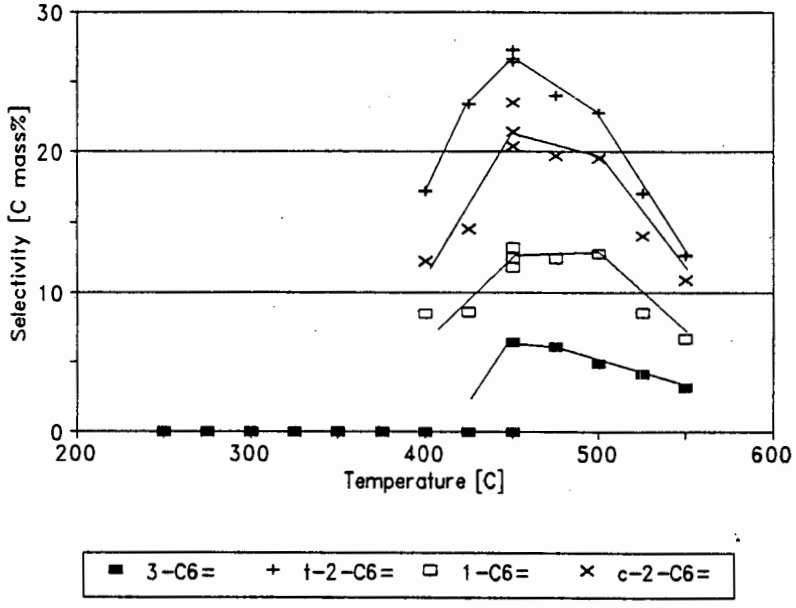

Figure 2-9 Selectivity to linear hexenes over KL

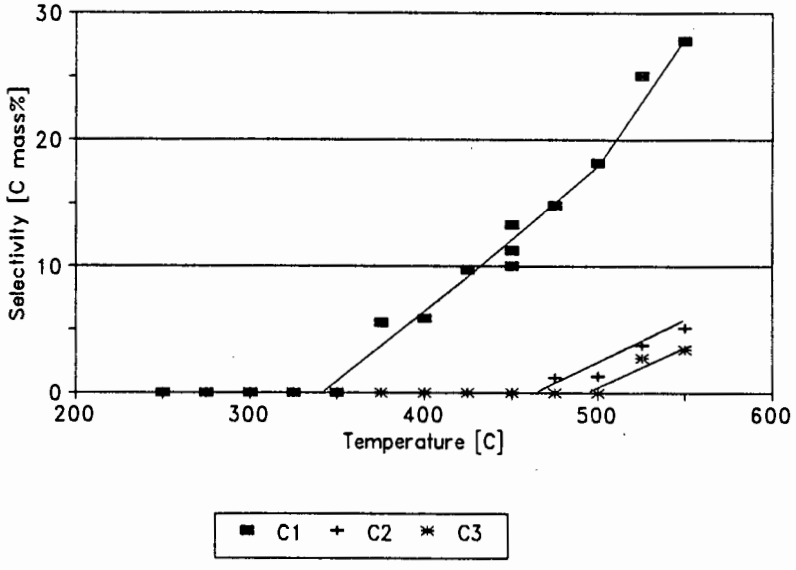

Figure 2-10 Selectivity to hydrogenolysis products on KL

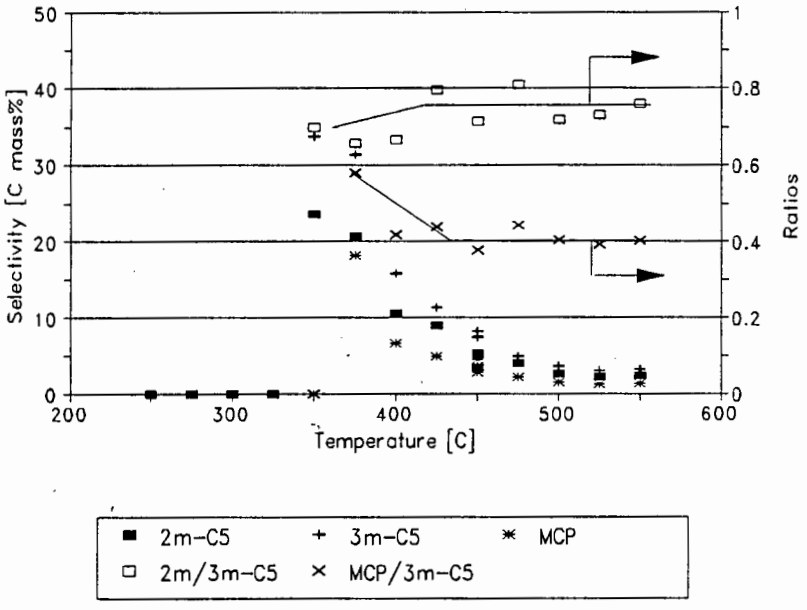

Figure 2-11 Selectivities and ratios of isomerized hexanes on KL

2.4.2.3 Conclusions on reactivity of KL

At reaction temperatures below 450°C, the conversion of n-hexane on KL is negligibly low (< 2.5%). The increase in selectivity to benzene above 450°C may be the result of dehydrocyclization of hexenes, which are thermodynamically more reactive than hexane (Appendices A.1.6.1) with respect to dehydrocyclization, e.g. cis-hexatriene is reported to dehydrocyclize to benzene, even in the absence of a catalyst, at 500°C (Section 1.6.1.5). The formation of methane as the major cracked product indicates non-acidic cracking (free radical hydrogenolysis, possibly nickel-catalyzed) and hence provides proof that the KL zeolite substrate has low acidity. Only trace amounts of butane were observed. Propane is possibly also produced by acid-catalyzed cracking, indicating some small amount of acidic activity is present at high temperatures.

Of the linear hexenes, trans-2-hexene is the major isomer. The trans isomers of hexene cannot undergo 1,6 ring closure to form benzene directly and thus this may explain its greater selectivity relative to the cis-2-hexene isomer, in contrast to that expected at thermodynamic equilibrium. The cis and trans isomers of 3-hexene could not be resolved by the GC column. The relative fractions of linear hexenes remained constant between 450°C and 550°C. The linear hexene thermodynamic equilibrium fractions remained constant in that temperature range as well. A comparison with the thermodynamic equilibrium ratios is made in Table 2-3. The fraction of 1-hexene is higher than expected while that of the 3-hexenes is lower. This could be indicative of a series dehydrogenation of 1-hexene ⇄ 2-hexene ⇄ 3-hexene.

Table 2-3 Comparison of the fraction of linear hexene isomers observed on KL with thermodynamic equilibrium

	1-hexene	t-2-hexene	c-2-hexene	3-hexene
KL (450°C)	0.19	0.39	0.33	0.09
Thermodynamic (450°)	0.07	0.32	0.38	0.24

2.4.3 Mass transfer (film diffusion effects)

For there to be negligible film diffusion (mass transfer between the gas phase and the bulk catalyst surface) the conversion of feed should be constant at different linear velocities, but at the same WHSV. The film diffusion effect becomes more pronounced with increase in reaction rate, which for aromatization on Pt/KL means higher reaction temperatures. Two masses of catalyst were used, 50 mg and 100 mg, each being tested at two reaction temperatures, *viz.* 450°C and 500°C. The superficial linear velocity of gas through the reactor at STP, assuming the catalyst bed and thermocouples are not present, was 3.14 cm/s at a volumetric flow of 30 sccm. For a catalyst bed 5 mm in length the residence time of the gas

at 30 sccm in the bed was 0.16 seconds. The linear velocity was at least twice as high due to the space taken by the thermocouples, quartz wool and the catalyst.

The usual method of presenting such data is a plot of conversion as a function of linear velocity (for the the same WHSV). The conversion usually increases with linear velocity, indicating that mass transfer effects are initially present at low linear velocities, and then remains constant with further increase in linear velocity, indicating that film diffusion effects are absent due to the high linear velocities. However, as only two catalyst masses where used in this experiment, such a plot would not be very informative. A better method of presenting the data is to superimpose the results of the experiments, plotted as a function of WHSV. Should the conversion of n-hexane and selectivities to different products lie on the same curve, *i.e.* at the same WHSV, but thus at different linear velocities, for the two catalyst masses, then it can be assumed that no film diffusion effects are present.

2.4.3.1 Results of film diffusion

In Figure 2-12 to Figure 2-15 it can be cleary seen that the conversions and selectivities, obtained using two different catalyst masses, lie on a common curve. This is a strong indication that film diffusion effects were absent. There was slightly less similarity at 500°C, but the selectivities were essentially the same. The differences at 500°C (at the same WHSV) can be summarized as follows:

- The conversion of n-hexane is, if anything, only slightly higher at higher linear velocities, *i.e.* 0.100 g Pt/KL.

- Dehydrocyclization selectivity (benzene) is somewhat greater at higher linear velocities.

- Dehydrogenation selectivity (hexenes) is slightly less at higher linear velocities.

- Hydrogenolysis selectivity (C_1-C_5) is similar at both linear velocities.

- Selectivity to n-hexane isomerization products is equal or very slightly lower at higher linear velocities.

Thus the only possible difference appears to be for benzene and the hexene products. One possible reason for these observations is that sintering of the platinum clusters had occurred at 500°C for the 0.050 g Pt/KL case (Section 3.1.1), thus resulting in lower benzene selectivites. However, this may be ruled out due to the fact that the hexene isomers were expected to show a greater degree of sensivity than benzene to sintering (Section 3.1.1.2). In any case the difference in selectivity to benzene is small (< 3% points).

2.4.3.2 Conclusions on film diffusion

Although a wider range of linear velocities should ideally have been tested, these results show that at 450°C for WHSV's between 1.5 hr^{-1} and 18 hr^{-1} there is no observable film diffusion effect. At 500°C there appears to be a slight effect, although only with regard to the formation of benzene and hexene products. However, the selectivity difference is small, being less than 3% points.

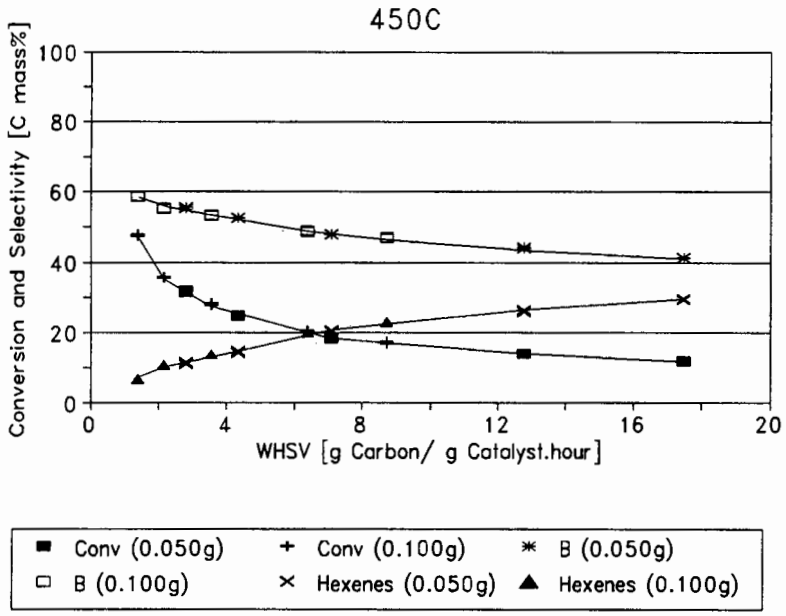

Figure 2-12 Film diffusion testing at 450°C

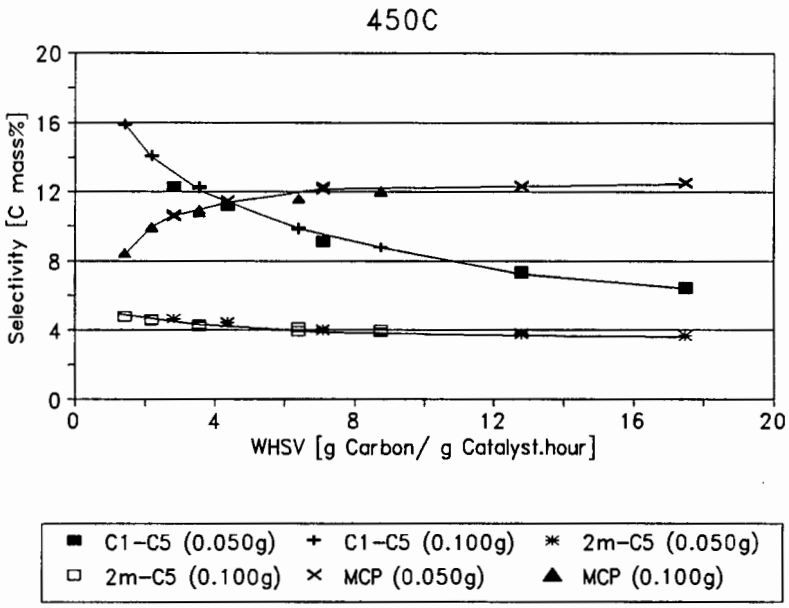

Figure 2-13 Film diffusion tests at 450°C (products)

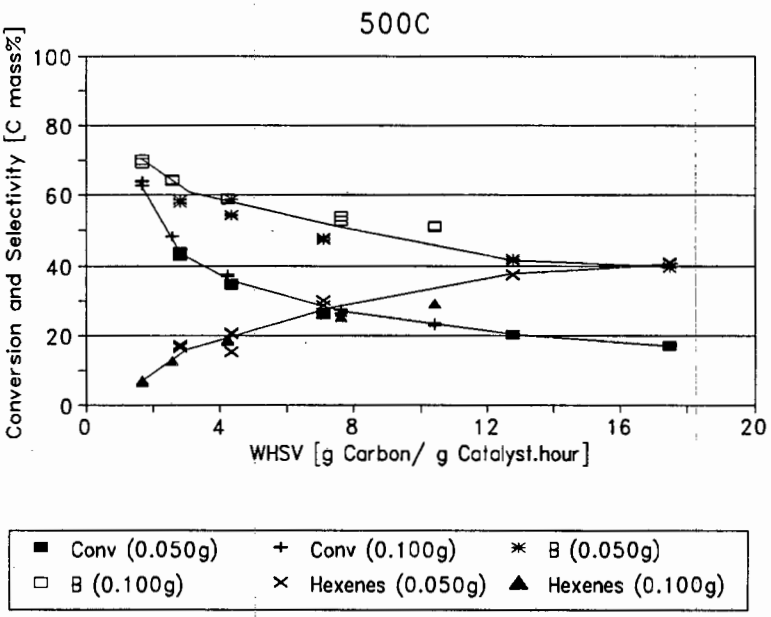

Figure 2-14 Film diffusion tests at 500°C.

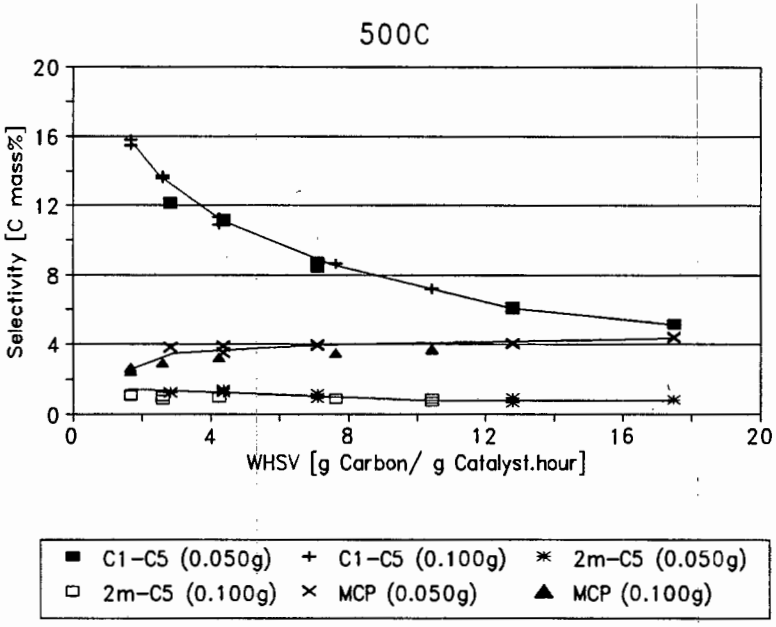

Figure 2-15 Film diffusion tests at 500°C (products)

2.4.4 Stability of Pt/KL

2.4.4.1 Different feeds

The n-hexane feedstocks used in this project was obtained from three different sources, viz Merck, Saarchem and Riedel de-Haen. Problems were encountered with the n-hexane feed from Merck which caused rapid deactivation of the catalyst (from a n-hexane conversion of 40% to 5% over 12 hours at 450°C), similar to that observed when sulphur impurities are present (Section 1.8.2). Thus, it can be reasonably speculated that some trace amounts of sulphur were present in the Merck n-hexane which, due to the high sensitivity of Pt/KL to sulphur impurities, caused the deactivation and resultant low activity. The n-hexane obtained from Riedel de-Haen and Saarchem showed very similar activity, *i.e* a decline in conversion from 60% to 37% over 48 hours and thereafter a steady state was reached. The 1-hexene feed (99% pure), used in later experiments was obtained from SASOL Ltd. and since it was produced in a Fischer-Tropsch process is expected to be sulphur-free.

2.4.4.2 Removal of sulphur

Due to the high sensitivity of Pt/KL to sulphur an attempt was made to determine the difference between an "off the shelf" n-hexane feed (Riedel de-Haen) and the same feed that had been "desulphurized". The catalyst is reported to be sensitive to sulphur compounds (thiophene) at concentrations greater than 50 ppb (Section 1.8.2). It is understandably difficult to determine the effectiveness of sulphur removal at these low levels as sophisticated analytical techniques are needed. In fact the limit of detection of sulphur for most analytical methods is well above 50 ppb. There are many sources of sulphur contamination and as the effectiveness of the procedure could not be determined directly (analytically) it was determined indirectly (by reaction on Pt/KL). The method employed to remove sulphur was by direct hydrogenation on palladium dispersed on activated charcoal, which is an active catalyst for the hydrogenation of sulphur containing compounds to hydrogen

sulphide, which can be removed by either washing with a basic aqueous solution or by the bubbling of an inert gas through the treated n-hexane. Palladium is the preferred catalyst for this reaction as it is relatively inactive for the isomerization of n-alkanes (Section 1.3.2.2). The following method was used:

- Wash 200ml n-hexane (4 x 60 ml) with conc. KOH soln.
- Hydrogenate n-hexane in autoclave over Pd/C (Aldrich 27,670 -7) at 200°C for 27 hours at a hydrogen partial pressure of 3 bar.
- Filter n-hexane, wash (3 x 60 ml) with conc. KOH soln.
- Dry n-hexane with anhydrous $CaCl_2$ and filter.

The desulphurized feed was tested at 450°C with Pt/KL as the catalyst. These results show that stable performance with respect to n-hexane conversion is obtained after *ca.* 48 hours time on stream (Figure 2-16). The conversion still declines slightly after this time, but the decrease is relatively small (a decrease in conversion of 3% over 90 hours). The benzene selectivity is stable at 59% over the entire run, however, the hexenes increase with time on stream, but reach a plateau after *ca.* 80 hours (Figure 2-17). The cracked products reach stready state after 24 hours time on stream (Figure 2-19) as do the isomerized hexane products (Figure 2-18). However, when untreated n-hexane was used as a reactant over fresh Pt/KL under identical reaction conditions, the activity and selectivity observed were identical to the treated catalyst. Thus, it was concluded that n-hexane feedstocks from Riedel de-Haen and Saarchem were sulphur free (containing less than 50 ppb thiophene). It is interesting to note that for the first analysis sample (t.o.s. of 15 minutes) the selectivity to methane was *ca.* 25%. The selectivity declined rapidly to 2% in subsequent samples. This behaviour was noted on all fresh catalysts. In fact if the t.o.s. was extrapolated to zero then methane would be the major product. This is discussed further in Section 3.2.

The deactivation exhibited by the catalysts is similar to that caused by initial coking or by thermal sintering, rather than by accelerated sintering as a result of sulphur impurities. In general, it can be assumed that the catalyst reaches steady state behaviour after 48 hours. The increase in selectivity to hexenes with time on stream can be rationalized if one assumes that dehydrogenation occurs more easily than other reactions on Pt/KL (*i.e.* because of low conversion more hexene is observed). Deactivation could occur by the adsorption of alkene products on platinum clusters, followed by coke formation.

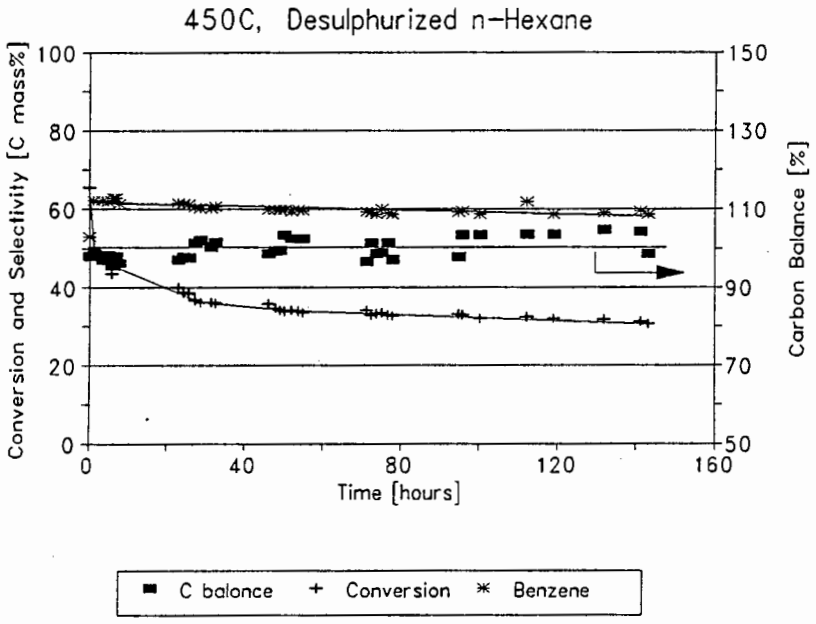

Figure 2-16 Stability of Pt/KL with desulphurized n-hexane feed at 450°C

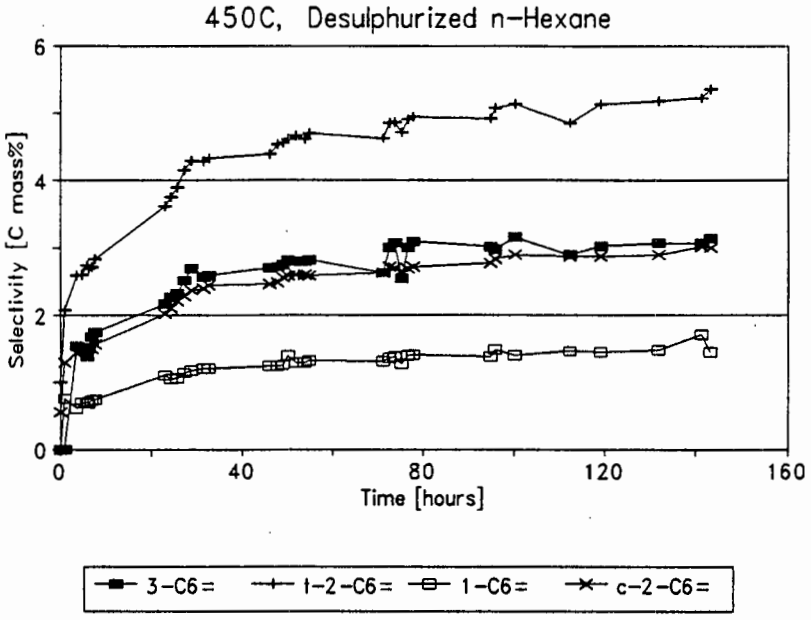

Figure 2-17 Stability of Pt/KL with desulphurized n-hexane feed at 450°C (hexene products)

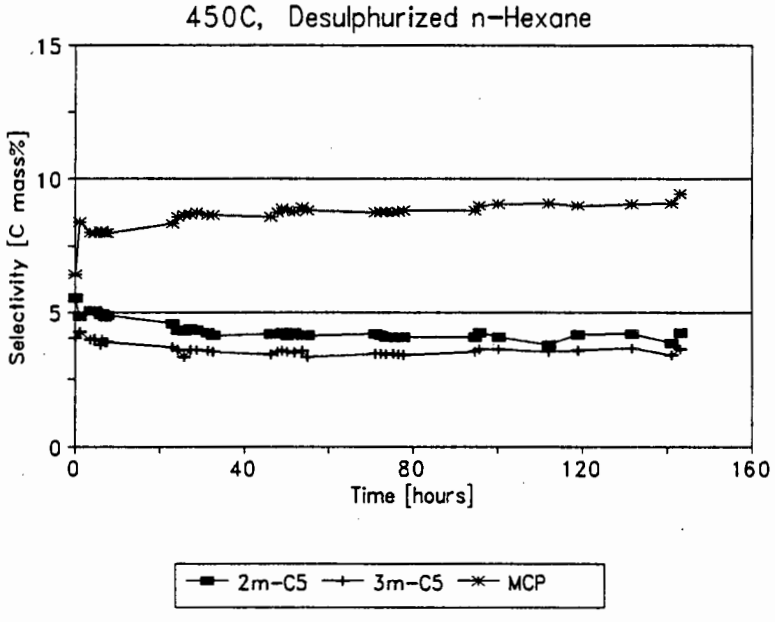

Figure 2-18 Stability of Pt/KL with desulphurized n-hexane at 450°C (isomerized products)

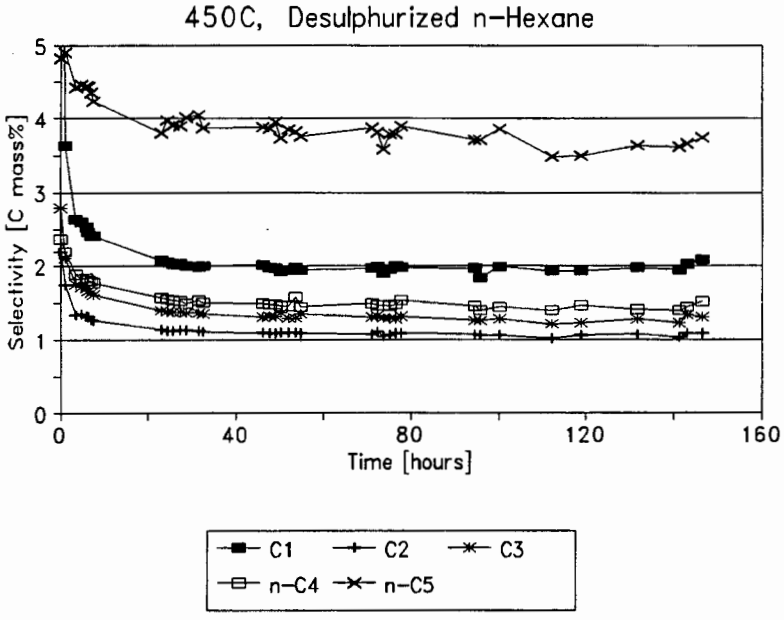

Figure 2-19 Stability of Pt/KL with desulphurised n-hexane at 450°C (cracked products)

2.5 Instrumental Analysis

2.5.1 X-ray Diffraction (XRD)

A Philips X-ray diffraction spectrometer was used to obtain XRD spectra of KL and Pt/KL catalysts. The following settings were used:

- CuKα radiation at 40kV and 30mA
- Step size 0.5°
- Scan time 1 second

Table 2-4 Comparison of experimental and simulated XRD data

d [Å]	I/Io	d[Å]	I/Io
Simulated XRD data (von Ballmoos and Higgins, 1990)		Experimental XRD data	
15.80	100	16.37	92
5.98	22	6.07	37
4.57	25	4.62	56
3.91	28	3.93	90
3.48	15	3.48	69
3.17	29	3.20	100
3.07	22	3.08	79
2.91	36	2.92	92
2.65	16	2.67	63
2.42	8	2.43	25
2.19	2	2.21	47

At at first glance there does not appear to be close correspondance between the simulated XRD data and experimental data. In particular the relative intensities are in general incorrect. A complicating factor was the fact that the peaks were in general quite broad. The reason for the deviation from ideality may be ascribed to the fact that the KL crystal sizes, as determined by SEM (Section 2.5.4), were very

small (<0.1 μm). It is obviously difficult to obtain good XRD data for such small crystals as line broadening effects become quite prevalent. However, at least the major XRD peaks appear at the correct d-spacing, thus indicating that crystalline zeolite LTL is present.

2.5.2 Temperature programmed desorption (TPD)

Temperature programmed desorption of adsorbed ammonia (NH_3) was carried out in the following manner:

- Load 250mg of catalyst into the cell
- Calcine at 450°C in air (heating rate 10°C/min)
- Cool to 150°C in air (cooling rate 5°C/min)
- Adsorption of 5% NH_3 in helium for 1 hour at 150°C
- Desorb physisorbed NH_3 for 12 hours at 150°C.
- Desorption of chemisorbed NH_3 by heating to 1000°C (heating rate 10°C/min).

Ammonia was detected by an on-line thermal conductivity detector (TCD). The TPD analysis of KL and Pt/KL are shown in Figure 2-20 and Figure 2-21 respectively. KL exhibits a low temperature desorption peak at 300°C and a high temperature peak at 650°C. Pt/KL has only one large desorption peak at 300°C.

The high temperature peak, for KL, is most likely due to dehydroxylation of the catalyst. This will result in the release of water which will be detected by the TCD. Dehydroxylation commonly occurs for zeolite catalysts at temperatures above 550°C. The Pt/KL catalyst chemisorbs more ammonia than KL (low temperature peak). This may be due to acidity induced during synthesis of Pt/KL or the result of chemisorbtion of ammonia on platinum clusters. The absence of the high temperature peak in the case of Pt/KL is puzzling. It appears that an unknown interaction, possibly introduced during the synthesis of Pt/KL, stablizes the Pt/KL

catalysts against dehydroxylation.

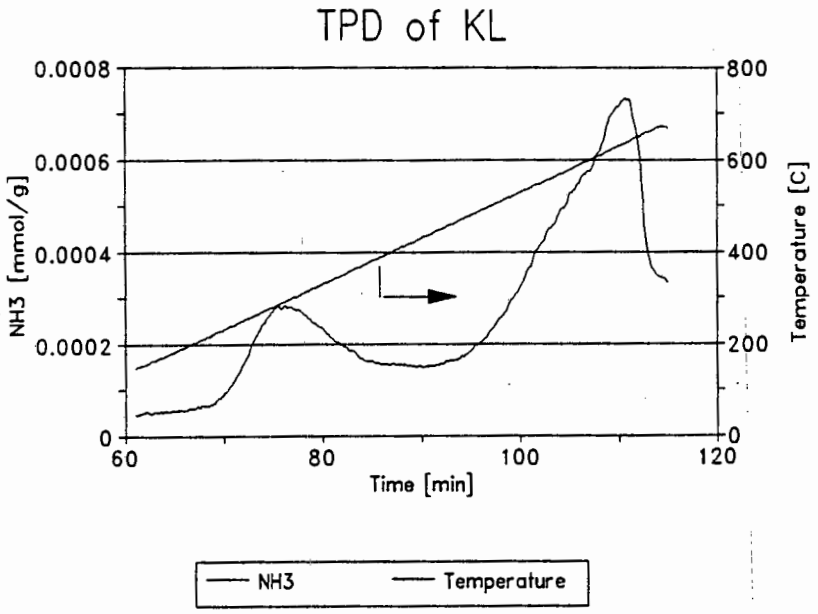

Figure 2-20 TPD analysis of KL

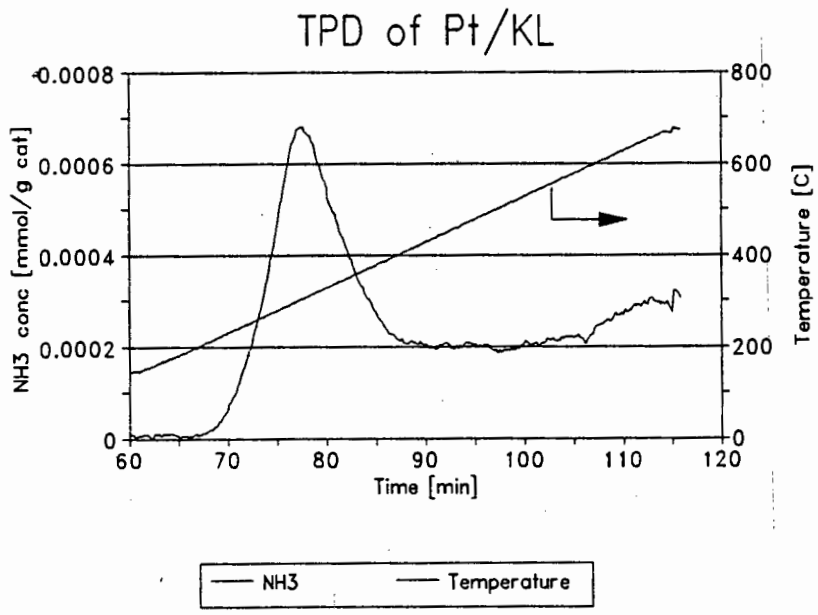

Figure 2-21 TPD analysis of Pt/KL

2.5.3 Scanning electron microscope (SEM)

A Cambridge Instruments S200 scanning electron microscope was used for SEM analysis of the KL zeolite (Figure 2-22). These micrographs show clearly that the KL zeolite consists of clusters of small KL crystals. The KL crystals are approximately 0.1 μm in diameter.

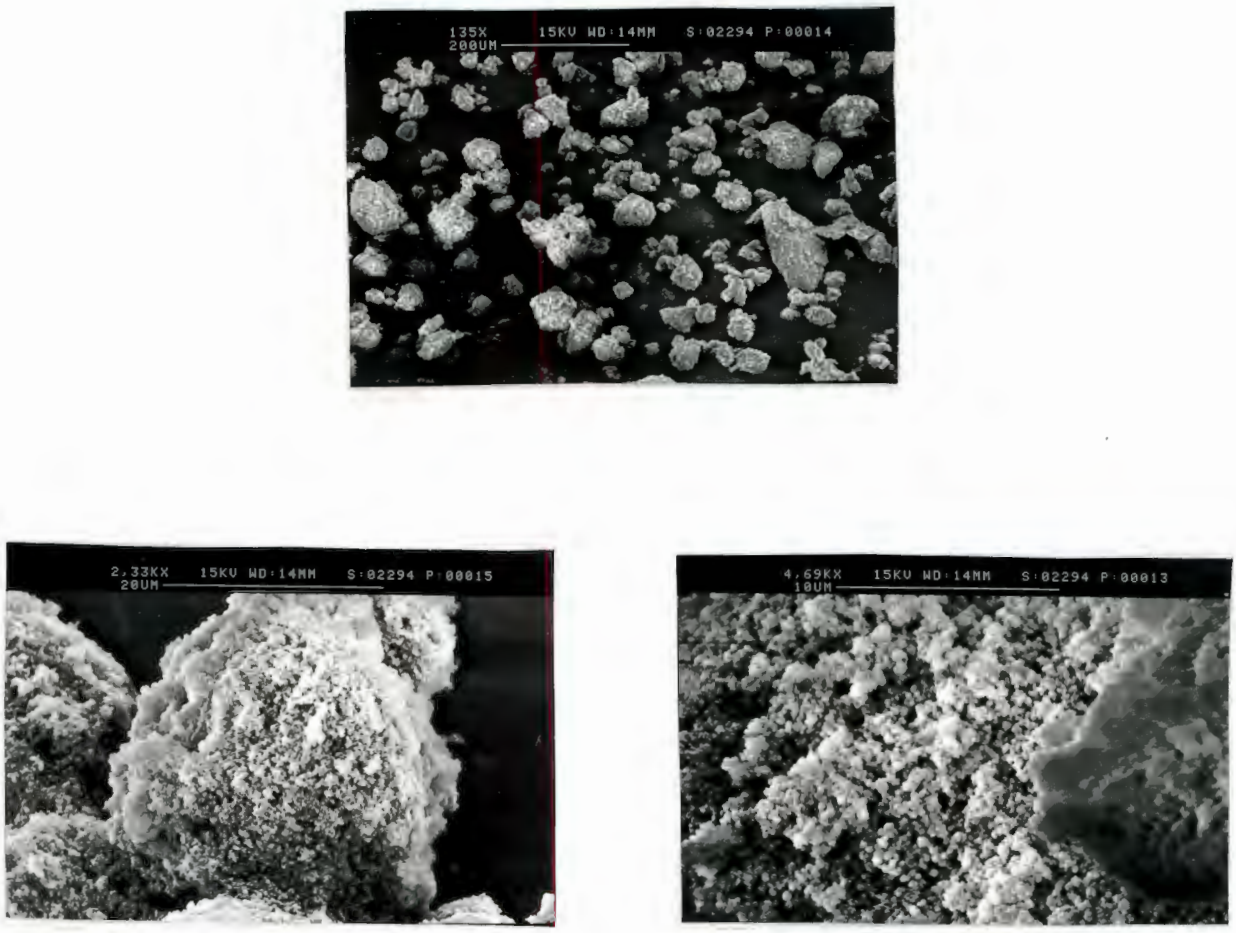

Figure 2-22 SEM micrographs for KL zeolite

2.5.4 Transmission electron microscopy (TEM)

TEM analysis was performed on Jeol 200 CX transmission electron microscope. The accelerating voltage was 200 keV. The micrographs show that platinum particles are not visible for freshly synthesized Pt/KL (Figure 2-23). This is indicative of very highly dispersed platinum. After reaction at 550°C large platinum clusters are observed (Figure 2-24). This indicates that platinum sintering had occured. A more detailed discussion of sintering is given in Section 3.1.1. The TEM analysis shows a small degree sintering of platinum after the co-feeding of n-butyraldehyde (Figure 2-25). After regeneration a larger degree of sintering can be seen to have occured (Figure 2-26). These results are discussed further in Section 3.2 and Section 3.4.

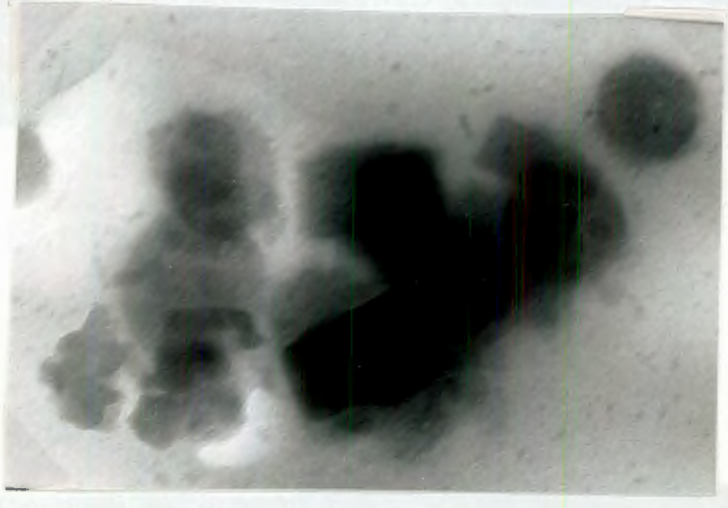

Figure 2-23 TEM of fresh Pt/KL (magnification of 100 000 times)

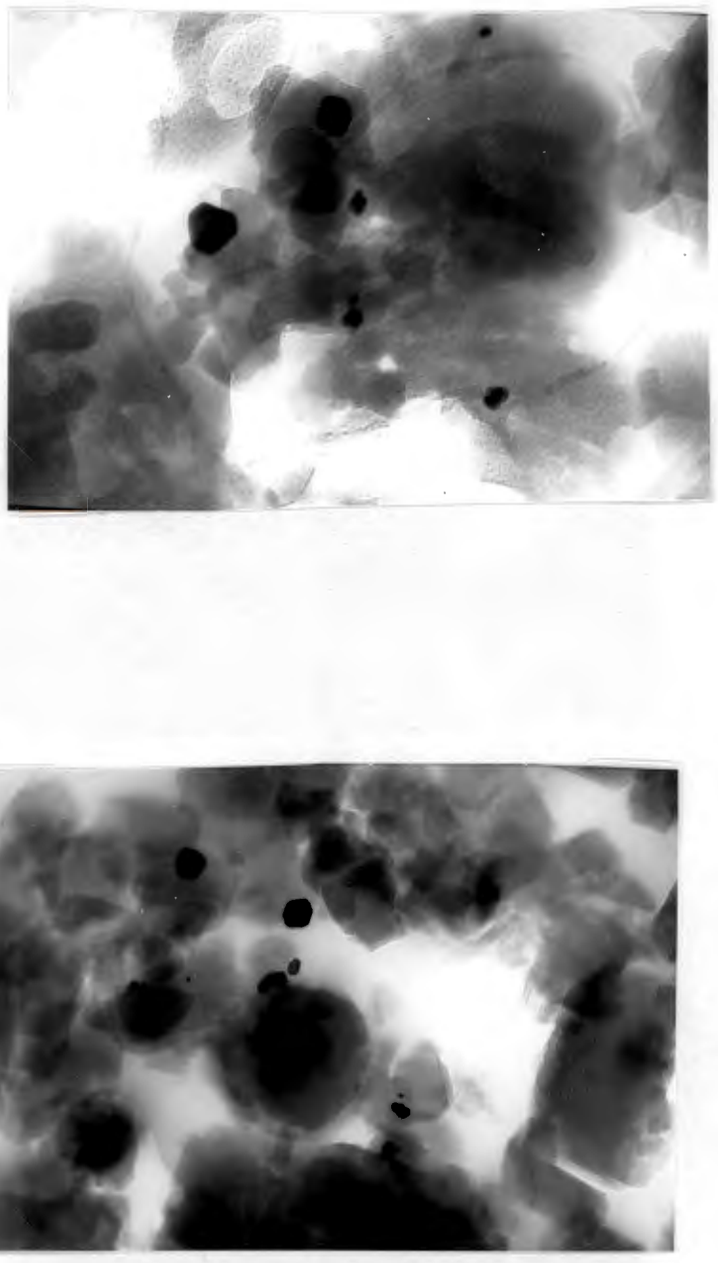

Figure 2-24 TEM of sintered Pt/KL, after reaction at 550°C (magnification of 100 000 and 132 000 times)

2.5.5 Atomic adsorption analysis (AA)

The platinum content of the Pt/KL catalysts were analysed on a Varian SpectrAA-30) spectrometer. Platinum standards were obtained from Saarchem Ltd. The catalyst was prepared for analysis by the following method:

- Dissolution of 200mg of Pt/KL catalyst in 5ml cold HF (98%). The dissolution took place in a Teflon parr bomb which was sealed and placed in an oven at 100°C for 24 hours.

- The Teflon parr bomb was removed from the oven and cooled. The HF solution from the Teflon parr bomb was transferred to a 50 ml polypropylene volumetric flask and deionized water added to make up the required volume (50 ml).

The platinum content of the Pt/KL catalysts was found to be 1% ± 0.02% by mass.

2.5.6 Fourier Transform Infrared Analysis (FTIR)

FTIR analysis was on a Nicolet 5ZDX infrared spectrometer. The resolution was 4 cm^{-1}. Wafers were from a 1:20 mixture of catalyst:KBr. The wafers were pressed at 10 kg/cm^2 and then dried in an oven at 80°C for 12 hours. The analysis was performed at room temperature. FTIR spectra of KL and Pt/KL are shown in Figure 2-27. The spectra for KL is identical to that in Figure 1.6 (Section 1.4.3). This is further confirmation that KL is present in the sample. The FTIR analysis of fresh Pt/KL and deactivated or "coked" Pt/KL is shown as well. The reaction conditions for the coked Pt/KL was 450°C, 1 bar hydrogen partial pressure with n-hexane as feed. Coke bands[201] are expected at *ca.* 2900 cm^{-1} and 1470 cm^{-1}. The spectra do not conclusively show that any coke had formed.

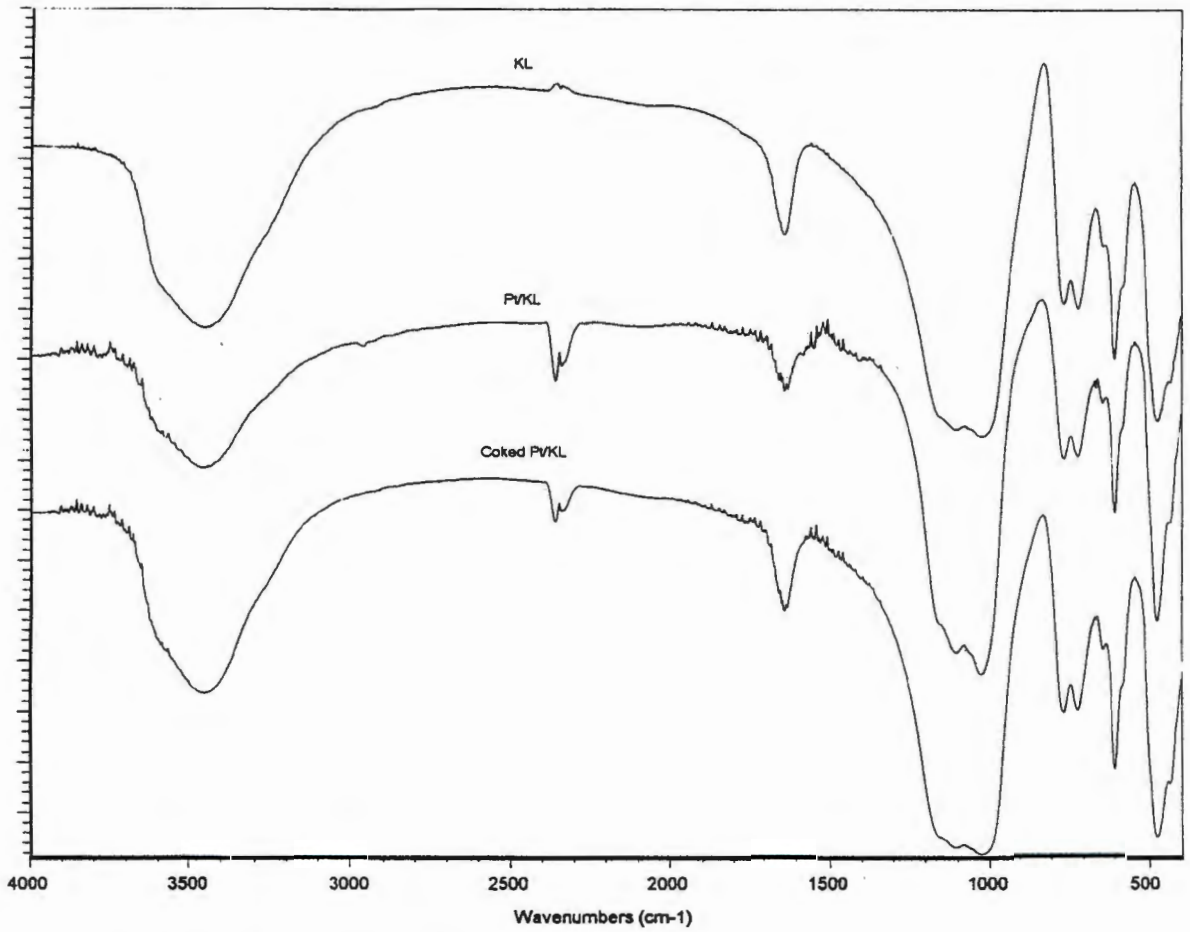

Figure 2-27 FTIR spectra of KL and Pt/KL

2.5.7 Thermogravimetric Analysis (TGA)

A Stanton Redcroft STA-780 TGA was used for thermogravimetric-differential temperature analysis (TG-DTA) of catalyst samples. The following method was applied:

- Load 25mg of catalyst sample into the sample holder (silica used as relative mass).
- Dry the samples in flowing nitrogen (30 ml/min) at 120°C for 2 hours.

- Inrease the sample temperature from 40°C to 500°C at 10°C/min in flowing nitrogen (30 ml/min)

- At 500°C switch from nitrogen to air (30 ml/min) and hold at 500°C for 30 minutes.

Various spectra for used Pt/KL catalysts are shown in Figure 2-28. The reaction conditions were 450°C and 1 bar hydrogen partial pressure. The feeds were:

A n-hexane, t.o.s. = 48 hours
B MEK/n-hexane, t.o.s. 90 = hours
C n-hexane, t.o.s. = 120 hours

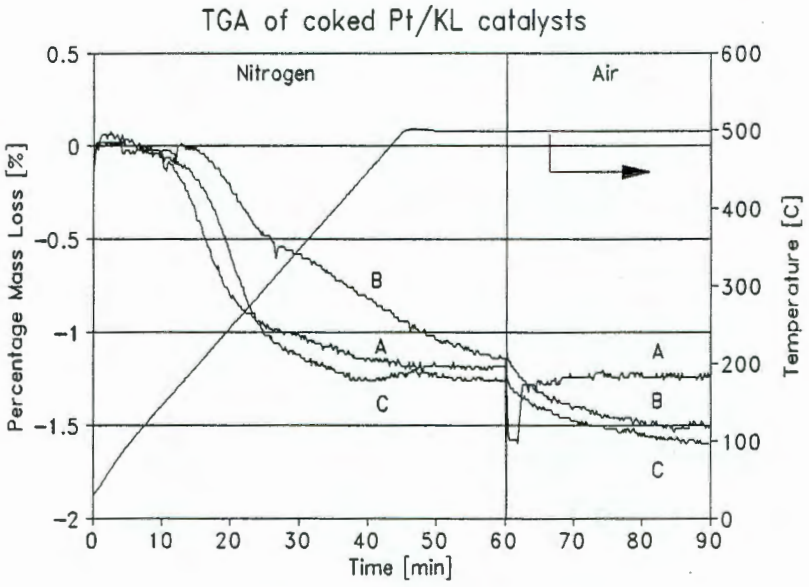

Figure 2-28 TGA spectra of Pt/KL catalysts

Under nitrogen, the percentage mass loss was similar in each case. The nitrogen should remove "soft coke" (desorbed heavy hydrocarbons), while calcination in air is necessary to remove "hard" coke (polynuclear aromatics). The mass percent of

soft coke was *ca.* 1.2 wt% for all three samples and the hard coke *ca.* 0.35 wt% for the case of sample B and C.

2.5.8 Chemisorption

The chemisorption experiments to determine the platinum metal dispersion of Pt/KL catalysts was performed on a Micromeritics ASAP 2000 instrument. Initially hydrogen was used as the chemisorbed gas to determine platinum metal dispersion. However, it proved problematic to obtain reproducible results using hydrogen. On the basis of the experimental difficulties encountered using hydrogen and on the basis of the discussion in Section 1.9 it was decided to use carbon monoxide as the chemisorbed gas to measure platinum metal dispersion.

The pretreatment conditions used for each catalyst sample are shown in Figure 2-29. The adsorption was performed at a temperature of 35°C. The different partial pressures of carbon monoxide were 150mmHg, 200mmHg, 300mmHg, 400mmHg and 500mmHg. The procedure used was, adsorption at the above pressures, degassing at 35°C for 1 hour and repetition of the CO adsorption. The difference between the two adsorption isotherms was taken as the chemisorbed amount of CO.

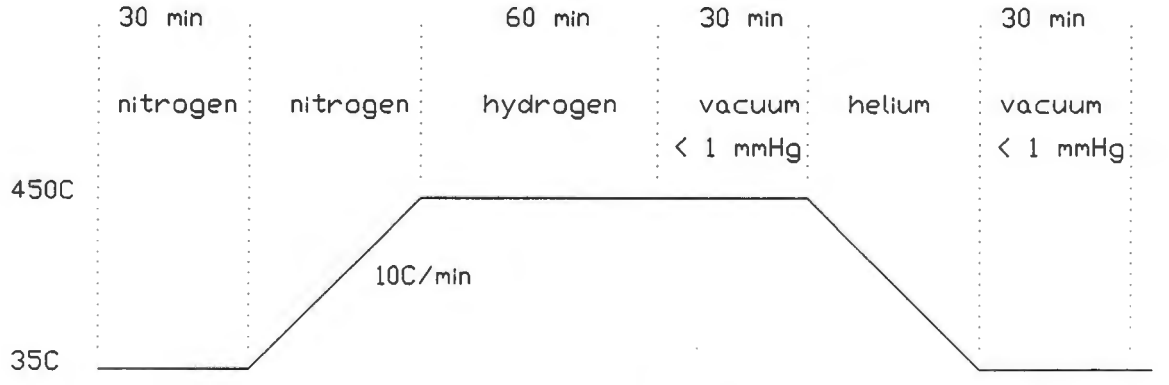

Figure 2-29 Pretreatment conditions for the Pt/KL catalysts during chemisorption experiments

The catalyst samples chosen for chemisorption analysis were:

- Fresh Pt/KL (synthesized as explained in Section 2.1.1).
- Pt/KL that had undergone reaction with n-hexane at 550°C (see Section 3.1.1 for a full description).

The results of the chemisorption experiments are shown in Table 2-5. Fresh Pt/KL had a metal dispersion of 90% indicating that the synthesis procedure for Pt/KL results in highly dispersed platinum particles. A degree of sintering occured when the catalyst was operated at 550°C. However, the decrease in platinum dispersion to 81% is quite small.

Table 2-5 Results of chemisorption of Pt/KL catalysts

Catalyst	Dry sample mass	Platinum dispersion
Fresh Pt/KL	0.4808g	90%
Sintered Pt/KL	0.2151g	81%

Chapter 3

Results and Discussion

3 Results and Discussion

3.1 Reaction pathways on Pt/KL

The effect of temperature, WHSV and hydrogen partial pressure on the selectivity to products for aromatization of n-hexane on Pt/KL were investigated. In addition, a reaction product, 1-hexene was also used as feed over Pt/KL. These results are summarized in the following subsections and allow the confirmation of the reaction pathways on Pt/KL to be made.

3.1.1 Sintering of platinum

Platinum loaded on inert supports (e.g. Zeolite L) is reported (Hughes *et al.* 1986) to sinter when exposed to temperatures greater than 450°C. The current sintering experiment was performed, with n-hexane as the feed, by increasing the reaction temperature from 450°C to 550°C in 25°C increments. After each 25°C increment the reaction temperature was returned to 450°C. Samples of the product gas were analysed at every temperature increment (and decrement). Sintering is a time-dependent phenomena; hence, the degree of sintering will be influenced by the length of time that the catalyst was exposed to elevated temperature. Thus the catalyst was held at each elevated temperature for 1.5 hours. Temperature, however, has an exponential effect on the rate of sintering in contrast to the linear effect of time.

University of Cape Town

3.1.1.1 Results of sintering experiments

These results are summarized in Table 3-1 and show clearly that a decline in conversion at 450°C of n-hexane occurs at and above reaction temperatures of 475°C. There is a concurrent slight decrease in benzene selectivity. The hexenes selectivities (at 450°C) increase after reaction at high temperatures, while the hydrogenolysis products (C_1-C_5) show a small decline. Hence, it appears that at 450°C, after reaction at 550°C:

- Conversion decreases by 26%
- Hexane isomerization selectivity (MCP, 2m-C_5, 3m-C_5) decreases by 7.5%
- Dehydrocyclization selectivity (benzene) decreases by 7%
- Hydrogenolysis selectivity (C_1-C_5) decreases by 19%
- Dehydrogenation selectivity (hexenes) increases by 39%

The ratio of 2m-C_5/3m-C_5 remains constant at about 1.25 after the sintering experiments. However, the ratio of MCP/2m-C_5 increases from 2.3 to 2.9 during the experiment (Table 3-1). In general, as the reaction temperature increases the ratio of MCP:methylpentanes decreases (and vice versa), while the ratio of 2m-C_5/3m-C_5 remains constant at about 1.25. Thermodynamic equilibrium calculations predict that the ratio of MCP/methylpentanes should increase with reaction temperature (Section A.2.2, MCP/2m-C_5 increases from 0.61 to 2.4 at 450°C and 550°C respectively). The thermodynamic equilibrium ratio of 2-mC_5:3m-C_5 decreases only slightly from 1.8 to 1.7 over the temperature range of the sintering experiments. Thus even though the experimental ratios of 2m-C_5/3m-C_5 are slightly different from the thermodynamically predicted ratios they remain constant over the temperature range studied.

Table 3-1 Sintering experiments on Pt/KL

Reaction temperature	450°C	475°C	500°C	525°C	550°C
n-C_6 conversion[a]	27	40	52	63	77
Conversion (450°C)	27	24	22	21	20
Benzene selectivity	54	58	60	68	78
Benzene (450°C)	54	52	51	50	50
MCP selectivity	12	7.8	5.2	1.8	0.2
MCP (450°C)	12	12	12	12	12
2m-C_5 selectivity	5.3	3.8	3.0	1.0	0.2
2m-C_5 (450°C)	5.3	4.9	4.6	4.4	4.2
3m-C_5 selectivity	4.0	3.3	2.5	1.0	0.2
3m-C_5 (450°C)	4.0	3.9	3.7	3.5	3.5
Methane selectivity	2.0	3.0	4.3	6.8	10
Methane (450°C)	2.0	1.9	1.8	1.8	1.7
Ethane selectivity	1.8	2.1	2.4	2.9	2.9
Ethane (450°C)	1.8	1.7	1.7	1.6	1.5
Propane selectivity	2.4	2.4	2.4	2.3	1.8
Propane (450°C)	2.4	2.3	2.0	1.9	1.7
n-Butane selectivity	2.3	2.0	1.8	1.4	0.8
n-Butane (450°C)	2.3	2.0	2.0	2.0	1.8
n-Pentane selectivity	3.7	3.7	3.0	2.0	0.8
n-Pentane (450°C)	3.7	3.6	3.4	3.3	3.2
ΣHexenes selectivity	10.9	11.3	13.3	10.6	2.7
ΣHexenes (450°C)	10.9	12.6	14.5	15.6	17.1
ΣC_1-C_5 selectivity	12.2	13.2	13.9	15.4	16.3
ΣC_1-C_5 (450°C)	12.2	11.5	10.9	10.6	9.9
Σi-C_6 selectivity	21.3	14.9	10.7	3.8	0.6
Σi-C_6 (450°C)	21.3	20.8	20.3	19.9	19.7
ΣSelectivities	98.4	97.4	97.9	97.8	97.6
ΣSelectivities (450°)	98.4	96.9	96.7	96.1	96.7
2m-C_5/3m-C_5	1.3	1.2	1.2	1.0	1.0
2m-C_5/3m-C_5 (450°C)	1.3	1.3	1.2	1.3	1.2
MCP/2m-C_5	2.3	2.1	1.7	1.8	1.0
MCP/2m-C_5 (450°C)	2.3	2.4	2.6	2.7	2.9

(a) n-hexane conversion and selectivities in carbon mass%
(b) p(n-C_6) = 0.083 bar, H_2:n-C_6 = 12:1, WHSV = 4.75 /hr

On platinum catalysts with low dispersion, the relative amount of n-hexane formed from the hydrogenolysis of MCP (to n-hexane and methylpentanes) is expected to decrease relative to highly dispersed platinum catalysts (Section 1.8.1.3). In the aromatization of n-hexane this would shift the reaction towards a greater relative amount of MCP and methylpentanes. However, this is can only be observed for the feeding of MCP. The ratio of n-C_6:(MCP + 2m-C_5 + 3m-C_5) at 450°C is 3.44 before sintering and 4.06 after sintering at 550°C. The thermodynamic ratio at 450°C is 0.34. The more highly dispersed catalyst should be more active and thus the ratio of n-C_6:i-C_6 should be lower. This is confirmed by the experimental ratios. At 550°C the experimental ratio is 38.3 and the thermodynamic ratio is 0.20. Thus the isomerization reaction, n-C_6 $\rightleftarrows$ i-C_6, is shifted further from equilibrium at higher reaction temperatures, presumably due to i-hexanes being converted to benzene and cracked products. The experimental ratio of MCP/2m-C5 decreases with temperature, while thermodynamics predicts that the ratio will increase with reaction temperature.

3.1.1.2 TEM and chemisorption analysis

TEM micrographs (Section 2.5.4) show clearly that sintering of the platinum clusters has occured after reaction at 550°C (compare Figure 2-24 and Figure 2-25). The platinum clusters on fresh Pt/KL catalysts cannot be resolved by the TEM as they are too highly dispersed (Figure 2-23). The TEM analysis of the sintered catalyst shows that large platinum particles $\approx$ 300Å to 600Å are present (Figure 2-24). These large platinum particles must, due to their large size, be located on the outer zeolite surface. Chemisorption of carbon monoxide (Section 2.5.8) gives a platinum metal dispersion of 81% (relative to 90% for fresh Pt/KL). This is further evidence that sintering has occured. Reaction temperatures at and below 450°C do not appear to cause much sintering of the platinum clusters.

3.1.1.3 Conclusions on sintering

Operation at temperatures above 450°C caused a decrease in the n-hexane conversion at 450°C over Pt/KL as discussed in section 3.1.1.1. There are two possibilities for these changes, *viz.* sintering of the platinum clusters and/or coke formation. Both mechanisms will cause a reduction in the number of active platinum sites and hence lower the conversion of n-hexane. If the primary cause of the deactivation observed after reaction at high temperatures was coke formation, resulting in pore blocking, then only the number of active platinum sites decreases. The intrinsic reactivity of the remaining platinum clusters should remain the same. However, if sintering had occured then a change in the physical and chemical properties of the platinum clusters would occur (as well as reduction in the number of active sites) and a deviation from a smooth selectivity-conversion plot would be expected, *i.e.* the curve should have a different slope and the product selectivities, at the same conversion should be different.

As shown in Section 2.4.4 the Pt/KL catalyst deactivates over the first 48 hours of operation resulting in an increase in the hexene selectivity, and a decrease in hydrogenolysis products (C_1-C_5) as well as a decrease in conversion. Benzene selectivity remains constant and the selectivity to isomerized hexane products (methylpentanes and MCP) remain approximately constant (Table 3-1). These results are compared qualitatively with the sintering experiments in Table 3-2.

Table 3-2 Qualitative comparison of the experimental selectivity and conversion trends for deactivation due to coking and sintering

Reaction pathway	Coking	Sintering
n-C_6 conversion	↓	↓
Dehydrocyclization (benzene)	→	↓
Isomerization (MCP + 2m-C_5 + 3m-C_5)	→	↓
Hydrogenolysis (C_1-C_5)	↓	↓
Dehydrogenation (hexenes)	↑	↑

University of Cape Town

Different trends are observed in the case of benzene selectivity and the hexane isomers for the sintering and coking experiments. Dehydrocyclization is sensitive to changes in platinum particle size (Section 1.8.1.3), while dehydrogenation and hydrogenolysis are not. Hence, the decrease in benzene selectivity during the sintering experiments tend to support the contention that sintering of the platinum clusters had occurred. Similarly the ring opening reactions of MCP on platinum are know to be sensitive to platinum particle size as well.

However, it is also quite likely that there was an increase in coke formation as there is a 39% increase in the selectivity to hexenes. The TGA analysis of Pt/KL (Section 2.5.7) shows that *ca.* 1.55 wt% coke is formed during the reaction of n-hexane with Pt/KL. Alkenes are known to form coke more rapidly than alkanes. The hexene products, in general, seem to be the reaction products most sensitive to any changes in the experimental conditions. This is most likely a result of the high reactivity of the hexenes relative to the alkane products. An increase in hexenes selectivity should result in an increase in benzene selectivity as the hexenes can undergo dehydrocyclization to form benzene. Thermodynamics predict that 1-hexene will undergo dehydrocyclization to benzene to a greater extent than n-hexane at the same temperature. However, the experimental evidence does not support this as benzene selectivity decreased slightly despite an increase in selectivity to hexenes.

If the dehydrocyclization pathway is inhibited (by sintering of platinum clusters) then the conversion of n-hexane will decrease, the selectivity to benzene will decrease and the selectivity to hexenes will increase. The sintering experiment results in different product selectivity trends to that observed during deactivation by coking, specifically with regard to ring closure/opening pathways. These reaction pathways are known to be sensitive to platinum particle size. In addition, the TEM micrographs and carbon monoxide chemisorption show that sintering of platinum particles has occured.

3.1.2 Effect of reaction temperature

The effect of reaction temperature on the performance of Pt/KL for n-hexane aromatization was tested. The catalyst was first allowed to reach steady state at 450°C and then the reaction temperature was decreased to 250°C in varying increments, returned to 450°C and then increased to 550°C, before being returned to 450°C. The results of these experiments are plotted with selectivity as a function of conversion, rather than reaction temperature. This experiment, performed in addition to the sintering experiment (Section 3.1.1) was with a fresh Pt/KL catalyst. The time that the catalyst was exposed to each elevated temperatures (>450°C), specifically 550°C, was less than 10 minutes. Thus the degree of sintering that could occur should be small. There are thus three selectivity and conversion values at 450°C. These show that no appreciable amount of sintering occurred.

3.1.2.1 Results at 1 bar hydrogen partial pressure

It was observed that the dehydrogenated products (linear hexenes) exhibit maxima at *ca.* 30% to 40% conversion (Figure 3-3) while the isomerized hexanes decline with increase in conversions above 5% (Figure 3-2, Figure 3-4). Of the cracked products, methane and ethane show an increase in selectivity with increase in conversion, while pentane and butane go through maxima at *ca.* 475°C (Figure 3-5). Benzene selectivity increases with increase in conversion (Figure 3-1). A good mass balance was attained. The reaction conditions were slightly different to that for the sintering experiments, *viz.* $p(\text{n-C}_6)$ = 0.064 bar, H_2:n-C_6 = 16:1, WHSV = 3.65 /hr. The selectivity/conversion data match quite well, however.

University of Cape Town

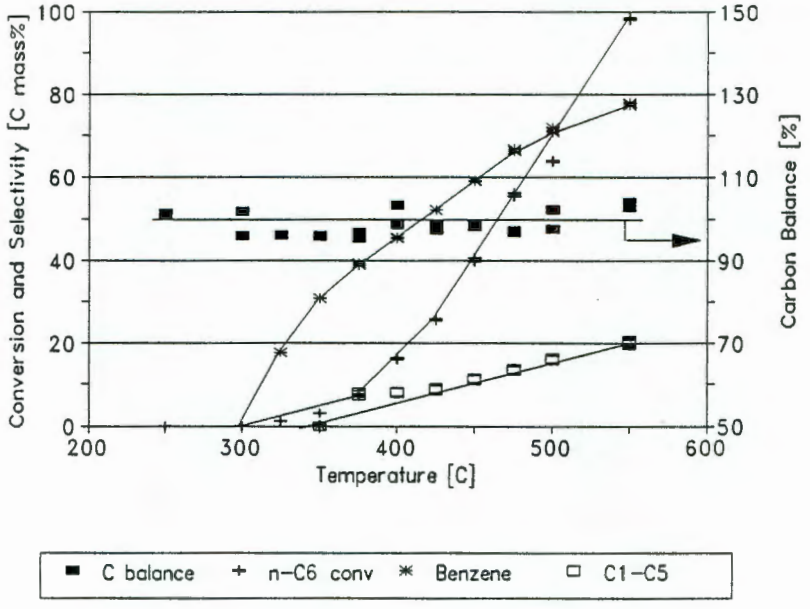

Figure 3-1 Selectivity/conversion relationship as a result of change in reaction temperature

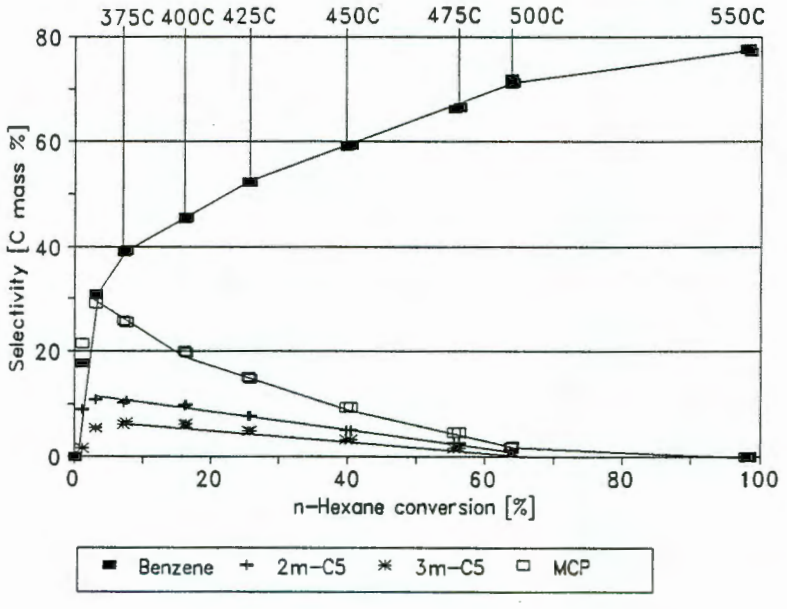

Figure 3-2 Selectivity/conversion relationship as a result of change in reaction temperature

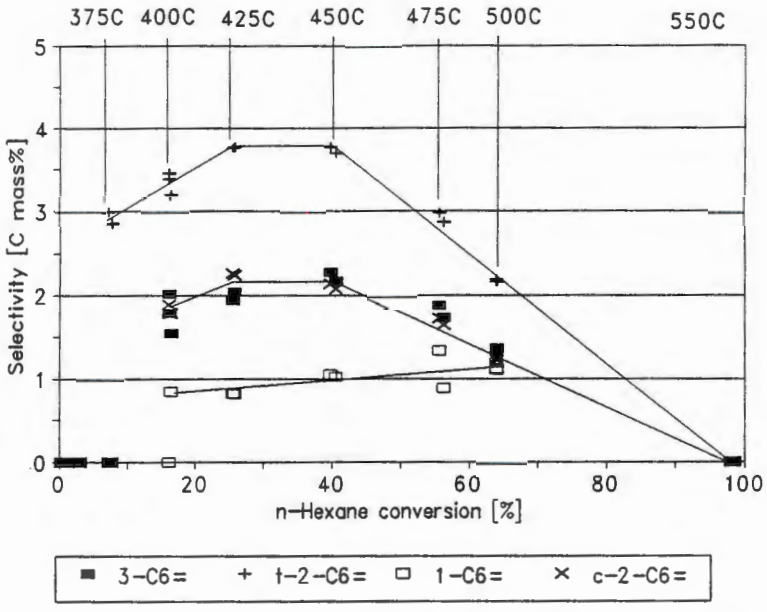

Figure 3-3 Selectivity/conversion relationship as a result of change in reaction temperature (hexene products)

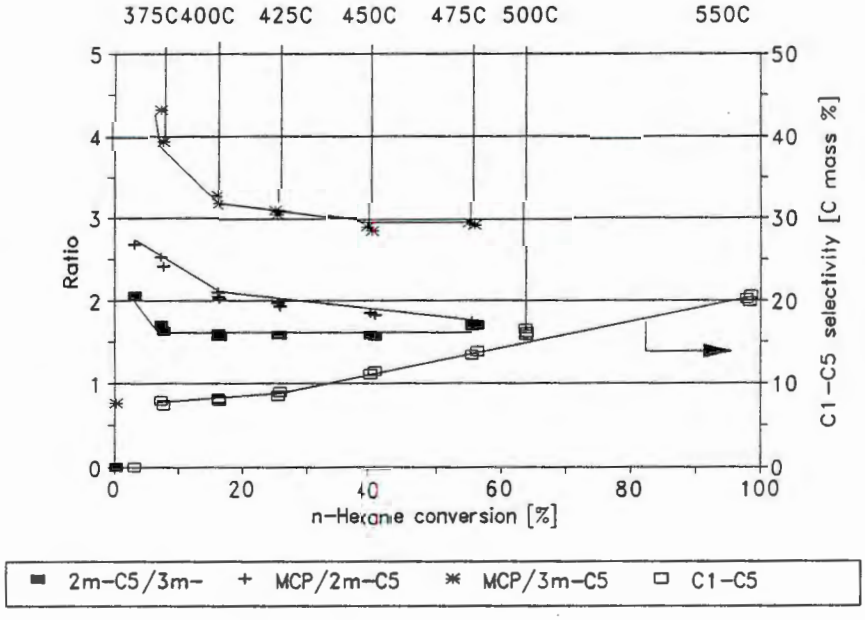

Figure 3-4 Selectivity/conversion relationship as a result of change in reaction temperature (isomerized hexane products)

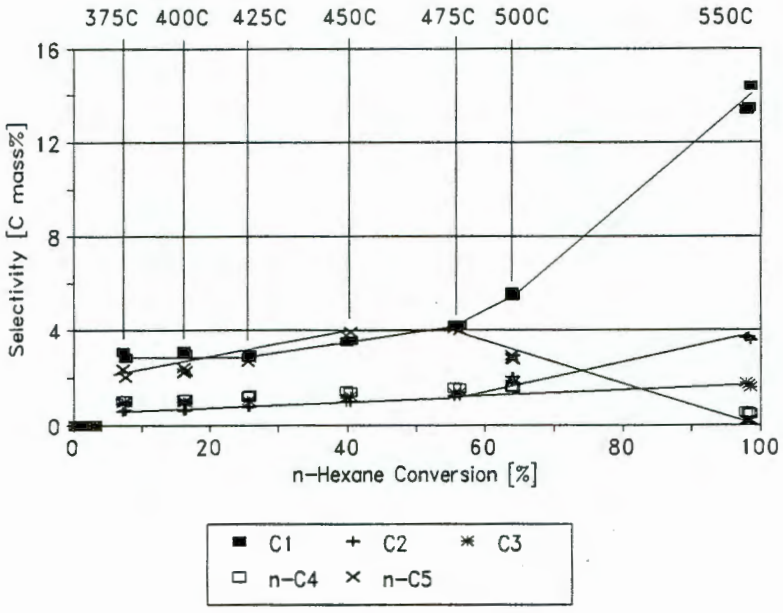

Figure 3-5 Selectivity/conversion relationship as a result of change in reaction temperature (cracked products)

3.1.2.2 Discussion of effect of reaction temperature

If all C_6 products are assumed to be able to undergo aromatization (via their transformation to n-hexane or hexenes) then the absolute selectivity to benzene (benzene + all C_6 products) decreases with increase in reaction temperature, due to the increase in selectivity to hydrogenolysis products. Cracked products (C_1-C_5) are not aromatizable with Pt/KL catalysts. Thus the absolute selectivity to benzene is 92% at 400°C, but only 80% at 550°C. Hence, increase in reaction temperature may be assumed to have an inhibitory effect on the ultimate selectivity to benzene.

It appears that both the isomerized hexanes and the dehydrogenated hexene products are intermediates, *i.e.* the selectivity decreases at high conversions Alternately they may just decrease because thay are in quasi-equlibrium with n-hexane. Dehydrogenation is an endothermic reaction and the extent to which it occurs should increase with increase in reaction temperature. However, this not

observed experimentally. Similarly, the extent of isomerization of n-hexane is thermodynamically expected to increase with temperature (Section A.2.2). Again this is not observed experimentally. The reason for this is that the hexenes and isomerized hexanes are reaction intermediates and hence are converted to the thermodynamically more favoured benzene with increase in reaction temperature.

From the selectivity data in Figure 3-5 it appears that the cracking activity is confined mainly to n-hexane at reaction temperatures below 475°C as the selectivity to both pentane and butane increase until that temperature. At higher temperatures there is a decline in selectivity to pentane and butane, presumably by their hydrogenolysis to methane, ethane and propane. At 550°C the selectivity to pentane and butane has dropped to *ca.* 0.5%, while the selectivity to propane and ethane are still increasing. Hence at high reaction temperatures both pentane and butane undergo further cracking. If it is assumed that only hexane undergoes hydrogenolysis, at low temperatures, then the molar ratios of n-pentane:methane and n-butane:ethane should be unity, assuming a low cracking activity for n-butane and n-pentane. The molar selectivities are shown in Table 3-3.

Table 3-3 Molar selectivities of cracked products as a function of reaction temperature at 1 bar hydrogen partial pressure

	C_1	C_2	C_3	C_4	C_5	Calc C_1[a]	C_2/C_4	C_1/C_5
375°C	2.9	0.28	0.48	0.26	0.43	3.5	1.1	6.7
400°C	3.0	0.30	0.49	0.27	0.44	3.7	1.1	6.8
425°C	3.0	0.39	0.51	0.31	0.56	4.3	1.3	5.4
450°C	3.6	0.48	0.60	0.35	0.78	5.2	1.4	4.6
475°C	4.2	0.61	0.68	0.41	0.93	6.2	1.5	4.5
500°C	5.5	1.02	0.91	0.45	0.82	8.5	2.3	6.7
550°C	13.4	1.84	0.86	0.18	0.04	10.3	10.2	335.0

(a) methane calculated assuming only terminal hydrogenolysis, *viz.* $C_1 = 4C_2 + 3C_3 + 2C_4 + C_5$

University of Cape Town

There is no correlation between the molar ratios of pentane:methane and butane:ethane. However, the molar ratios of butane:ethane are close to unity below 450°C. The molar selectivity of methane is about an order of magnitude greater than any of the other cracked products. The amount of methane calculated, assuming only terminal hydrogenolysis also does not match very well with the experimentally observed methane molar selectivity. The possible hydrogenolysis reactions are shown below. Note that metals, specifically nickel, which is present in the stainless steal reactor walls, can catalyze the complete hydrogenolysis of hydrocarbons to methane

$$a\ C_6 \rightarrow 6a\ C_1 \quad \ldots(1)$$

$$b\ C_6 \rightarrow b\ C_5 + b\ C_1 \quad \ldots(2)$$

$$c\ C_6 \rightarrow c\ C_4 + c\ C_2 \quad \ldots(3)$$

$$d\ C_6 \rightarrow 2d\ C_3 \quad \ldots(4)$$

$$e\ C_5 \rightarrow e\ C_4 + e\ C_1 \quad \ldots(5)$$

$$f\ C_5 \rightarrow f\ C_3 + f\ C_2 \quad \ldots(6)$$

$$g\ C_4 \rightarrow g\ C_3 + g\ C_1 \quad \ldots(7)$$

$$h\ C_4 \rightarrow 2h\ C_2 \quad \ldots(8)$$

$$i\ C_3 \rightarrow i\ C_2 + i\ C_1 \quad \ldots(9)$$

The ratio of methane:pentane remains approximately constant until 500°C, above which temperature it increases. If only platinum catalyzed cracking was taking place then the ratio would be expected to show a steady increase with increase in reaction temperature, *i.e.* the percentage cracked molar selectivity to pentane would be highest at the lowest reaction temperature at which cracking was observed. However, it appears that there must be a hydrogenolysis pathway that completely cracks hexane to methane, probably catalyzed by nickel, due to the very high selectivity to methane. Nickel is present in the reactor walls. The conversion of n-hexane in the empty reactor was less than 3% (Section 2.4.2.1) and hence the reactor walls should only have a small influence on the total amount

of cracked products.

Anyway, this calls into contention the work of Tauster and Steger (1990) who propose a direct relationship between the TCI ($n\text{-}C_5/n\text{-}C_4$) and benzene selectivity. The TCI assumes that only hexane cracking occurs and that no secondary cracking of n-pentane and n-butane takes place. This only holds for reaction temperatures below 425°C as it appears that n-butane cracks at higher temperatures (the molar ratio of C_2:C_4 is no longer unity). The experimental benzene selectivities and TCI values for this work is shown in Table 3-4.

Table 3-4 TCI and benzene selectivity data

Reaction temperature	$n\text{-}C_6$ conversion	Benzene selectivity	TCI (C_5/C_4)
375°C	8%	39%	1.65
425°C	26%	52%	1.81
500°C	64%	71%	1.82
550°C	99%	78%	0.22

The ratios of isomerized products and the linear hexenes fraction is shown in Table 3-5. The methylpentanes appear to be in equilibrium as their ratio is close to that expected from thermodynamics. However, the ratios of MCP:methylpentanes is not close to the thermodynamically expected values. If the reaction scheme shown below (cyclic mechanism for isomerization) is used, then it follows that $2m\text{-}C_5$ and $3m\text{-}C_5$ cannot be in thermodynamic equilibrium with each other, but not in equilibrium with MCP as well (assuming MCP readily desorbs).

$$n\text{-}C_6 \rightleftarrows MCP \rightleftarrows 2m\text{-}C_5,\ 3m\text{-}C_5$$

Table 3-5 Ratios of isomerized hexanes and linear hexene mole fractions at 1 bar hydrogen partial pressure

	2m-C_5/ 3m-C_5	MCP/ 2mC_5	MCP/ 3m-C_5	n-C_6/ MCP	1-C_6=	t-2-C_6=	c-2-C_6=	3-C_6=
Experimental data								
375°C	1.67	2.41	3.94	3.5	0	1	0	0
400°C	1.59	2.05	3.21	4.2	0	0.48	0.27	0.25
425°C	1.58	1.95	3.08	4.9	0.09	0.43	0.26	0.22
450°C	1.58	1.85	2.91	6.8	0.11	0.41	0.23	0.25
475°C	-	1.73	2.96	11.3	0.14	0.39	0.22	0.24
Thermodynamic equilibrium data (molar ratio H_2:hydrocarbon = 20:1)								
375°C	1.89	0.15	0.28	4.43	0.05	0.33	0.39	0.23
400°C	1.87	0.27	0.51	2.52	0.05	0.33	0.38	0.24
425°C	1.86	0.41	0.76	1.72	0.06	0.33	0.38	0.24
450°C	1.84	0.55	0.89	1.19	0.07	0.32	0.37	0.24
475°C	1.82	0.89	1.61	0.86	0.07	0.32	0.37	0.24

If the ratio of n-C_6/MCP was not in equilibrium (due to the n-C_6 → benzene reaction) then the ratios of MCP/methylpentanes should be lower than expected. However, the ratio of MCP/methylpentanes was found to be higher than expected. This can be rationalized if the reaction of MCP ⇄ methylpentanes is slow, relative to the reaction of n-C_6 ⇄ MCP. However, the statistically expected ratio of 2-m-C_5/ 3-m-C_5 is 2 which is also close to the observed value of 1.6. Thus, it appears that the methylpentanes are not in thermodynamic equilibrium at all, the ratios observed are merely the statistically expected values.

Another, possible explanation is that the formation of methylpentanes from n-hexane also proceeds via a bond shift mechanism, *viz.* MCP is not involved as a reaction intermediate. In this case the methylpentanes could be in thermodynamic equilibrium with each other, but not with MCP. However, on highly dispersed platinum catalysts the bond shift isomerization mechanism has been shown to be a minor pathway compared to the cyclic mechanism (Section 1.9.1.2)

The experimental ratio of n-C_6/MCP increases with increase in reaction temperature, while the thermodynamic ratios decrease. Thus at higher reaction temperatures, isomerization is shifted further from equilibrium, presumably as the iso-hexanes are reaction intermediates and are converted to benzene and C_1-C_5 hydrogenolysis products.

The ratios observed on Pt/KL differ significantly to those observed on pure KL (Section 2.4.2.2) where the ratio of 2m-C_5/3m-C_5 and MCP/2m-C_5 is 0.75 and 0.4 respectively at 450°C. This may indicate a different reaction mechanism on KL, *i.e.* an acid-catalyzed reaction pathway rather than a metal-catalyzed pathway, although it is difficult to see how this would result in more 3m-C_5 than that statistically expected. A possible explanation may be that 2m-C_5 and MCP react at a faster rate than 3m-C_5, but again the reason for this is unknown.

The linear hexenes show a fairly close correlation between the experimentally observed fractions and the calculated thermodynamic equilibrium fractions, except for cis-2-hexene. The experimental ratios of c-2-hexene:t-2-hexene remain constant at 0.56. The thermodynamic ratio is 1.15. A possible explanation is that dehydrocyclization to benzene occurs for the cis-isomer, but not for the trans-2-hexene isomer, thus lowering the ratio. As the 3-hexene isomers could not be resolved, this hypothesis could not be extended to the 3-hexenes.

University of Cape Town

However, the linear hexenes fraction is considerably different to that observed on KL (Table 2-3). If the dehydrogenation proceeds in the order 1-hexene → 2-hexene → 3-hexene, then on KL where the reaction is slow, less 3-hexene is expected, and more 1-hexene is expected, relative to thermodynamic equilibrium. This is observed on KL, but not on Pt/KL where reaction is much faster and the hexenes are close to thermodynamic equilibrium. The sum of the molar fractions of the observed 2-hexene isomers at 400°C and 475°C is 0.75 and 0.61 respectively while the sum of the thermodynamic equlibrium 2-hexene isomers is 0.72 and 0.69 at 400°C and 475°C respectively. Thus if the isomers are grouped as 1-hexene, 2-hexenes and 3-hexenes they can considered to be very close to thermodynamic equilibrium.

3.1.2.3 Effect of temperature at a hydrogen partial pressure of 6 bar

The effect of reaction temperature (300°C to 450°C), at a hydrogen partial pressure of 6 bar, was investigated. A fresh Pt/KL catalyst was used. A good mass balance was achieved (Figure 3-6). For all reaction work at high pressure, the residence time in the catalyst bed was kept constant by increasing the flowrate of the carrier gas in proportion to the increase in pressure. The n-hexane partial pressure was kept constant. The experimental conditions were $p(n\text{-}C_6)$ = 0.064 bar, molar ratio H_2:n-C_6 = 94 and WHSV = 3.65 /hr.

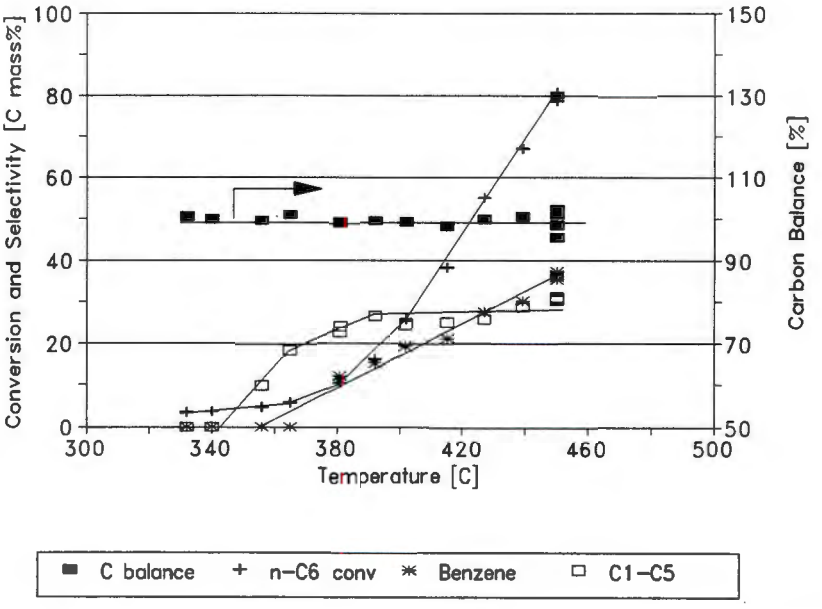

Figure 3-6 Effect of reaction temperature at 6 bar hydrogen partial pressure

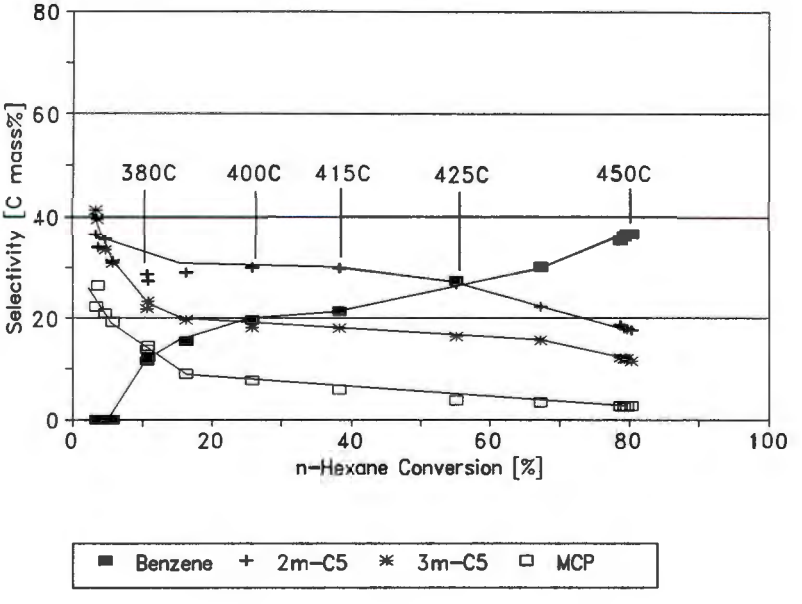

Figure 3-7 Selectivity as a function of n-hexane conversion at 6 bar hydrogen partial pressure (isomerized products and benzene)

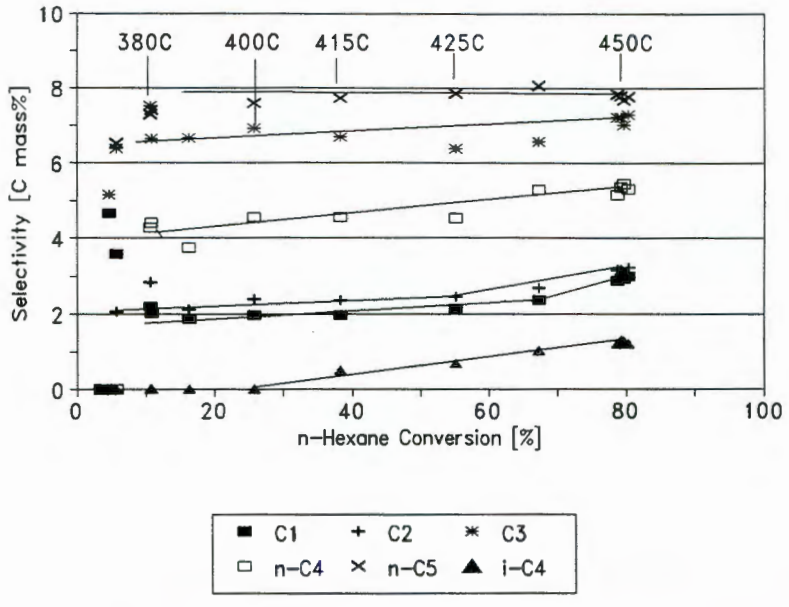

Figure 3-8 Selectivity as a function of n-hexane conversion at 6 bar hydrogen partial pressure (cracked products)

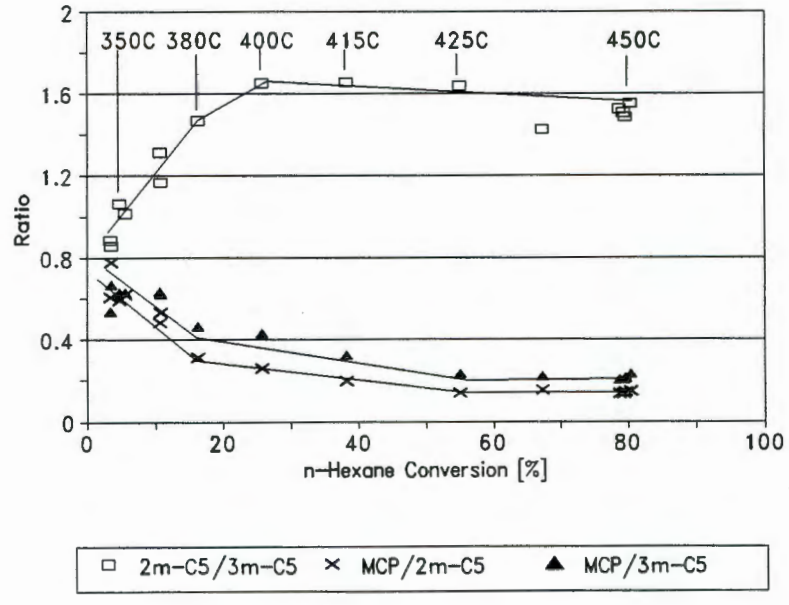

Figure 3-9 Isomerized hexanes ratios as a function of conversion at 6 bar hydrogen partial pressure

3.1.2.4 Discussion of the effect of reaction temperature at 6 bar

The effect of higher hydrogen partial pressure (6 bar) relative to low hydrogen partial pressure (1 bar) is summarized below:

- Conversion of n-hexane increases.
- Selectivity to benzene is lowered.
- Selectivity to methylpentanes increases, while selectivity to MCP decreases.
- Hexenes selectivity is zero.
- Hydrogenolysis selectivity increases, but the relative methane selectivity is suppressed.

Table 3-6 Molar selectivities of cracked products at 6 bar

	methane	ethane	propane	butane	pentane	Calc C_1[a]	C_2/C_4	C_1/C_5
380°C	1.97	1.08	2.21	1.10	1.48	14.63	0.98	1.33
400°C	1.95	1.16	2.24	1.11	1.68	15.26	1.05	1.16
425°C	2.13	1.25	2.13	1.14	1.57	15.24	1.10	1.36
450°C	2.89	1.58	2.41	1.29	1.57	17.70	1.22	1.84

(a) Calculated methane molar selectivity, for terminal hydrogenolysis only: $4C_2 + 3C_3 + 2C_4 + C5$

A summary of the molar selectivities of the cracked products are shown in Table 3-6. The ratio of ethane:butane is close to unity, but increases slightly with increase in reaction temperature, probably as a result of an increase in the cracking rate of butane. The ratio of methane:pentane is also close to unity with the ratio increasing with increase in reaction temperature. When these results are compared to those at 1 bar, the most obvious difference is the suppression of methane relative to the other cracked products. The increase in selectivity to cracked products with increase in reaction temperature, at 6 bar, decreases the absolute selectivity of benzene from 67% to 65% at 400°C and 450°C respectively. The absolute selectivity to benzene at 1 bar is 92% and 88% at 400°C and 450°C respectively. Thus the same trend is evident, *viz.* a decrease in absolute benzene selectivity with increase in reaction temperature. These results lead to the

selectivity with increase in reaction temperature. These results lead to the conclusion that at 6 bar the following hydrogenolysis reactions are dominant (especially below 425°C):

$$C_6 \rightarrow C_5 + C_1 \qquad \because C_1 \approx C_5 \text{ below } 425°C$$
$$C_6 \rightarrow C_4 + C_2 \qquad \because C_2 \approx C_4 \text{ below } 425°C$$
$$C_6 \rightarrow 2C_3$$

Propane is the major hydrogenolysis product at 6 bar (on a molar basis). It appears that terminal hydrogenolysis, which will always produce methane, is suppressed strongly at high pressure. This is well known for nickel catalysts. The hydrogenolysis reaction of n-hexane to produce methane is endothermic. It is thus expected that the extent of terminal hydrogenolysis will increase with both temperature and hydrogen partial pressure. There does appear to be a slight increase in terminal hydrogenolysis with increase in reaction temperature, as indicated by the ratio of C_1/C_5.

A summary of the ratios of isomerized hexanes at 6 bar are shown in Table 3-7. The formation of MCP is suppressed at 6 bar relative to 1 bar. This is expected as the formation of MCP from n-hexane and methylpentanes results in the formation of an equimolar amount of hydrogen. The ratio of 2m-C_5:3m-C_5 (1.6) is not much affected by the increase in hydrogen partial pressure to 6 bar relative to 1 bar where the ratio is 1.6 as well. As expected this is also observed in the case of the thermodynamic calculations.

Table 3-7 Ratios of isomerized hexanes at 6 bar

	2m/3m-C_5	MCP/2m-C_5	MCP/3m-C_5
Experimental data at 6 bar			
380°C	1.17	0.53	0.62
400°C	1.65	0.26	0.43
425°C	1.64	0.14	0.23
450°C	1.53	0.13	0.20
Thermodynamic equilibrium data at 6 bar			
375°C	1.90	0.027	0.051
400°C	1.88	0.043	0.080
425°C	1.86	0.066	0.122
450°C	1.84	0.098	0.179

At 450°C, the isomerization reactions of MCP appear to be fairly close to thermodynamic equilibrium at 6 bar (Table 3-7). This is in contrast to that observed at 1 bar. At 1 bar, the dehydrogenation reactions appear to be fast relative to hydrogenolysis At 6 bar, the dehydrogenation reactions are suppressed (less benzene and MCP) relative to hydrogenolysis as indicated by the ratios in Table 3-8.

Table 3-8 Experimental and thermodynamic selectivity ratios at 450°C

	Experimental		Thermodynamic	
	1 bar	6 bar	1 bar	6 bar
Benzene/(C_1-C_5)	4.9	1.06	≈0	≈0
MCP/(C_1-C_5)	0.75	0.11	≈0	≈0
n-C_6/(MCP + 2,3m-C_5)	3.1	5.0	0.34	0.55
n-C_6/(C_1-C_5)	5.0	0.59	≈0	≈0

The following reaction scheme may be proposed for the reaction of n-hexane on Pt/KL (Figure 3-10).

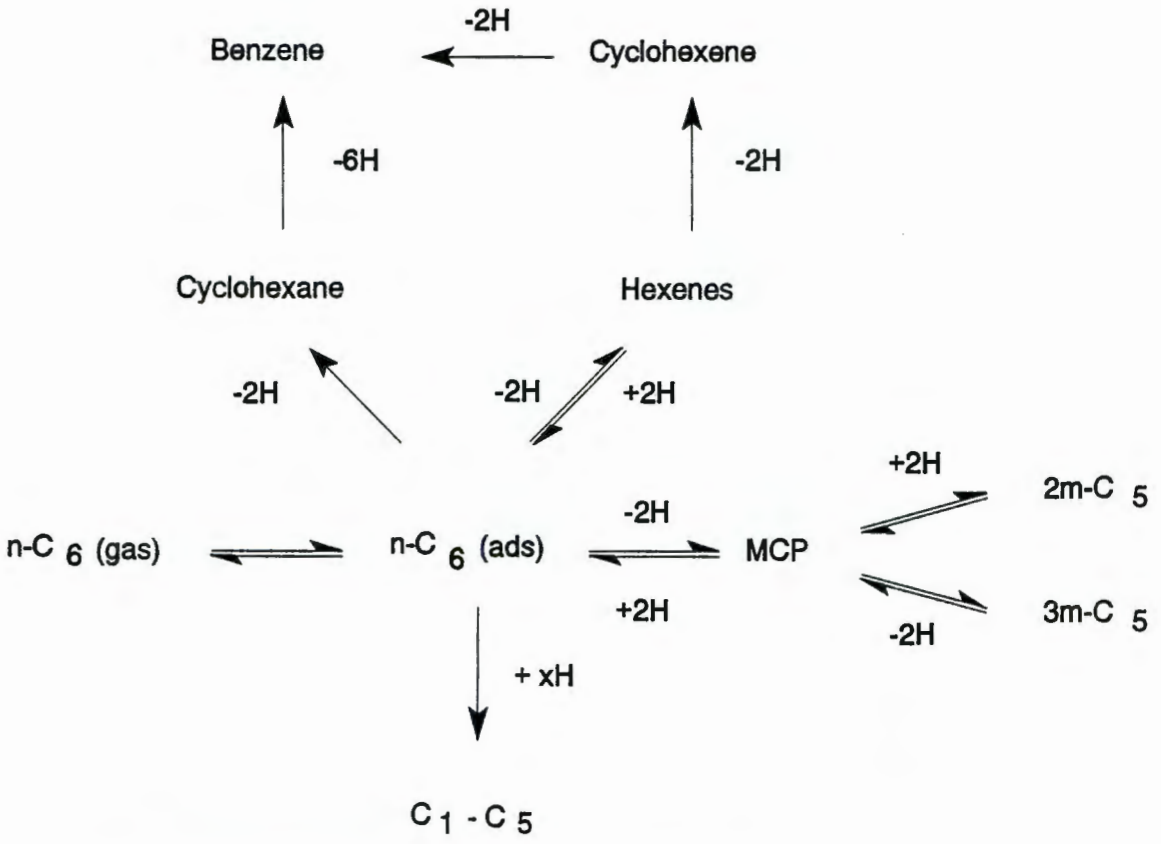

Figure 3-10 Reaction scheme for n-hexane on Pt/KL

The following suggestions can be made:

$n\text{-}C_6$(gas)	⇄	$n\text{-}C_6$(ads)	Slow, because $n\text{-}C_6$/benzene is greater than expected from thermodynamics.
$n\text{-}C_6$(ads)	→	$C_1\text{-}C_5$	Slow because thermodynamically hydrogenolysis is favoured.
$n\text{-}C_6$(ads)	⇄	MCP	Fast, because MCP/2m-C_5 and MCP/3m-C_5 are greater than expected
MCP	⇄	2,3m-C_5	Slow, because MCP/2m-C_5 and MCP/3m-C_5 are greater than expected
Cyclohexane	→	benzene	Fast because cyclohexane is low

At 1 bar cyclohexene is observed as a trace product (no cyclohexane is observed). At 6 bar trace amounts of cyclohexane are observed (but no cyclohexene). This supports the proposal that cyclohexene is an intermediate in the cyclization of hexenes at 1 bar. At 6 bar, dehydrogenation is suppressed (benzene formation) and thus some cyclohexane is observed.

3.1.3 Changes in WHSV at constant temperature

The WHSV was changed for n-hexane aromatization at a reaction temperature of 450°C and 350°C for a hydrogen partial pressure of 1 bar. The selectivities are plotted as a function of n-hexane conversion (Figure 3-11 to Figure 3-14). If a product selectivity tends to zero as the conversion approaches zero then it is most likely not a primary product. However, it was not always possible to determine the product selectivities at n-hexane conversions below 10% (for the reaction temperature of 450°C). However, if with increasing contact time (*i.e.* conversion) the product increases it may be a secondary product and if it decreases it may be a primary product. At 350°C (Figure 3-11) the main products were isomerized hexanes, with low selectivity to hexenes and cracked products observed. The conversion of n-hexane was below 5%.

The results at 450°C, which were obtained independently of the film diffusion work, can be superimposed with those of the film diffusion (Section 2.4.3) and the same trends are observed.

3.1.3.1 Discussion of the change in WHSV

The selectivity to benzene and hydrogenolysis products increases with increase in n-hexane conversion, thus indicating that they are final reaction products. All the other products (isomerized hexanes and hexenes) are intermediates or products of a side reaction not involved in benzene or C_1-C_5 formation. The absolute selectivity

University of Cape Town

to benzene (benzene + all C_6 products) decreases with increase in conversion as a result of the increase in selectivity to cracked products. This is as expected, because the hydrogenolysis products are thermodynamically favoured over benzene. It does indicate that the hydrogenolysis reaction step is slow.

Once again the increase in benzene selectivity coincides with a decrease in selectivity to hexenes. The increase in selectivity to benzene of 15% points (42% to 57%) is close to the decrease in selectivity to hexenes of 16% points (25% to 9%) as shown in Figure 3-12 and Figure 3-13. This may be taken as evidence that direct cyclization of linear hexenes (to benzene) occurs.

A summary of the molar selectivities of cracked products at 450°C and 500°C at different conversions (as a result of change in WHSV) is shown in Table 3-9. The relative proportion of pentane and butane is expected to decrease with increase in conversion. This trend is observed at both 450°C and 500°C, although it is less convincing at 450°C than at 500°C. Methane is the major cracked product at both temperatures. However, the proportion of methane increases at 500°C relative to 450°C at the same conversion of n-hexane.

Table 3-9 Molar selectivities of cracked products at 450°C and 500°C due to change in WHSV

Conv	C_1	C_2	C_3	C_4	C_5	C_2/C_4	C_1/C_5	$(C_4+C_5)/(C_1-C_5)$
				450°C				
12%	1.23	0.54	0.43	0.30	0.44	1.80	2.80	0.25
20%	1.58	0.72	0.54	0.44	0.63	1.64	2.51	0.27
35%	2.26	0.95	0.70	0.57	0.80	1.67	2.83	0.26
47%	2.76	1.18	0.98	0.69	0.90	1.71	3.07	0.24
				500°C				
23%	2.09	0.66	0.42	0.22	0.33	3.00	6.33	0.15
37%	3.45	0.99	0.59	0.31	0.43	3.19	8.02	0.13
48%	4.52	1.20	0.69	0.37	0.48	3.24	9.42	0.12
63%	5.66	1.36	0.79	0.43	0.51	3.16	11.10	0.11

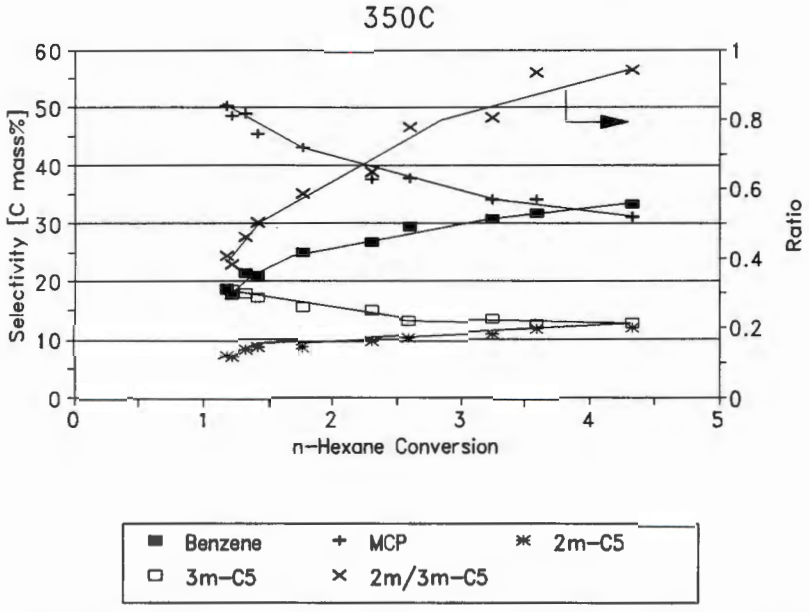

Figure 3-11 Selectivity\conversion plot as a result of changes in WHSV at 350°C for n-hexane aromatization

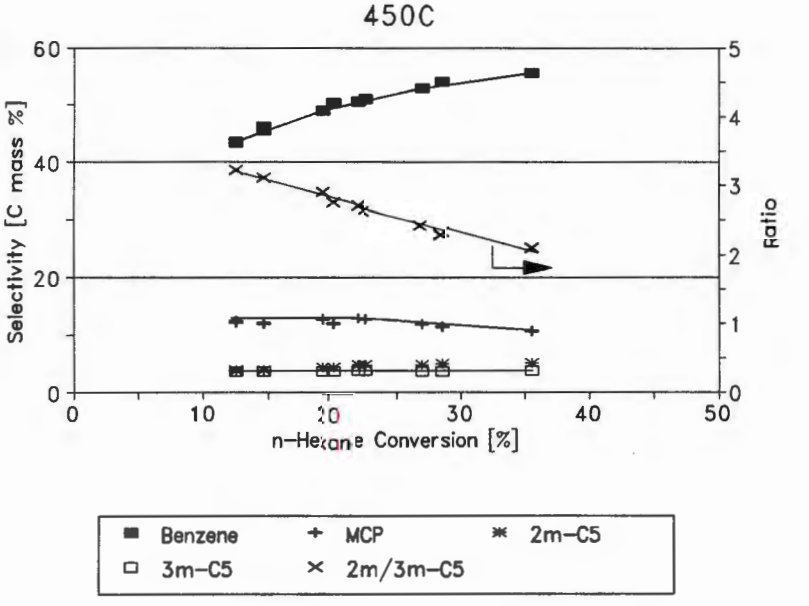

Figure 3-12 Selectivity\conversion plot for changes in WHSV at 450°C for n-hexane aromatization

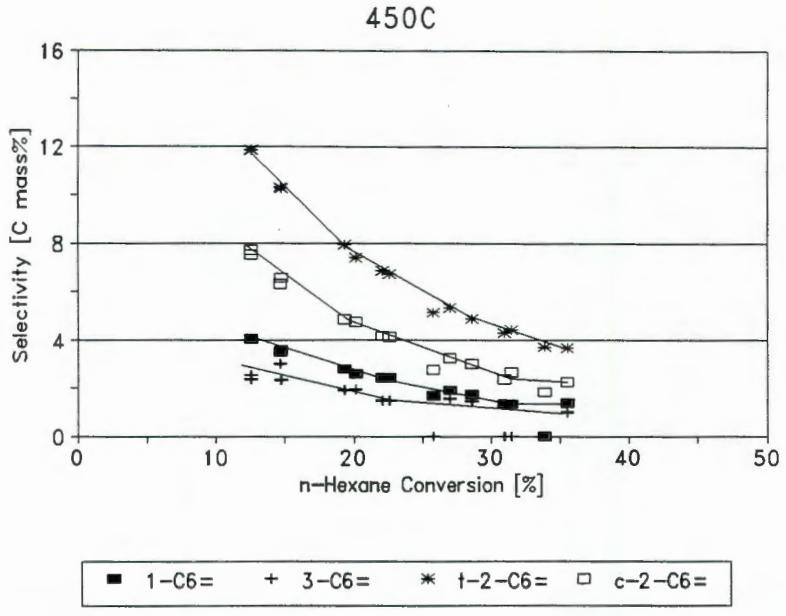

Figure 3-13 Selectivity\conversion plot for changes in WHSV for n-hexane aromatization at 450°C (hexene products)

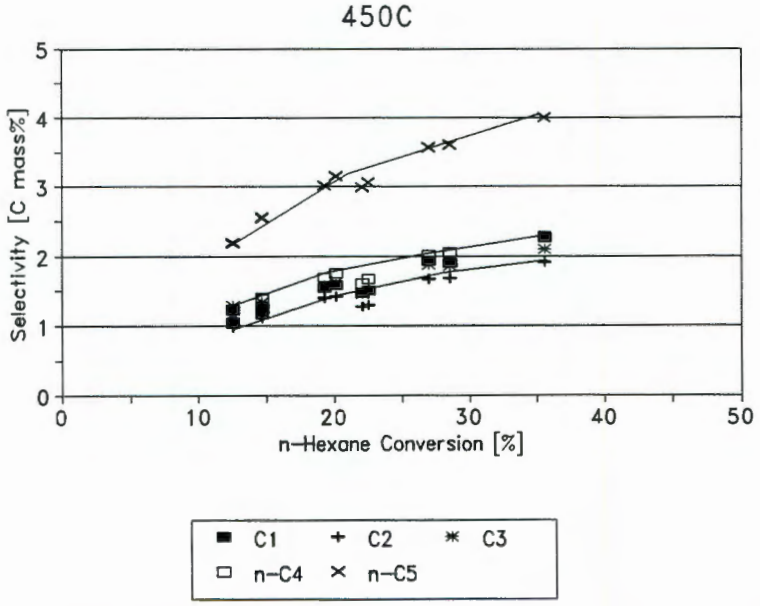

Figure 3-14 Selectivity\conversion plot as a result of changes in WHSV for n-hexane aromatization at 450°C (cracked products)

3.1.4 Effect of hydrogen partial pressure

3.1.4.1 Constant total pressure

The hydrogen partial pressure was varied at a total pressure of 2 bar by compensating for the hydrogen flowrate with nitrogen. Thus a total pressure of 2 bar was maintained as well as a fixed residence time over the catalyst bed (*i.e.* the total flowrate remained constant). The partial pressure of n-hexane remained constant.

A decline in selectivity to hexene isomers is observed with increase in hydrogen partial pressure as would be expected (Figure 3-17). There is also a decrease in hydrogenolysis products with increase in hydrogen partial pressure (except for pentane) as shown in Figure 3-18. The selectivity to benzene increases markedly (Figure 3-15) and this can be rationalized in terms of the platinum surfaces being more active due to less carbon fouling at higher hydrogen partial pressure. The increase in benzene formation could also be a result of the direct cyclization of hexenes to benzene on a more active catalyst. In support of this statement, the conversion of n-hexane did increase. The increase in benzene selectivity is 22% points (45% to 67%), while the decrease in selectivity to hexene is 37% points (42% to 5%). Thus not all the hexene isomers could have been converted to benzene. At higher hydrogen partial pressures, the selectivity to benzene is expected to fall, due to inhibition of the dehydrogenation pathway. This was observed at hydrogen partial pressures greater than 2 bar and is discussed in Section 3.1.4.2. The suppression of terminal hydrogenolysis (methane selectivity) is observed Figure 3-18 with increase in hydrogen partial pressure. This is in agreement with the results at 1 bar and 6 bar of Section 3.1.2. Overall hydrogenolysis selectivity increases slightly with increase in hydrogen partial pressure.

University of Cape Town

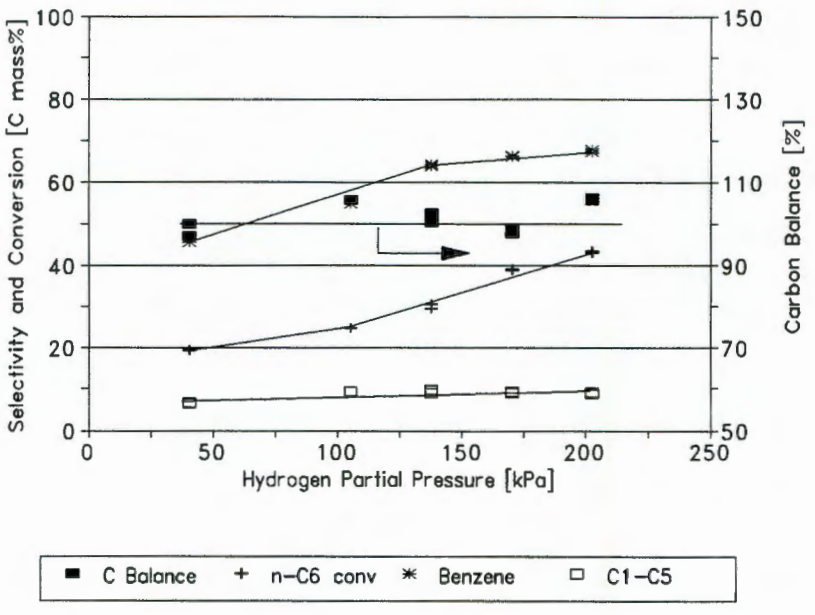

Figure 3-15 Effect of hydrogen pressure at fixed residence time and n-hexane partial pressure

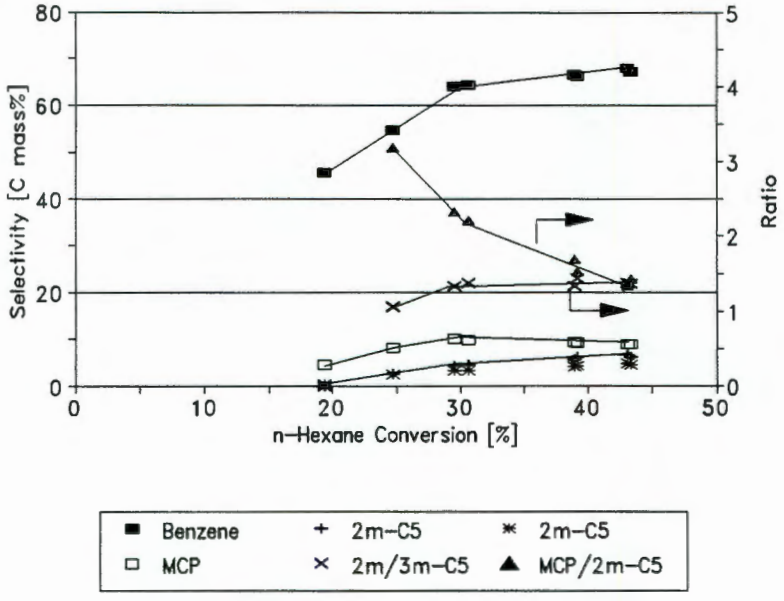

Figure 3-16 Effect of hydrogen partial pressure at 450°C

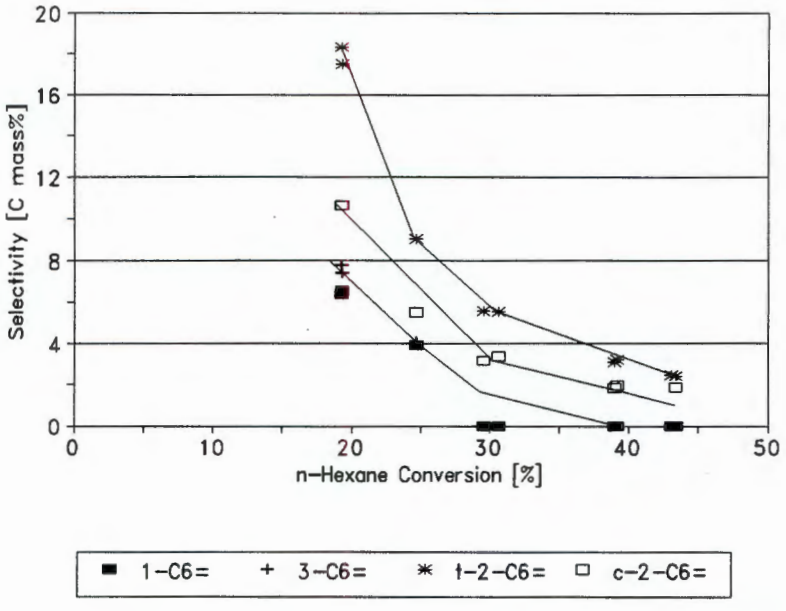

Figure 3-17 Effect of hydrogen partial pressure at 450°C

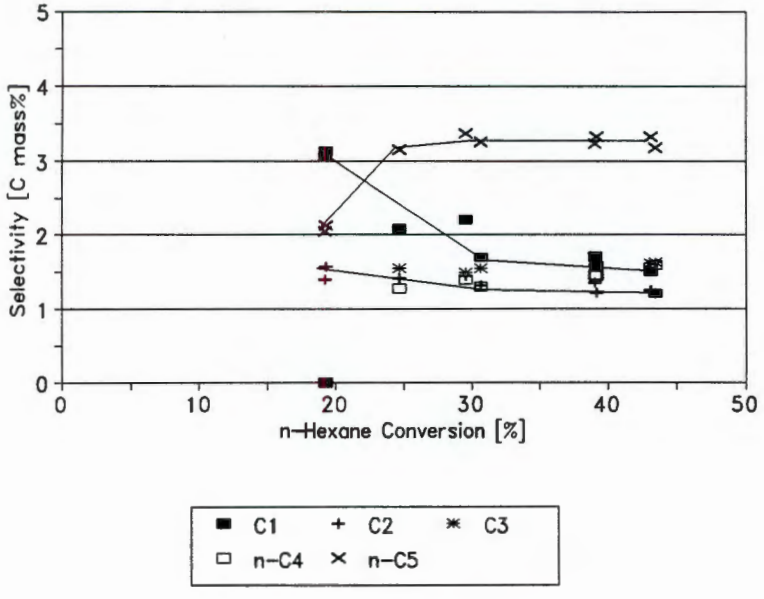

Figure 3-18 Effect of hydrogen partial pressure at 450°C

3.1.4.2 Effect of higher hydrogen partial pressure

The effect of hydrogen partial pressure (1-6 bar) is shown in Figure 3-19 to Figure 3-21. The total pressure, as well as the hydrogen partial pressure was increased. The residence time over the catalyst bed was constant at all pressures. The reaction temperature was 450°C.

As expected, benzene selectivity peaked at about 2 bar hydrogen partial pressure and then declined, due to the inhibitory effect of hydrogen pressure on dehydrogenation. This resulted in a decline in n-hexane conversion. As expected the selectivity to MCP also declined with increase in hydrogen partial pressure as dehydrogenation is involved in converting n-hexane to MCP. The dominant trends that are observed with increase in hydrogen partial pressure from (1 bar to 6 bar) are :

- n-Hexane conversion decreases by 16% (95% at 2 bar to 80% at 6 bar).
- Benzene selectivity decreases 46% (70% at 2 bar to 38% at 6 bar).
- Selectivity to MCP decreases by 63% (5.7% at 1 bar to 2.1% at 6 bar).
- Selectivity to methylpentanes increase by 172% (11% at 1 bar to 30% to 6 bar). This is expected since their formation from MCP involves hydrogenation.
- Selectivity to hydrogenolysis products increases by 100% (15% at 1 bar to 30% at 6 bar).

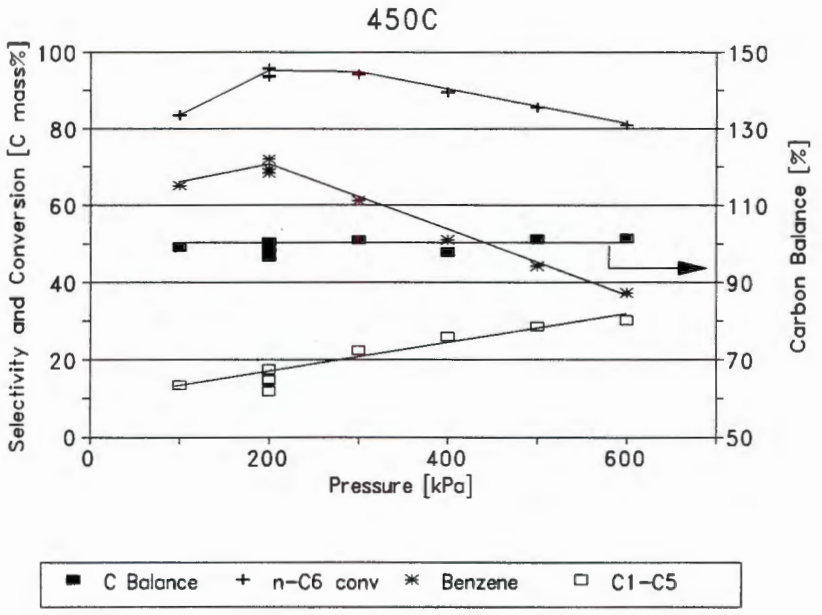

Figure 3-19 Effect hydrogen partial pressure at 450°C

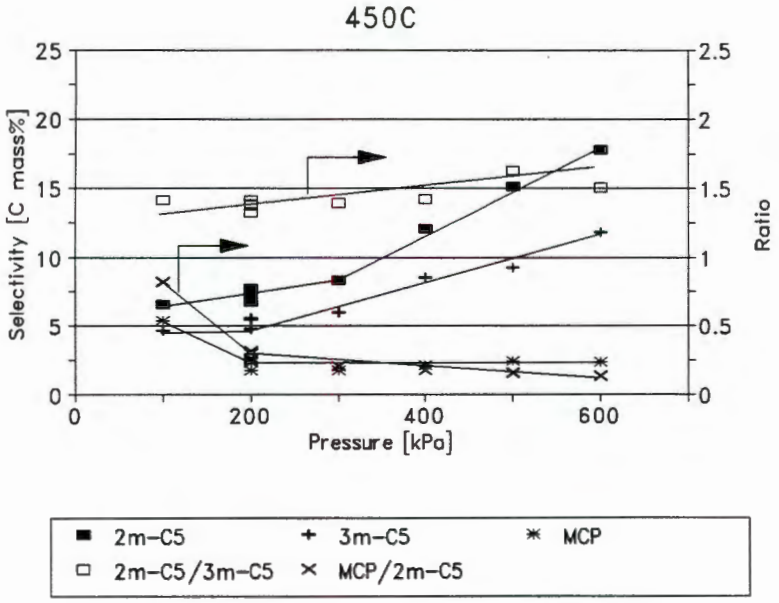

Figure 3-20 Effect of hydrogen partial pressure at 450°C (isomerized products)

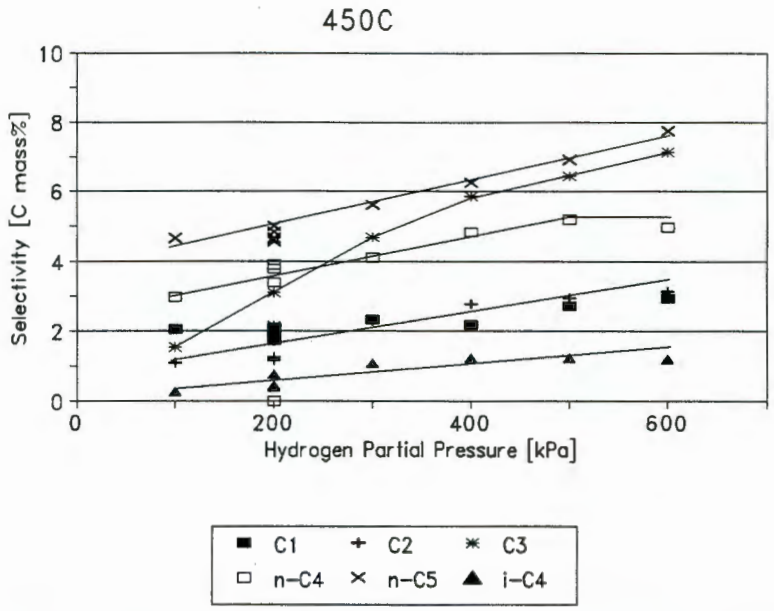

Figure 3-21 Effect of hydrogen partial pressure at 450°C (cracked products)

As previously mentioned terminal hydrogenolysis is suppressed by increase in hydrogen partial pressure (the relative molar selectivity to methane decreases slightly, Table 3-11), while the overall hydrogenolysis selectivity increases (15% to 30%).

3.1.4.3 Discussion of the effect of higher hydrogen pressure

A summary of the ratios of isomerized products are shown in Table 3-10. These results show a decline in the MCP:methylpentane ratios. This is a result of the decline in MCP selectivity and concomitant increase in methylpentane selectivities with increase in hydrogen partial pressure. This trend is also exhibited by the thermodynamic equilibrium results. The experimental and thermodynamic ratios are all fairly close, indicating that the isomerization reactions are close to equilibrium.

Table 3-10 Ratios of isomerized hexanes at 450°C

$p(H_2)$	2m/3m-C_5	MCP/2m-C_5	MCP/3m-C_5
Experimental data at 450°C			
1 bar	1.42	0.82	1.17
2 bar	1.41	0.26	0.37
3 bar	1.40	0.21	0.29
4 bar	1.42	0.17	0.26
5 bar	1.63	0.16	0.26
6 bar	1.51	0.13	0.20
Thermodynamic equilibrium data at 450°C			
1 bar	1.84	0.61	1.13
2 bar	1.84	0.30	0.55
3 bar	1.84	0.20	0.36
4 bar	1.84	0.15	0.27
5 bar	1.84	0.12	0.22
6 bar	1.84	0.10	0.18

A summary of the molar selectivities to the cracked products is shown in Table 3-11. There is an overall increase in selectivity to hydrogenolysis products with increase in hydrogen partial pressure. Propane shows the largest relative increase. The ratio of ethane:n-butane increases with pressure and is close to unity at high hydrogen partial pressures. The smaller amount of ethane relative to n-butane at 1 bar and 2 bar is an anomaly and does not fit with the results in the previous sections. A possible explanation is that the catalysts operated at 1 bar and 450°C in the aforementioned sections were allowed to stabilize for 48 hours which would have resulted in coke formation on the catalyst. As shown in Section 2.4.4 the hydrogenolysis products exhibit a decline in selectivity as a result of deactivation of Pt/KL. The deviation from unity is small, however, and thus does not indicate cause for concern.

Once again the primary hydrogenolysis reactions appear to be n-$C_6 \rightarrow 2C_3$, n-$C_6 \rightarrow C_5 + C_1$ and n-$C_6 \rightarrow C_4 + C_2$. Of interest is the appearance of i-butane with

increase in hydrogen partial pressure as shown in Figure 3-21. The hydrogenolysis of methylpentanes can result in the formation of i-butane. The large increase in selectivity to methylpentanes (by 172%) with increase in hydrogen partial pressure parallels the increase in selectivity to i-butane. However, it appears that the methylpentanes are not cracked as easily as n-hexane (note the smaller amount of i-butane relative to n-butane. Hence, some sort of selective hydrogenolysis mechanism should be present, with a preference for n-alkanes over i-alkanes. It may also be possible that isomerization of n-butane to i-butane occurs with increase in hydrogen partial pressure. This is less likely as acid sites will be required (Pt/KL is relatively non acidic) and they tend to require unsaturated molecules that are disfavoured at high hydrogen pressure. Also, if acid catalysed cracking occured then i-butane would be expected as a product at 1 bar as well.

Table 3-11 Molar selectivities of cracked products at 450°C

$p(H_2)$	methane	ethane	propane	butane	pentane	C_2/C_4	C_1/C_5	$C_1/\Sigma(C_1\text{-}C_5)$
1 bar	2.06	0.55	0.51	0.74	0.93	0.74	2.22	0.43
2 bar	2.08	0.70	0.71	0.97	0.96	0.72	2.17	0.38
3 bar	2.31	1.15	1.56	1.02	1.12	1.13	2.06	0.32
4 bar	2.18	1.39	1.90	1.21	1.25	1.15	1.74	0.27
5 bar	2.72	1.46	2.15	1.50	1.30	0.97	2.09	0.30
6 bar	2.94	1.57	2.38	1.24	1.55	1.27	1.90	0.30

A hypothesis will now be put foward to explain both the large relative selectivity to methane at one bar as well as large selectivity to methane observed for the intial time on stream (as shown in Section 2.4.4.2 and Figure 2-19):

At low pressure the formation of graphitic coke on Pt/KL is prevalent. The high methane selectivity at low pressure could be due to hydrogenation of graphitic coke from the platinum particles ($C + 2H_2 \rightarrow CH_4$). At partial pressures of hydrogen greater than 1 bar, the formation of graphitic coke is suppressed and hence methane selectivity is mainly the result of terminal hydrogenolysis. On fresh Pt/KL

graphitic coke formation is very fast and hence there is an abundance of graphitic coke on the surface. The hydrogenation of this coke leads to the observed high initial methane selectivities. With increasing time on stream the mass percent of graphitic coke decreases, possible due to stronger adsorption of alkenes or polynuclear coke precursors (not graphitic coke) and hence the methane selectivity decreases.

3.1.5 Aromatization of 1-hexene

It has been previously seen that 1-hexene is a reaction product of the reactions of n-hexane below 2 bar. It is also reported in the literature that 1-hexene is a reaction intermediate in the cyclization of n-hexane to benzene (Section 1.9.1.5). The hexene isomers are thermodynamically expected to be more reactive than n-hexane for the aromatization reaction. Thus feeding 1-hexene could result in a higher reaction rate of benzene formation.

Thus 1-hexene was fed over Pt/KL at 1 bar hydrogen partial pressure and a wide temperature range. At temperatures below 70°C only double bond isomerization of 1-hexene occured. Above 100°C the 1-hexene feed was hydrogenated to n-hexane which only reacts further at temperatures above *ca.* 350°C. These results are shown in Figure 3-22 to Figure 3-25. In this section n-hexane is considered as a product and the conversions shown are for 1-hexene.

University of Cape Town

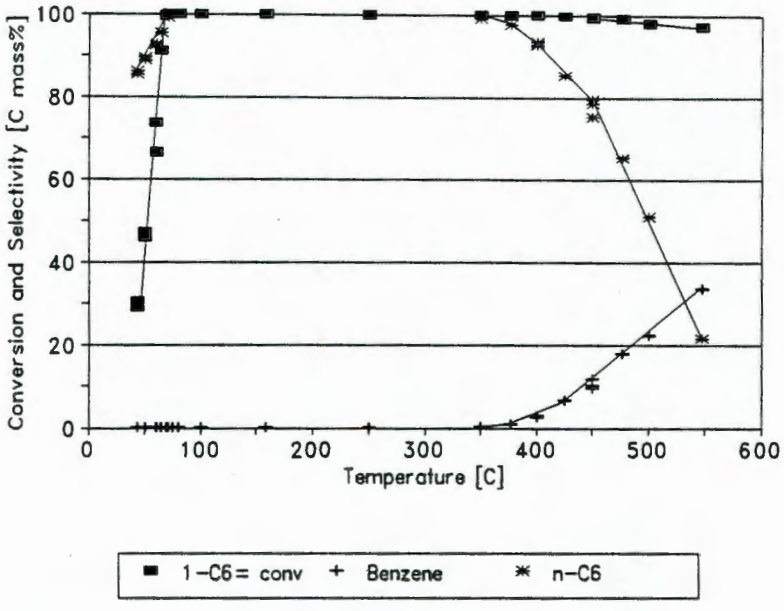

Figure 3-22 Effect of temperature on 1-hexene aromatization

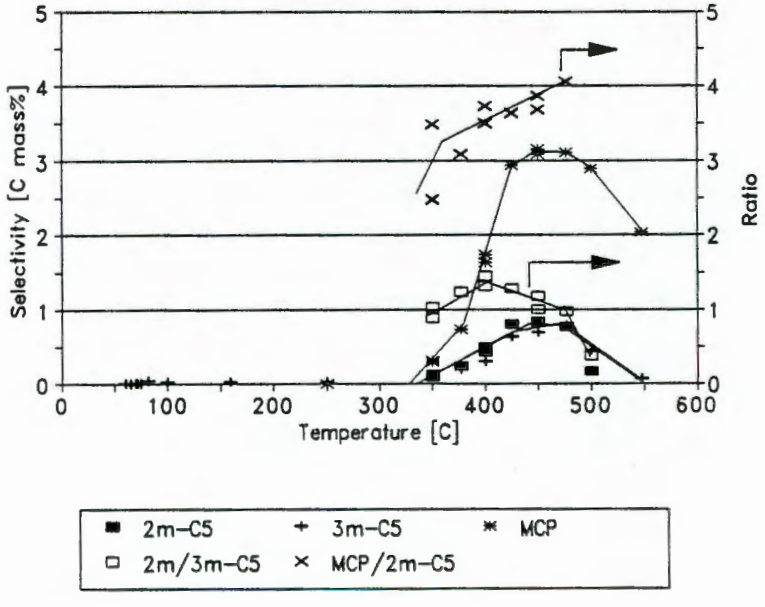

Figure 3-23 Effect of reaction temperature on 1-hexene aromatization

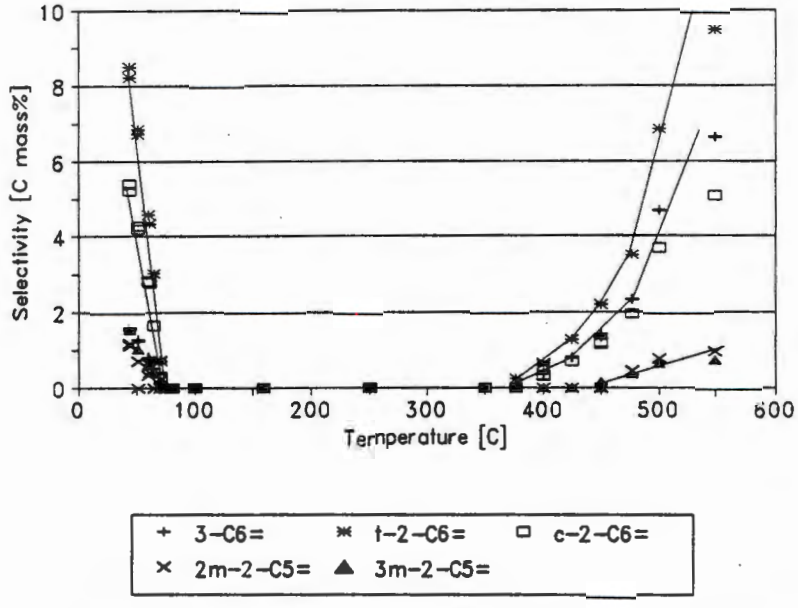

Figure 3-24 Effect of temperature on 1-hexene aromatization

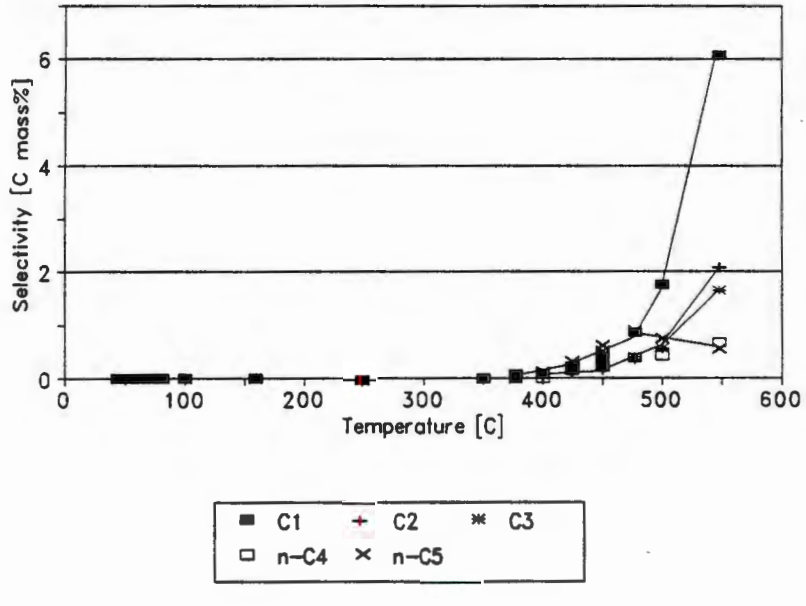

Figure 3-25 Effect of temperature on 1-hexene aromatization

3.1.5.1 Discussion of the feeding of 1-hexene

Between reaction temperatures of 70°C and 350°C n-hexane is the only product. Below 70°C double bond isomerization of 1-hexene to 2-hexene and 3-hexene occurs. Trans-2-hexene and cis-2-hexene are the major hexene isomers at these low temperatures. A summary of the hexene fractions at low and high temperatures are shown in Table 3-12. The experimental ratio of trans-2-hexene:cis-2-hexene is 1.62 below 70°C and is 1.88 above 400°C. Thus even at low temperatures there is less cis-2-hexene formed than trans-2-hexene. This would tend to count as evidence against the hypothesis postulated in Section 3.1.2.2 that the lower selectivity to cis-2-hexene relative to trans-2-hexene is due to cis-2-hexene being preferentially cyclized to form benzene. However, the ratio does increase at higher temperatures (> 400°C) which means that at higher temperatures at least some of the cis-2-hexene may cyclize to form benzene at a greater rate than trans-2-hexene. The fraction of 2-hexenes and 3-hexenes remains constant at *ca.* 70% and 30% above 400°C. At low temperatures there is much less 3-hexene than expected from thermodynamics, which indicates again that a series reaction for double bond isomerization of 1-hexene occurs, *viz.* 1-hexene ⇄ 2-hexene ⇄ 3-hexene. In contrast to that observed for n-hexane aromatization, the selectivity to the hexenes does not decrease at temperatures above 475°C, rather it continues to increase.

At low temperatures (< 70°C) there also appear to be a low selectivity to branched hexene isomers, 2-methyl-2-hexene and 3-methyl-2-hexene. This is unexpected as isomerization is highly unlikely to take place at such low temperatures. There is also no MCP or methylpentane isomers present, which could undergo dehydrogenation to methylhexenes. Thus it is speculated that these "methylhexene" products are actually hexadienes, *viz.* cis and trans 1,3-hexadiene. This is then an analysis problem. No GC standards were available to indentify these low temperature products, but they appeared at the same approximate retention times as the high temperature methylpentene products, which were identified using the relevant GC standards. Ideally GC-MS could be used for identification.

Table 3-12 Hexene isomer fractions for the aromatization of 1-hexene

Temperature	t-2-hexene	c-2-hexene	3-hexenes	t:c-2-hexene
		Experimental results		
44°C	0.55	0.34	0.10	1.62
60°C	0.55	0.35	0.10	1.57
400°C	0.47	0.25	0.28	1.88
450°C	0.46	0.25	0.28	1.84
500°C	0.45	0.24	0.31	1.88
550°C	0.45	0.24	0.31	1.88
		Thermodynamic equilibrium fractions		
< 70°C	0.35	0.41	0.24	0.85
> 350°C	0.34	0.40	0.26	0.85

There is a large increase in selectivity to methane for reaction temperatures above 475°C, with a concurrent decrease in pentane and butane. This indicates that hydrogenolysis of pentane and butane occur at reaction temperatures above 475°C. The selectivity to ethane and propane show a consistent increase with increase in reaction temperature. When Figure 3-5 (n-hexane hydrogenolysis products) is compared with Figure 3-25 (1-hexene hydrogenolysis products) it is clear that the selectivity to cracked products is less in the latter case. The hexene molar selectivities are tabulated in Table 3-13.

Table 3-13 Hydrogenolysis products molar selectivities at 1 bar for 1-hexene

Temperature	C_1	C_2	C_3	C_4	C_5	C_2/C_4	C_1/C_5
400°C	0.08	0.00	0.02	0.00	0.03	-	2.67
425°C	0.22	0.04	0.04	0.03	0.06	1.33	3.67
450°C	0.31	0.07	0.06	0.05	0.09	1.40	3.44
475°C	0.91	0.15	0.12	0.08	0.12	1.88	7.58
500°C	1.76	0.27	0.19	0.11	0.15	2.45	11.73
550°C	6.07	1.04	0.55	0.17	0.11	6.12	55.18

When these molar selectivity results are compared with Table 3-3 the following observations can be made:

- The values of the C_2:C_4 and C_1:C_5 ratios are similar and have the same overall trend, *i.e.* the ratios increase with reaction temperature.

- The molar selectivity for n-pentane goes through a maximum at *ca.* 475°C to 500°C in both cases.

- The molar selectivity for n-butane increases in the case of the 1-hexene feed while it goes through a maximum in the case of n-hexane.

The reason for the lower overall hydrogenolysis selectivity is unknown.

3.1.6 Summary of the reaction pathways

The following salient points can be made, with regard to the data presented in this section:

Benzene and hydrogenolysis products are the final reaction products. All other products (hexenes and hexanes) are intermediates and can react to form either benzene or hydrogenolysis products. Thermodynamically hydrogenolysis is favoured over dehydrocyclization and thus operation at high temperatures will tend to lower the absolute benzene yield. Hydrogenolysis is also favoured by increase in hydrogen partial pressure. Terminal hydrogenolysis, which always results in methane, is suppressed by increase in hydrogen partial pressure.

3.2 Deactivation of Platinum/KL

3.2.1. Deactivation by coke formation

Deactivation of Pt/KL can occur by either coke formation or sintering of platinum particles. In the absence of sulphur-containing compounds and at reaction temperatures below 500°C, the deactivation of Pt/KL is the result of coke formation (Section 3.1.1). If the deactivation scheme proposed in Section 1.6.1.1 is followed then the activity of the catalyst declines as a power function of time. This relationship was first proposed by Voorhies (1945)[202] based on deactivation of catalysts used in the cracking of gas-oil feed stocks.

$$C(t) = A_o t^n$$

C(t) : rate of coke formation at time t
A_o : Initial rate of coke formation
t : time on stream
n : reaction exponent

Voorhies further determined that the value of n was *ca.* 0.5. An implication of his work is that the diffusion of reactants to the reaction site is limited by the thickness of the coke layer. The Voorhies equation correlates coke formation for a large variety of reactions and catalysts[203,204]. The Voorhies exponent was generally found to be in the range of 0.5 to 0.91. The Voorhies equation is an empirical formulation as coke formation is often distributed nonuniformly in catalysts. Activity is not directly related to coke levels mechanistically for three major reasons

- Coke can deposit on nonreactive surfaces as well as active surfaces.
- Coke can deposit on coke.
- Coke can deposit non-uniformly and plug pores.

The rate of deactivation of Pt/KL was approximated by exponential decay at hydrogen partial pressures of 1 bar for n-heptane aromatization (Kooh *et al.* 1993).

$$r = a.t^b$$

r : rate of feed turnover [mol/g.hour]
t : time
a : initial rate at t = 0
b : deactivation exponent

Thus a log-log plot of conversion rate as a function of time on stream will yield a straight line with the gradient and y ordinate intercept equal to the variables b and a respectively. These were found by Kooh *et al.* (1993) to be -0.22 and 0.017 for n-heptane aromatization on Pt/KL at a hydrogen partial pressure of one atmosphere and a reaction temperature of *ca.* 450°C (Section 1.6.1.1). The exponent 'b' is henceforth referred to as the deactivation exponent and is related to the rate of catalyst deactivation. A negative value for the deactivation exponent for n-hexane conversion indicates that the rate of conversion decreases with time on stream (and vice versa for positive values of b). As the deactivation is not caused by sintering, it is assumed to be caused by coke formation. Increasing the hydrogen partial pressure is expected to result in a lower rate of coke deposition and hence a lower rate of deactivation, *viz.* 'b' will be closer to zero at higher hydrogen partial pressures.

3.2.1.1 Effect of hydrogen partial pressure on deactivation

The stability of Pt/KL for n-hexane aromatization at 450°C and 1 bar hydrogen partial pressure was shown in Section 2.4.4. A plot of the log of the rates of formation as a function of log time on stream is shown in Figure 4-1. Linear regression of the data is summarized in Table 4-1. The stability of Pt/KL was also tested at 6 bar hydrogen partial pressure. A log-log plot of rates of formation as function of time on stream is shown in Figure 4-2. At 6 bar no hexene products are observed. In both cases a good linear relationship is observed.

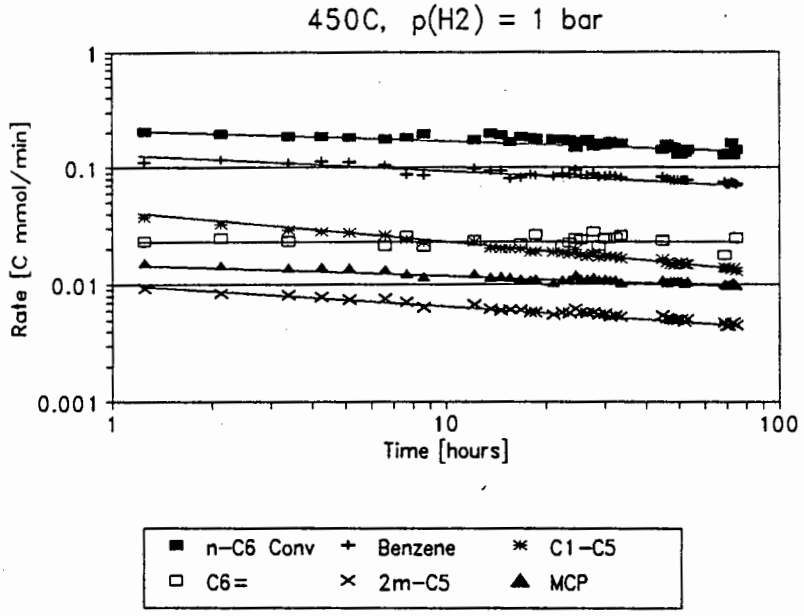

Figure 4-1 Deactivation of Pt/KL at 450°C and 1 bar hydrogen partial pressure for n-hexane aromatization

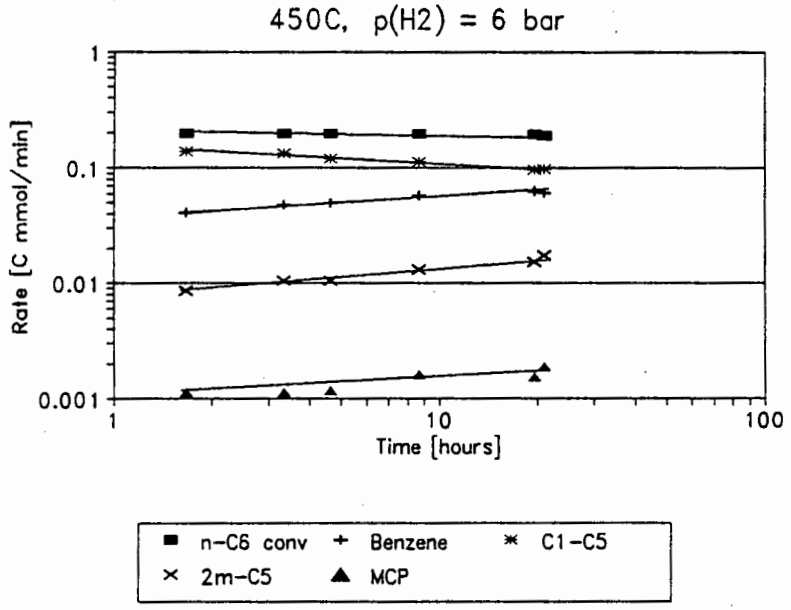

Figure 4-2 Deactivation of Pt/KL at 6 bar hydrogen partial pressure and 450°C for n-hexane aromatization

Deactivation at 1 bar hydrogen pressure and 450°C is always characterized by a decrease in n-hexane conversion. The selectivity to benzene remains steady, while the selectivity to hexenes increases with time on stream. The isomerized hexanes and hydrogenolysis products show a slight decrease with time on stream (Section 2.4.4). As the conversion of n-hexane decreases the rate of formation of benzene will decrease even though the selectivity remains constant. The deactivation exponents of benzene, MCP, methylpentanes and n-hexane conversion are all negative, while the deactivation exponent of the hexene isomers is positive, because they are at equilibrium. The variance, "r^2" value, is an indication of the goodness of fit of the data to the linear regression, values close to unity imply that data scatter is low. The hexenes generally showed the greatest amount of scatter and this is a result of difficulty in resolving the closely spaced hexene isomers chromatographically.

Table 4-1 Summary of the linear regression data for n-hexane aromatization on Pt/KL at 450°C

	n-C_6 conv	Benzene	C_1-C_5	C_6=	2m-C_5	MCP
1 bar hydrogen partial pressure						
Initial rate [C mmol/min]	0.208	0.092	0.040	0.017	0.013	0.018
Deactivation exponent	-0.119	-0.800	-0.209	0.059	-0.144	-0.079
r^2	0.74	0.87	0.99	0.26	0.97	0.93
3 bar hydrogen partial pressure						
Initial rate [C mmol/min]	0.295	0.119	0.089	-	0.010	0.014
Deactivation exponent	-0.073	-0.735	-0.178	-	-0.026	0.048
r^2	0.69	0.73	0.86	-	0.94	0.92
6 bar hydrogen partial pressure						
Initial rate [C mmol/min]	0.415	0.064	0.303	-	0.013	0.0014
Deactivation exponent	-0.063	0.124	-0.204	-	0.486	0.452
r^2	0.72	0.78	0.83	-	0.98	0.80

At a hydrogen partial pressure of 6 bar the rate of n-hexane conversion and the rate of formation of hydrogenolysis products decrease with time on stream, *viz.* the

exponents are negative. The rates of formation of benzene and isomerized products (MCP and methylpentanes) increase with time on stream. At hydrogen partial pressures greater than 2 bar no hexene isomers are observed. The linear regression represents a good fit at 6 bar as can be observed from the variance ("r^2"). These results, as well as results at 3 bar, are shown graphically in Figure 4-3 and Figure 4-4. The values in the graphs are the averages of 5 runs at 1 bar and 2 runs at 3 bar and 6 bar. In all cases fresh Pt/KL was used.

The initial rates of formation were calculated by extrapolation to a time on stream of 1 minute for the linear regression of the log rate versus log time on stream plots. The initial rate for n-hexane conversion increases with pressure. The initial formation rate of MCP decreases with increase in pressure, presumably due to the inhibitory effect of hydrogen partial pressure on dehydrocyclization reaction pathways. At 3 bar the initial rate of benzene is slightly higher than at 1 bar, while at 6 bar it is lower. This maximum is also observed for the benzene selectivities (Section 3.1.4.2), although the maximum occurs at 2 bar.

Thermodynamically the formation of benzene and MCP from n-hexane is inhibited by increase in hydrogen partial pressure (Appendice A.6.1). However, an increase in hydrogen partial pressure will also result in less coke deposition and hence a more active catalyst, which will tend to offset the inhibitory effect of hydrogen partial pressure on the rate of formation on benzene and MCP. As shown in Figure 4-4 the initial rate of formation of benzene remains constant up to 3 bar. At higher hydrogen partial pressures (6 bar) the initial rate declines. The initial rate of MCP declines with increase in hydrogen partial pressure.

The initial rate of formation of hydrogenolysis products increases with increase in hydrogen partial pressure. This trend is opposite to that observed for the cracking of waxes, where terminal hydrogenolysis activity, producing methane, decreases with increase in hydrogen partial pressure[205]. Thermodynamics predict that the molar ratios of methylpentanes, for n-hexane isomerization, will not be affected by changes in hydrogen partial pressure (Appendice A.6.1). The initial rate of

formation of 2-methylpentane remains constant (Figure 4-4) between 1 bar and 6 bar, in agreement with thermodynamic expectations. The initial rate of conversion of n-hexane increases with increase in hydrogen partial pressure, presumably due to the inhibition of coke deposition on platinum particles which results in a more active catalyst.

The deactivation exponent for the hydrogenolysis products (C_1-C_5) remains constant at *ca.* -0.205 with increase in hydrogen partial pressure (Figure 4-3). Thus the rate of formation of cracked products always decreases with time on stream. The deactivation exponent for n-hexane conversion increases slightly, but remains below zero, for increase in hydrogen partial pressure. This indicates that deactivation of Pt/KL occurs up to 6 bar hydrogen partial pressure. The increase in hydrogen partial pressure results in a slightly lower rate of deactivation, presumably due to inhibition of coke formation. The deactivation exponent for benzene is below zero at 1 bar, indicating that the rate of formation of benzene decreases with time on stream. The deactivation exponent for benzene increases to 0.124 at 6 bar. Thus the rate of formation of benzene increases with time on stream at higher pressures. A similar effect is observed for MCP and the methylpentanes (Figure 4-3). At 1 bar the only products for which the rate of formation increase with time on stream are the hexene isomers.

An interesting observation made during these experiments was that methane selectivity was initially very high (30% - 50%) and decreased sharply to *ca.* 3% after 1-2 hours time on stream. This is well known in catalytic reforming and is the reason why catalysts are pre-treated with sulphur. Chromatographic analysis of the products by on- line sampling allowed samples to be taken at intervals no closer than 30 minutes. To better quantify this effect samples should be taken at closer intervals, *i.e.* every minute. The initial very high selectivity to methane is not represented in the initial rates shown in this section. A possible explanation is offered in Section 3.1.4.3.

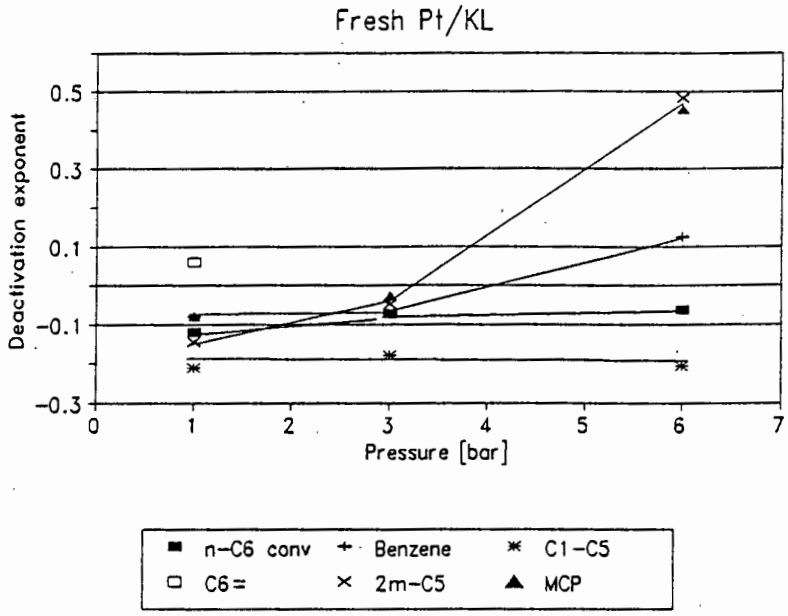

Figure 4-3 Effect of hydrogen partial pressure on the deactivation exponent for n-hexane aromatization at 450°C

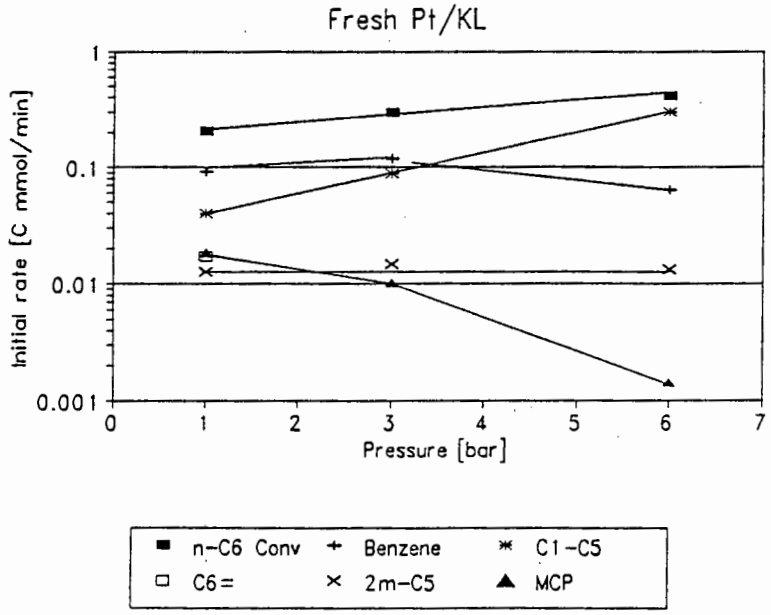

Figure 4-4 Effect of hydrogen partial pressure on the initial rates of formation for n-hexane aromatization at 450°C

3.2.2 Regeneration at 450°C

If the reason for the deactivation of the Pt/KL was coke formation then regeneration of the catalyst by calcination in air should restore the initial activity. Calcinations were performed *in situ* at 450°C in air (60 sccm) for 8 hours. After calcination, the catalyst was flushed with nitrogen (60 sccm) for 15 minutes, followed by reduction in hydrogen (60 sccm) for 2 hours. The catalyst was then considered to be "regenerated".

The effect of regeneration on the initial reaction rates as well as the deactivation exponent are shown in Figure 4-5 and Figure 4-6. These results are the average value from five different catalysts. The reaction temperature was 450°C and the hydrogen partial pressure was 1 bar.

The initial rate of conversion of n-hexane before regeneration is similar after regeneration while the initial rate of formation of benzene appears to be slightly higher. However, the deactivation exponent for benzene decreases sharply after regeneration (-0.073 to -0.174), while for n-hexane conversion it remains almost constant. In general the initial rates of formation are similar after regeneration with the hydrogenolysis products showing a slight decrease.

The deactivation exponents for 1-hexene and MCP changed very little after regeneration. The hydrogenolysis products and methylpentanes do not exhibit any change in the deactivation exponent after regeneration. Thus there must be some change to the catalyst, caused by regeneration, that specifically effects the rate of formation of benzene. Sintering of platinum could possibly cause this effect and is discussed in Section 3.2.3.

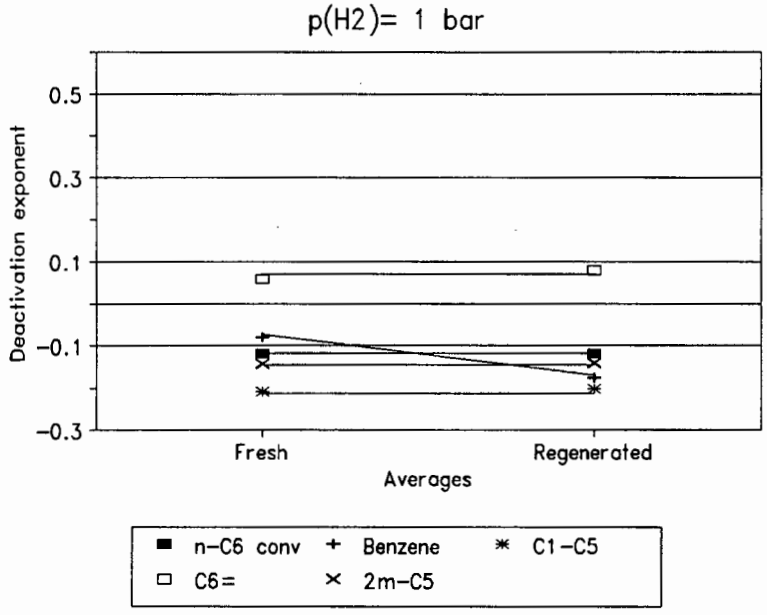

Figure 4-5 Deactivation exponent at 450°C and 1 bar for n-hexane aromatization on Pt/KL

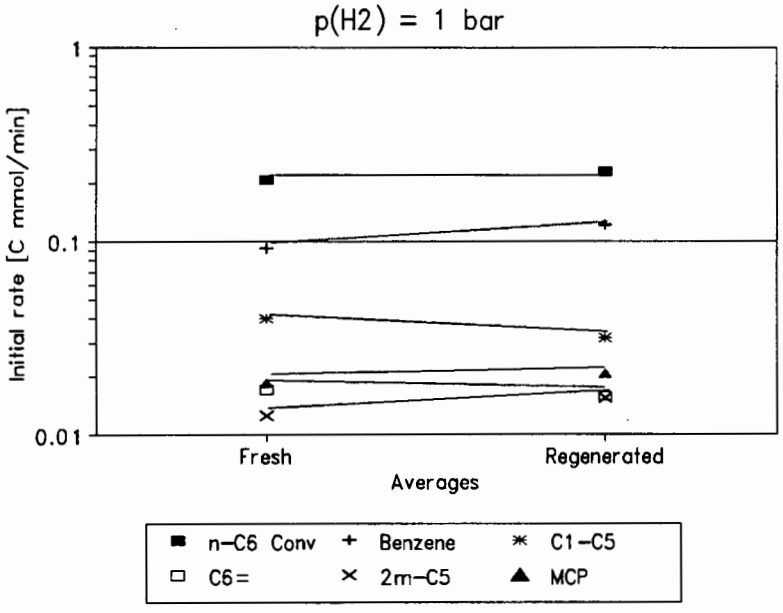

Figure 4-6 Initial rates at 450°C and 1 bar hydrogen pressure for n-hexane aromatization on Pt/KL

3.2.2.1 Multiple regenerations at 450°C

The effect of multiple regenerations on Pt/KL was investigated. The catalyst underwent 4 successive regenerations at 450°C in air, as described in Section 3.2.2. The reaction conditions were once again 450°C and 1 bar hydrogen partial pressure. These results are shown in Figure 4-7 and Figure 4-8. This regeneration series was performed separately to the results in Section 3.2.2.

The initial rate of conversion of n-hexane clearly shows a decline with increase in the number of regenerations (Figure 4-8). A similar trend is observed for the initial rate of formation of benzene, the hydrogenolysis products and hexene isomers. The initial rate of formation of MCP remains approximately constant, while the methylpentanes show a slight increase.

The deactivation exponent for benzene and n-hexane conversion decreases with increase in the number of regenerations. The decrease is larger for benzene than for n-hexane. The deactivation exponent for MCP and the hydrogenolysis products remain constant. The methylpentanes shown a small increase in the deactivation exponent after the first regeneration, thereafter the deactivation exponent remains constant. A similar trend is observed for the hexene isomers for which the deactivation exponent increases sharply after the first regeneration and thereafter remains essentially constant. Thus, in summary, the greatest change in the deactivation exponent is observed after the first regeneration for benzene, n-hexane conversion, methylpentanes and hexene isomers. The relatively large decline after the first regeneration is possibly indicative of sintering. Sintering of highly dispersed platinum will initially be rapid. However, after repeated regeneration only a small amount of further sintering will tend to occur. TEM evidence supports this conclusion (Section 2.5.4).

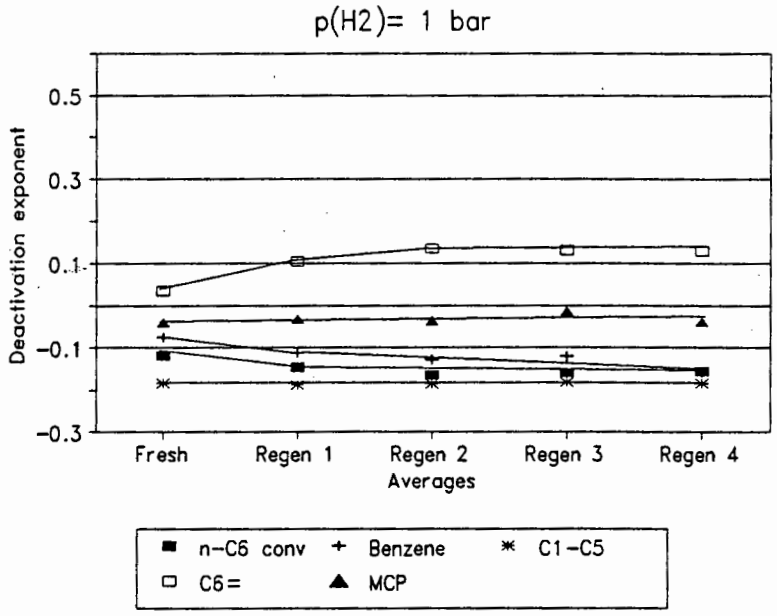

Figure 4-7 Multiple regenerations at 450°C and 1 bar

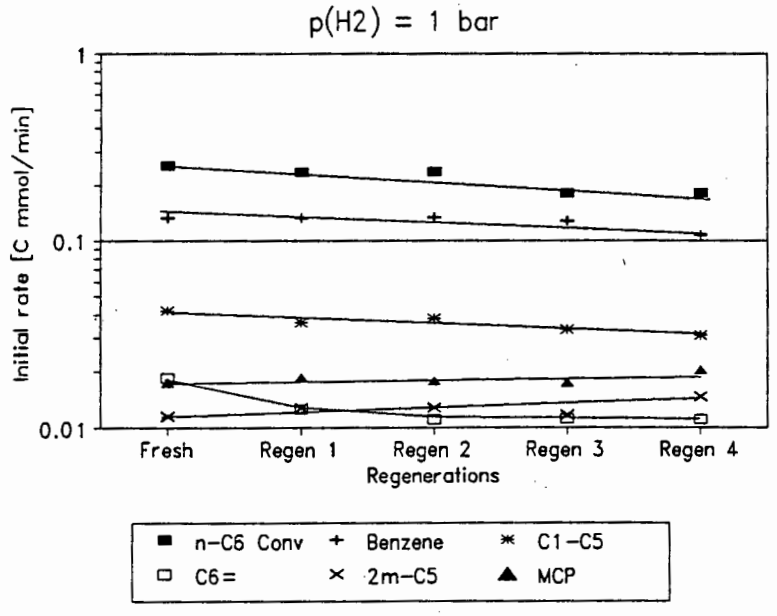

Figure 4-8 Multiple regenerations at 450°C and 1 bar

3.2.2.2 Effect of hydrogen partial pressure on regenerated Pt/KL

The fresh Pt/KL catalysts, which originally underwent reaction at 450°C and a hydrogen partial pressure of 6 bar, were regenerated, as previously described, at 450°C and 1 bar. The regenerated catalyst then underwent further reaction at 450°C and 6 bar hydrogen partial pressure. The results of the fresh and regenerated catalysts are shown in Figure 4-9 and Figure 4-10.

The effect of regeneration on the reaction of n-hexane over Pt/KL at 6 bar hydrogen partial pressure is much less marked than for reaction at 1 bar. The initial rates of formation are constant, except for 2-methylpentane which has a slightly higher initial rate of formation after regeneration. The deactivation exponents are also essentially unchanged by regeneration. There is a very slight increase in the deactivation exponent of 2-methylpentane.

A possible explanation for the above results is that at low partial pressures of hydrogen (1 bar) the amount of coke deposited is expected to be larger than at 6 bar. Calcination in air of heavily coked catalysts may result in local "hot spots", for which the temperature may exceed 500°C and thus lead to sintering of the platinum particles. For less heavily coked catalysts, the probability of local hot spots developing are much lower and hence sintering is unlikely to occur. Of course regenerations should be carried out in such a manner as to avoid this type of overheating. This is usually achieved by using diluted air and by starting at low temperatures. The temperature is then increased slowly to the required regeneration temperature and the oxygen content of the air may be slowly increased as well. High gas flowrates are better if the air is diluted as better heat transfer is achieved. The synthetic air used during these regenerations contained 21% oxygen and 79% nitrogen.

The deactivation curves are continuous and the plot of log rate as a function of log time on stream show a good linear correlation. Thus it can be postulated that coke formation leads to Pt/KL catalyst deactivation during the runs. However, sintering

of platinum occurs during regeneration of the heavily coked catalysts and leads to the observed decrease in initial activity.

Sintering of platinum would lower the initial conversion rate of n-hexane as there would be a smaller number of platinum sites. This was observed in Figure 4-8. The large decrease in the deactivation exponent of benzene is difficult to rationalize though.

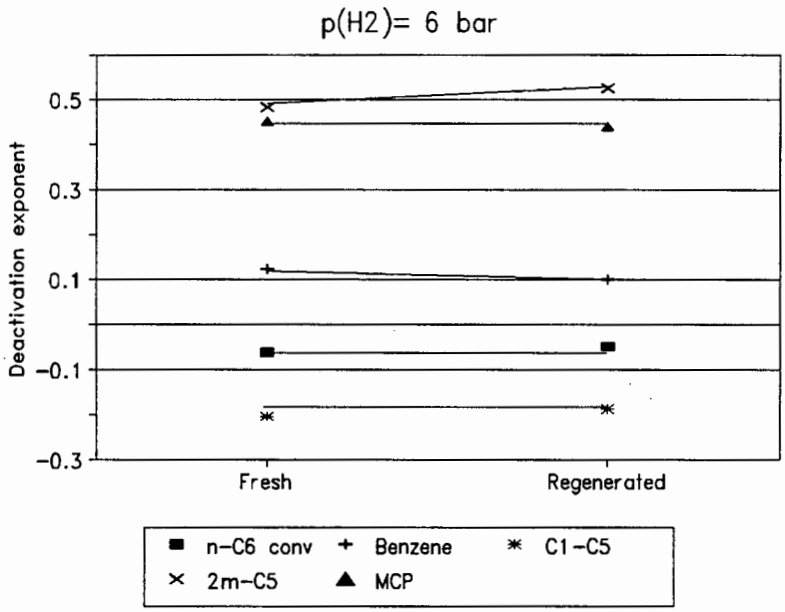

Figure 4-9 Effect of hydrogen partial pressure on regenerated Pt/KL

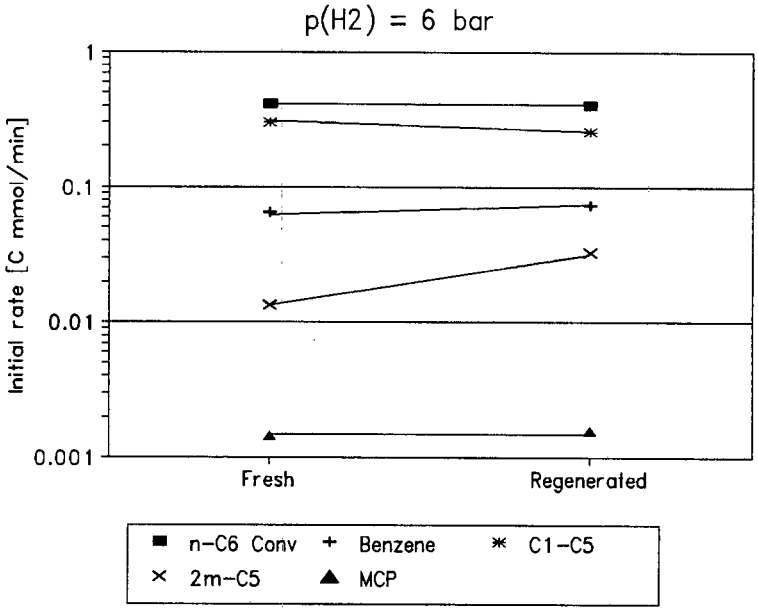

Figure 4-10 Effect of hydrogen partial pressure on regenerated Pt/KL at 450°C

3.2.3 Summary of the deactivation of Pt/KL

In summary it is postulated that deactivation occurs primarily by coking of platinum sites. A small degree of platinum sintering may occur after regeneration in oxygen, as indicated by the decline in initial activities after a series of regenerations. Sintering of platinum in oxidising atmospheres should only occur at reaction temperatures above 600°C (Section 1.7.4.3). As the calcination temperatures were 450°C the sintering must have been caused by the formation of local "hot spots" on the coked catalyst. The unidimensional nature of the channel system of zeolite L makes it very susceptible to deactivation by sintering, as pore blockages easily occur. Hence a small degree of sintering may have a large influence on the catalyst activity. Increase in hydrogen partial pressure results in less deactivation, supporting the postulate that the deactivation mechanism is by coke formation. As explained in Section 1.7.5 regeneration of deactivated catalysts in air is unlikely to

cause redispersion of platinum particles as no chlorine is present. It is doubtful if chlorine introduced during the synthesis of Pt/KL from zeolite L will have any effect on the redispersion of platinum as the chlorine content will be low. In the synthesis of Pt/KL by impregnation of $Pt(NH_3)_4Cl_2$, most of the Cl^- anions will react with H^+ cations formed during reduction thus forming $HCl_{(gas)}$ which will desorb from the catalyst surface (Section 1.5.1). In addition, exposure to the Pt/KL catalyst to a reducing atmosphere, at 450°C, should not cause much sintering. Hence, sintering is unlikely to occur during n-hexane aromatization.

3.3 Reactions of Oxygenates

3.3.1 Introduction

The main purpose of this project was to investigate the effect of oxygenated impurities on Pt/KL activity and selectivity for the aromatization of n-hexane. The primary oxygenates produced by the Fischer-Tropsch process are alcohols, butyraldehydes and ketones. The oxygenate compounds to be tested as impurities in this work were chosen on the basis of the boiling points, *i.e.* they had a boiling point in the same range as C_6 to C_7 alkanes. The boiling point of n-hexane is 68.7°C and that of n-heptane is 98°C. Thus ethanol (EtOH, b.p. 79°C), n-butyraldehyde (n-BuHO, b.p. 75°C), i-butyraldehyde (i-BuHO, b.p. 63°C) and methylethylketone (MEK, b.p. 80°C) were tested as impurities. Carbon monoxide (CO) and water were additionally tested, as both these latter compounds are produced as products in the reactions of the oxygenates over Pt/KL.

The co-feeding of the oxygenates with n-hexane is discussed in Section 3.4. This section deals with the feeding of only the oxygenates over Pt/KL. Five different oxygenated compounds were fed over Pt/KL, *viz.* ethanol, methylethylketone, n-butyraldehyde, i-butyraldehyde and carbon monoxide. The oxygenated compounds were fed via a single stage stainless steel saturator. The residence time over the catalyst bed and the hydrogen partial pressure was the same as for the feeding of n-hexane. This was achieved by the use of auxillary hydrogen. The feed rates of the oxygenated compounds were 14% to 20% of the n-hexane feed rate (Section 3.4.1 , Table 6.1).

The oxygenated compounds can react through either hydrogenation or hydrogenolysis pathways, in both cases producing alkanes in the C_1 - C_4 range. A summary of the different products expected, as a result of reaction of oxygenates on Pt/KL, are shown in Table 5-1. Any alkenes formed will be rapidly hydrogenated to alkanes over Pt/KL.

Table 5-1 Reaction products from reaction of oxygenated compounds on Pt/KL

	Ethanol	MEK	n-BuHO	i-BuHO	CO
hydrogenation[a]	C_2	n-C_4	n-C_4	i-C_4	C_1
hydrogenolysis[a]	C_1	C_1, C_2	C_1, C_3	C_1, C_3	-

(a) all products are alkanes

Hydrogenolysis is expected to occur alpha to the oxygenated carbon atom. The oxygenated compound will have slight positive polarization on the carbon atoms as a result of the electronegativity of the oxygen atom relative to carbon. As the platinum in Pt/KL zeolites is commonly reported to be electron rich, the oxygenated molecule will be preferentially adsorbed via the carbon atom adjacent to the oxygen atom. Hydrogenolysis should result in the formation of a carbonyl group on the platinum active site. Hydrogenation of the carbonyl group will result in the formation of an equimolar amount of methane and water. Carbon monoxide was detected by online analysis of the flue gas by infrared spectroscopy as explained in Section 2.2.1.5. No carbon dioxide was found in the flue gas in any of the runs.

3.3.2. Effect of temperature

An increase in reaction temperature resulted in a greater degree of hydrogenolysis products relative to hydrogenation products for the feeding of n-hexane over Pt/KL (Section 3.1.2). Thus the ratio of hydrogenolysis to hydrogenation was expected to increase with increase in reaction temperature for the feeding of oxygenates over Pt/KL.

3.3.2.1 n-Butyraldehyde

The effect of temperature on the feeding n-butryaldehyde (n-BuHO) over Pt/KL at different hydrogen partial pressures is shown in Figure 5-1 to Figure 5-3. In all cases the conversion of n-BuHO was 100%. There was an increase in

hydrogenation products (butane) with increase in reaction temperature (Figure 5-1 to Figure 5-3). It is also of interest to note that the selectivity to i-butane increases with increase in hydrogen partial pressure (Table 5-2 and Table 5-6). Direct hydrogenation of n-BuHO should yield n-butane only. Thus i-butane must be formed via the isomerization of n-butane, especially at higher partial pressures of hydrogen. The total selectivity to hydrogenation must be the sum of the butanes, *viz.* i-butane and n-butane. The selectivity to propane, formed by hydrogenolysis of n-BuHO declines with increase in temperature. Selectivity to methane increases with increase in reaction temperature, presumably due to increased hydrogenation of carbon monoxide formed by hydrogenolysis of n-BuHO. At 6 bar partial pressure of hydrogen no carbon monoxide was detected. Thus the molar ratios of propane:(methane + carbon monoxide) should be unity, assuming no adsorbed CO remains on the catalyst (as coke). A summary of the normalized molar selectivities are shown in Table 5-2. These indicate that the ratio is close to unity at 450°C and increases at lower reaction temperature. Note that the figures show selectivity calculated on a carbon mass basis.

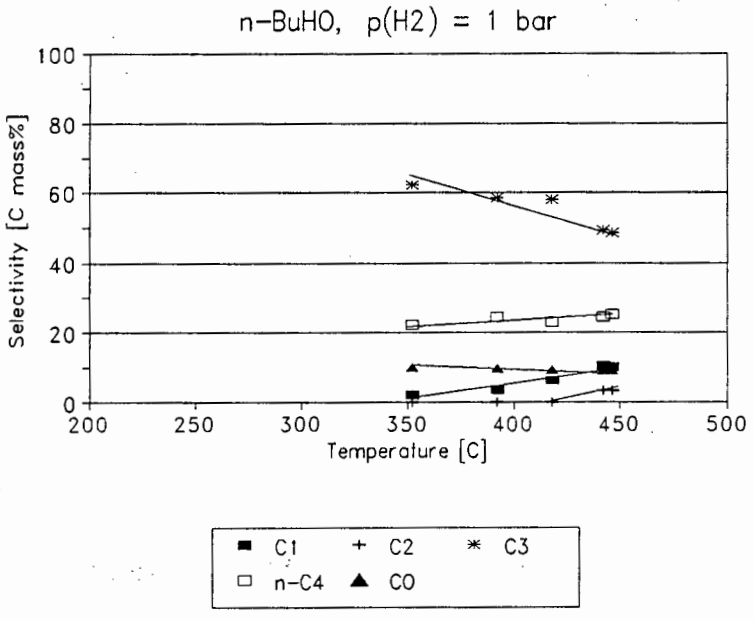

Figure 5-1 Effect of reaction temperature on reaction of n-BuHO at 1 bar hydrogen partial pressure

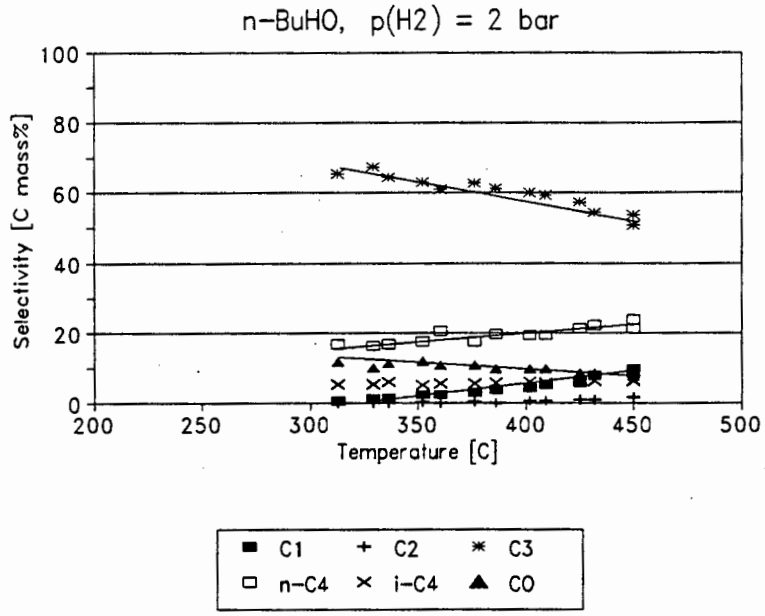

Figure 5-2 Effect of temperature for n-butyraldehyde reacted on Pt/KL at 2 bar hydrogen partial pressure

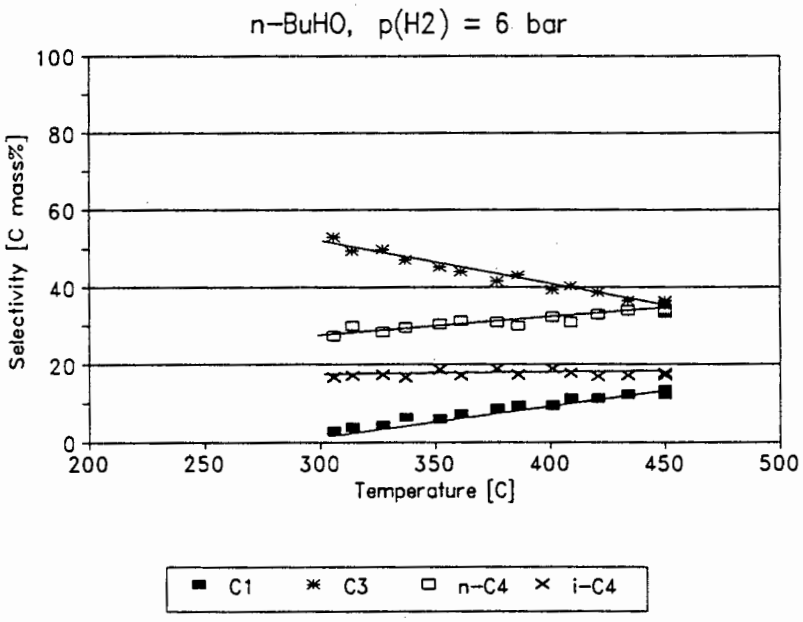

Figure 5-3 Effect of reaction temperature on n-butyraldehyde reaction on Pt/KL at 6 bar hydrogen partial pressure

Table 5-2 Molar selectivities of products for n-butyraldehyde reaction on Pt/KL

	Hydrogenolysis				Hydrogenation			
Temperature	C_1	C_2	C_3	CO	n-C_4	i-C_4	C_3:(C_1 + CO)	C_4:C_3
1 bar hydrogen partial pressure								
352°C	5.1	0.0	52.9	25.6	14.2	2.1	1.72	0.31
392°C	9.3	0.0	49.1	24.2	15.3	2.3	1.47	0.36
450°C	23.7	1.2	37.8	20.8	15.5	2.1	0.85	0.47
2 bar hydrogen partial pressure								
350°C	5.5	0.3	51.5	28.9	10.7	3.1	1.50	0.27
400°C	10.6	0.9	49.4	23.8	11.9	3.6	1.44	0.31
450°C	23.0	1.8	39.8	17.5	14.1	3.8	0.98	0.45
6 bar hydrogen partial pressure								
350°C	17.5	0.4	45.3	0.0	22.9	14.2	2.59	0.82
400°C	26.9	1.2	37.4	0.0	22.9	12.7	1.39	0.95
450°C	31.4	5.3	30.6	0.0	21.3	11.1	0.97	1.06

The reaction temperature has a small effect on the selectivity to i-butane, which can be assumed to be constant (Figure 5-2 and Figure 5-3). In general the mass selectivity to n-butane increases slightly with increase in reaction temperature. The ratio of hydrogenation to hydrogenolysis (C_4:C_3, Table 5-2) increases with increase in reaction temperature at all pressures. At 6 bar the ratio is close to unity. The ratio of propane:(methane + CO) decreases to close to unity with increase in reaction temperature. Thus the ratio of hydrogenolysis to hydrogenation decreased, in contrast to that observed for the feeding of n-hexane. No CO is detected at 6 bar hydrogen pressure. This supports the hypothesis that CO is adsorbed on the catalyst at low temperatures (< 400°C) and desorbs (at low hydrogen pressure) or is hydrogenated to methane (at high hydrogen pressure or higher reaction temperature). It may be speculated that at higher hydrogen pressures, the platinum surfaces should be largely free of coke deposits, possibly allowing CO to be adsorbed more strongly on platinum clusters than at lower hydrogen partial pressures.

3.3.2.2 i-Butyraldehyde

The reaction product selectivities for the reaction of i-butyraldehyde (i-BuHO) on Pt/KL are shown in Figure 5-4 and Table 5-3. The ratios of hydrogenation: hydrogenolysis (C_4:C_3) are similar for n-BuHO and i-BuHO and increase with reaction temperature. The ratio of propane:(methane + CO) is close to unity at 400°C and 450°C. As expected the greatest difference between i-BuHO and n-BuHO is that more i-butane than n-butane is produced in the former case. The appearance of n-butane at 1 bar hydrogen pressure for i-BuHO implies isomerization of i-butane takes place. This corresponds well with i-butane formed in the case of n-BuHO. In agreement the ratio of n-butane:i-butane decreases with increase in hydrogen partial pressure, from 7.4 at 1 bar to 1.9 at 6 bar and 450°C (Table 5-2). As only trace amounts of i-butane are formed in the feeding of n-hexane (at 1 bar), it is postulated that i-butane is not formed directly from n-butane (which is a hydrogenolysis product when feeding n-hexane), but rather by some mechanism involving the adsorbed n-butyraldehyde molecule. The assumed reaction pathways of n-BuHO on Pt/KL are shown below:

n-BuHO	→	n-C_4 + i-C_4	Hydrogenation
n-BuHO	→	C_3 + CO	Hydrogenolysis
CO	→	C_1 + H_2O	Hydrogenation

The reactions are the same for i-BuHO, with the exception being that the ratio of n-C_4:i-C_4 is *ca.* 18:82 at 450°C and 1 bar. For n-BuHO this ratio of n-C_4:i-C_4 is *ca.* 86:14 at the same reaction conditions.

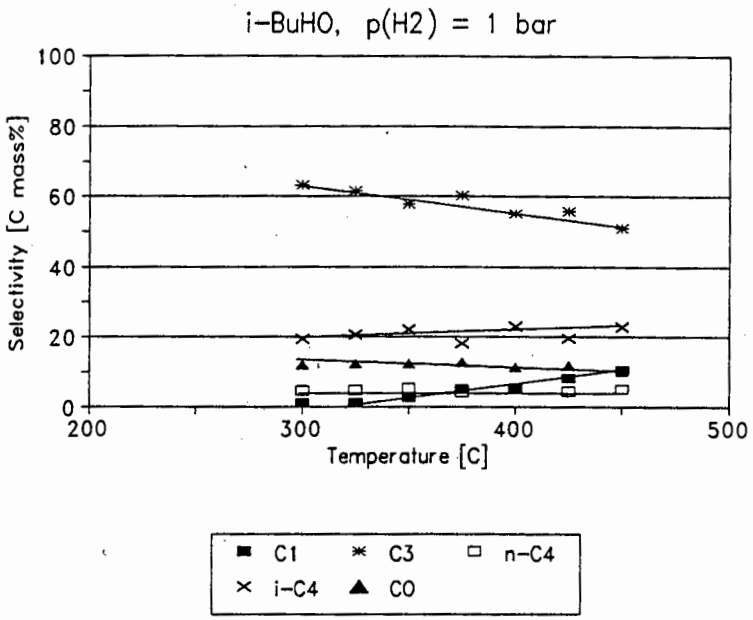

Figure 5-4 Effect of temperature on i-butyraldehyde reaction on Pt\KL at 1 bar hydrogen partial pressure

Table 5-3 Molar selectivities of products for i-butyraldehyde reaction on Pt/KL

	Hydrogenolysis				Hydrogenation			
Temperature	C_1	C_2	C_3	CO	n-C_4	i-C_4	C_3:(C_1 + CO)	C_4:C_3
1 bar hydrogen partial pressure								
350°C	6.2	0.02	47.2	29.8	3.3	13.5	1.31	0.36
400°C	12.8	0.02	43.8	26.6	3.2	13.7	1.11	0.39
450°C	23.3	0.64	37.9	22.3	2.8	13.0	0.83	0.42

3.3.2.3 Methylethylketone

Methylethylketone (MEK) was fed at a hydrogen partial pressure of 2 bar and 6 bar over Pt/KL (Figure 5-5 and Figure 5-6). The complete hydrogenation of MEK will yield n-butane, while the hydrogenolysis products are mainly ethane, methane and carbon monoxide. The molar ratios of ethane:(methane + CO) is expected to be 0.5 (see reaction equations below). The molar ratio of C_4:C_2 is taken as the ratio of hydrogenation to hydrogenolysis. In contrast to the butyraldehydes, the feeding of MEK results in a greater amount of hydrogenation relative to hydrogenolysis and the ratio declines with increase in temperature. In addition, at 2 bar, the amount of CO produced increases with reaction temperature (Table 5-4).

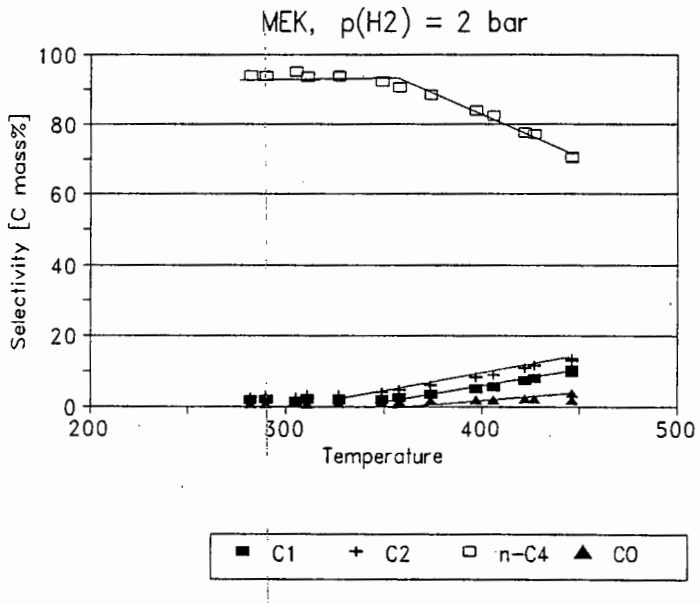

Figure 5-5 Effect of temperature on MEK reaction on Pt/KL at 2 bar hydrogen partial pressure

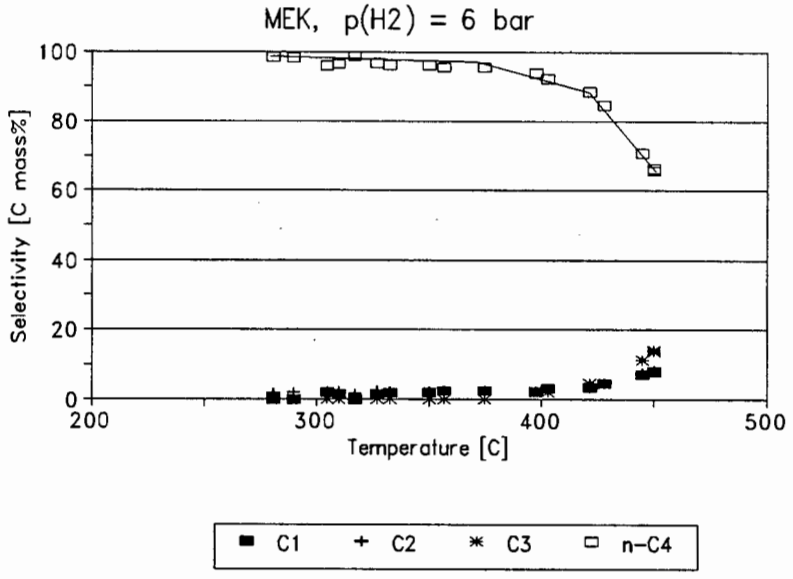

Figure 5-6 Effect of temperature on MEK reaction on Pt/KL at 6 bar hydrogen partial pressure

Table 5-4 Molar selectivities of products for MEK reaction on Pt/KL

	Hydrogenolysis				Hydrogenation			
Temperature	C_1	C_2	C_3	CO	n-C_4	i-C_4	C_2:(C_1 + CO)	C_4:C_2
2 bar hydrogen partial pressure								
350°C	9.1	8.3	0.6	4.5	77.5	0.0	0.61	9.34
400°C	15.8	13.1	0.9	5.8	64.2	0.2	0.61	4.92
450°C	26.4	17.3	1.9	8.1	46.2	0.8	0.50	2.72
6 bar hydrogen partial pressure								
350°C	6.7	3.7	0.0	0.0	89.6	0.0	0.55	24.22
400°C	7.3	4.0	2.6	0.0	86.1	0.0	0.55	21.53
450°C	23.0	11.5	12.4	0.0	50.1	2.9	0.50	4.61

The ratio of C_2:(C_1 + CO) is close to the expected value of 0.5 at both 2 bar and 6 bar. The selectivity to propane is low. Propane is most likely formed by hydrogenolysis of n-butane or by hydrogenolysis of MEK, producing methane and and an adsorbed propanal species, that is then hydrogenated to propane. The ratio of hydrogenation:hydrogenolysis (C_4:C_2) increases at higher pressures at the same reaction temperature. In contrast to the feeding of butyraldehydes, only small amounts of i-butane are produced when feeding MEK. The ratio of n-butane: i-butane at 450°C is 57 and 18 at 2 bar and 6 bar respectively. The ratio decreases with increase in reaction temperature due to increase in selectivity to i-butane, *i.e.* the ratio is 350 at 400°C and 2 bar. The relatively small amount of i-butane is similar to that observed when feeding n-hexane. Thus the reaction pathway that produces i-butane and n-butane in the feeding of n-BuHO and i-BuHO respectively is absent in the case of MEK. A proposed reaction pathway for MEK is shown below:

MEK	→	n-C_4	Hydrogenation
MEK	→	C_2 + C_1 + CO	Hydrogenolysis
CO	→	C_1 + H_2O	Hydrogenation

The increase in selectivity to CO with increase in reaction temperature is not expected, (see Section 3.2.2.4) and is in contrast with the results for the feeding of n-BuHO. This may be indicative of another reaction mechanism for MEK on Pt/KL.

3.3.2.4 Carbon monoxide

Carbon monoxide was detected as reaction product in both the feeding of oxygenates over Pt/KL as well as the co-feeding of oxygenates with n-hexane over Pt/KL (Section 3.4). No carbon dioxide was detected. Thus it was decided to investigate the effect of reaction temperature on the reaction of CO over Pt/KL. Carbon monoxide (CO) was fed via a mass flow controller. The residence times

over the catalyst bed and the hydrogen partial pressures were kept constant by the feeding of auxillary hydrogen. The only observed product was methane. However, water is also expected as reaction product in the hydrogenation of carbon monoxide. The rate of formation of methane as well as the conversion of CO are shown in Figure 5-7. The rate of formation of methane increases with reaction temperature and consequently so does the conversion of CO. The reactions of CO on Pt/KL may be postulated to be the following:

$CO_{(g)}$	$\rightleftarrows$	$CO_{(ads)}$	CO adsorption on platinum
$CO_{(ads)} + 6H_2$	$\rightarrow$	$CH_4 + H_2O$	Hydrogenation

An Arrhenius plot of the rates of formation of methane as a function of inverse temperature yielded a straight line (Figure 5-8) from which the activation energy E_a for methane formation may be calculated using the Arrhenius relationship, as shown below:

$$k = Ae^{-Ea/RT}$$

k : reaction rate	[/s]
E_a : Activation energy	[J/mol]
R : gas constant = 8.314	[J/(K.mol)]
T : reaction temperature	[K]
A : Pre-exponential factor taking entropy into account	

The activation energy was calculated as E_a = 139 kJ/mol and the pre-exponential factor as 0.26 s^{-1}.

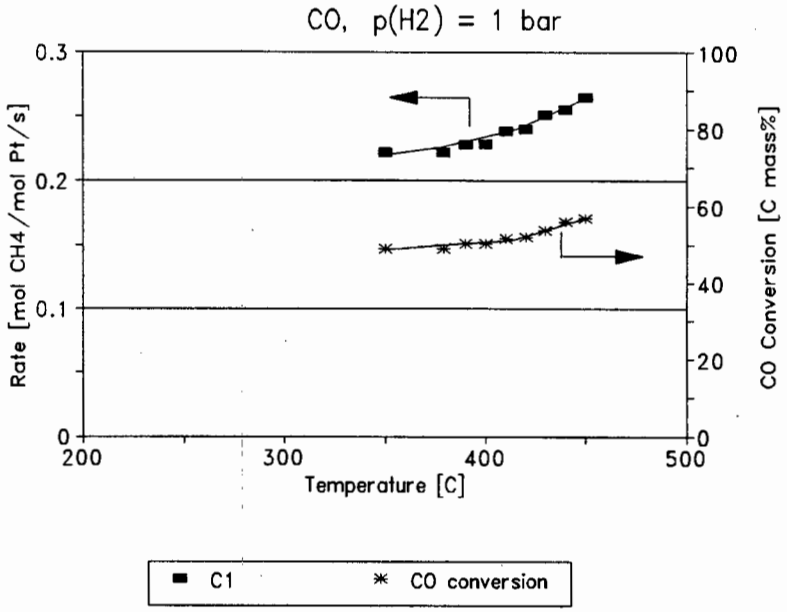

Figure 5-7 Effect of temperature on the reaction of CO on Pt/KL at 1 bar hydrogen partial pressure

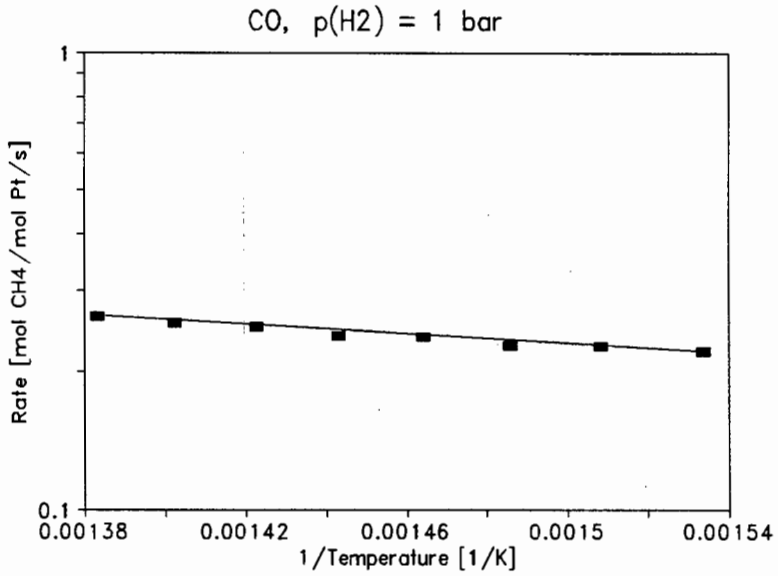

Figure 5-8 Arrhenius plot for reaction of CO on Pt/KL at 1 bar hydrogen partial pressure

3.3.2.5 Ethanol

The complete hydrogenation of ethanol should yield ethane, while hydrogenolysis should produce methane and CO. Unfortunately no CO analysis was performed in the feeding of ethanol over Pt/KL for this experiment. However, CO was detected during the co-feeding of ethanol with n-hexane at 450°C and 1 bar hydrogen pressure. Dehydration of ethanol could also occur, producing ethene and water. However, the ethene would be hydrogenated to ethane, especially at higher temperatures and hydrogen partial pressure. Note that no C_2 to C_5 alkenes were observed for the feeding of n-hexane over Pt/KL at 1 bar hydrogen partial pressure.

The ratio of hydrogenation to hydrogenolysis can be expressed by the ratio $2C_2$:(C_1 + CO). However, as no detection of CO was performed, the ratio of methane:CO is assumed from the data in Section 3.2.2.4, that is the feeding of carbon monoxide only.

Table 5-5 Molar selectivities for the reaction of ethanol on Pt/KL at 1 bar hydrogen partial pressure

	Hydrogenolysis		Hydrogenation		
Temperature	C_1	CO[a]	C_2	C_2:C_1	$2C_2$:(C_1 + CO)
350°C	54.1	27.9	18.0	0.33	0.44
400°C	58.1	27.4	14.5	0.25	0.34
450°C	61.4	25.4	13.1	0.21	0.30

(a) Estimated CO molar selectivity

The reaction pathways on Pt/KL can be assumed as:

EtOH	→	C_2	Hydrogenation
EtOH	→	C_1 + CO	Hydrogenolysis
CO	→	C_1 + H_2O	Hydrogenation

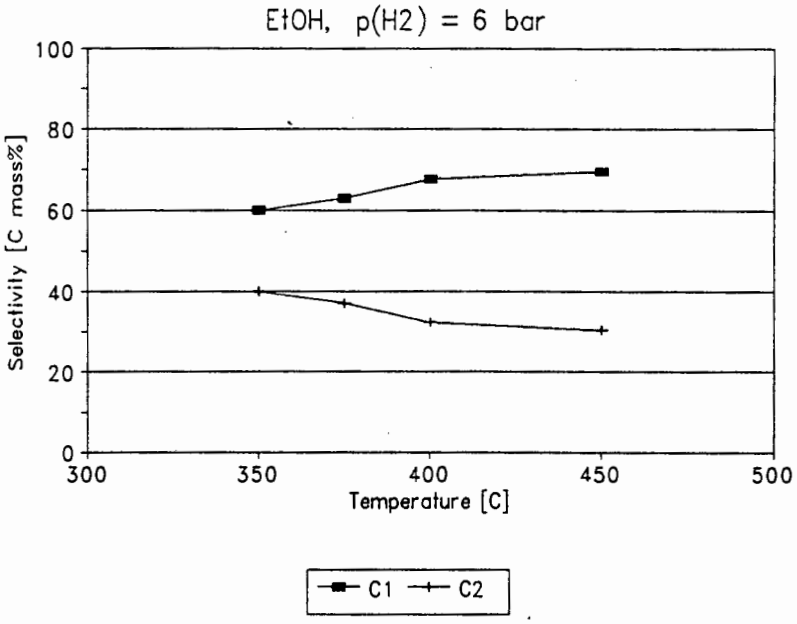

Figure 5-9 Effect of temperature on the reaction of ethanol over Pt/KL at 2 bar hydrogen partial pressure

As was found for MEK, the ratio of hydrogenation:hydrogenolysis (C_2:C_1) decreases with increase in reaction temperature. The ratio of $2C_2$:(C_1 + CO) is expected to be close to unity, but is in the range of 0.44 to 0.30. The reason for the lower than expected value may be ascribed to the fact that the CO molar selectivity was estimated from the C_1:CO ratio obtained from the reaction of CO on Pt/KL. It seems likely that this ratio is different in the case of ethanol. Thus more CO is probably produced for the reaction of ethanol, possibly due to inhibition of the hydrogenation reaction. The reason is unknown.

3.3.3 Effect of hydrogen partial pressure

The effects of changing hydrogen partial pressure (1 bar to 6 bar) on the reaction of various oxygenated compounds on Pt/KL were investigated. These experiments were performed in addition to those is Section 3.2.2. In all cases the Pt/KL catalyst was allowed to reach steady state operation at 6 bar and 450°C for n-hexane aromatization. Once steady state had been achieved the flow of n-hexane was terminated and only the oxygenated compound was fed. The residence time over the catalyst bed was kept constant at all pressures.

The selectivity to hydrogenolysis for n-hexane increased with increase in hydrogen partial pressure over Pt/KL (Section 3.1.2.4 and Section 3.1.4.2). However, terminal hydrogenolysis was suppressed, resulting in lower relative selectivity to methane at high partial pressures than at low partial pressures. The hydrogenolysis reactions of the oxygenates over Pt/KL are mainly terminal hydrogenolysis. Thus increasing the hydrogen partial pressure may favour hydrogenation of the oxygenates relative to hydrogenolysis on Pt/KL. However, hydrogenation of CO to form methane is a complicating factor in evaluating whether terminal hydrogenolysis has been suppressed. Thus methane should not be taken into account in evaluting the ratio of hydrogenation:hydrogenolysis.

3.3.3.1 n-Butyraldehyde

The reaction products for n-BuHO at 450°C as a result of change in hydrogen partial pressure as shown Figure 5-10 and Table 5-6. An increase in the ratio of hydrogenation:hydrogenolysis, expressed as C_4:C_3, is observed with increase in hydrogen partial pressure. The ratio of C_3:(C_1 + CO) is fairly close to unity and increases slightly with increase in pressure. The ratio of n-butane:i-butane increases with hydrogen pressure from 2.3 to 3.0 at 1 bar and 6 bar respectively. The selectivity to CO decreases with increase in hydrogen partial pressure.

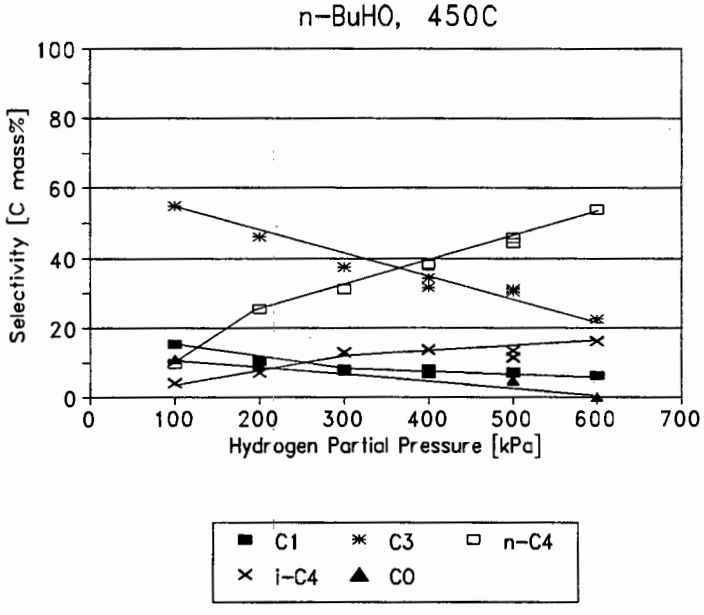

Figure 5-10 Effect of hydrogen partial pressure for the reaction of n-BuHO on Pt/KL at 450°C

Table 5-6 Molar selectivities of products for n-butyraldehyde reaction on Pt/KL at 450°C

	Hydrogenolysis				Hydrogenation			
Pressure	C_1	C_2	C_3	CO	n-C_4	i-C_4	C_3:(C_1 + CO)	C_4:C_3
1 bar	30.3	4.9	36.3	21.6	5.4	2.4	0.70	0.21
2 bar	22.2	4.1	31.4	20.9	16.7	3.9	0.73	0.66
3 bar	20.2	3.7	31.2	18.6	19.5	6.7	0.80	0.84
4 bar	19.5	0.8	28.4	19.2	24.7	7.3	0.73	1.13
5 bar	19.3	0.2	28.6	12.9	31.0	8.1	0.89	1.37
6 bar	19.9	0.3	23.4	0.0	42.3	12.7	1.18	2.35

The molar selectivities in Table 5-6 and Table 5-2 do not match particulary well, although the trends for the ratios of C_4:C_3 and C_3:(C_1 + CO) are similar. The

reason for the differences may be due to increased fouling at low reaction temperatures, which may have had an adverse effect on the results at higher reaction temperatures (Table 5-2). The trends for the molar selectivities are much more clear in Table 5-6 than in Table 5-2.

3.3.3.2 Methylethylketone

The product selectivities for MEK at 450°C as a result of change in hydrogen partial pressure are shown in Figure 5-11 and Table 5-7. The ratio of hydrogenation:hydrogenolysis (C_4:C_2) increases with hydrogen partial pressure, as was found previously (Table 5-4). The ratio of n-butane:i-butane is 21 at 1 bar and increases to 63 at 4 bar. No i-butane is observed above this pressure. The ratio of C_2:(C_1 + CO) is in the region of the expected 0.5, but appears to decrease slightly with increase in pressure. The selectivity to CO also decreases with increase in pressure, again as per Table 5-4.

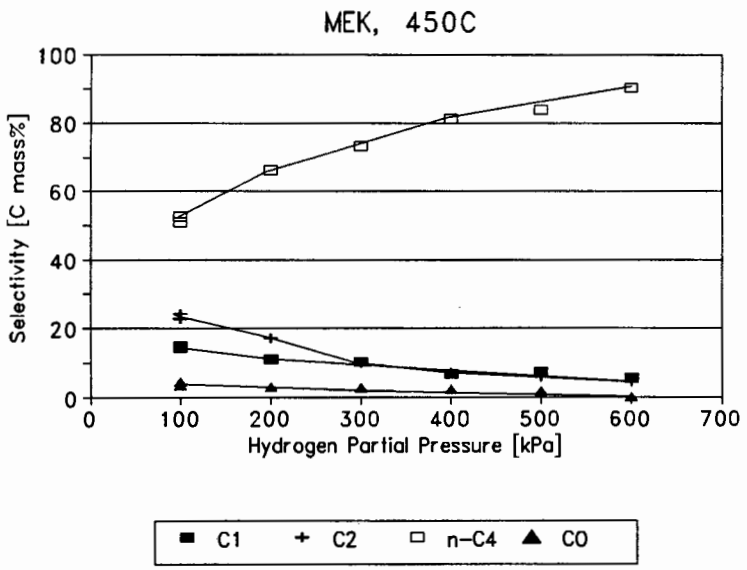

Figure 5-11 Effect of hydrogen partial pressure on MEK reaction on Pt/KL at 450°C

Table 5-7 Molar selectivities of products for MEK reaction on Pt/KL

	Hydrogenolysis				Hydrogenation			
Pressure	C_1	C_2	C_3	CO	n-C_4	i-C_4	C_2:(C_1 + CO)	C_4:C_2
1 bar	32.5	25.9	2.9	8.8	28.6	1.33	0.63	1.13
2 bar	27.6	21.3	1.9	6.8	41.3	1.17	0.62	1.96
3 bar	27.4	13.3	2.0	6.8	49.4	1.08	0.39	3.74
4 bar	24.1	9.4	1.7	5.5	54.6	0.86	0.32	5.84
5 bar	22.0	8.6	1.7	4.5	63.2	0.00	0.32	7.35
6 bar	18.2	6.9	0.0	0.0	74.6	0.00	0.38	10.81

When the results of Table 5-7 and Table 5-4 are compared, it is observed that there is fairly close correspondance between the molar selectivities at 2 bar, but less so at 6 bar. Specifically at 6 bar the molar selectivities for n-butane are much higher in Table 5-7 than in Table 5-4. The molar selectivity to i-butane is, however higher at 6 bar in Table 5-4 than in Table 5-7. The reason for these discrepancies is unknown, but may possibly be due to fouling of the catalyst as a result of working at lower reaction temperatures in the case of data shown in Table 5-4. However, the clear trends observed for the data in Table 5-7 support the use of that experiment to show the effect of changes in hydrogen partial pressure on the reaction products for MEK.

3.3.3.3 Carbon monoxide

The effect of hydrogen partial pressure on the reaction of CO over Pt/KL is shown in Figure 5-12. The rate of formation of methane increases with pressure as is expected. The conversion of CO increases with increase in pressure as a result. The carbon balance is close to 100% at all pressures at 450°C. The conversion of CO, to methane, approaches 100% at 6 bar.

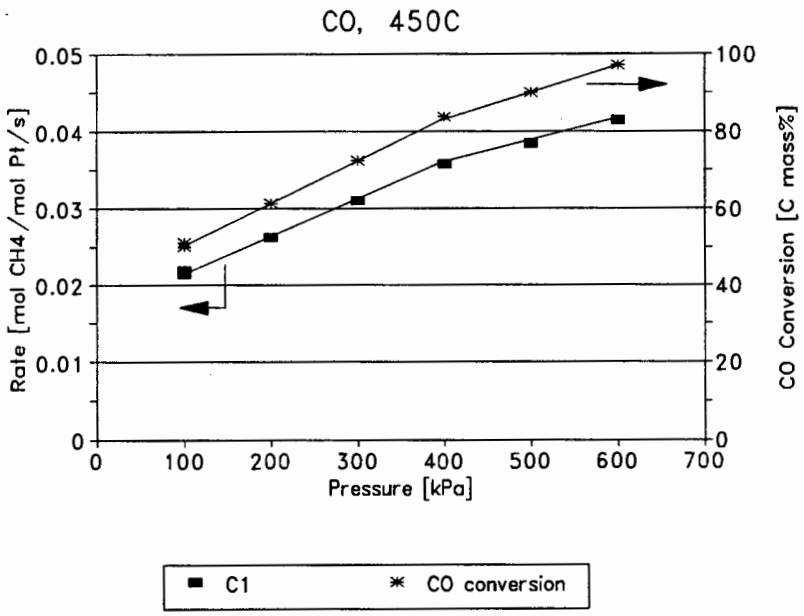

Figure 5-12 Effect of hydrogen pressure on carbon monoxide reaction on Pt/KL at 450°C

3.3.3.4 Ethanol

The effect hydrogen partial pressure on the reaction of ethanol over Pt/KL is shown Figure 5-13. No analysis of the CO in the flue gas was performed. The ratio of hydrogenation:hydrogenolysis (C_2:C_1) increases from 0.06 to 0.86 at 1 bar and 6 bar respectively.

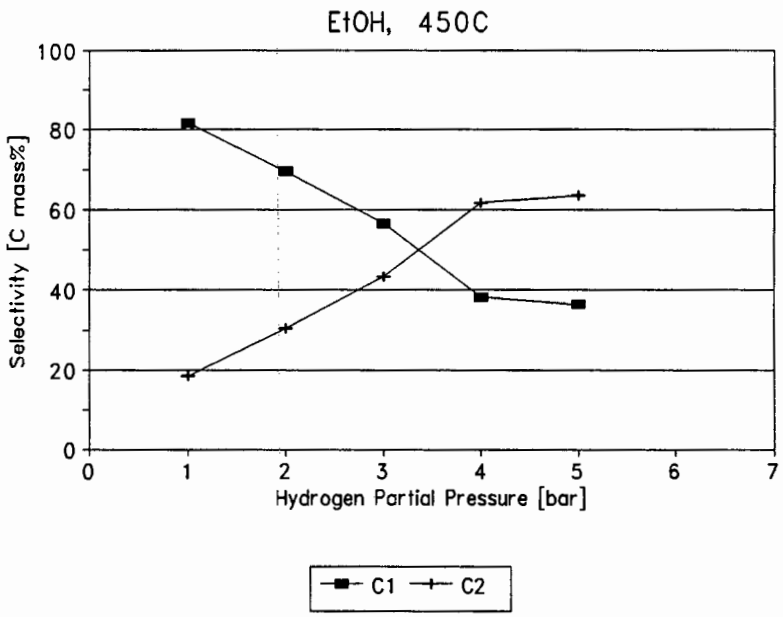

Figure 5-13 Effect of hydrogen partial pressure on reaction of ethanol over Pt/KL at 450°C

3.3.4. Summary of the reaction of oxygenates on Pt/KL

The oxygenated feed can react either through hydrogenation or hydrogenolysis pathways. Hydrogenolysis seems to occur mainly alpha to the oxygenated carbon atom, leaving a carbonyl group adsorbed on the platinum clusters. However, platinum carbonyls are unstable and thus at higher temperatures the carbonyl may undergo complete hydrogenation to methane and water or it may desorb as carbon monoxide. An alternate proposal is the formation of "hard coke", *i.e.* the reaction of CO to form water and carbon. At higher partial pressures of hydrogen it is feasible that this coke may be hydrogenated to methane. No carbon dioxide was observed and thus the Boudouard reaction $2CO \rightarrow C + CO_2$, can be assumed to be negligible. The catalysts were analysed by TGA (Section 2.5.7) after the reaction and coke identified.

In general, the effect of increase in hydrogen partial pressure at 450°C is to increase the ratio of hydrogenation to hydrogenolysis (for n-BuHO, MEK, CO, ethanol).

The effect of reaction temperature is more complex. The ratio of hydrogenation to hydrogenolysis increases with reaction temperature for n-BuHO and i-BuHO, while the ratio decreases for MEK and ethanol. In addition both n-BuHO and i-BuHO produce both i-butane and n-butane as reaction products. Thus it appears that there is some isomerization activity (n-butane $\rightleftarrows$ i-butane) during the feeding of the butyraldehydes. However, no i-butane is formed by the isomerization of n-butane in n-hexane aromatization and negligible amounts of i-butane are formed in the reaction of MEK on Pt/KL, where n-butane is a major product. Thus the reaction mechanism for butyraldehydes on Pt/KL appears to differ from that of MEK, which is strange as ketones and aldehydes are, at least at a first glance, very similar in structure and hence it is expected that their reactivity would be similar.

In all cases selectivity to methane increases with reaction temperature. As hydrogenolysis of C_2-C_4 alkanes are not expected below 450°C, the increase in

selectivity to methane is presumably by hydrogenation of the CO. This is supported by the reaction of CO on Pt/KL, for which the conversion to methane increases with reaction temperature.

3.3.4.1 Water gas shift and steam reforming reactions

Other possible reactions of CO on the catalyst are the water gas shift (WGS) reaction and steam reforming. Both require that water be present, however. Water may be formed by dehydrydration of alcohols on acid sites as well as by the complete hydrogenation of CO or the oxygenate. Due to the low acidity of the KL substrate, dehydrogenation is not expected to be a major reaction pathway, so complete hydrogenation can be assumed as the source of water.

WGS	$CO + H_2O \rightleftarrows CO_2 + H_2$	
Steam reforming	$CH_4 + H_2O \rightleftarrows CO + 3H_2$	forward $\geq$ 700°C reverse $\leq$ 700°C
Naphtha reforming	$1/6C_6H_{12} + H_2O \rightleftarrows CO + H_2$	

However, these reactions can be ruled out on the following grounds:

Steam/naptha reforming: On co-feeding H_2O with n-hexane no CO was detected (Section 3.4.2.1) and the reaction temperature is too low (450°C). The reverse steam reaction does, however, take place when feeding CO. The detection of water was not performed and thus its existance as a reaction product cannot be confirmed.

WGS: No CO_2 is detected in the exit gas.

3.4 Co-Feeding of Oxygenates with n-Hexane

3.4.1 Introduction

Six oxygenated compounds were used as co-feeds with n-hexane over Pt/KL at 450°C. These compounds are listed below, along with shorthand nomenclature and boiling points:

- ethanol (EtOH, 79°C)
- n-butyraldehyde (n-BuHO, 75°C)
- i-butyraldehyde (i-BuHO, 63°C)
- methylethylketone (MEK, 80°C)
- carbon monoxide (CO)
- water (100°C)

The first four compounds were chosen on the basis of their boiling point range, which was similar to that of n-hexane (68°C) and n-heptane (98°C). Water and carbon monoxide were co-fed as they are products of reaction of the former four oxygenates over Pt/KL, as discussed in Section 3.3.

3.4.1.1 Experimental method of co-feeding

The co-feeding was performed in the following manner:

- The run was started by feeding n-hexane and hydrogen only. The catalyst was allowed to reach a steady state for the aromatization of n-hexane (*ca.* 48 hours at 1 bar and *ca.* 24 hours at 6 bar)

- After steady state was reached the co-feeding of the oxygenated compound with n-hexane commenced. The residence time and hydrogen partial pressure was kept constant by decreasing the flow of auxillary hydrogen by an amount equivalent to the flowrate of the

hydrogen carrier gas through the single stage saturator containing the oxygenated compound (see Section 2.2, Figure 2.1).

- The co-feeding was terminated after 24 hours. Thereafter n-hexane only was fed for a further 8-24 hours. The residence time was once again kept constant by increasing the flow of auxillary hydrogen

The reaction products of the oxygenated compounds are C_1-C_4 alkanes, carbon monoxide and water (see Section 3.3 for a detailed description of the feeding of oxygenated compounds only over Pt/KL). The carbon monoxide was detected and quantified by infrared spectroscopy of the flue gas. The amount of water produced was not quantified. The C_1-C_4 alkanes produced by the oxygenated co-feed were subtracted from the n-hexane products during co-feeding . This was achieved by:

- Assuming the fraction of C_1-C_4 cracked products from both the oxygenated feed as well as from n-hexane remained constant during the experiment.

- The C_1-C_4 products from the oxygenated feed were subtracted from the total C_1-C_4 products during co-feeding. The amount subtracted for each co-feed was based on knowledge of the reaction products from the reaction of oxygenated compounds on Pt/KL (using data from Section 3.2).

Hence a correction could be made to account for the increase in cracked products due to co-feeding.

A summary of the flowrates, at 1 bar total pressure, of the various compounds are shown in Table 6-1. At higher total pressure the flowrates of the carrier gases were increased to keep the residence time of gas (in the catalyst bed and in the saturators) constant. The molar flow rates can be converted to carbon molar flowrates (C mmol/min) by multiplication with the number of carbon atoms for the

compound in question.

Table 6-1 Molar flowrates for the co-feeding experiments

Compound	Saturator temperature [°C]	Vapour pressure [bar]	Carrier gas flowrate[a] [sccm]	Molar flowrate [mmol/min]	Mole% of n-hexane [%]
n-hexane	1.8	0.064	25	0.0708	-
ethanol	15	0.044	5	0.0097	13.7
MEK	14	0.064	5	0.0142	20.1
n-BuHO	3	0.045	5	0.0100	14.1
i-BUHO	0.5	0.067	3.2	0.0095	13.4
water	30	0.043	5	0.0095	13.4
CO	-	100% CO	5	0.2232	315.3
CO	-	5.9% CO in H_2	5	0.0132	18.6

(a) Flowrate of carrier gas through saturator

3.4.2 The effect of co-feeding oxygenates with n-hexane

The effect of different co-feeds, various partial pressures of hydrogen as well as the amount of co-feed were quantified with regard to n-hexane conversion and product selectivity. Unless otherwise stated, fresh Pt/KL was used for each experiment.

3.4.2.1 The effect of co-feeding at low pressure

The co-feeding of various oxygenates with n-hexane was performed at a hydrogen partial pressure of 1 bar and 2 bar and a reaction temperature of 450°C. In all cases fresh catalyst was used. The hydrogen partial pressure and residence time over the catalyst bed was kept constant by use of auxillary hydrogen before and during co-feeding. The absolute changes in activity and selectivity during the co-feeding of MEK (Figure 6-1 and Figure 6-2), carbon monoxide (Figure 6-3 and Figure 6-4), ethanol (Figure 6-5) and n-butyraldehyde (Figure 6-6) with n-hexane

at 1 bar hydrogen partial pressure is shown to illustrate the effects of the oxygenates.

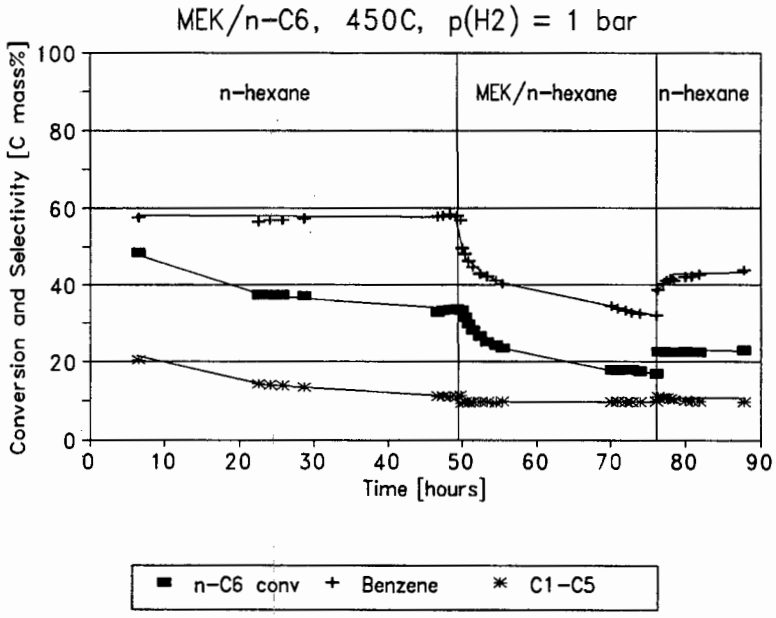

Figure 6-1 The effect of co-feeding MEK with n-hexane

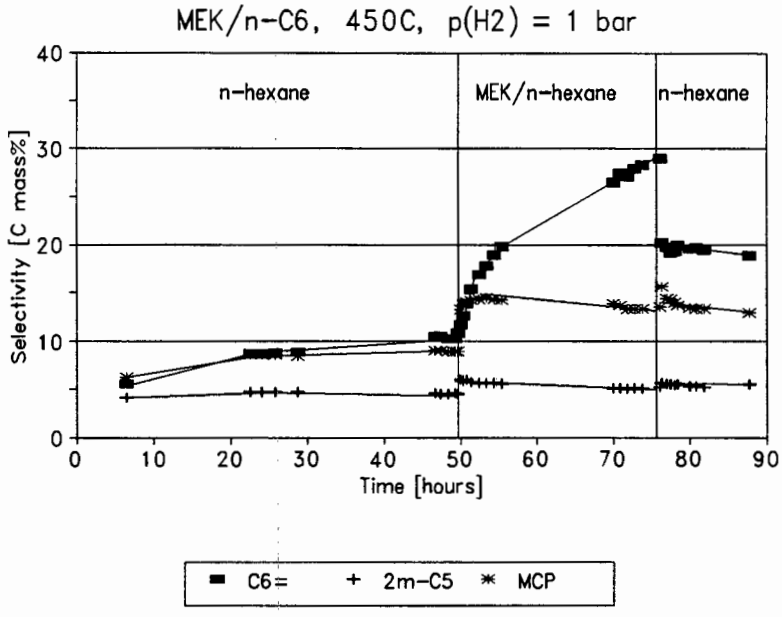

Figure 6-2 The effect of co-feeding of MEK with n-hexane

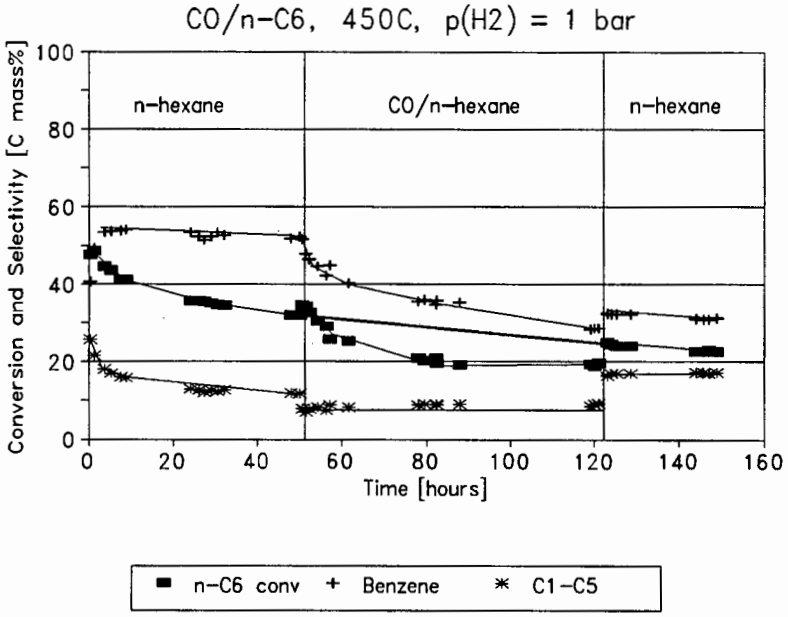

Figure 6-3 Effect of co-feeding CO with n-hexane (CO 18.6 mole% of n-C_6) at 1 bar and 450°C

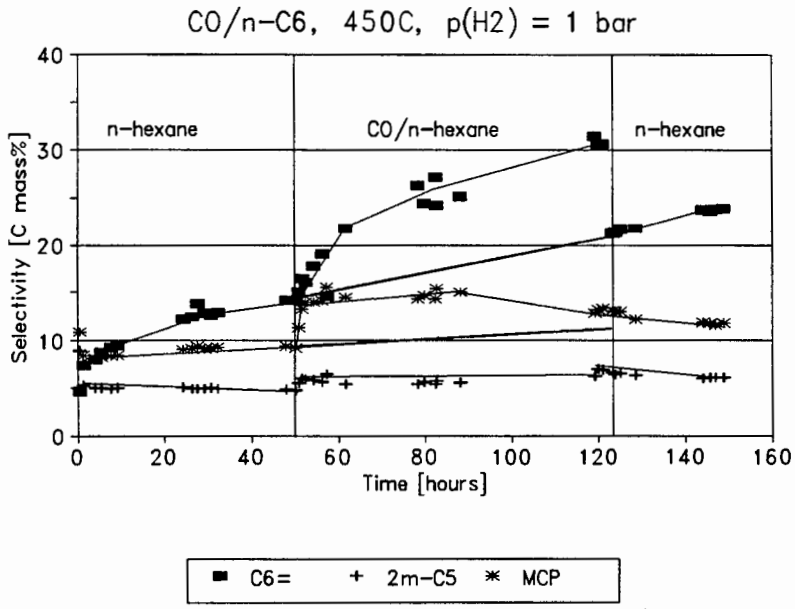

Figure 6-4 Effect of co-feeding CO with n-hexane (CO 18.6 mole% of n-C_6) at 450°C and 1 bar hydrogen partial pressure

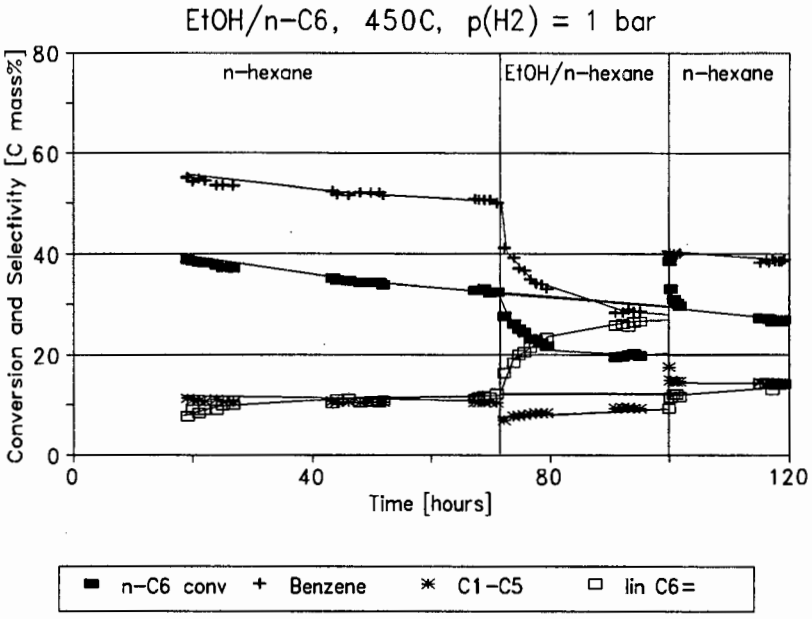

Figure 6-5 Co-feeding of ethanol with n-hexane at 450°C and 1 bar hydrogen partial pressure

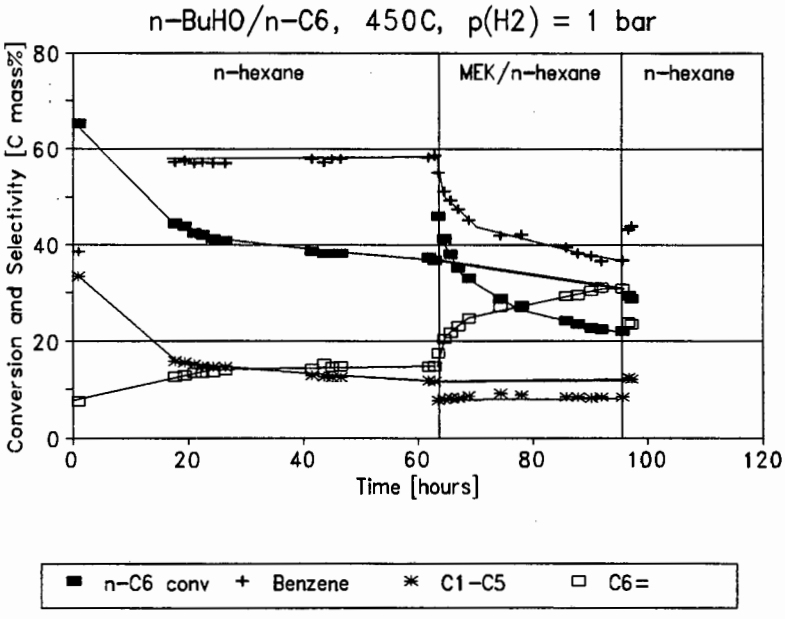

Figure 6-6 Co-feeding of n-butyraldehyde with n-hexane at 450°C

Water is an expected product from the hydrogenation of CO or other carbonyl species as well as from the dehydration of ethanol. Initially it was thought that the presence of water, produced in the reaction of other oxygenates on Pt/KL, may have had an adverse effect on the catalyst activity. An additional possibility was that water could increase the acidity of the catalyst by leaching the aluminum from the zeolite structure (mild steaming). This would result in a greater degree of cracking activity.

To quantify any effect, water was co-fed with n-hexane at 450°C and 1 bar hydrogen partial pressure. Two co-feeding experiments were performed with the molar ratio of water to n-hexane 8 mole% and 13.5 mole%. In each case fresh Pt/KL was used. During these co-feeding experiments no deactivation or shift in selectivities was observed. Hence, it was concluded that water, at the molar ratios used in these experiments, had a negligible effect.

The results for the co-feeding of MEK, CO, ethanol and n-BuHO (Figure 6-1 to Figure 6-6) were typical for the co-feeding of all the oxygenated compounds with n-hexane, with the sole exception being water. A summary of the relative changes in n-hexane conversion and product selectivities during CO co-feeding (CO 18.6 mole% of n-C_6) at 1 bar is given:

- n-Hexane conversion decreased ($\approx$ 45%)
- Benzene selectivity decreased ($\approx$ 42%)
- Selectivity to hexene products increased ($\approx$ 120%)
- Hydrogenolysis selectivity decreased ($\approx$ 20%)
- Selectivity to MCP increased ($\approx$ 40%)
- Selectivity to methylpentanes increased ($\approx$ 20%)

After co-feeding was terminated a recovery in catalyst activity is observed. This is discussed in Section 3.4.3. In general a linear extrapolation from before co-feeding to after co-feeding shows very little change, the exception being benzene

selectivity. All the C_6 products, except benzene, show an increase in selectivity during co-feeding, while the hydrogenolysis products and benzene show a decrease in selectivity. Benzene and the C_1-C_5 products are the result of irreversible reaction pathways (Figure 3.10). Thus the inhibition of aromatization and hydrogenolysis pathways is expected to decrease n-hexane conversion and increase the selectivity to other C_6 products. The relative decrease in benzene selectivity is much greater than would be expected from simple reduction in the overall reaction rate, *i.e.* the rate of formation of benzene is affected more severely than any of the other rates of formation. This is discussed further in Section 3.4.4. (See Table 6-5 and Table 6-11).

The relative changes in selectivity for the co-feeding of the various oxygenates with n-hexane are shown in Table 6-2. The relative magnitude of deactivation is the relative change in selectivity, or conversion, between the steady state value during co-feeding and the steady state value before co-feeding (n-hexane only). Thus for CO the relative magnitude of deactivation for n-hexane conversion is (20-35)/35 = -0.42 and is expressed as a percent in Table 6-2 (-42% change). The effect of co-feeding on conversions and selectivities is expressed in this relative manner, rather than as an absolute change, to take into account slight variations in selectivity and conversion for the different runs. The CO evolved during the experiment is shown as the molar percent of the oxygenated co-feed.

Negative values for the relative magnitude of deactivation imply that the selectivity or conversion decreases during co-feeding (and vice versa for positive values). The co-feeding of MEK and n-BuHO was also performed at 2 bar hydrogen partial pressure. The relative magnitude of deactivation for these experiments are shown Table 6-3. The selectivity to benzene and hydrogenolysis products decreases during co-feeding while the selectivities of the hexenes and iso-hexanes increase (Table 6-2 and Table 6-3). This implies that the hexenes and iso-hexanes are reaction intermediates and that benzene and the C_1-C_5 alkanes are final reaction products. No hexene products are formed at 2 bar hydrogen partial pressure.

Table 6-2 Relative magnitudes of deactivation at 1 bar for the co-feeding of oxygenates with n-hexane

	EtOH	MEK	n-BuHO	i-BuHO	CO	H_2O
Co-feed mole%	13.7%	20.1%	14.1%	13.4%	18.6%	13.4%
n-C_6 conversion	-38%	-49%	-42%	-38%	-42%	≈0%
Benzene[b]	-44%	-45%	-38%	-40%	-46%	≈0%
C_1-C_5[b]	-12%	-12%	-12%	-16%	-33%	≈0%
Hexenes[b]	125%	170%	109%	107%	222%	≈0%
i-C_6[b]	36%	33%	46%	23%	39%	≈0%
CO evolved[a]	n/a	n/a	47%	51%	44%	0%

(a) The amount of CO evolved expressed as a mole% of the co-feed
(b) Selectivities

Table 6-3 Relative magnitudes of deactivation at 2 bar for the co-feeding of oxygenates with n-hexane

	MEK	n-BuHO
Co-feed mole%	20%	14%
n-C_6 conversion	-27%	-12%
Benzene[b]	-29%	-15%
C_1-C_5[b]	-14%	-3%
i-C_6[b]	167%	185%
CO evolved [mole%][a]	29%	30%

(a) Amount of CO evolved expressed as a mole% of the co-feed
(b) Selectivities
(c) The selectivities to hexene products are zero at 2 bar

A plot of the product selectivities for all the co-feeding experiments at 450°C and 1 bar and 2 bar are shown in Figure 6-7 and Figure 6-8 respectively. The data is for the steady state values before co-feeding, during co-feeding and after co-feeding was terminated. In both cases a linear selectivity-conversion relationship is evident.

The plots (Figure 6-7 and Figure 6-8) tend to support the hypothesis that the effect of the oxygenates is due to adsorption of an oxygenated species on the platinum clusters, thus reducing the number of active sites. The fact that the effects of the oxygenates are similar points to a common factor, possibly carbon monoxide. The selectivity data at the highest conversions in the plots at 1 bar and 2 bar are for n-hexane only.

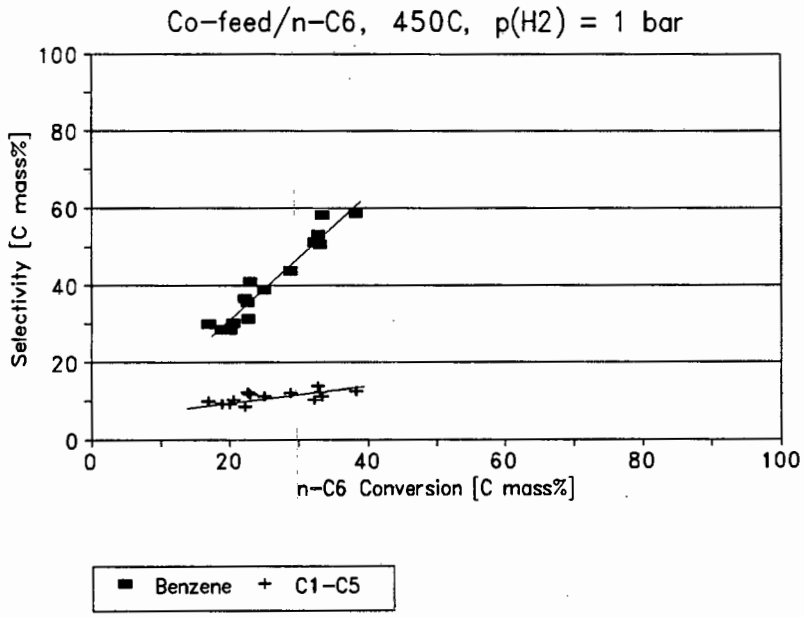

Figure 6-7 Selectivity data for co-feeding at 1 bar and 450°C

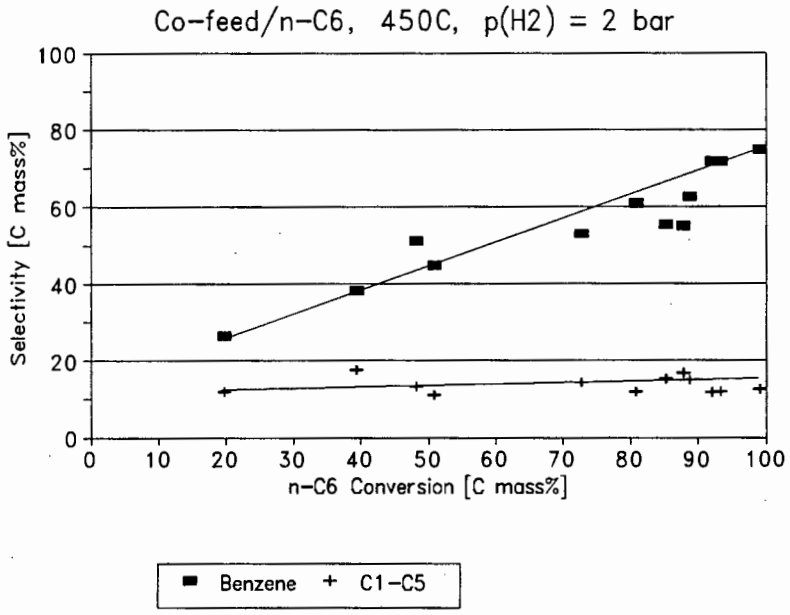

Figure 6-8 Selectivity data for co-feeding at 2 bar

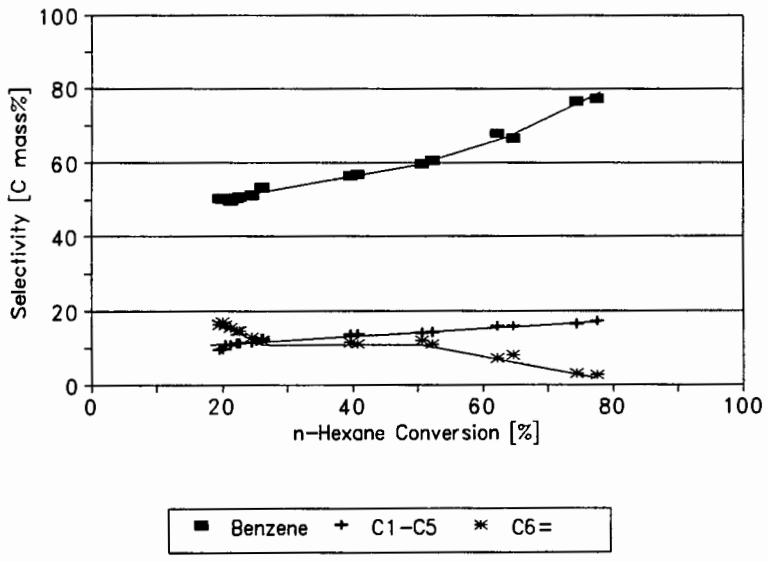

Figure 6-9 Selectivity-conversion plot for the sintering of platinum at 1 bar partial pressure of hydrogen

The plots (Figure 6-7 and Figure 6-8) may be compared with the data from the sintering experiment in Section 3.1.1 for which a similar selectivity conversion plot is shown (Figure 6-9). The selectivity to hydrogenolysis products are similar in all three plots. However, the selectivity to benzene is suppressed in the case of co-feeding (Figure 6-7 and Figure 6-8), relative to that for the feeding of n-hexane only (Figure 6-9). Thus the co-feeding of oxygenates must alter the reactivity of the platinum clusters in such a way as to inhibit the formation of benzene. Linear regression of the benzene and hydrogenolysis product selectivity is shown in Table 6-4.

Table 6-4 Linear regression data for benzene and hydrogenolysis selectivity data during co-feeding at 1 bar and 2 bar

	$p(H_2)$ = 1 bar		$p(H_2)$ = 2 bar	
	Benzene	C_1-C_5	Benzene	C_1-C_5
Gradient	1.36	0.14	0.44	0.03
Y-intercept	4.2	7.4	21.6	11.7
r^2	0.68	0.39	0.69	0.11

There seems to be a fair amount of spread in the relative changes in conversion and selectivity during co-feeding (Table 6-2). However, the decrease in n-hexane conversion and benzene selectivity seem to be of similar magnitude for all the oxygenated cases. There is a greater variation in the change in selectivities for the methylpentane and hexene isomers.

In Table 6-5 the selectivity-conversion data for the co-feeding experiments is compared with selectivity-conversion data for hexane only at different space velocities, but at the same reaction temperature and hydrogen partial pressure.

Table 6-5 Comparison of selectivity-conversion data for the co-feeding experiments and WHSV experiments at 1 bar and 450°C

Conversion	20%	25%	30%	35%
	n-Hexane (1 bar, 450°C, changes in WHSV)[a]			
Benzene	50	54	55	57
C_1-C_5	9	10	11	12
Hexenes	18	14	11	9
2m-C_5	6	6	6	6
3m-C_5	4	4	4	4
MCP	14	13	13	12
ΣSelectivities	101	101	100	100
	co-feeding with n-hexane (1 bar, 450°C)[b]			
Benzene	33	40	48	56
C_1-C_5	6	6	7	10
Hexenes	31	26	22	15
2m-C_5	8	8	7	6
3m-C_5	7	7	6	5
MCP	15	14	11	9
ΣSelectivities	100	101	101	101

(a) Data from Section 3.1.3
(b) Data from linear regression of selectivity data for co-feeding as shown in Figure 6-7 for benzene and hydrogenolysis products

At a n-hexane conversion of 35% only n-hexane was fed for both sets of data in Table 6-5. Hence the product selectivities are similar. The decrease in benzene selectivity is mainly reflected by a similar increase in selectivity to hexene products. This may be taken as evidence that the hexene isomers are possible intermediates in the formation of benzene.

3.4.2.2 The effect of hydrogen partial pressure

Carbon monoxide, n-butyraldehyde and methylethylketone were co-fed with n-hexane at 6 bar hydrogen pressure. In each case a fresh Pt/KL catalyst was used. The molar ratios of co-feed:n-hexane were the same at 6 bar as for 1 bar and 2 bar. The results of co-feeding CO with n-hexane are shown in Figure 6-10 and Figure 6-11. Both MEK and n-BuHO co-feeding produced similar results.

At 1 bar the co-feeding of oxygenates with n-hexane produces smooth and continuous deactivation curves (Figure 6-1 to Figure 6-6). However, co-feeding of oxygenates at a hydrogen partial pressure of 6 bar produces a sharp discontinuous change (Figure 6-10 and Figure 6-11) in the product selectivities. The effect of co-feeding oxygenates with n-hexane at 6 bar produces similar trends to that at 1 bar. As 1-hexene is not observed as a reaction product at 6 bar, the greatest increase in selectivity is for the isomerized hexanes. The relative changes in n-hexane conversion and product selectivities are shown below.

- n-Hexane conversion decreases ($\approx$ 10%)
- Benzene selectivity decreases ($\approx$ 13%)
- Selectivity to hydrogenolysis products decreases ($\approx$ 30%)
- MCP selectivity increases ($\approx$ 110%)
- Selectivity to methylpentanes increases ($\approx$ 80%)

The results of the co-feeding experiments are shown in Table 6-6. At 6 bar no alkene products are observed. After co-feeding was terminated the catalyst activity and product selectivities return to the values expected had there been no co-feeding (Figure 6-10 and Figure 6-11).

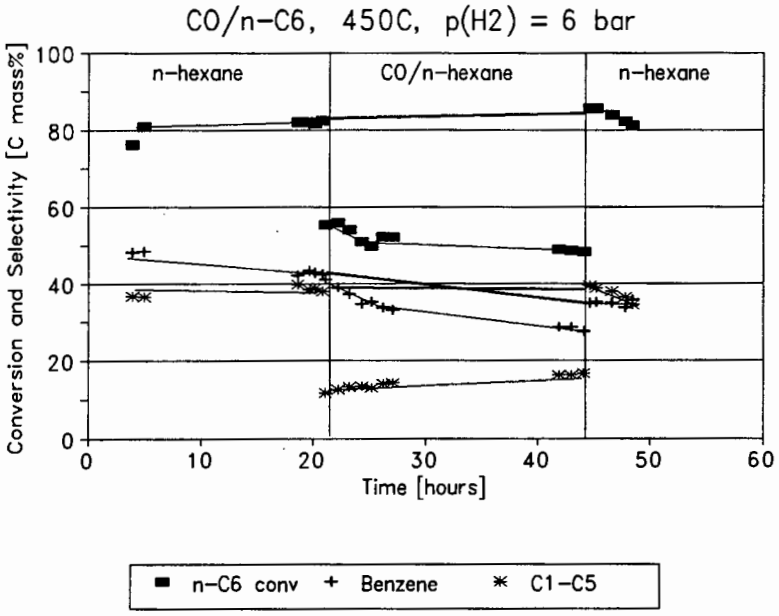

Figure 6-10 Effect of co-feeding CO with n-hexane at 6 bar and 450°C

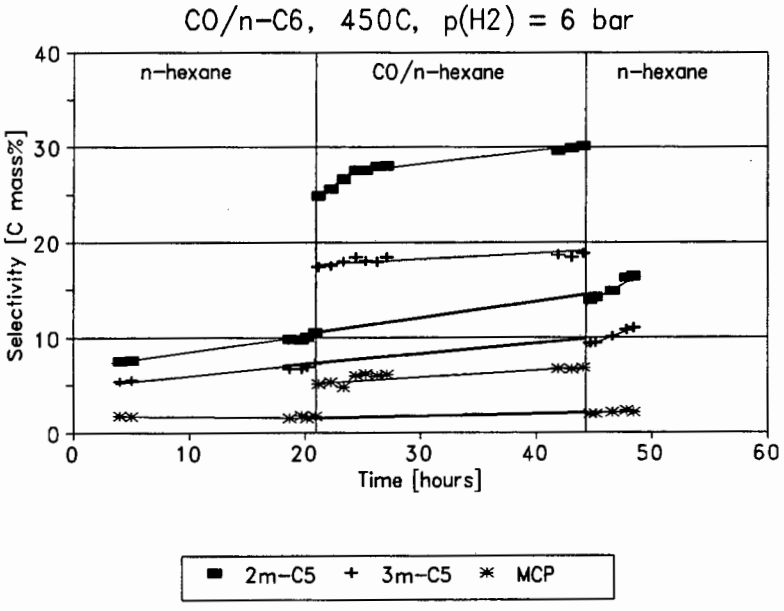

Figure 6-11 Effect of co-feeding CO with n-hexane at 450°C and 6 bar hydrogen partial pressure

At the higher partial pressures of hydrogen it is more informative to look at the relative magnitude of changes in selectivity. The relative magnitude of deactivation is defined, as before, as the change in product selectivity (or n-hexane conversion) at steady state during co-feeding relative to the steady value before co-feeding. These are shown in Table 6-6. No CO was produced at 6 bar hydrogen partial pressure, *i.e.* no CO emerged from the reactor.

Table 6-6 Relative magnitudes of deactivation at 6 bar for the co-feeding of oxygenates with n-hexane

	MEK	n-BuHO	CO
Co-feed mole%	20%	14%	18%
n-C_6 conversion	-9%	-13%	-10%
Benzene[a]	-11%	-16%	-13%
C_1-C_5[a]	-23%	-44%	-30%
2m-C_5[a]	60%	118%	86%
3m-C_5[a]	64%	102%	75%
MCP[a]	102%	136%	110%

(a) Selectivities

Co-feeding at 6 bar caused a decrease in n-hexane conversion of *ca.* 11% while the selectivity to benzene decreased by *ca.* 13%. A summary of the average relative changes during co-feeding is shown in Table 6-7.

The absolute magnitude of change in product selectivity and n-hexane conversion during co-feeding is not very informative for comparison at different hydrogen partial pressures as the conversion of n-hexane will be different at different partial pressures. The percentage change in selectivity and conversion may be a better method of presenting such data, *i.e.* the relative magnitude. However, ideally the catalysts should be compared at the same conversion of n-hexane before co-feeding the oxygenated compounds. It was not possible to maintain both the same residence time over the catalyst bed as well as keeping the n-hexane conversion constant at different partial pressures of hydrogen.

Table 6-7 Summary of the average relative changes in selectivity and conversion for the co-feeding of oxygenates with n-hexane at 450°C

	1 bar[b]	2 bar[b]	6 bar[b]
n-C_6 conversion	-42%	-20%	-11%
Benzene	-43%	-22%	-13%
C_1-C_5	-17%	-9%	-34%
Hexenes	146%	n/a	n/a
2m-C_5	28%	126%	90%
3m-C_5	31%	90%	83%
MCP	45%	203%	120%
CO produced [mole%][a]	51%	30%	0%

(a) Amount of CO produced expressed as a mole% of the co-feed
(b) Average values from Table 6-2, Table 6-3 and Table 6-7 respectively

The relative change in benzene selectivity and n-hexane conversion decreases with increase in hydrogen partial pressure. The amount of carbon monoxide evolved also decreases. At higher partial pressures of hydrogen increased hydrogenation of the oxygenated compounds occurs (Section 3.3.3). The main oxygen-containing compound at 6 bar will be water as no carbon monoxide is detected at this partial pressure of hydrogen. Water has been shown to have negligible effect on either selectivity or conversion when co-fed with n-hexane (Section 3.4.2.1). The magnitude of the relative changes in product selectivity also seem to be related to the amount of carbon monoxide evolved, *i.e.* the greater the amount of carbon monoxide evolved, the greater the extent of deactivation. However, at 6 bar no CO is observed, yet deactivation still occurs. This implies that although CO may be a contributing factor causing the poisoning, it is not the only factor. The fact that no carbon monoxide is observed at 6 bar does not necessarily preclude the presence of carbon monoxide in the upper portion of the catalyst bed, where it may still deactivate the catalyst. Lower in the catalyst bed the carbon monoxide is hydrogenated to form "harmless" methane and water. It is thus proposed that adsorbed carbonyl species (including CO), formed from the hydrogenolysis of the oxygenates, are the main cause of the deactivation of Pt/KL.

The conversion of CO for the co-feeding of CO with n-hexane at 450°C is shown in Figure 6-12. Carbon monoxide conversion data for the reaction of CO only over Pt/KL (from Section 3.3.3.3) is shown as well for comparision. The residence time over the catalyst bed was kept constant at each hydrogen partial pressure. At 6 bar hydrogen partial pressure the conversion of CO to methane and water goes to completion for the co-feeding case. Thus there should be no CO available for adsorbtion on platinum sites. If deactivation of the catalyst only occured as the result of preferential CO adsorbtion, then at 6 bar this effect should be small due to the absence of free CO. However, a decrease in activity is still observed at 6 bar (Figure 6-10). These results for the co-feeding of carbon monoxide showed that the conversion of CO was higher when co-fed with n-hexane compared to the case when only CO was fed.

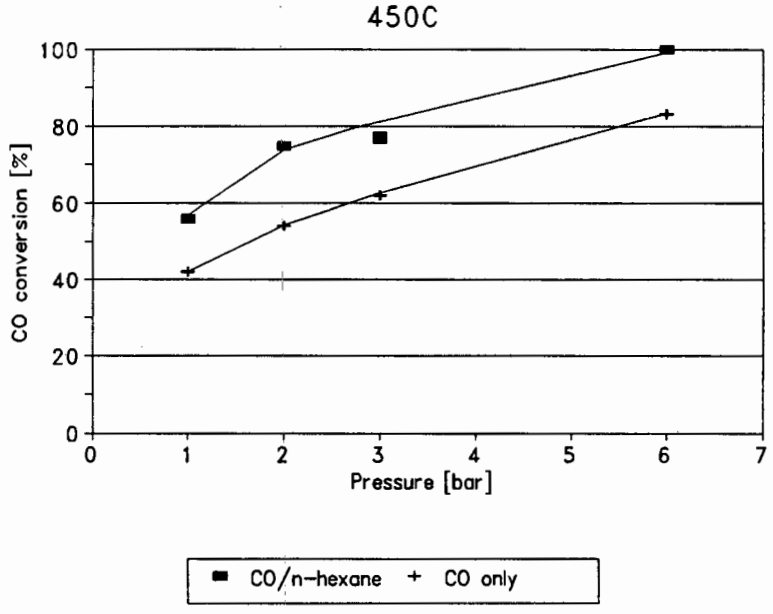

Figure 6-12 Effect of hydrogen pressure on the conversion of CO for the co-feeding of CO with n-hexane (CO 18.6 mole%) and the feeding of CO only at 450°C

The yields (selectivity multiplied by conversion) of benzene and hydrogenolysis products during co-feeding are shown in Table 6-8. The highest benzene yields occur at 2 bar while the hydrogenolysis yields show a steady increase with increase in hydrogen partial pressure. This is not surprising as hydrogenolysis products are the thermodynamically favoured products. Operating at high pressure and high temperature will bring the system closer to thermodynamic equilibrium, thus resulting in higher yields of hydrogenolysis products.

Table 6-8 Comparison of product yields at different hydrogen partial pressures during co-feeding and 450°C

co-feed	n-hexane		n-BuHO/n-C_6		MEK/n-C_6		CO/n-C_6	
yield	benzene	C_1-C_5	benzene	C_1-C_5	benzene	C_1-C_5	benzene	C_1-C_5
1 bar	13.9	2.2	8.1	1.9	5.4	1.7	5.4	1.8
2 bar	66.2	15.1	37.6	7.9	27.6	6.9	20.4	4.9
6 bar	30.4	28.3	28.5	18.3	21.5	13.4	13.3	8.2

3.4.2.3 The effect of reaction temperature

The reaction temperature was changed during the co-feeding of n-butyraldehyde and i-butyraldehyde. The temperature was varied after steady state had been reached during co-feeding, *i.e.* after 24 hours. The hydrogen partial pressure was 1 bar. Thus selectivity-conversion plots as a result of change in reaction temperature can be obtained and compared to those obtained for n-hexane only.

The effect of reaction temperature is similar for the co-feeding of n-butyraldehyde and i-butyraldehyde with n-hexane (compare Figure 6-13 and Figure 6-14). The results of the co-feed/n-hexane reaction are compared with the results of Section 3.1.2 for the aromatization of n-hexane in Table 6-9.

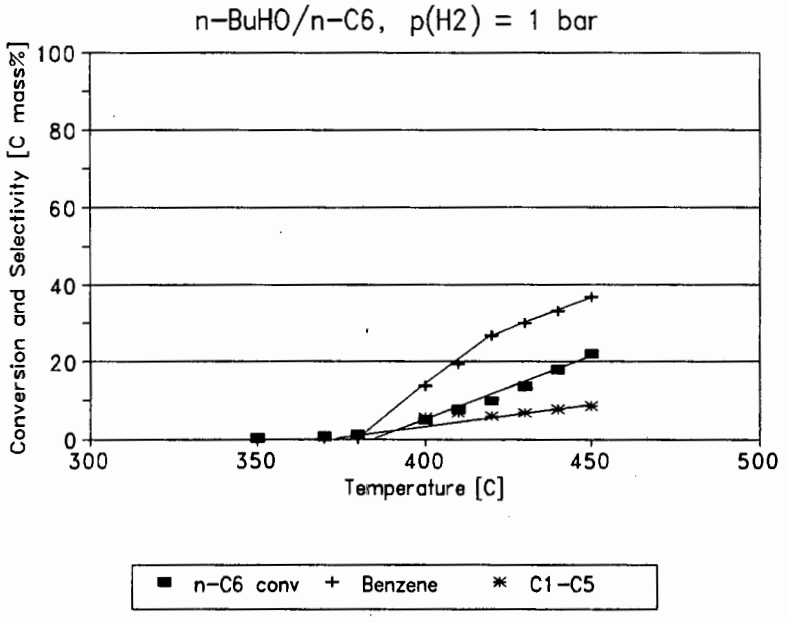

Figure 6-13 Effect of reaction temperature during co-feeding of n-butyraldehyde with n-hexane at 1 bar hydrogen partial pressure

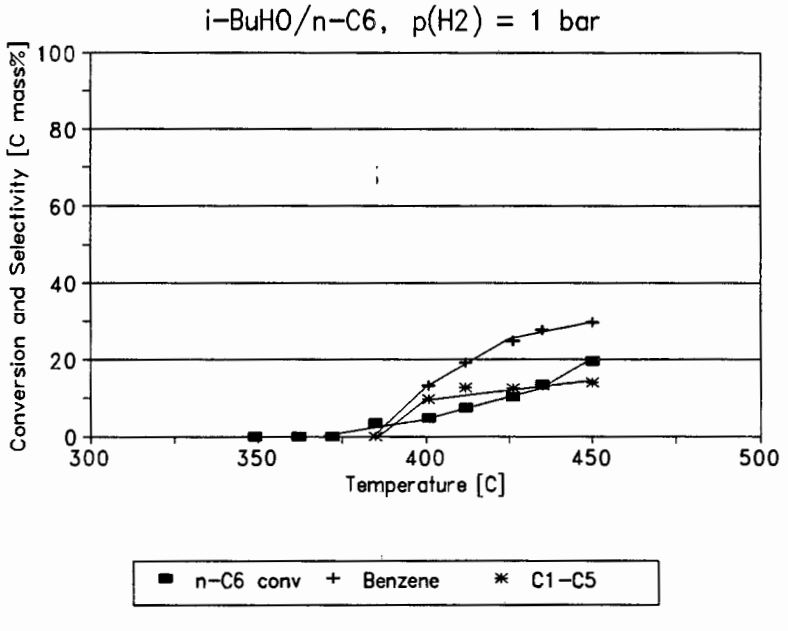

Figure 6-14 The effect of reaction temperature for the co-feeding of i-butyraldehyde with n-hexane at 1 bar

The amount of carbon monoxide evolved during co-feeding decreases with increase in reaction temperature, presumably by reaction to methane and water. The conversion of n-hexane is zero below 375°C. As in the case of n-hexane only an increase in selectivity to benzene and hydrogenolysis products is observed with increase in reaction temperature.

Table 6-9 Comparision of n-BuHO co-feeding with n-hexane aromatization at 1 bar hydrogen partial pressure

Feed	n-hexane		n-BuHO/n-hexane	
Temperature	400°C	450°C	400°C	450°C
n-C_6 conversion	16	40	5	22
Benzene[c]	47	60	14	37
C_1-C_5[c]	8	12	5	8
C_6=[c]	8	9	41	30
Σi-C_6[a,c]	36	19	40	25
ΣSelectivity	99	100	100	100
CO evolved[b]	n/a	n/a	47%	43%

(a) methylpentanes and MCP
(b) Amount of CO evolved expressed as a mole% of the co-feed
(c) Selectivities

The hexene isomer ratios (the ratios of 1-hexene:c,t-2-hexene:3-hexene) remain approximately constant over the n-hexane conversion range. The hexene isomer selectivity, however, decreased as the conversion of n-hexane increased (Figure 6-15). During all the co-feeding experiments the hexene isomer ratios were constant and did not change during or after co-feeding. The ratio of 2-methylpentane:3-methylpentane increases very slightly with increase in n-hexane conversion. The ratio of MCP:methylpentanes increases with n-hexane conversion. These results are thermodynamically expected, *viz.* higher conversions of n-hexane imply a more active catalyst and hence the reaction is shifted closer to thermodynamic equilibrium.

A more representative way of comparing the effect of co-feeding would be to compare the product selectivities at similar conversions of n-hexane. To this end plots of product selectivities as a function of n-hexane conversion are shown in Figure 6-15.

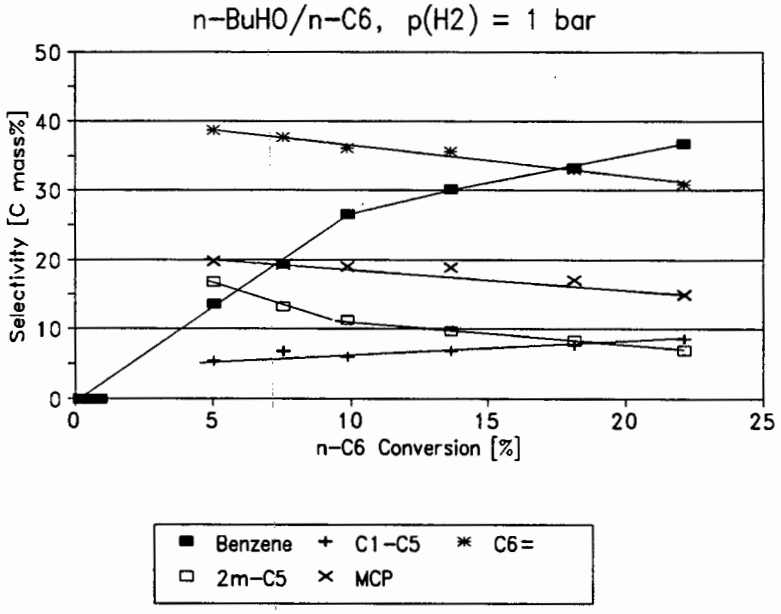

Figure 6-15 Selectivity as a function of n-hexane conversion for the the co-feeding of n-BuHO with n-hexane for changes in reaction temperature

The results shown Figure 6-15 can be compared with those for reaction of n-hexane over Pt/KL (Section 3.1.2) as illustrated in Table 6-10. The most obvious differences are the decrease in selectivity to benzene and hexenes at comparable n-hexane conversions in the case of the co-feeding experiments. With the exception of benzene and the hexene isomers the product selectivities are remarkably similar at the same conversion of n-hexane (Table 6-10). This may be presented as evidence that the co-feed alters the reactivity of the platinum clusters in such a way as to inhibit benzene formation. Inhibition of the aromatization

pathway will result in an increase in selectivity to hexenes. At higher partial pressures of hydrogen the hexenes will be hydrogenated to n-hexane which will result in an increase in the selectivity to methylpentanes as shown in Section 3.1.4.2.

Table 6-10 Product selectivities as a function of n-hexane conversion for changes in reaction temperature at 1 bar

Conversion	10%	15%	20%
		n-Hexane (1 bar)	
Temperature	380°C	395°C	405°C
Benzene	43	46	49
C_1-C_5	8	9	10
Hexenes	3	8	9
Σi-C_6[a]	43	35	30
ΣSelectivities	97	98	98
		n-Butyraldehyde/n-hexane (1 bar)	
Temperature	415°C	425°C	450°C
Benzene	26	32	35
C_1-C_5	5	6	8
Hexenes	35	33	31
Σi-C_6[a]	36	31	27
ΣSelectivities	102	102	101

(a) Methylpentanes and MCP

However, the results of Table 6-10 may be misleading as the reaction temperatures are different. Hence, the selectivities were compared at the same reaction temperature (450°C) and the same n-hexane conversions (Table 6-11). The n-hexane conversions were varied in the case of feeding n-hexane only due to changes in WHSV. In the case of the co-feeding experiments the different n-hexane conversion data was obtained as a result of catalyst deactivation during co-feeding. Thus the residence times over the catalyst bed will differ for the two cases. The residence for all the co-feeding data was the same.

Table 6-11 Product selectivities as a function of n-hexane conversion for changes in WHSV at 1 bar and 450°C

Conversion	10%	15%	20%	25%	30%
		n-Hexane (1 bar)			
Benzene	41	45	50	54	57
C_1-C_5	6	9	10	11	13
Hexenes	30	23	19	15	12
Σi-C_6[a]	21	20	19	18	16
ΣSelectivities	98	97	98	98	98
Absolute benzene[b]	92	88	88	87	85
		Co-feed/n-hexane (1 bar)			
Co-feed	i-BuHO	MEK	i-BuHO	EtOH	i-BuHO
Benzene	22	31	30	33	37
C_1-C_5	15	9	13	15	11
Hexenes	28	29	27	23	21
Σi-C_6[a]	34	30	30	29	31
ΣSelectivities	99	99	100	100	100
Absolute benzene[b]	84	90	87	85	89

(a) Methylpentanes and MCP
(b) Benzene + hexene + i-C_6

The co-feeding of oxygenates with n-hexanes results in a decrease in benzene selectivity relative to feeding n-hexane only, at the same conversion of n-hexane. The selectivities to hydrogenolysis products are similar in both cases. This is further proof that the oxygenates do not merely reduce the number of active sites. The reactivity of the platinum clusters is altered as well.

The absolute selectivity to benzene (benzene plus all C_6 reaction products) is the same for n-hexane and for the co-feeding of oxygenates with n-hexane. This implies that high selectivities to benzene can be retained during co-feeding by decreasing the WHSV of the feed.

It thus appears that to minimize selectivity to hydrogenolysis products, which cannot undergo 1-6 ring closure and subsequent aromatization, the system must be operated at low pressure and temperature. Higher partial pressures (6 bar) minimize the deactivating effects of the oxygenate co-feeds. However, this beneficial result is offset by an increase in selectivity to hydrogenolysis products at 6 bar. The deactivating effect of the oxygenate compounds appears to inhibit the overall reaction rate (although the aromatization pathway is the most sensitive to the oxygenate poisoning). This effect appears to be reversible. Thus the system can tolerate oxygenate impurities. Lower benzene yields and lower hydrogenolysis yields will both result during co-feeding. The effect of hydrogen partial pressure on deactivation by coke formation must also be taken into account. At 1 bar the rate of deactivation by coke formation is high. Thus it appears that operating at 2 bar to 3 bar hydrogen partial pressure and at 400°C to 450°C will maximize benzene yields and result in tolerable rates of deactivation by coke formation. It may be neccessary to operate a high pressure (6 bar) to completely prevent coke formation for catalysts that are intended to have long reactor life times. However, greater losses of the feed to hydrogenolysis will occur.

3.4.2.4 The effect of amount of ethanol co-fed

The amount of ethanol co-fed was varied by increasing the temperature of the saturator. In this series the same Pt/KL catalyst was used. However, it was regenerated, as explained in Section 3.2, after each co-feeding experiment. The hydrogen partial pressure was 1 bar and the reaction temperature 450°C. The relative magnitude of deactivation for this series of experiments are shown in Table 6-12.

Table 6-12 Relative magnitudes of deactivation for different molar amounts of ethanol co-fed with n-hexane

EtOH mole%[a]	1.1%	2.8%	14%	23%
n-C_6 conv	-11%	-28%	-38%	-49%
Benzene	-9%	-18%	-44%	-51%
C_1-C_5	-4%	-13%	-16%	-18%
C_6=	38%	45%	116%	160%

(a) mole % of EtOH relative to n-hexane feed rate

The salient point that can be made with regard to the data in Table 6-12 is once again that the decrease in benzene selectivity is reflected mainly by the large increase in selectivity to hexene products. This implies that hexene products are reaction intermediates in the formation of benzene. The decrease in selectivity to benzene is larger than for hydrogenolysis products. Hence, it may be speculated that the co-feeding of oxygenates alters the reactivity of the platinum clusters such that the formation of benzene is inhibited. The degree of decrease in n-hexane conversion is related to the amount of ethanol co-fed. This tends to support the hypothesis that the deactivation is the result of competitive adsorbtion on platinum sites. Even low levels of ethanol (2.8 mole%) cause a large decrease in n-hexane conversion and selectivity to benzene.

3.4.3 Recovery after co-feeding

After co-feeding of the oxygenated compounds with n-hexane was terminated a recovery in the activity of the catalyst, relative to that during co-feeding, was observed. This is represented schematically in Figure 6-16. The letters A, B and C represent the n-hexane conversion at the "steady state" before co-feeding (*ca.* 48 hours at 1 bar), 24 hours after co-feeding and 12 hours after co-feeding was terminated. A similar scheme can be made for the selectivity values as well.

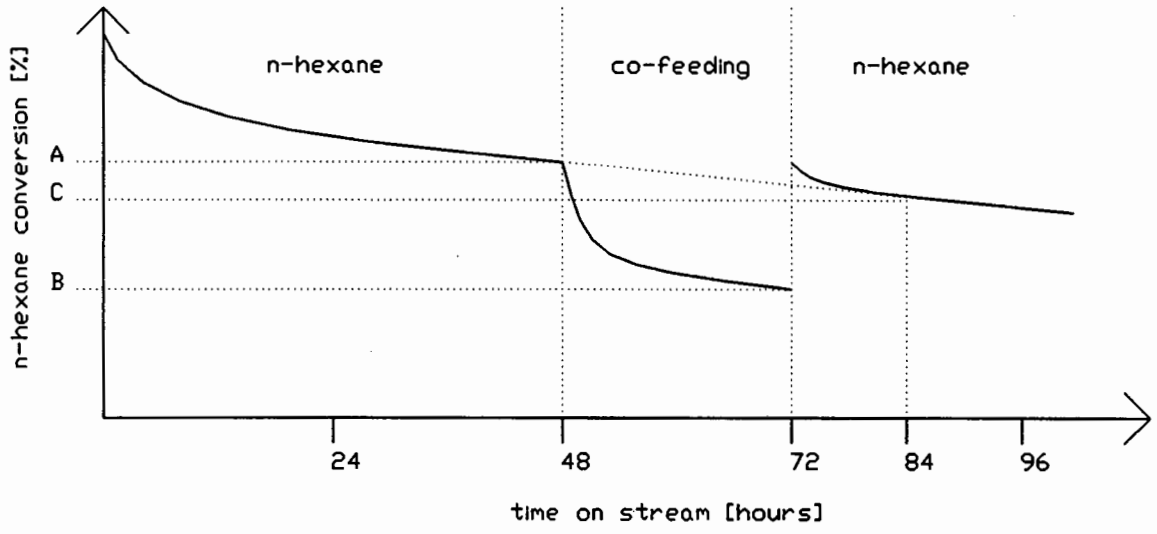

Figure 6-16 Schematic representation of the effect of co-feeding on n-hexane conversion

This recovery also included an increase in selectivity to benzene and a decrease in selectivity to hexene isomers (at 1 bar). The hexane isomers also showed a decline. The recovery was calculated by two different methods:

- The recovery is calculated as the percentage difference between the "steady state" value before co-feeding and after co-feeding, *viz.* (C-A)/A. It may be argued that this represents the normal deactivation of the catalyst as a result of the feeding of n-hexane only. The closer the values are to zero the greater the extent of recovery, *i.e.* 0% implies 100% recovery after co-feeding.

- An alternative method is to calculate the recovery as the percentage difference between the steady state value during co-feeding and 12 hours after co-feeding, *viz.* (C-B)/B. The difficulty with this method is that the catalyst did not always reach a steady state value with regard to activity and product selectivity during co-feeding. Thus the activity and selectivity values after 24 hours of co-feeding were used in all cases.

The recoveries after co-feeding are shown in Table 6-13, Table 6-14 and Table 6-15 for co-feeding at 1 bar, 2 bar and 6 bar respectively. The reaction temperature was 450°C. The problem with a constantly deactivating catalyst is that the selectivities are a function of time on stream. As can be seen from the plots of selectivity and conversion with time on stream, at both 1 bar and 6 bar, (Figure 6-1 to Figure 6-4 and Figure 6-10 to Figure 6-11) a satisfatory steady state with regard to n-hexane conversion and product selectivity was not always attained. This obviously introduces errors in the relative changes in conversion and selectivity. Also relatively large errors are caused by products with low selectivities. To overcome these problems it was neccessary, in certain cases, to extrapolate conversion and selectivity to assumed "steady state" values.

Table 6-13 Relative magnitudes of recovery at 1 bar after the co-feeding of oxygenates with n-hexane

	EtOH	MEK	n-BuHO	i-BuHO	CO
Co-feed mole%	14%	20%	14%	13%	19%
	Recovery expressed as percent of (C-A)/A				
n-C_6 conv	-23%	-31%	-25%	-32%	-31%
Benzene	-24%	-25%	-25%	-29%	-41%
C_1-C_5	37%	4%	26%	7%	24%
Hexenes	16%	76%	60%	71%	120%
i-C_6	10%	19%	24%	10%	29%
	Recovery expressed as percent of (C-B)/B				
n-C_6 conv	25%	36%	30%	10%	20%
Benzene	37%	36%	19%	18%	10%
C_1-C_5	22%	18%	42%	19%	30%
Hexenes	-49%	-35%	-24%	-17%	-32%
i-C_6	-12%	-2%	-5%	-7%	-12%

Table 6-14 Relative magnitudes of recovery at 2 bar after the co-feeding of oxygenates with n-hexane

	MEK	n-BuHO	CO
Co-feed mole%	20%	14%	19%
	Recovery expressed as percent of (C-A)/A		
n-C_6 conv	-11%	-4%	-9%
Benzene	-27%	-13%	-23%
C_1-C_5	32%	28%	29%
i-C_6	91%	22%	78%
	Recovery expressed as percent of (C-B)/B		
n-C_6 conv	21%	10%	67%
Benzene	4%	3%	23%
C_1-C_5	17%	25%	39%
i-C_6	-40%	-52%	-57%

Table 6-15 Relative magnitudes of recovery at 6 bar after the co-feeding of oxygenates with n-hexane

	MEK	n-BuHO	CO
Co-feed mole%	20%	14%	19%
	Recovery expressed as percent of (C-A)/A		
n-C_6 conv	0%	6%	1%
Benzene	0%	1%	-16%
C_1-C_5	-4%	-30%	-6%
i-C_6	32%	97%	75%
	Recovery expressed as percent of (C-B)/B		
n-C_6 conv	9%	6%	68%
Benzene	10%	7%	30%
C_1-C_5	25%	14%	104%
i-C_6	-20%	-8%	-47%

The salient point observed here is that increasing hydrogen partial pressure resulted in almost complete recovery (see (C-A)/A values). At lower partial pressures the recovery was less, possibly due to coke formation. An alternative explanation would be that the lower relative recovery at 1 bar was due to the adsorption of the reaction products formed during co-feeding on platinum sites. At higher partial pressures of hydrogen (6 bar) these species are presumably hydrogenated to alkanes and water and hence desorb more easily from the active platinum sites.

The relative change in n-hexane conversion and benzene selectivity appear to be linked, *i.e.* they are of similar magnitude. The hydrogenolysis products show an increase in selectivity after co-feeding at 1 bar and 2 bar. This would tend to support the hypothesis that sintering of the platinum clusters had occurred during co-feeding. Sintered platinum clusters are thought to be more active for hydrogenolysis (Section 1.8.1.3). At 6 bar the hydrogenolysis selectivity decreases after co-feeding, relative to that before co-feeding. The selectivity to hydrogenolysis products decreases with time on stream (for n-hexane reaction only), presumably due to coke formation. During co-feeding the rate of aromatics formation is suppressed, however, benzene selectivity is not affected by coke deposition (Section 2.4.4).

3.4.4 Rate of deactivation

To overcome the problem of determining when a steady state had been reached, before, during and after co-feeding, the rates of reaction were investigated. Deactivation caused by coking could be empirically modeled by exponential decay (Section 3.2). Similarly deactivation as a result of co-feeding could also be modelled by an exponential function of the form:

$$r = A_o t^n$$

r : rate of reaction [C mmol/min]
A_o : rate at time on stream = 0
n : deactivation exponent
t : time on stream

Thus a linear relationship between a plot of log rate as a function of log time on stream is observed. The time on stream for the log-log plots during co-feeding is corrected by subtracting the first 48 hours during which deactivation with n-hexane occured, *i.e.* time on stream = 0 occurs as co-feeding begins. At 1 bar a good linear relationship for all products is obtained for the log of rate of formation with log time on stream (Figure 6-17 and Figure 6-18). The slope of this line gives an indication as to the severity of the deactivation However, at 6 bar the slope obtained by this method is not very informative due to the discontinuous nature of the the change in reaction rates during co-feeding.

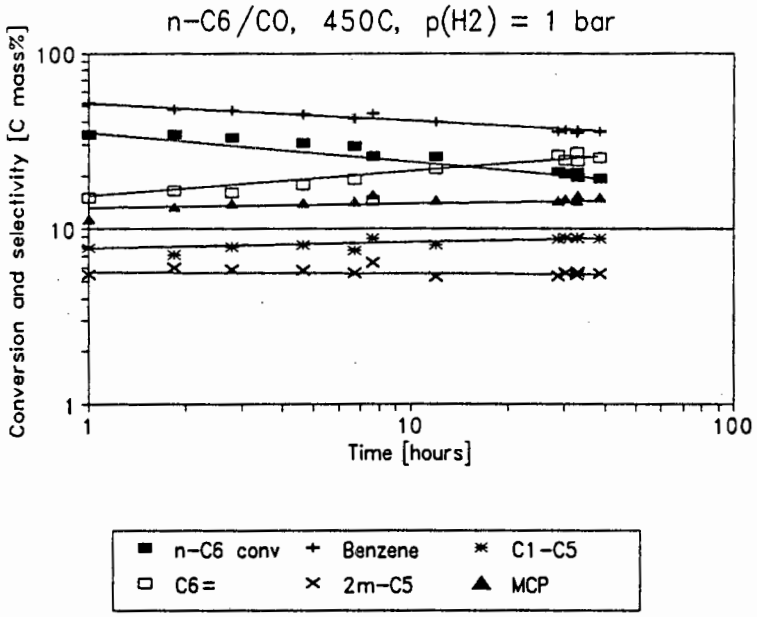

Figure 6-17 Plot of log selectivity and conversion as function of log time for co-feeding

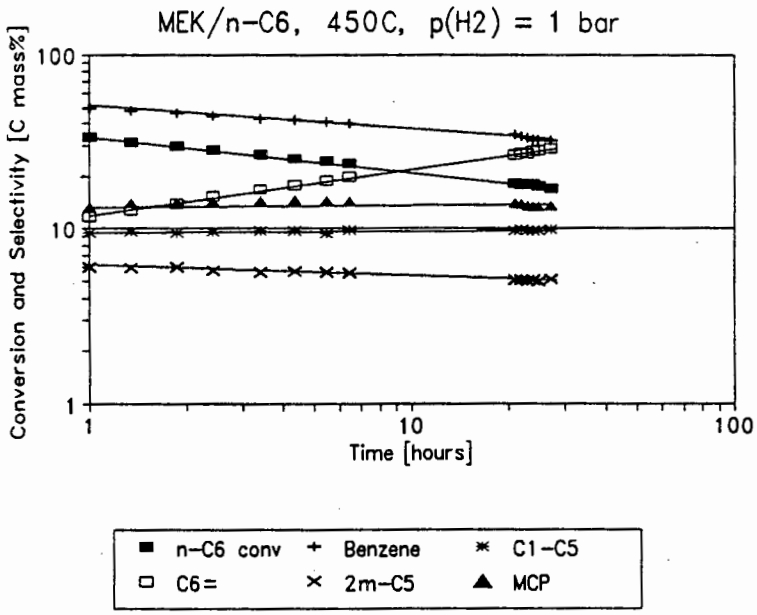

Figure 6-18 Plot of log selectivity and conversion as function of log time for co-feeding

3.4.4.1 The effect of different co-feeds on deactivation rates

The deactivation exponents of the gradients of plots of log rate as a function of log time on stream, for the co-feeding of various oxygenates with n-hexane, were obtained by linear regression. Fresh Pt/KL was used for each experiment which were performed at either 1 bar or 2 bar hydrogen partial pressure.

Within the bounds of experimental error it appears that the co-feeding of oxygenated compounds have a similar effect on the activity of Pt/KL. Any differences are not statisically significant. The deactivation exponents for different co-feeds at 1 bar and 2 bar hydrogen partial pressure are shown in Figure 6-19 and Figure 6-20 respectively. There is remarkable similarity between the different co-feeds. The largest decrease in the rate of benzene formation and n-hexane conversion is for MEK and the butyraldehydes at 1 bar. The molar ratio of MEK and CO to n-hexane was *ca.* 20% while for the other compounds it was *ca.* 14%. At both partial pressures of hydrogen benzene shows the greatest rate of decline. The hexene isomers increase with time on stream at 1 bar while at 2 bar the n-hexane isomers (MCP and methylpentanes) increase with time on stream, as expected. The deactivation exponent for n-hexane conversion, hydrogenolysis products and benzene is greater at 1 bar than at 2 bar.

The decline in activity during co-feeding is most likely caused by competitive (or preferential) adsorbtion of an oxygenated species, *e.g.* CO, on platinum active sites. The recovery observed after co-feeding was terminated is also supporting evidence for this hypothesis. If deactivation was caused by increased coking then no recovery would be expected after co-feeding was terminated.

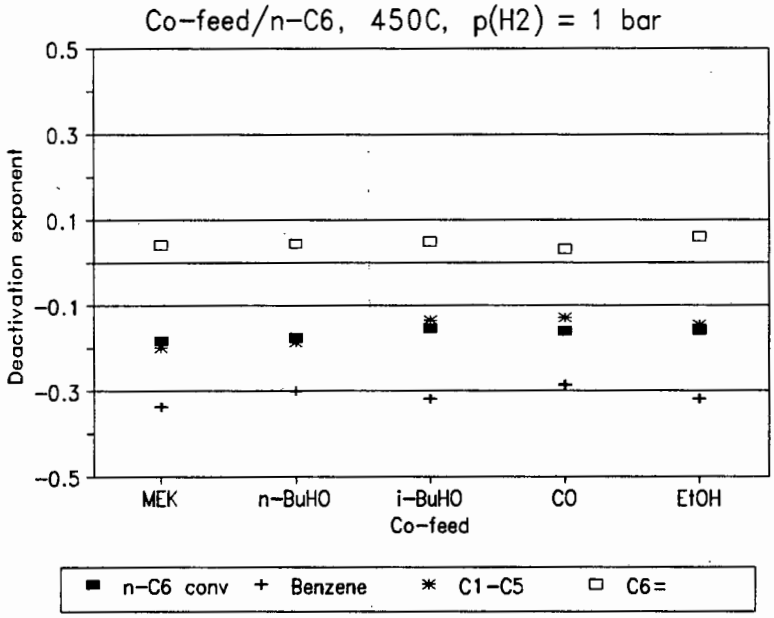

Figure 6-19 Effect of different co-feeds on the deactivation exponent

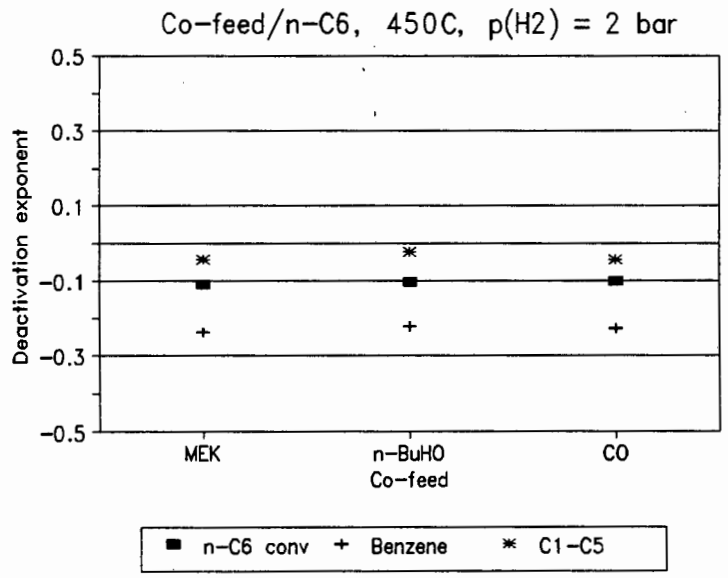

Figure 6-20 Deactivation exponents at 2 bar hydrogen partial pressure for the co-feeding of oxygenates with n-hexane at 450°C

The CO produced by the co-feeding of oxygenated compounds was ca. 50% ± 7% (mole % of the co-feed) at 1 bar hydrogen partial pressure (see Table 6-2). The amount of CO evolved at 2 bar hydrogen partial pressure was 30% ± 5% (expressed as mole % of the co-feed) for the different co-feeds.

The differences in the deactivation exponents for co-feeding of oxygenates with n-hexane to the exponents for deactivation of n-hexane only (Section 3.2) are summarized in Table 6-16 at different partial pressures of hydrogen.

Table 6-16 Deactivation exponents over Pt/KL at 450°C

	n-Hexane only			Co-feeding with n-hexane		
Pressure	1 bar	3 bar	6 bar	1 bar	2 bar	6 bar
n-C_6 conv	-0.12	-0.08	-0.07	-0.15	-0.10	-0.04
Benzene	-0.07	-0.06	0.11	-0.30	-0.22	-0.09
C_1-C_5	-0.20	-0.19	-0.19	-0.14	-0.04	-0.03
Hexenes	0.06	n/a	n/a	0.05	n/a	n/a

There is a reasonably close corresponance between the deactivation exponents for the co-feeding and for deactivation during the n-hexane only runs. The largest discrepancy is for benzene, which declines much more severely during co-feeding than during normal n-hexane runs. Thus the co-feeding of oxygenates with n-hexane must inhibit the pathway for the formation of benzene more than the other pathways. Both coke and the co-feed are expected to adsorb on platinum sites and hence should simply decrease the number of available sites. This could result in a similar deactivation effect. However, an hypothesis can be proposed whereby the electronegative oxygen group has an additional electronic effect which adversely effects the formation of benzene. The high selectivity to benzene on Pt/KL is variously attributed to electronic interactions, that stabilize small platinum clusters in the L zeolite structure. Thus local electronic effects may have

a large role to play with regard to the high selectivity to benzene observed on Pt/KL catalysts. The oxygenated co-feed may interact with the platinum clusters in such a way that a strong platinum-oxygen bond does not form, but rather a weak interaction predominates. Thus a strong interaction, which would lead to sintering of the platinum is absent (see Section 3.3.3). The weak interaction of the oxygenated species with platinum may be sufficient to perturb its electronic properties and result in the inhibition of the pathway for the formation of benzene. This is discussed further in Section 3.4.6

3.4.4.2 Deactivation rates at higher pressures of hydrogen

There is a remarkable similarity between the deactivation exponents for the co-feeding of n-butyraldehyde and MEK with n-hexane (Figure 6-21 and Figure 6-22). The amount of carbon monoxide evolved is also similar in both cases (at 1 bar and 2 bar). For all pressures benzene undergoes the greatest deactivation rate during co-feeding.

At 6 bar hydrogen partial pressure (Figure 6-21 and Figure 6-22) the effect of the co-feeding appears to be less than at lower pressure, as seen by the deactivation exponents being closer to zero (Table 6-16). However, this may be misleading, due to the discontinuous nature of the change in selectivity during co-feeding at 6 bar. As the partial pressure of hydrogen increases the exponents decrease, but with the effect decreasing as the pressure increases.

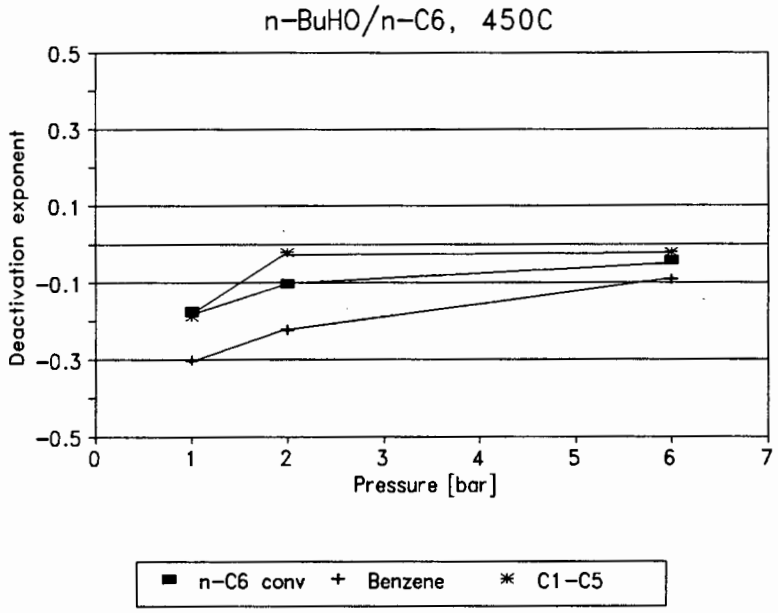

Figure 6-21 The effect of hydrogen partial pressure for the co-feeding of n-butyraldehyde with n-hexane on the deactivation exponents

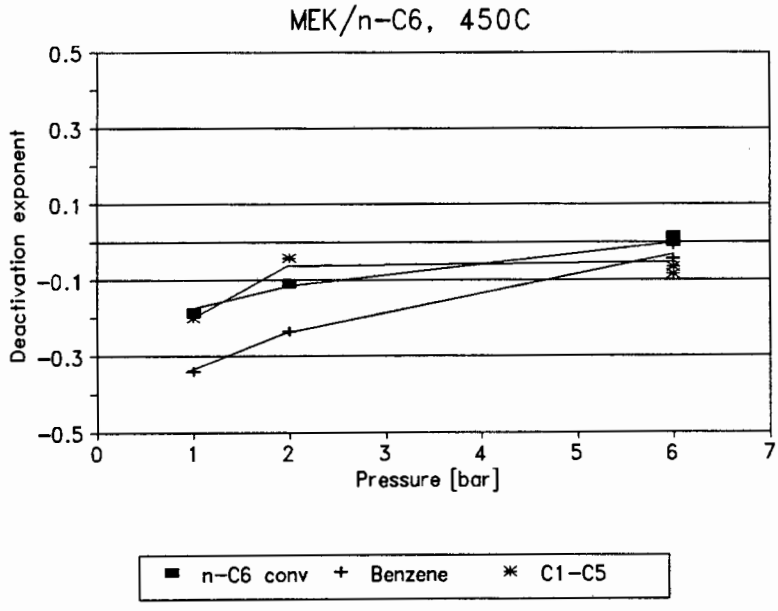

Figure 6-22 Effect of hydrogen partial pressure for the co-feeding of MEK with n-hexane on the deactivation exponent

3.4.4.3 Effect of amount co-fed on deactivation rates

A clear increase in the rate of deactivation with increase in the the molar amount of ethanol co-feed is observed. The exponent for the hexene isomers remains constant at *ca.* 0.07 for the co-feeding series. Once again benzene shows the largest decrease. At low levels of the ethanol co-feed, *viz.* 1.8 mole% there is hardly any observable change in the n-hexane conversion or product selectivity. Thus it appears from these results that if the oxygenates could be lowered to about 2 mole% of the alkane feed, then the process could tolerate Fischer-Tropsch feed.

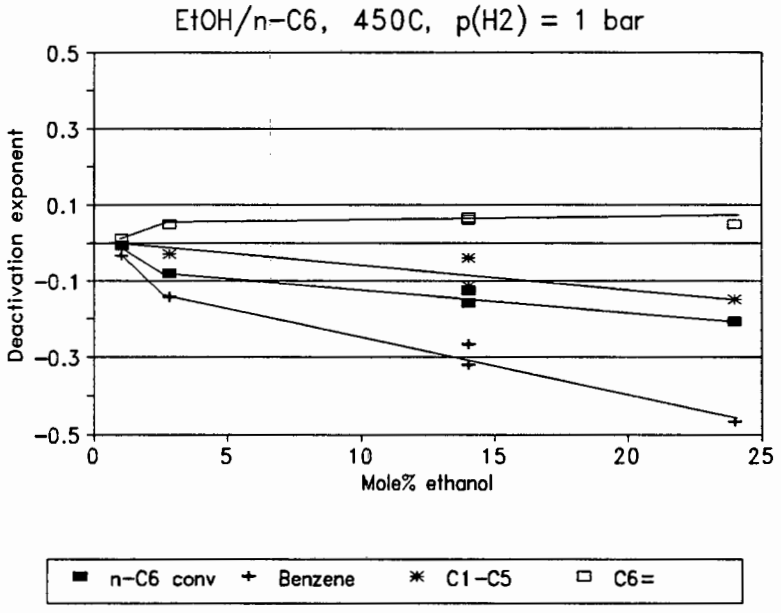

Figure 6-23 The effect of different amounts of ethanol co-fed with n-hexane on the deactivation exponent

The increase in deactivation rate with increase in the ethanol co-feed also tends to support the hypothesis of competitive adsorbtion on platinum sites. However, at a certain level of co-feed saturation coverage of platinum sites should occur, after which the decline in activity should be less. In these experiments there appears to be a linear correlation between the molar ratio of the co-feed and the rate of decline in activity. This does not support the saturation concept. However, higher levels of ethanol may be needed to reach saturation coverage.

3.4.5 Summary of the co-feeding of oxygenates

The different oxygenates, co-fed with n-hexane, cause a similar effect with regard to decrease in n-hexane conversion and changes in product selectivity. The effect is directly related to the molar ratio of co-feed:n-hexane as well as the partial pressure of hydrogen. Increased hydrogen partial pressure (6 bar) strongly suppresses the deactivating effects of the co-feed. However, a deactivating effect is still observed at this partial pressure of hydrogen. Furthermore the yield of benzene is lower and hence the best operating pressure appears to be at 2 bar to 3 bar.

The deactivation is not permanent, however, and almost full recovery occurs after termination of co-feeding. This is especially true for co-feeding at 6 bar hydrogen partial pressure. The co-feeding appears to mainly inhibit the aromatization pathway and the hydrogenolysis pathway to a lesser extent. This results in an increase in C_6 products. These C_6 products can still undergo aromatization, but the residence time of the feed in the reactor will have to be increased.

The reason for the inhibition of the aromatization pathway is postulated as being due to adsorption or interaction of carbon monoxide or carbonyl compounds with the platinum clusters. Thus the electronic state of the platinum cluster is altered and hence the reactivity towards benzene formation. The carbonyl compounds are expected to interact with platinum via an electropostive carbon atom adjacent to an oxygen atom (Section 1.8.3.1). The interaction is weak (Section 1.8.3.3), however, thus the effect is easily reversible when the flow of the co-feed is terminated. Sulphur-containing compounds interact much more strongly with platinum clusters due to the presence of d-orbitals on sulphur. Due to the weak interaction of the carbonyls with platinum, the platinum-support interaction is not weakened sufficiently to cause sintering. The absence of sintering is confirmed by TEM analysis. Water, which can only interact with platinum via relatively weak hydrogen bonds, has a negligible effect.

Chapter 4

Concluding Remarks

4 Concluding Remarks

Pt/KL was found to be a stable and active catalyst for the aromatization of n-hexane. Benzene and C_1-C_5 hydrogenolysis products were formed via irreversible reaction pathways. Hexene isomers and isomerized hexanes were converted to benzene at high n-hexane conversions. The selectivity to benzene and hydrogenolysis products increased with increase in reaction temperature. The maximum selectivity to benzene was at 2 bar hydrogen partial pressure. Higher partial pressures of hydrogen inhibit the aromatization reaction. Hydrogenolysis products increase with increase in hydrogen partial pressure. Thus to maximize benzene selectivity relative to hydrogenolysis, the Pt/KL catalyst must be operated at low partial pressures of hydrogen (1 bar - 2 bar) and low temperature (*ca.* 400°C). As the hydrogenolysis products are thermodynamically favoured over benzene, the Pt/KL catalyst must be operated far from equilibrium conditions. At 1 bar the catalyst undergoes deactivation due to coke formation. Hexene isomers are major reaction products at 1 bar hydrogen partial pressure and are known to easily form coke precursors. Increasing the hydrogen partial pressure results in less rapid deactivation. At 6 bar the Pt/KL catalyst is very stable with regard to conversion and product selectivity with time on stream. Benzene selectivity and yield are low at 6 bar hydrogen pressure. Terminal hydrogenolysis is more prevalent at low pressure (1 bar to 2 bar). At 6 bar the selectivity to hydrogenolysis increases but terminal hydrogenolysis (methane selectivity) is heavily suppressed. Lower reaction temperatures (< 400°C) also result in less terminal hydrogenolysis.

Sintering of Pt/KL occurs to a limited extent when the reaction temperature is below 475°C for both n-hexane feeds and oxygenated feeds. Oxygenated feeds do not not result in significant sintering. High reaction temperatures (500°C to 550°C) do, however, result in sintering of platinum clusters. Sintering alters the reactivity of the platinum clusters as well as reducing the number of activity sites. Hence, there is a decrease in n-hexane conversion as well as changes in product selectivity that is distinct from deactivation caused by coking.

The Pt/KL catalyst deactivates during the n-hexane aromatization reaction due to coke formation. The deactivation is most prevalent at low hydrogen partial pressures (1 bar). At hydrogen partial pressures of 6 bar this deactivation is slight. The deactivated Pt/KL catalyst can be succesfully regenerated by calcination in oxygen containing atmospheres. However, it is important to make sure that overheating of the catalyst does not occur during calcination. Overheating will lead to sintering of platinum clusters. The deactivation can be modelled successfully by use of an exponential rate function of the form: $r = A_o t^n$.

The reaction products of the oxygenates fed over Pt/KL can be divided into hydrogenation products and hydrogenolysis products. Hydrogenation leads to the formation of an alkane and water. Hydrogenolysis leads to the formation of methane, carbon monoxide and C_2-C_3 alkanes (depending on the oxygenate feed). The hydrogenation reaction is suppressed relative to hydrogenolsis with increase in reaction temperature for all oxygenates. The hydrogenation reaction is favoured by increase in hydrogen partial pressure. At 6 bar hydrogen partial pressure no carbon monoxide is observed in the product gas.

The co-feeding of oxygenated products with n-hexane causes a decrease in selectivity to benzene and hydrogenolysis products. The n-hexane conversion decreases as well. The magnitude of decline was found to be related to the amount of co-feed as well as the hydrogen partial pressure. Increase in hydrogen partial pressure resulted in less deactivation during co-feeding. Water and carbon monoxide, which are products of the reaction of oxygenates on Pt/KL, were co-fed with n-hexane as well. Water was found to have no observable effect on activity or product selectivities. Carbon monoxide caused a similar deaction effect to that observed for the other oxygenates. The deactivation caused by co-feeding of oxygenates could be modelled by an exponential rate function, similar to that for deactivation caused by coking. The deactivation exponents for n-hexane conversion and benzene formation were similar for all co-feeds. The deactivation exponents decreased with increase in hydrogen partial pressure.

The co-feeds appear to effect the aromatization pathway more strongly than other reaction pathways. This effect is proposed to be caused by interaction of carbonyl species, formed by hydrogenolysis reaction of oxygenates, with platinum clusters. The platinum clusters in Pt/KL are well know to be electron rich relative to platinum clusters dispersed on other supports such as silica. The carbon adjacent to the oxygen atom in the carbonyl group is proposed to interact with the platinum cluster, thus altering the electronic properties of the platinum. This results in lower selectivity to benzene (at similar n-hexane conversion levels) than would be expected. The carbonyl-platinum interaction is not strong enough to weaken the platinum-support interaction as this would lead to sintering. It is well known that strong sulphur-platinum bonding causes sintering of platinum clusters for Pt/KL catalysts poisoned by sulphur containing compounds. Water is presumed to interact with platinum by weak hydrogen bonding. This weak bonding is insufficient to alter the reactivity of platinum clusters. The use of FTIR spectroscopy to probe the nature of the proposed carbonyl-platinum interaction would be both interesting and revealing.

The deactivation caused by co-feeding is reversible as after co-feeding is terminated the catalyst returns to an activity similar to that expected had co-feeding not occured. The catalyst deactivated by co-feeding can also be regenerated by calcination in air, in a manner similar to that for catalysts deactivated by the n-hexane aromatization reaction.

The Pt/KL catalyst is not suitable for the aromatization of the C_6-C_8 cuts from heavy naphtha from crude oil as extensive (and expensive) hydrotreating to remove sulphur containing compounds must first be performed. This makes the process economically unfeasible. The Pt/KL catalyst may, however, find use for the aromatization of sulphur-free C_6-C_8 alkane products from the Fischer-Tropsch process as it is tolerant towards oxygenated impurities. In addition Pt/KL can aromatize alkenes, which cause rapid fouling of conventional bi-functional Pt-Re/Al_2O_3 reforming catalysts. High hydrogen pressure (6 bar) will provide maximum catalyst lifetime, but at the cost of increased yields of unwanted hydrogenolysis

products. Low hydrogen pressure (1 bar - 2 bar) will result in minimum selectivity to hydrogenolysis products, but will result in shortened catalyst cycle times due to deactivation by coke formation.

References

References

1. Weissermel K., Arpe H.-J., *Industrial Organic Chemistry*, 2nd ed., Verlagsgesellschaft mbH, Weinheim, Germany, 1993, p 333.

2. Szmant H.H., *Organic Building Blocks of the Chemical Industry*, John Wiley and Sons, New York, 1989, p 424.

3. Catalytica Inc., *Oxygenate Fuels: Challenge and Opportunity*, Multiclient Study Number 4190 Z, Catalytica Studies Division, Mountain View, CA, 1991.

4. *Informations Chimie*, 1990, **316**, p 143.

5. Olson D.H., Haag W.O., In *Structure-Selectivity Relationships in Xylene-Isomerization and Selective Toluene Disproportionation*, ACS Symposium Series 248, Whyte T.E., Jr., Ed., American Chemical Society, Washington, DC, 1984, p 275.

6. Hughes T.R., Jacobson R.L., Tamm P.W., In *Catalysis 1987*, J.W. Ward ed., Elsevier Science, Amsterdam, 1987, p 167.

7. D'Auria, J.H., Weiszmann J.A., Tieman W.C., *Proceedings*, UOP Division Technology Conference, UOP, Des Plaines, IL, 1980.

8. Jacques G., *Proceedings*, Symposium on Catalytic Reforming, Hydrotreating and Hydrocracking, Damascus, OPEC, Kuwait, 1981, p 122.

9. Bennett R.W., Peer R.L., Bakas S.T., NPRA, Annual Meeting, San Antonia, TX, 1988, Paper AM-88-65.

10. Chen N.Y., Garwood W.E., *Adv. Chem. Ser.*, 1973, **121**, p 575.

11. Chen N.Y., Yan T.Y., *Ind. Eng. Chem. Process Des. Dev.*, 1986, **25**, p 151.

12. Chen N.Y., Garwood W.E., Heck R.H., *Ind. Eng. Chem. Res.*, 1987, **26**, p 706.

13. Gosling C.D., Wilcher F.P., Sullivan L., Mountford R.A., *Hydrocarbon Process.*, 1991, December, p 69.

14. Saito S., Hirabayashi K., Shibata S., Kondo T., Adachi K., Inoue S., *NPRA Annual Meeting*, New Orleans, LA, March 22-24, 1992, Paper AM-92-38.

15. Doolan P.C., Pujado P.R., *Hydrocarbon Process.*, 1989, September, p 72.

16. Mowry J.R., Anderson R.F., Johnson J.A., *Oil Gas J.*, 1985, December 2, p 128.

17. Guisnet M., Gnep N.S., *Appl. Catal.*, **89**, 1992, p 1.

18. Hansen J.B., *A Short Description of the Topas Process from Haldor Topsoe A/S*, Haldor Topsoe A/S, Lyngby, Denmark, 1993.

19. Derouane E.G., In *Catalysis on Acids and Bases, Stud. Surf. Sci. Catal.*, Imelik B., Naccache C., Coudrier G., Ben Taarit Y., Vedrine J.C., Eds., Elsevier Science, Amsterdam, 1985, Vol. 20, p 221.

20. Mills G.A., Heinemann H., Milliken T.H., Oblad A.G., *Ind. Eng. Chem.*, 1953, **45**, p 134.

21. Tamm P.W., Mohr D.H., Wilson C.R., In *Catalysis 1987, Stud. Surf. Sci. Catal.*, Ward J.W. Ed., Elsevier Science, Amsterdam, 1988, Vol. 38, p 335.

22. HYSIM, Hyprotech Ltd., 1994, Ver. 2.40.

23. Bernard J.R., *Proceedings*, 5th International Conference on Zeolites, Naples, Ress L.V.C., Ed., Heyden, London, 1980, p 686.

24. Besoukhanova C., Breyesse M., Bernard J.R., Barthomeuf D., *Proceedings*, 7th International Congress on Catalysis Tokyo, 1980, Seiyama, T., Tanabe, K., Eds., Godansha/Elsevier Science, Tokyo/Amsterdam, 1981, p 1410.

25. Larsen G., Haller G.L., *Catal. Today*, 1992, **15**, p 431.

26. Gargarin S.V., Komarov V.S., Urbanovich I.I., Gintovt T.I., Teterin Y.A., In *Structure and Reactivity of Modified Zeolites, Stud. Surf. Sci. Catal.*, Jacobs P.A., Jaeger N.L., Jiru P., Kzansky V.B., Schultz-Ekloff G., Eds., Elsevier Science, Amsterdam, 1984, Vol. 18, p 345.

27. Lane G.S., Miller G.T., Modica F.S., Barr M.K., *J. Catal.*, 1993, **141**, p 465.

28. Sugimoto M., Katsuno H., Murakawa T., *Appl. Catal. A: General*, 1993, **96**, p 201.

29. Iglesia E., Baumgartner J.E., Price G.L., *J. Catal.*, 1992, **134**, p 549.

30. Nash R.J., Dry M.E., O'Connor C.T., *Appl. Catal. A: General*, 1995, **134**, p 285.

31. Meitzner G.D., Iglesia E., Baumgartner J.E., Huang E.S., *J. Catal.*, 1993, **140**, p 209.

32. Tennison S.R., Foster A.I., McCarroll J.J., Joyner R.W., *Prepr. ACS. Pet. Div.*, 1983, p 439.

33. Paal Z., Groeneweg H., Paal-Lukacs J., *J. Chem. Soc. Faraday Trans.*, 1990, **86**, p 3159.

34. Derouane E.G., Jullien-Lardot V., Davis R.J., Blom N.J., Hojlund-Nielsen P.E., In *New Frontiers in Catalysis, Stud. Surf. Sci. Catal.*, Guzci L., Solymosi F., Tetenyi P., Eds., Elsevier Science, Amsterdam, 1993, Vol. 75, p 1031.

35. Davis R.J., Derouane E.G., *Nature (London)*, 1991, **349**, p 313.

36. Davis R. J., Derouane E.G., *J. Catal.*, 1991, **132**, p 269.

37. Johnson I.D., Chu P., Kresge C.T., US Patent 5 008 481, 1991, assigned to Mobil Oil Corp.

38. Kinomoto Y., Watanabe S., Takahashi M., *Surf. Sci.*, 1991, **242**, p 538.

39. Parades Olivera P., Estin G.L., Castro E.A., Ariva A.J., *J. Mol. Struct.*, 1990, **210**, p 393.

40. Derouane E.G., Vanderveken D., *Appl. Catal.*, 1988, **45**, L15.

41. Blom N.J., Derouane E.G., EP 475 357, 1992, assigned to Haldor Topsoe A/S.

42. Germain J.E., *Catalytic Conversion of Hydrocarbons*, Academic Press, New York, 1969

43. Manninger I.,Xu X.L., Tetenyi P., Paal Z., *Appl. Catal.*, 1989, **51**, L7.

44. Tauster S.J., Steger J., *Mater. Res. Soc. Symp. Proc*, 1988, **111**, p 149.

45. Karpinski Z., Gandhi S.N., Sachtler W.M.H., *J. Catal.*, 1993, **141**, p 337.

46. Iglesia E., Baumgartner J.E., *Proceedings*, 9th International Zeolite Conference, Montreal, 1992, von Ballmoos R., Higgins J.B., Treacy M.M.J., Eds., Butterworth-Heinemann, Stoneham, MA, 1993, p 421.

47. Barrer R.M., Villiger H., *Z. Kristallogr., Kristallgeom., Kristallphys., Kristallchem.*, 1969, **128**, p 352.

48. Szostak R., *Handbook of Molecular Sieves*, Van Nostrand Reinhold, New York, 1992, p 274.

49. Meier W.M., Olson D.H., *Atlas of Zeolite Structure Types*, Butterworth Scientific Ltd., London, 1987, p 89.

50. Newsam J.M., Silbernagel B.G., Garcia A.R., Melchior M.T., Fung S.C., In *Structure-Activity Relationships in Heterogeneous Catalysis*, Elsevier Science, Amsterdam, 1991, p 211.

51. Hughes J.R., Buss W.C., Tamm P.W., Jacobson R.L., *Aromatization of Hydrocarbons over Platinum Earth Zeolites, Stud. Surf. Sci. Catal.*, Gates B.C. *et al.* (Eds.), Vol. 28, 1986, p 725.

52. Von Ballmoos R., Higgins J.B., *Collection of simulated XRD Powder Patterns for Zeolites*, Butterworth-Heinemann Ltd, New York, 2nd Ed., 1990, p 430S.

53. Ostgard D., Kustov L., Poeppelmeier K.R., Sachtler W.M.H., *J. Catal.*, 1992, **133**, p 342.

54. Anderson J.R., In *Structure of Metallic Catalysts*, Academic Press, New York, 1975, p 360.

55. Hughes T.R., Buss W.C., Tamm P.W., Jacobson R.L., *Proc. 7th Int. Zeolite Conf.*, Tokyo, Aug 17-22, 1986, Kodansha, Tokyo, Elsevier Science, Amsterdam, 1987, p 725.

56. Hicks R., Han W.-J., Kooh A.B., In *New Frontiers in Catalysis, Proc. 10th Int. Congr. on Catalysis*, 19-24 July, 1992, Budapest, Hungary, Elsevier Scientific Ltd., 1993, p 1042.

57. Besoukhanova C., Giudot J., Barthomeuf D., *J. Chem. Soc., Faraday Trans. 1*, 1981, **77**, p 1595.

58. Yashima P., Suzuki H., Hara N., *J. Catal.*, 1974, **33**, p 486.

59. Kooh A.B., Han W-J., Hicks R., *Catal. Lett.*, 1993, **18**, p 209.

60. Paal Z., Lun X.X., *Appl. Catal.*, 1988, **43**, L 1.

61. Kern-Talas E., In *Preparation of Catalysts IV*, Delmon B., Grange P., Jacobs P.A., Poncelet G., (Eds.), Elsevier, Amsterdam, 1987, p 689.

62. Bragin O.V., Karpinski Z., Matusek K., Paal Z., Tetenyi P., *J. Catal.*, 1979, **56**, p 219.

63. Rohrer J.C., Hurwitz H., Sinfelt J.H., *J. Phys. Chem.*, 1961, **65**, p 1458.

64. Pacheco M.A., Petersen E.E., *J. Catal.*, 1984, **86**, p 75.

65. Sharma S.B., Ouraipryvan P., Nair H.A., Balaraman P., Root W., Dumesic J.A., *J. Catal.*, 1994, **150**, p 234.

66. Sinfelt J.H., Hurwitz H., Rohrer J.C., *J. Phys. Chem.*, 1960, **64**, p 892.

67. Sinfelt J.H., *Catalysis, Science and Technonlogy*, Anderson J.R., Boudart M. (Eds.), Springer Verlag, Berlin, 1981, Vol. 1, Chap. 5, p 257.

68. Zaera F., Godbey D., Somorjai G.A., *J. Catal.*, 1986, **101**, p 73.

69. Moretti G., Sachtler W.M.H., *J. Catal.*, 1989, **116**, p 350.

70. Vaarkamp M., Dijkstra P., van Grondelle J., Miller J.T., Modica F.S., Konisberger D.C., van Santen R.A., *J. Catal.*, 1995, **151**, p 330.

71. Sharma S.B., Miller J.T., Dumesic J.A., *J. Catal.*, 1994, **148**, p 198.

72. Tauster S.J., Steger J., *J. Catal.*, 1990, **125**, p 387.

73. Iglesia E., Baumgartner J.E., *Proc. 9th Int. Zeolite Conf.*, Montreal, July, 1992

74. Kopelman R., *Science*, 1988, **241**, p 1620.

75. Hughes R., *Deactivation of Catalysts*, Academic Press, London, 1984, Chap. 2, p 17.

76. Iglesia I., Baumgartner, *New Frontiers in Catalysis, Proc. 10th Int. Congr. on Catalysis*, 19-24 July, 1992, Budapest, Hungary, Elsevier Ltd., Amsterdam, 1993, p 993.

77. Gallezot P., *J. Chim. Phys.*, 1981, **78**, p 881.

78. Bergeret G., Gallezot P., in *Proc. 7th Int. Congr. on Catalysis*, Berlin 1984, Dechema, Frankfurt, 1984, Vol. 5, p 659.

79. Butt J.B., Joyal C.L.M., Megiris C.E., in *Catalyst Deactivation*, Petersen E.E. and Bell A.T. eds., Marcel Dekker Inc., New York, 1987, Chapter 1, p 3.

80. Herrington E.F.G., Rideal E.K., *Trans. Faraday Soc.*, 1944, **40**, p 505.

81. Maxted E.B., *Adv. Catal.*, 1951, **3**, p 129.

82. Dorling T.A., Eastlake M.J., Moss R.L., *J. Catal.*, 1969, **14**, p 23.

83. Schlatter J., Boudart M., *J. Catal.*, 1972, **14**, p 482.

84. Manogue W.H., Katzer J.R., *J. Catal.*, 1974, **32**, p 166.

85. Onal I., Butt J.B., *J. Chem. Soc. Faraday Trans. I*, 1982, **8**, p 1887.

86. Damiani D.E., Butt J.B., *J. Catal.*, 1984, **93**, p 132.

87. Rabo J.A., Schomaker V., Pickert P.E., in *Proceedings of the 3rd Int. Congr. on Catalysis*, Amsterdam 1964, North Holland, Amsterdam , 1965, Vol. 2, p 1264.

88. Gallezot P., Datka J., Massardier J., Primet M., Imelik B., in *Proc. 6th Int. Congr. on Catalysis*, Bond G.C. *et al.* Eds., The Chemical Society, London, 1977, p 144.

89. Besoukhanova C., Breyesse M., Bernard J.R., Barthomeuf D., in *Catalyst Deactivation*, Delmon D. and Froment G. Eds., Elsevier, Amsterdam, 1980, p 201.

90. McVicker G.B., Lao J.K., Ziemiak J.J., Gates W.E., Robbins J.L., Treacy M.M.J., Rice S.B., Vanderspurt T.H., Cross V.R., Ghosh A.K., *J. Catal.*, 1993, **143**, p 48.

91. Kao J.L., McVicker G.B., Treacy M.M.J., Rice S.B., Robbins J.L., Gates W.E., Ziemiak J.J., Cross V.R., Vanderspurt T.H., In *New Frontiers in Catalysis, Proc. 10th Int. Congr. on Catalysis*, Guczi L. *et al.* Eds., 19-24 July, 1992, Budapest, Hungary, Elsevier Ltd., Amsterdam, 1993, p 1019.

92. Bartholomew C.H., Agrawal P.K., Katzer J.R., *Adv. Catal.*, 1982, **31**, p 135.

93. Fukunaga T., Ponec V., *J. Catal.*, 1995, **157**, p 550.

94. Guenin M., Breysse M., Frety R., Tifouti K., Marecot P., Barbier J., *J. Catal.*, 1987, **105**, p 144.

95. Biloen P., Dautzenberg F.M., Sachtler W.M.H., *J. Catal.*, 1977, **50**, p 77.

96. Barbier J., Marecot P., Tifouti L., Guenin M., Frety R., *Appl. Catal.*, 1985, **19**, p 375.

97. Zubova I.E., Rabina P.D., Pavlova N.Z., Kuznetsov L.D., Chudinov M.G., Le Kong S., *Kinet. Catal.*, 1974, **15**, p 1118.

98. Besoukhanova C., Breysse M., Bernard J.R., Barthomeuf D., *Stud. Surf. Sci. Catal.*, Elsevier Ltd., Amsterdam, 1980, **18**, p 201.

99. Lieske H., Lietz G., Spindler H., Volter J., *J. Catal.*, 1983, **81**, p 8.

100. Fiedorow R.M.J., Wanke S.E., *J. Catal.*, 1976, **43**, p 34.

101. Straguzzi G.I., Aduriz H.R., Gigola C.E., *J. Catal.*, 1980, **66**, p 171.

102. Foger K., Jager H., *J. Catal.*, 1985, **92**, p 64.

103. Wilson G.R., Hall W.K., *J. Catal.*, 1972, **24**, p 306.

104. Wanke S.E., Szymura J.A., Yu T.T., in *Catalyst Deactivation*, Petersen E.E., Bell A.T. eds., Marcel Dekker Inc., New York, 1987, Chapter 3.

105. Hughes J.R., Houston R.J., Sieg R.P., *Ind. Eng. Chem. Proc. Des. Dev.*, **1**, 1962, p 96.

106. Herrmann R.A., Adler S.F., Goldstein M.S., Debaun R.M., *J. Phys. Chem.*, 1961, **65**, p 2189.

107. Wanke S.E., Flynn P.C., *Catal. Rev.*, 1975, **12**, p 93.

108. Mills G.A., Weller S., Cornelius E.B., *Actes du Deuxieme Congres International de Catalyse, Paris, 1960*, Technip, Paris, 1961, p 2221.

109. Ruckenstein E., Pulvermacher B., *J. Catal.*, 1973, **29**, p 224.

110. Flynn P.C., Wanke S.E., *J. Catal.*, 1974, **34**, p 390.

111. Wanke S.E., in *Process in Catalyst Deactivation*, Figueiredo J.L., Ed., Martinus Nijhoff, The Hague, 1982 p 315.

112. Lee H.H., Ruckenstein E., *Catal. Rev.*, 1983, **25**, p 475.

113. Ruckenstein E., Malhotra M.L., *J. Catal.*, 1976, **41**, p 303.

114. Birke P., Engels S., Becker K., Nuebauer H.D., *Chem. Techn.*, 1979, **31**, p 473.

115. Lietz G., Lieske H., Spindler H., Hanke W., Volter J., *J. Catal.*, 1983, **81**, p 17.

116. Sugimoto M., Murakawa T., Hirano T., Ohashi H., *Appl. Catal.: A General*, 1993, **95**, p 257.

117. Sugimoto M., Katsuno H., Hayasaka T., Hirasawa K-I., Ishikawa N., *Applied Catalysis A: General*, 1993, **106**, p 9.

118. Parera J.M., Beltramini J.N., Querini C.A., Martinelli E.E., Churin E.J., Aloe P.E., Figoli N.S., *Proc. 8th Int. Congr. Catal.*, Berlin, Vol. 2, 1984, Verlag Chemie, Weinheim, 1984, p 593.

119. Foger K., Jaeger H., *Appl. Catal.*, 1989, **56**, p 137.

120. Maire G.L.C., Garin F.G., In *Catalysis Science and Technology*, Anderson J.R., Boudart M., Eds., Springer-Verlag, Berlin, Vol. 6, 1984, p 165.

121. Somorjai G.A., in *Catalysis Design, Progress and Perspectives*, John Wiley and Sons, New York, 1987, p 11.

122. Gates B.C., *Catalytic Chemistry*, John Wiley and Sons Inc., New York, 1992, p 369.

123. Somorjai G.A., *Proc. 8th Int. Congr. Catal.*, Berlin, Vol. 1, 1984, p 113.

124. Kemball C., *Advan. Catal.*, 1959, **11**, p 223.

125. Anderson J.R., Baker B.G., *Proc. Roy. Soc. Ser.*, 1963, **A 271**, p 402.

126. Barron Y., Cornet D., Maire G., Gault F.G., *J. Catal.*, 1963, **2**, p 152.

127. Maire G., Plouidy G., Prudhomme J.C., Gault F.G., *J. Catal.*, 1965, **4**, p 556.

128. Barron Y., Maire G., Muller J.M., Gault F.G., *J. Catal.*, 1966, **5**, p 428.

129. Gault F.G., *Acad. Sci. Paris*, 1957, **245**, p 1620.

130. Anderson J.R., Avery N.R., *J. Catal.*, 1966, **5**, p 446.

131. Boudart M., Ptak L.D., *J. Catal.*, 1970, **16**, p 90.

132. Muller J.M., Gault F.G., *J. Catal.*, 1972, **24**, p 361.

133. Anderson J.R., Shimoyama Y., *Proc. Int. Conf. Catal. 5th*, Miami, Hightower, 1973, **1**, p 695.

134. Shephard F.E., Rooney J.J., *J. Catal.*, 1964, **3**, p 129.

135. Anderson J.R., Shimoyama Y., *Proc. 5th Int. Congr. Catal.*, Miami, Hightower, Vol. 1, 1973, p 695.

136. Paal Z., Tetenyi P., *J. Catal.*, 1973, **30**, p 350.

137. Paal Z., Tetenyi P., *Acta. Chim. Acad. Sci. Hung.*, 1968, **54**, p 175.

138. Kazanskii B.A., In *Mechanisms of Hydrocarbon Reactions, A Symposium*, Marta F., Kallo D., (Eds.), Akademiai Kiado, Budapest, 1975, p 26.

139. Rozanov V.V., Sklyarov A.V., *Kinet. Katal.*, 1978, **19**, p 1533.

140. Zimmer H., Rozanov V.V., Sklyarov A.V., Paal Z., *Appl. Catal.*, 1982, **2**, p 51.

141. Paal Z., Tetenyi P., *Acta. Chem. Acad. Sci. Hung.*, 1968, **55**, p 273.

142. Rozengart M.I., Mortikov E.S., Kazanskii B.A., *Dokl. Akad. Nauk. SSSR*, 1966, **166**, p 619.

143. Bragin O.V., Karpinski Z., Matusek K., Paal Z., Tetenyi P., *J. Catal.*, 1979, **56**, p 219.

144. Mitrofanova A.N., Boronin V.S., Poltorak O.M., *Vest. Mosk. Univ. Ser. II, Khim.*, 1966, **5**, p 40.

145. Mitrofanova A.N., Boronin V.S., Poltorak O.M., *Mosk. Univ. Ser. II, Khim.*, 1967, **1**, p 95.

146. Poltorak O.M., Boronin V.S., *Zh. Fiz. Khim.*, 1966, **40**, p 2671.

147. Boudart M., Aldag A., Benson J.E., Dougharty A.N., Harkins Girvin C., *J. Catal.*, 1966, **6**, p 92.

148. Maurel R., Leclercq G., Leclercg L., *Bull. Soc. Chim. Fr.*, 1972, p 491.

149. Boudart M., Aldag A., Ptak L.D., Benson J.E., *J. Catal.*, 1968, **11**, p 35.

150. Maat H.J., Moscou L., *Proc 3^{d} Inter. Congr. Catal. Amsterdam (1964)*, North Holland Pub. Co., Amsterdam, 1965.

151. Dartigues J.M., Chambellan A., Corolleur S., Gault F.G., Renouprez A., Moraweck B., Bosch-Giral P., Dalmai-Imelik G., *Nouv J. Chim.*, 1979, **3**, p 591.

152. Gingerich K.A., *Faraday Symp. Roy. Soc. Chem.*, 1980, **14**, p 109.

153. Cotton F.A., Wilkinson G., *Advanced Inorganic Chemistry*, 4th ed., Wiley and Son Ltd., New York, 1980, p 10.

154. Baetzold R.C., *J. Phys. Chem.*, 1978, **82**, p 738.

155. Gingerich K.A., Shim I., Grupta S.K., Kingcade J.E., Surf. Sci., 1985, **156**, p 495.

156. Stakheev A.Y., Shipiro E.S., Jaeger N.I., Schultz-Ekloff G., *Catal. Lett.*, 1995, **32**, p 147.

157. Vannice M.A., *Catalytic Activation of Carbon Monoxide on Metal Surfaces*, In *Catalysis Science and Technology*, Anderson J.R., Boudart M. Eds., Springer-Verlag, Berlin, 1982, Vol. 3, p 140.

158. Jorgensen W.L., Salem L., in *The Organic Chemist's Book of Orbitals*, Academic Press, New York, 1973.

159. Blyholder G., Allen M.C., *J. Am. Chem. Soc.*, 1969, **91**, p 3158.

160. Jones L.H., *J. Mol. Spectroscopy*, 1962, **9**, p 130.

161. Broden G., Rhodin T.N., Brucker C., Benbrow R., Hurych Z., *Surface Sci.*, 1976, **59**, p 593.

162. Doyen G., Ertl G., *Surface Sci.*, 1974, **43**, p 197.

163. Froitzheim H., Hopster H., Ibach H., Lewald S., *Appl. Phys.*, 1977, **13**, p 147.

164. Hopster H., Ibach H., *Surface Sci.*, 1978, **77**, p 109.

165. Larsen G., Haller G., *Catal. Lett.*, 1993, **17**, p 127.

166. Stakheev A.Y., Shipiro E.S., Jaeger N.I., Schultz-Ekloff G., *Catal. Lett.*, 1995, **34**, p. 293.

167. Kappers M.J., van der Maas J.V., *Catal. Lett.*, 1991, **10**, p 365.

168. Kustov L., Ostgard D., Sachtler W.M.H., *Catal. Lett.*, 1991, **9**, p.121

169. Calabrese J.C., Dahl L.F., Chini P., Longoni G., *J. Am. Chem. Soc.*, 1974, **96**, p 2614.

170. Roundhill D.M., *Comprehensive Coordination Chemistry*, Vol. 5, Wilkinson G. ed., Pergamon Press Ltd., Oxford, 1987, p 351.

171. Kundig E.P., McIntosh D., Moskovits M., Ozin G.A., *J. Am. Chem. Soc.*, 1973, **95**, p 7234.

172. Vaarkamp M., Miller J.T., Modica F.S., Lane G.S., Koningsberger D.C., *J. Catal.*, 1993, **138**, p 675.

173. Guy Opren A., Brammer L., Allen F.H., Kennard O., Watson D.G., Taylor R., *J. Chem. Soc. Dalton Trans.*, 1989, s1.

174. Sachtler W.M.H., Zhang G., Stakheev A.Y., Feeley J.S., *New Frontiers in Catalysis, Stud. Surf. Sci. Catal.*, Vol. 75, Guczi L. *et al.* Eds., Elsevier Ltd., Amsterdam, 1993, p 271.

175. Dong J-L., Zhu J-H., Xu Q-H., *Appl. Catal. A: General*, 1994, **112**, p 105.

176. Hathaway P.E., Davis M.E., *J. Catal.*, 1989, **116**, p 263.

177. Chow M., Park S.H., Sachtler W.M.H., *Appl. Catal.*, 1985, **19**, p 349.

178. Chen H-W., Chen C-S., *Catal. Lett.*, 1996, **39**, p 39.

179. Emmett P.H., Brunauer S., *J. Am. Chem. Soc.*, 1937, **59**, p 310.

180. Benson J.E., Boudart M., *J. Catal.*, 1965, **4**, p 704.

181. Prasad J., Murthy K.R., Menon P.G., *J. Catal.*, 1978, **52**, p 515.

182. Menon P.G., Froment G.F., *Appl. Catal.*, 1981, **1**, p 31.

183. Menon P.G., Froment G.F., *J. Catal.*, 1979, **59**, p 138.

184. Kip B.J., Duivenvoorden F.B.M., Koningsberger D.C., Prins R., *J. Catal.*, 1987, **105**, p 26.

185. Vaarkamp M., Grondelle J.V., Miller J.T., Sajkowski D.J., Modica F.S., Lane G.S., Gates B.C., Koningsberger D.C., *Catal. Lett.*, 1990, **6**, p 369.

186. Mielczarski E., Bong Hong S., Davis R.J., Davis M.E., *J. Catal.*, 1992, **134**, p 359.

187. Larsen G., Haller G., *Catal. Lett.*, 1989, **3**, p 103.

188. Hathaway P.E., Davis, M.E., *J Catal.*, 1989, **119**, p 497.

189. Han W.J., Kooh A.B., Hicks R.F., *Catal. Lett.*, 1993, **18**, p 193.

190. Lane G.S., Modica F.S., Miller J.T., *J. Catal.*, 1991, **129**, p 145.

191. Ehwald H., Leibnitz U., *Catal. Lett.*, 1996, **38**, p 149.

192. Miller J.T., Meyers B.L., Modica F.S., Lane G.S., Vaarkamp M., Koningsberger D.C., *J. Catal.*, 1993, **143**, p 395.

193. Modica S., Miller J.T., Meyers B.L., Koningsberger D.C., *Catal. Today*, 1994, **21**, p 37.

194. M'Kombe C., MSc Thesis, *Incorporation of Platinum onto Zeolite KL for Aromatization Reactions*, University of Cape Town, 1994.

195. Schnitzler A., Private communication, 1995.

196. Reid R.C., Prausnitz J.M., Poling B.E., *Properties of Gases and Liquids*, 4th Ed., McGraw-Hill Book Company, New York, 1987.

197. *Perry's Chemical Engineering Handbook*, 1988, p 3-101.

198. Weitkamp J., In *Innovation in Zeolite Materials Science*, Grobet P.J. *et al.* (Ed.), Elsevier Science Publishers B.V., Amsterdam, 1988, p 515.

199. Karagozler A.E., Simpson C.F., *J. Chromatogr.*, 1978, **150**, p 329.

200. Maire G.L.C., Garin F.G., In *Catalysis Science and Technology*, Anderson J.R., Bourdart M. (eds.), Springer-Verlag, Berlin, 1984, Vol. 6, Chap. 3, p 167.

201. Karge H.G., in "*Introduction to Zeolite Science and Technology*", van Bekkumm H., Flanigen E.M., Jansen J.C., Eds., Elservier Ltd., Amsterdam, 1991, Chap. 4, p 531.

202. Voorhies A., *Ind. Eng. Chem.*, **37**, 1945, p 318.

203. Ruderhausen C.G., Watson C.C., *Chem. Eng. Sci.*, **3**, 1954, p.110.

204. Eberly P.H., Kimberlin C.N., Miller W.H., Drushel H.V., *Ind. Eng. Proc. Des. Dev.*, **7**, 1968, p 67.

205. Dry M.E., private communication, 1996.

Appendices

Appendices

A.1 Calculations

A.1.1 Selectivity

Selectivity (S) to product$_i$ is defined as the carbon mass% of product$_i$ in the total products. For the feeding of n-hexane, all compounds (except n-hexane) are considered products. However, n-hexane is considered a product in the feeding of 1-hexene (whereas in this case 1-hexene is not considered a product).

$$S_i = (\text{carbon mass product}_i / \text{carbon mass of all products}) \times 100$$

A.1.2 Conversion

Conversion (X) of the feed is the mass percentage of feed converted to products and is determined on a carbon mass basis:

$$X = (\text{mass feed in} - \text{mass feed out})/(\text{mass feed in}) * 100$$

A.1.3 Feed flowrates

The flowrates (Fr), in ml/min, of feed from the saturators is calculated assuming full saturation of the feed in the gas stream:

$$Fr_i = (Vp_i / (\text{total pressure} - Vp_i)) * \text{Flowrate of carrier gas through saturator}$$

Vp_i : Vapour pressure of feed$_i$ in saturator.

As the vapour pressure of the organic feeds, as a result of the saturator temperatures, were much smaller than the ambient pressure of 1 bar (*ca.* 15 times)

the equation can be simplified to:

$$Fr_i = (Vp_i / (\text{total pressure})) * \text{Flowrate of carrier gas through saturator}$$

An error of *ca.* 7% is introduced by this approximation. The molar flowrates of the feed are calculated by use of the ideal gas equation.

A.1.4 Product flowrates

The flowrate of products was calculated relative to the flowrate of the internal standard, dimethyl ether (DME). A response factor, R_f, takes into account the different relative response of the flame ionization detector for alkanes and DME. For alkanes a value of 0.70 was used. Thus for product$_i$ the following relationship was used:

$$Fr_i = Fr_{DME} * R_f * area_i / area_{DME}$$

$R_f(n\text{-}C_6/DME) = 0.70$

$area_i$ = area of product i on GC trace

$area_{DME}$ = area of DME on GC trace

Fr_{DME} in g/s

The molar flowrate is determined for each product by dividing by the molar mass for that product. The carbon mass flowrate is calculated as the mass of carbon per unit time, *i.e.* dividing the mass flowrate by the carbon mass in the molecule (for hexane 6 x 12.011 = 72.066 g/mol).

A.1.5 Mass balances

The mass balance was determined relative to the flowrate of DME for the feed and products on a carbon mass basis.

$$\text{mass balance} = ((\text{mass feed} - \text{mass out})/ \text{mass feed}) * 100$$

A.2 Thermodynamic calculations

The thermodynamic equlibrium calculations were made in two different manners, by the use of the Hysim (ver. 2.50) computer program as well as by use of the relevant thermodynamic equations.

A.2.1 Thermodynamic equations

The data used in thermodynamic equations was obtained from Taubert (1987) and the the Gibbs free energy calculated by the following relationships. The Van't Hoff approximation of constant heat capacity, C_p, was found to be valid (Figure A-1).

basis: n-hexane $C_6H_{14} \rightarrow C_6H_6 + 4H_2$

1-hexene $C_6H_{12} \rightarrow C_6H_6 + 3H_2$

For n-hexane:

$$\Delta_r G = \Delta_f G_{benzene} + 4\Delta_f G_{hydrogen} - \Delta_f G_{n\text{-}hexane}$$

$$\Delta_f G_{hydrogen} = 0 \text{ kJ/mol}$$

$$RT\ln K_p = -\Delta_r G$$

$$\Delta_r G = \Delta_r H - T\Delta_r S$$

$$\Delta_r S = \Sigma S_{products} - \Sigma S_{reactants}$$

$$\Delta_r H^\circ = \Sigma \Delta_f H_{products} - \Sigma \Delta_f H_{reactants}$$

$$\ln K' - \ln K = -[\Delta_r H/R][1/T' - 1/T] \qquad \text{(Van't Hoff approximation)}$$

The temperatures at above which benzene will form spontaneously for n-hexane and 1-hexene is 350°C and 175°C, respectively (Figure A-1).

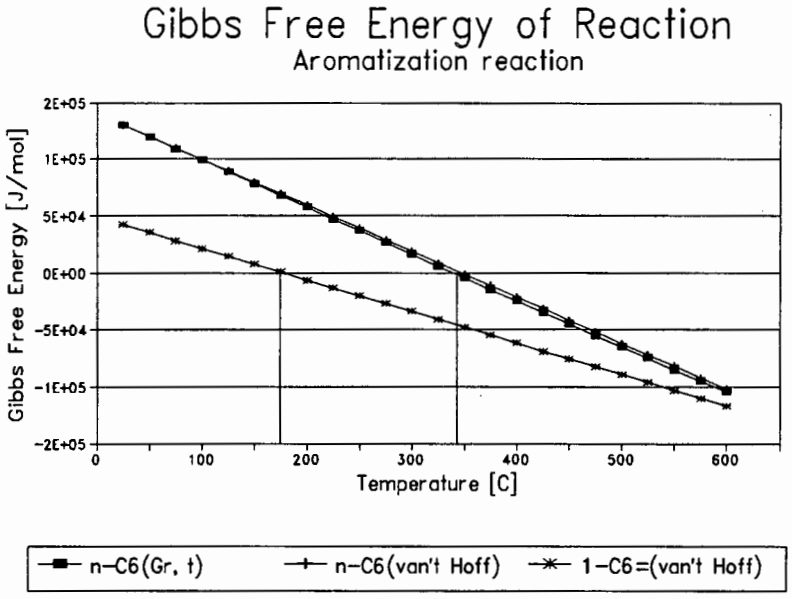

Figure A-1 Change in Gibbs free energy for aromatization of n-hexane and 1-hexene with change in temperature

A.2.2 Hysim

Thermodynamic equilibrium data was also obtained for:

- linear hexene isomerization
- hexane isomerization (n-hexane, MCP, methylpentanes)
- n-hexane aromatization (excluding cracking reactions)

The data was obtained at different temperatures and molar ratios of hydrogen to the hydrocarbons using the UNIQUAC module of the Hysim program. A Gibbs reactor was specified with a pressure drop of 10 kpa, which is similar to that observed experimentally in this project. The reaction pressure was set at 1 bar, except for the data shown in Figure A-4.

For n-hexane aromatization (Figure A-5) isomerization, dehydrogenation and dehydrocylization, including cyclohexane formation, were specified. Hydrogenolysis

was excluded. Effectively no dehydrogenation products were observed.
The thermodynamic equilibrium data for the isomerization of n-hexane is shown in Figure A-3 to Figure A-4. The data for the isomerization of linear hexenes is shown in Figure A-2.

When hydrogenolysis is taken into account, thermodynamics predicts that methane is the sole product. This is true for both the hydrogenolysis of hexane to C_1-C_5 products as well as for the aromatization of n-hexane (aromatization, isomerization and hydrogenolysis reactions allowed).

Table A-1 Thermodynamic data at different temperatures and 1 bar hydrogen partial pressure

molar ratios	350°C	400°C	450°C
n-hexane isomerization (H_2:hydrocarbon molar ratio = 20:1)			
n-hexane	0.276	0.271	0.248
2m-C_5	0.442	0.397	0.338
3m-C_5	0.229	0.211	0.185
MCP	0.046	0.108	0.208
cyclohexane	0.006	0.013	0.021
Linear hexene isomerization			
1-hexene	0.045	0.054	0.062
c-2-hexene	0.334	0.329	0.324
t-2-hexene	0.387	0.382	0.377
c-3-hexene	0.068	0.072	0.076
t-3-hexene	0.166	0.164	0.162
n-hexane aromatization			
n-hexane	0.1042	0.0000	0.0000
benzene	0.6250	0.9895	1.0000
2m-C_5	0.1666	0.0105	0.0000
3m-C_5	0.0833	0.0000	0.0000
MCP	0.0208	0.0000	0.0000
cyclohexane	0.0000	0.0000	0.0000

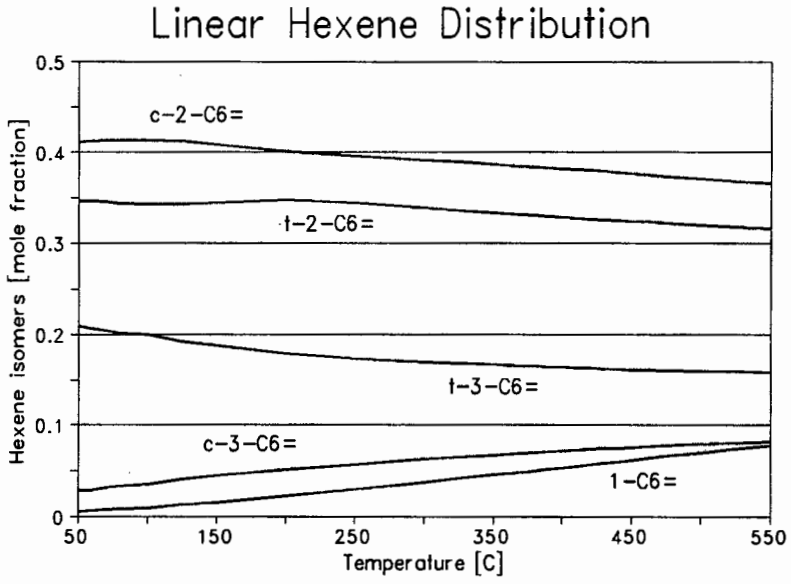

Figure A-2 Linear hexene isomer distribution

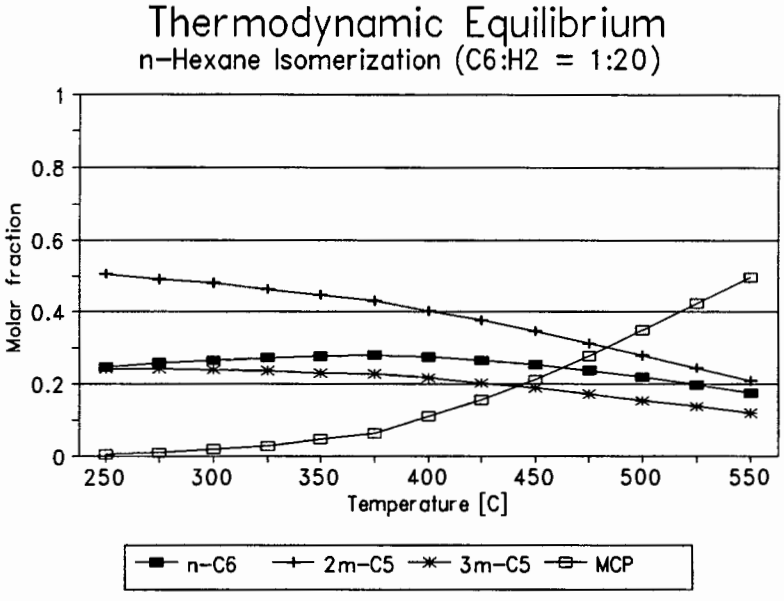

Figure A-3 Effect of temperature on the molar fractions for n-hexane isomerization

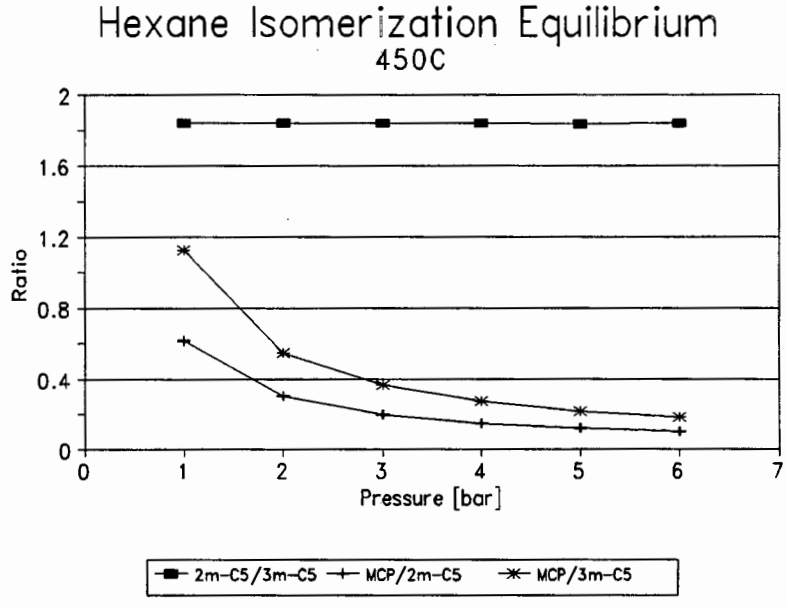

Figure A-4 Effect of hydrogen partial pressure on the isomerization of n-hexane at 450°C

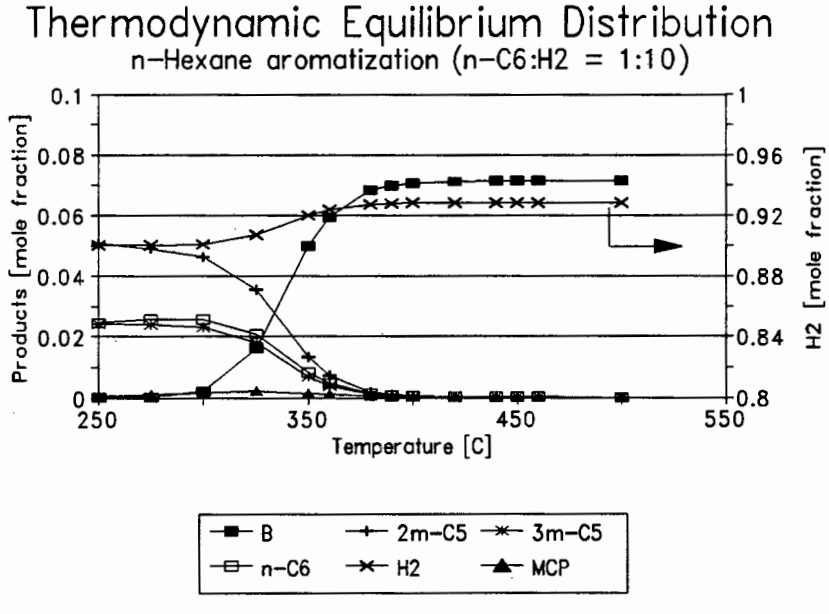

Figure A-5 Effect of temperature on the aromatization of n-hexane

A.3. Mass flow calibrations

A.3.1 Inorganic gases (nitrogen, hydrogen, air)

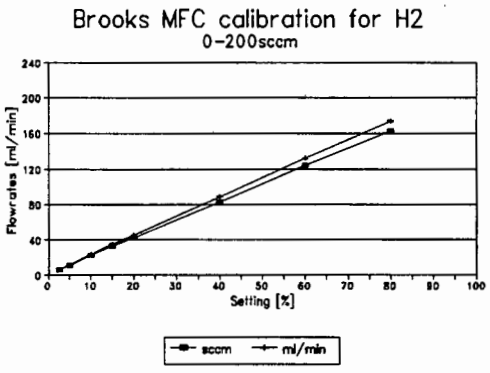

Figure A-6 Hydrogen calibration

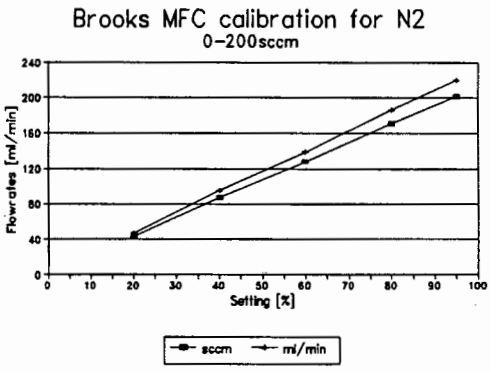

Figure A-7 Nitrogen calibration

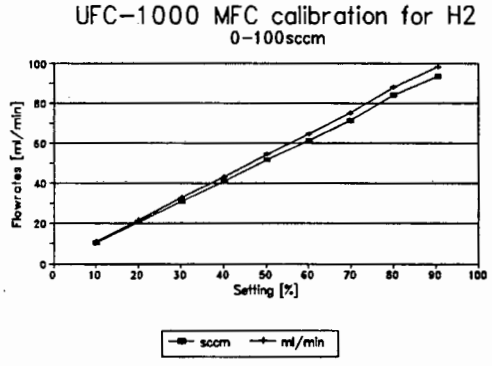

Figure A-8 Hydrogen calibration

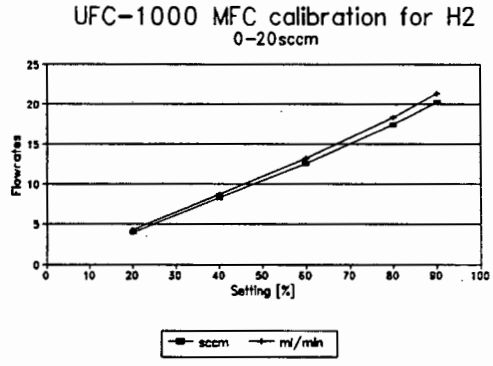

Figure A-9 Hydrogen calibration

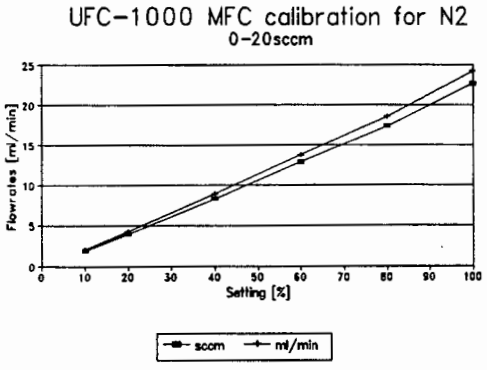

Figure A-10 Nitrogen calibration

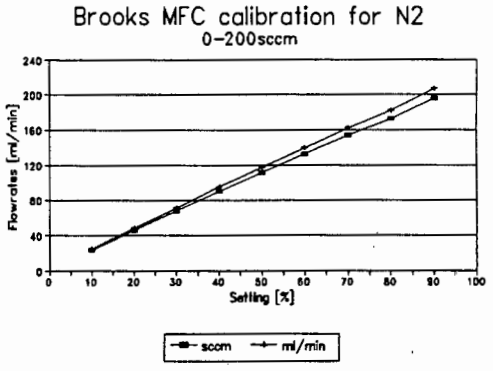

Figure A-11 Nitrogen recalibration

A.3.2 Dimethylether (DME)

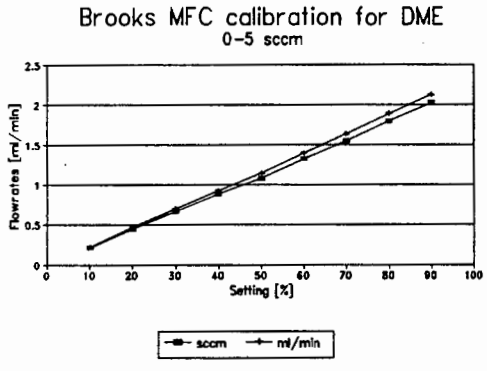

Figure A-12 DME calibration

A.3.3 Carbon monoxide

During the calibration of 5.89% CO in hydrogen the concentration of CO was monitored (downstream of the bubblemeter) by IR spectrscopy. As expected it remained constant at 5.89 vol% of the flue gas.

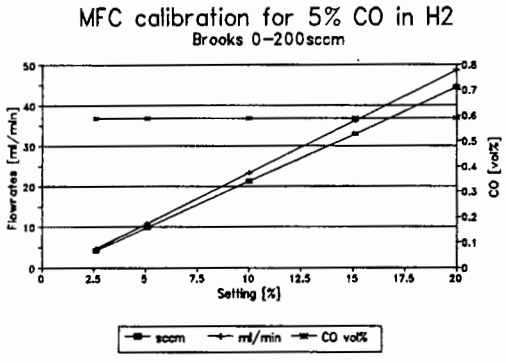

Figure A-13 Calibration of 5% CO in hydrogen

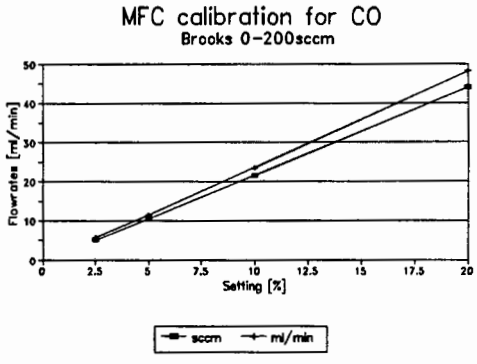

Figure A-14 Calibration of CO

A.4 Physical Data for Organic Compounds

Table A-2 Alkane hydrocarbon data

Compound	Code	Boiling point [°C]	Molecular mass [g/mol]
methane	C_1	-161.5	16.04
ethane	C_2	-88.6	30.70
propane	C_3	-42.1	44.10
n-butane	n-C_4	-0.5	58.12
i-butane	i-C_4	-11.7	58.12
n-pentane	n-C_5	36.1	72.15
2,2-dimethylbutane	2,2-d-m-C_4	49.5	86.18
n-hexane	n-C_6	68.7	86.18
3-methylpentane	3-m-C_5	60.3	86.18
2-methylpentane	2-m-C_5	63.3	86.18
methylcyclopentane	MCP	72.0	84.16

Table A-3 Alkene hydrocarbon data

Compound	Code	Boiling point [°C]	Molecular mass [g/mol]
ethene	$C_2=$	-104.0	28.05
propene	$C_3=$	-48.0	42.08
1-butene	1-$C_4=$	-6.3	56.11
i-butene	i-$C_4=$	-6.9	56.11
t-2-butene	t-2-$C_4=$	0.9	56.11
c-2-butene	c-2-$C_4=$	3.7	56.11
1-pentene	1-$C_5=$	29.9	70.14
1-hexene	1-$C_6=$	63.5	84.14
c-2-hexene	c-2-$C_6=$	68.8	84.14
t-2-hexene	t-2-$C_6=$	67.9	84.14
c-3-hexene	c-3-$C_6=$	66.4	84.14
t-3-hexene	t-3-$C_6=$	67.1	84.14
benzene	B	78.1	80.00

Table A-4 Oxygenated compound data

Compound	Code	Boiling point [°C]	Molecular mass [g/mol]
ethanol	EtOH	79.0	46.07
methylethylketone	MEK	80.0	72.11
acetic acid	EtOOH	116	44.05
n-butyraldehyde	n-BuHO	75	72.11
i-butyraldehyde	i-BuHO	63	72.11
carbon monoxide	CO	-	28.01
water	H_2O	100	18.02

A.5 Vapour pressure data

Vapour pressure data was calculated by the method of Reid *et al.* (1987) The data obtained from these equations is shown in Figure A-15 and Figure A-16.

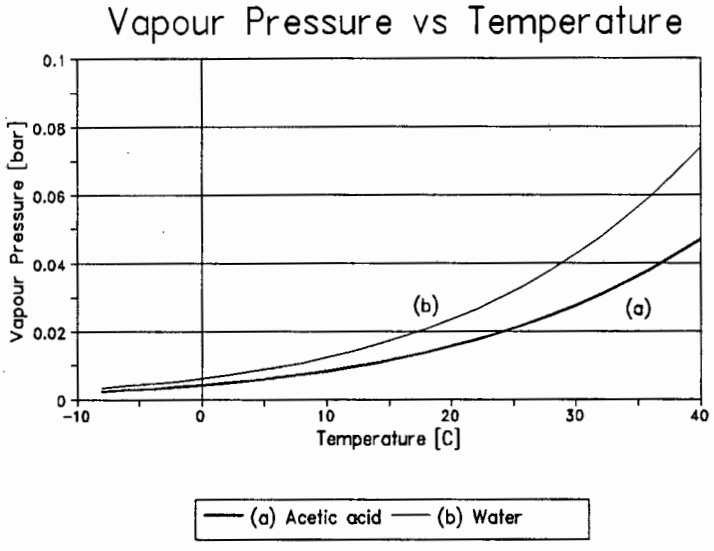

Figure A-15 Vapour pressure of water and acetic acid

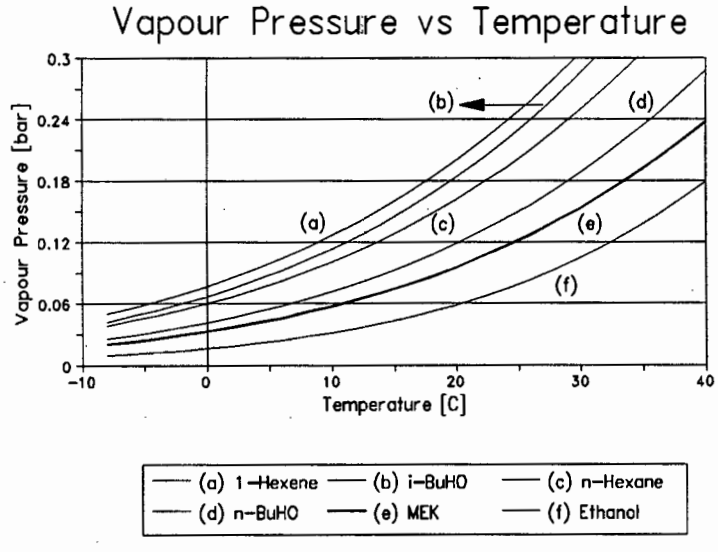

Figure A-16 Vapour pressure data